

University of Windsor

Scholarship at UWindor

Electronic Theses and Dissertations

Theses, Dissertations, and Major Papers

2016

Exploiting Cancer Cell Mitochondria as a Therapeutic Strategy: Structure Activity Relationship Analysis of Synthetic Analogues of Pancratistatin

Dennis Ma
University of Windsor

Follow this and additional works at: <https://scholar.uwindsor.ca/etd>

Recommended Citation

Ma, Dennis, "Exploiting Cancer Cell Mitochondria as a Therapeutic Strategy: Structure Activity Relationship Analysis of Synthetic Analogues of Pancratistatin" (2016). *Electronic Theses and Dissertations*. 5744.

<https://scholar.uwindsor.ca/etd/5744>

This online database contains the full-text of PhD dissertations and Masters' theses of University of Windsor students from 1954 forward. These documents are made available for personal study and research purposes only, in accordance with the Canadian Copyright Act and the Creative Commons license—CC BY-NC-ND (Attribution, Non-Commercial, No Derivative Works). Under this license, works must always be attributed to the copyright holder (original author), cannot be used for any commercial purposes, and may not be altered. Any other use would require the permission of the copyright holder. Students may inquire about withdrawing their dissertation and/or thesis from this database. For additional inquiries, please contact the repository administrator via email (scholarship@uwindsor.ca) or by telephone at 519-253-3000ext. 3208.

**Exploiting Cancer Cell Mitochondria as a Therapeutic Strategy:
Structure Activity Relationship Analysis of Synthetic Analogues of
Pancratistatin**

Dennis Ma

A Dissertation
Submitted to the Faculty of Graduate Studies
through the Department of Chemistry and Biochemistry
in Partial Fulfillment of the Requirements for
the Degree of Doctor of Philosophy at the
University of Windsor

Windsor, Ontario, Canada

© 2016 Dennis Ma

**Exploiting Cancer Cell Mitochondria as a Therapeutic Strategy:
Structure Activity Relationship Analysis of Synthetic Analogues of
Pancratistatin**

By

Dennis Ma

APPROVED BY:

S. Ray, External Examiner
Manchester University

P. Vacratsis
Department of Chemistry and Biochemistry

M. Boffa
Department of Chemistry and Biochemistry

M. Crawford
Department of Biological Sciences

S. Pandey, Advisor
Department of Chemistry and Biochemistry

May 25, 2016

Declaration of Co-authorship & Previous Publication

I. Declaration of Co-Authorship

I hereby declare that this dissertation incorporates material that is result of joint research as follows:

This dissertation incorporates the outcome of joint research efforts undertaken in collaboration with Daniel Tarade, Tyler Gilbert, Christopher Pignanelli, Fadi Mansour, Scott Adams, Colin Curran, Alexander Dowhayko, Megan Noel, Melissa Cowell, Manika Gupta, Ian Tuffley, Sabrina Ma, Phillip Tremblay, Kevinjeet Mahngar, Pardis Akbari-Asl, Sergey Vshyvenko, Jonathan Collins, Tomas Hudlicky, and James McNulty under the supervision of Dr. Siyaram Pandey. In all cases, experimental design, execution, data analysis, interpretation, and manuscript preparation were performed by the author. All authors have read and approved the final manuscript prior to submission.

Collaboration with James McNulty is covered in Chapters 2 and 4 of this dissertation; this contribution was through provision of chemical compounds and write-up of synthesis details.

Collaboration with Sergey Vshyvenko, Jonathan Collins, and Tomas Hudlicky is covered in Chapters 2-5 (and Appendices A and B) of this dissertation; this contribution was through synthesis and provision of chemical compounds and write-up of synthesis details.

Collaboration with Phillip Tremblay, Kevinjeet Mahngar, and Pardis Akbari-Asl is covered in Chapters 2 and 3 (and Appendix A) of this dissertation; there was partial contribution to experimental execution and data interpretation.

Collaboration with Daniel Tarade, Tyler Gilbert, Christopher Pignanelli, Fadi Mansour, Scott Adams, Colin Curran, Alexander Dowhayko, Megan Noel, Melissa Cowell, Manika Gupta, Ian Tuffley, and Sabrina Ma is covered in Chapters 4 and 5 of this dissertation; there was partial contribution to experimental execution and data interpretation.

I am aware of the University of Windsor Senate Policy on Authorship and I certify that I have properly acknowledged the contribution of other researchers to my dissertation, and have obtained written permission from each of the co-authors to include the above materials in my dissertation. I certify that, with the above qualification, this dissertation, and the research to which it refers, is the product of my own work.

II. Declaration of Previous Publication

This dissertation includes 4 original papers that have been previously published:

CHAPTER 2

Ma D, Tremblay P, Mahngar K, Akbari-Asl P, Collins J, Hudlicky T, McNulty J, Pandey S. A Novel Synthetic C1 Analog of 7-deoxypancratistatin Induces Apoptosis in p53 Positive and Negative Human Colon Cancer Cells by Targeting the Mitochondria: Enhancement of Activity by Tamoxifen. *Investigational New Drugs* 2012;30(3):1012-27. doi: 10.1007/s10637-011-9668-7. Epub April 15, 2011.

CHAPTER 3

Ma D, Tremblay P, Mahngar K, Collins J, Hudlicky T, Pandey S. Selective Cytotoxicity Against Human Osteosarcoma Cells by a Novel Synthetic C-1 Analogue of 7-deoxypancratistatin is Potentiated by Curcumin. *PLoS One* 2011;6(12):e28780. doi: 10.1371/journal.pone.0028780. Epub December 21, 2011.

APPENDIX A

Ma D, Tremblay P, Mahngar K, Akbari-Asl P, Collins J, Hudlicky T, Pandey S. Induction of Apoptosis and Autophagy in Human Pancreatic Cancer Cells by a Novel Synthetic C-1 Analogue of 7-deoxypancratistatin. *Am. J. Biomed. Sci.* 2011;3(4):278-291; doi: 10.5099/aj110400278. Published September 5, 2011.

APPENDIX B

Ma D, Collins J, Hudlicky T, Pandey S. Enhancement of apoptotic and autophagic induction by a novel synthetic C-1 analogue of 7-deoxypancratistatin in human breast adenocarcinoma and neuroblastoma cells with tamoxifen. *J Vis Exp.* 2012;(63). pii: 3586. doi: 10.3791/3586. Published May 30, 2012.

CHAPTERS 4 & 5

These chapters are manuscripts in preparation for submission.

II. Declaration of Previous Publication (Continued)

I certify that I have obtained written permission from the copyright owners to include the above published materials in my dissertation. I certify that the above material describes work completed during my registration as graduate student at the University of Windsor.

I declare that, to the best of my knowledge, my dissertation does not infringe upon anyone's copyright nor violate any proprietary rights and that any ideas, techniques, quotations, or any other material from the work of other people included in my dissertation, published or otherwise, are fully acknowledged in accordance with the standard referencing practices. Furthermore, to the extent that I have included copyrighted material that surpasses the bounds of fair dealing within the meaning of the Canada Copyright Act, I certify that I have obtained a written permission from the copyright owners to include such materials in my dissertation.

I declare that this is a true copy of my dissertation, including any final revisions, as approved by my doctoral committee and the Graduate Studies office, and that this dissertation has not been submitted for a higher degree to any other University or Institution.

Abstract

Distinct characteristics, including decreased dependence on mitochondrial respiration and high levels of oxygen radicals, provide opportunities for cancer targeting. We have shown the compound pancratistatin (PST) to selectively induce apoptosis in cancers by mitochondrial targeting. However, its low availability in nature was limiting its preclinical development. Various PST analogues were synthesized to circumvent this limitation. In this dissertation, these analogues were screened and several had comparable or greater anti-cancer activity compared to PST. The analogue, SVTH-7, demonstrated the most potent anti-cancer activity, followed by SVTH-6 and -5 *in vitro* and *in vivo*. These compounds had greater efficacy than PST, 7-deoxyPST analogues, and multiple standard chemotherapeutics, and were found to induce apoptosis in cancer cells by acting on cancer cell mitochondria. Furthermore, the anti-cancer effects of PST analogues were enhanced when used with agents known to target cancer cell mitochondria and oxidative vulnerabilities, including tamoxifen, curcumin, and piperlongumine. Interestingly, functional complex II and III of the electron transport chain were required for SVTH-7 to inflict its pro-apoptotic effects on cancer cells, suggesting exploitation of a mitochondrial vulnerability by SVTH-7. Therefore, these findings demonstrate a novel approach to treat cancer by exploiting cancer cell mitochondria with PST analogues alone or in combination with other compounds. These PST analogues have high therapeutic potential and this work will lay the groundwork for the identification and characterization of distinct mitochondrial features of cancer cells.

Acknowledgements

I would like to thank my mentor and supervisor, Dr. Siyaram Pandey, for taking me into his lab in the summer of 2007 as an undergraduate student and giving me the opportunity to work in his lab for all these years to the completion of my undergraduate research project and this dissertation. He was the first to spark my interest in research and his guidance, expertise, patience and encouragement have been invaluable to my growth as a scientist. He is an example of having all the right intensions as a researcher to benefit others, and genuinely cares and advocates for his students.

Thank you to my doctoral committee, including Dr. Siyaram Pandey, Dr. Panayiotis Vacratsis, to Dr. Michael Boffa, Dr. Michael Crawford, and Dr. Sidhartha Ray for their valuable input, critical evaluation of my work, and encouragement during my graduate studies.

Thank you for the heartfelt local support to this work and our lab by the Knights of Columbus Chapter 9671 (Windsor, ON), the Pajama Angels, and the Couvillon Family, in memory of Kevin Couvillon. Your kindness, generosity, and encouragement have been extremely motivational to us and is greatly appreciated. Thank you for believing in us. Thank you to the Lotte & John Hecht Memorial Foundation for funding the pancratistatin project and the Jesse & Julie Rasch Foundation for supporting the natural health products research in our laboratory.

My graduate studies have been funded by a Vanier Canada Graduate Scholarship, a CIHR Frederick Banting and Charles Best Canada Graduate Scholarship, and an Ontario Graduate Scholarship.

Thank you to our collaborators, Dr. Tomas Hudlicky, Sergey Vshyvenko and Jonathan Collins of Brock University, for synthesizing and providing the synthetic derivatives of pancratistatin for this project. Thank you to Dr. James McNulty, for providing natural pancratistatin to our laboratory, as well as combretastatin A4 (CA4) analogues for the synthetic CA4 project. Thank you to Dr. Yi Wang at Wenzhou Medical University in China for providing synthetic analogues of curcumin for the synthetic curcumin project. Thank you to Dr. James Gault in the capacity as both a mentor and collaborator. Having you next door was like having a second supervisor. You have gone out of your way and have done so much for me and it is greatly appreciated; please also give my regards to Oscar and Frank. Thanks to Dan Simard and Mohamed Aboelnga for performing computation studies for my projects. Also, thanks to the rest of the Gault Group, that I have gotten to know, for their support and friendship from across the hall: Phil De Luna, Bogdan Ion, Grant Fortowsky, Hisham Dokainish, Sameer Jafar, Wanlei Wei, Travis Dewolfe, Danielle, Rami Gherib, Eric Bushnel.

Thank you to Dr. Michael Boffa, Dr. Sirinart Ananvoranich, Dr. Bulent Mutus, Dr. Barbara Zielinski, and Dr. Porter for the use of their lab equipment. Thank you to our secretaries in the Department of Chemistry and Biochemistry, Marlene Bezaire, Elizabeth Kickham, Cathy Wilson, and Michelle Miglietta for keeping our department running and for your support and encouragement. All of

your work is much appreciated. Special thanks to Marlene for going out of her way to let me know about deadlines and scholarship opportunities; you are the reason why I am graduating as planned. You have gone above and beyond, moving the whole world around for me, and your help throughout these years has been extremely valuable and greatly appreciated. Also thank you to Beth for addressing all my financial matters and concerns with general lab maintenance.

Thank you to the Chemical Control Center crew, including Jerry Vriesacker, Alina Jaworska-Sobiesiak, Tina Lepine, Francis Arnaldo, and Sherri Menard, for all your assistance in obtaining lab supplies and materials. Special thanks to Jerry for dealing with all my extra ordering concerns in a very timely and efficient manner.

Special thanks to Janice Tubman, Elizabeth Fidalgo da Silva, Dorota Lubanska, Joe Lichaa, Bob Hodge, Elaine and Linda Sterling for their technical support. Also thank you to Ionut Pricop, Biju Vasavan, Urszula Liwak, Anna Crater-Potter, Michael Holmes, Farzana Afrin, Andei, Justin Garabon, Jessica Snyder, Sera Sayegh, Matt Gemin, Jackson McAiney, Mousa Gawanmeh, Victor Igbokwe, Zainab Bazzi, Tanya Marar, Rocco Romagnuolo, Hyder Ali Khan, Ryan McLarty, Adam Faccenda, Terence Yep, Chris Bonham, Robert Gombar, Besa Xhabija, Jas Sohi, Justin Roberto, Quidi Geng, Norah Franklin, Colleen Mailloux, Anna Kozarova, Jordan Prince, Michael-Anthony Ferrato, Derek Lanoue, Akhil Vohra, Giorgio, Manar Shoshani, Heather Filiatrault, Ronan San Juan, Chris Mireault, Chris Caputo, Vedran Vukotic, Ryan Mills, Laura Allen, Bryan Lucier, Chris O'Keefe, Leslie Hernandez, Max Nascimento, and Mitchell Nascimento for

their support and friendship during my time in the Chemistry and Biochemistry Department.

Thank you to the original graduate students and group members of the Pandey Lab that were present when I first joined. You took me in, trained me, and made me feel welcomed. You have all been a positive influence in my experience in the lab, showing me how to perform lab techniques while being patient and offered me your friendship.

Thank you to Dr. Peter Seidlakowski, who was the graduate student on the natural pancratistatin (PST) project when I first joined, for initially encouraging and helping me get into the Pandey Lab. You always had a positive attitude and were great to work with. You were my first mentor in the lab, trained me on the PST project, and have been supportive to this present day as my dentist.

Thank you to Mallika Somayajulu-Nitu who was a role model, mentor, and the mother figure of the lab. For me, you were the gold standard of what every graduate student and mentor should be and I have strived to become the mentor you were for me for my mentees. Your disciplined work ethic, guidance, life advice, and continued support throughout the years and after your time in the lab has been greatly appreciated.

Thanks to Carly Griffin for her work on natural PST.

Thank you to Sudipa June Chatterjee, who quickly became a leader in the lab, for addressing any of my questions and concerns with great patience and encouragement during my undergraduate thesis. You were a dedicated, hard worker and still made time to help me for which I am extremely grateful for.

Thank you to Katrina McGonigal who mentored and worked with me on the Bax project during my first NSERC summer research award tenure. Your patience, positive attitude, and instruction was much appreciated and I am thankful for everything you have done for me.

Thank you to Danijela Domazet who worked on the fibroblast project and co-authored a manuscript with me later in my graduate career. You were a great role model in the lab and your friendship and assistance was much appreciated.

Thank you to my peers who did their undergraduate work with me in the Pandey Lab for your friendship and support. It was great to work and learn with all of you: Justin Kale, Sakshi Jasra, Kristen Church, Cynthia Tran, Natasha Rafo, Parvati Dadwal, Kanika Jaggi, Aditya Karnik, Edward Schwartzenberger, Brandon Gagne, Anca Matei and Subitha Rajakumaran.

Thank you to the other graduate students in the lab for being great colleagues. Thank you Krithika Muthukumaran, for your continued support, encouragement and friendship. I enjoyed our tea and refreshments breaks and classes together. Thank you to Katie Facecchia for your support and friendship over the years. Thank you to Mike Stanesic for your friendship, support, and fitness wisdom. I strive to one day squat as much as you.

Thank you to everyone in the Neurodegeneration Research Group or "PDG" as well as the Natural Health Products Group in Pandey Lab. Thank you for being great colleagues and for your friendship and support: Kate Harrison, Jessica Smith, Samantha Leahy, Harshil Jasra, Miranda Mazza, Melissa Macksoud, Joseph Correia, Alexandra Marginean, Annie Kanwar, Austin Elliott,

Simon Pupulin, Adrian Di Meo, Leah Nicoletti, Karishma Desai, Alessia Roma, Matt Steckle, Grace Teskey, Diego Vazquez, Patrick Malolepszy, Bayan Aloran, Ivan Ruvinov, Dayna Mastronardi, Emmanuel Igbokwe, Abbey Nicoletti, Emily Kogel, Chris Nguyen, Sabrina Cardillo, Tanya Tewari, Saniya Jain, Bianca Grier.

My greatest experience as a doctoral student was working and mentoring 28 undergraduate and 2 masters researchers. As well as getting an opportunity to build my leadership abilities, I thoroughly enjoyed working and learning together with all of you. You have all earned my respect, gratitude, and lifelong friendship working together in this laboratory. I have viewed all of you as my peers, colleagues and equals, as opposed to my subordinates; you have all worked as hard as I have, and I owe much of my research success to your efforts and our teamwork. All of you maintained great patience, a positive attitude, accommodated to each other's schedules, troubleshooted each other's problems, facilitated communication, and played to everyone's strengths to synergize productivity. This unprecedented level of teamwork and productivity has been something I thoroughly enjoyed being a part of and I can only hope to achieve this with my colleagues and mentees in the future. You all have the skills and mentality to become successful contributing members of society in your future careers and I wish you all the best: Cory Phillion, Kristen Larocque, Colin Curran, Alexander Dowhayko, Simon Pupulin, Fadi Mansour, Jesse Ropat, Megan Noel, Christopher Pignanelli, Tyler Gilbert, Mark Rodriguez, Inderpal Singh, Rabia Hadi, Krishan Parashar, Scott Adams, Cody Caba, Fatmeh Hourani, Daniel Tarade, Kyle Stokes, Adam Kadri, Julia Church, Seema Joshi, Sabrina Ma, Ian

Tuffley, Manika Gupta, Jashan, Phillip Tremblay, Kevinjeet Mahngar, Pardis Akbari-Asl, Cynthia Tran, and Surbhi Garg.

In particular, I would like to thank Danny Tarade, Chris Pignanelli, and Kyle Stokes. The three of you are not human. You are super-human or possibly robots. Even as undergraduate students, I have never seen people so enthusiastic, independent, talented, and hard working with unbelievable time management skills. Despite being extremely busy with things outside of the lab, you still had time to work extremely hard. You took initiative, read up on new ideas and techniques for the lab, performed experiments properly, were the most productive individuals I have ever witnessed in Pandey Lab (including graduate students and postdoctoral researchers), and helped both me and your peers as well as others who were not even working on our projects. You put in more time than anyone else in the lab even when you weren't getting paid and were always there when I needed an extra hand. More importantly, I would like to thank you for reminding me of my initial enthusiasm for research. You indirectly helped me get back on track when I was burnt out, kept me on my toes, and pushed me to reach my full potential. The three of you have made me very proud as your mentor and there is no doubt in my mind that you will become extremely successful in your respective careers. I wish you all the best and hope we can be colleagues and collaborators in the future.

I would like to thank Team AD, including Phil Tremblay and Jeet Mahngar (and Pardis). You were my first students and really helped me get on my feet inside and outside of the lab. I owe most of my initial success to your hard work

and friendship which we have maintained to this day. You have become successful on your respectively career paths and I could not be more proud.

Thank you to Kate, Nelson, and Rico Suave Harrison-Ho. The three of you have been great friends. Your support and encouragement throughout the years has been greatly appreciated. You are all extremely hard working and I am proud of your accomplishments as they are well deserved.

Thank you to the Quiz Crew. Thank you Tyler Gilbert for your help, support, stylish hats, cute puppies, and friendship. You have been like a little brother to me and I feel privileged to have been part of several of your life changing experiences. I look forward to more in the future! Thank you to Mark and Inderpal, two hard workers, for your assistance, support and friendship. Even just as undergraduate volunteers, the both of you (along with Alessia) are easily the hardest working individuals on the natural health products project in our lab. Your initiative, discipline, independence, and work ethic have been outstanding and I wish you the best in the future. Thank you to my male nurse Sasha, who played a pivotal role in the completion of my dissertation. As a fellow mature student, I appreciate your friendship, company, and shared enthusiasm for school. I wish you the best and hope all this school pays off for the both of us.

Thank you to Fadi, Colin, and Megan who have helped me tremendously in my final stages of my doctoral studies. Even as junior members of lab, you have been extremely valuable and have demonstrated great maturity, team work, work ethic, and enthusiasm for our research. I could always depend on you for help when I needed it and wish you all the best in the future.

Special thanks to Scott, Fatmeh, Seema (PITA1), Julia (PITA2), Alessia, Joe, Harshil, Austin, Emmanuel, Simon, Cody, Jashan, Cynthia, Annie, Leah, Abbey, Emily, Mrs. Potter, Ionut, Diego, Tanya, David, Justin, Zainab, Victor, Pat, Trish, Nick, Arthur, and the rest of the Windsor 2015's for your support and friendship. I enjoyed our time together and hope to stay in touch in the future.

Thank you to Cory and Lemur. You both started out with no experience in the lab and have grown into independent scientists. I am very proud of you both! You played a huge role in helping me figure out my future career plans and I am grateful for your friendship and support. I will miss you both.

I would, most importantly, like to thank my friends and family for supporting me throughout my life and during my studies at the University of Windsor. To all my cousins, aunts, uncles, and grandparents, thank you for being there for me and for your support and encouragement. Thank you to my aunt Efa and uncle Weiser for their love, encouragement and support. Thank you uncle Tim and auntie Helen for supporting me as well. Thank you to my sister, Sabrina, and my brother, William, who have always been there for me for any of my problems or concerns as siblings do. You were always there for advice and suggestions all my life and have played a huge role in achieving my goals. And thank you to my parents, who have sacrificed everything for my siblings and I. I have not seen more hardworking and selfless people. Your hard work and dedication to us has been unparalleled and we are extremely grateful for everything you have done for us.

**Permissions have been given to post the pictures on the following page.*

MY RESEARCH TEAM IN PANDEY LAB



Dennis Dr. Pandey Kristen Cory



Mark Inderpal Sasha Rabia Colin Simon



Fadi Megan Chris Krishan Tyler Jesse



Scott Cody Danny Kyle Fatmeh Adam



Seema Julia Manika Ian Sabrina Jashan



Phil Jeet Pardis Cynthia Surbhi

Table of Contents

Declaration of Co-authorship & Previous Publication	iii
Abstract	vi
Acknowledgements	vii
List of Figures	xxiii
List of Appendices	xxviii
CHAPTER 1: General Introduction	1
List of Abbreviations	2
Cancer.....	4
Apoptosis.....	5
Extrinsic and Intrinsic Apoptosis	5
Apoptogenic Factors.....	8
The Bcl-2 Family of Proteins	10
Mitochondrial Membrane Permeabilization	11
Evasion of Apoptosis by Cancer Cells.....	12
The p53 Tumor Suppressor	13
Metabolic Reprogramming in Cancer Cells.....	14
Reactive Oxygen Species (ROS) Scavengers & Generators	16
Cancer Cell Mitochondria and Mitocans.....	18
Vitamin E Analogues	19
Taxol.....	19
Pancratistatin and Narciclasine.....	20
Synthetic Analogues of Pancratistatin	23
Objectives.....	26
References	27
CHAPTER 2: A Novel Synthetic C1 Analogue of 7-deoxypancratistatin Induces Apoptosis in p53 Positive and Negative Human Colorectal Cancer Cells by Targeting the Mitochondria: Enhancement of Activity by Tamoxifen	41

List of Abbreviations	42
Summary	44
Introduction.....	46
Materials and Methods	49
<i>Cell Culture</i>	49
<i>Cell Treatment</i>	49
<i>Nuclear Staining</i>	50
<i>Annexin V Binding Assay</i>	50
<i>WST-1 Assay for Cell Viability</i>	50
<i>Tetramethylrhodamine Methyl Ester (TMRM) Staining</i>	51
<i>Mitochondrial Isolation</i>	51
<i>Amplex Red Assay</i>	52
<i>Cellular Lysate Preparation</i>	53
<i>Western Blot Analyses</i>	53
<i>Z-VAD-FMK Caspase Inhibition</i>	54
<i>Monodansylcadaverine (MDC) Staining</i>	54
<i>Long-term Analysis on Growth Rate</i>	55
Results	56
<i>JCTH-4 Effectively Induces Apoptosis in Human CRC Cells</i>	56
<i>TAM Enhances the Apoptotic Efficacy of JCTH-4 in CRC Cells</i>	60
<i>JCTH-4 and TAM Target the Mitochondria in HT-29 and HCT 116 Cells</i>	64
<i>JCTH-4 Induces Apoptosis in a Caspase-Independent Manner</i>	70
<i>JCTH-4 Induces Autophagy in HT-29 and HCT 116 Cells</i>	72
<i>Long-Term Effect on Human CRC Cells Post Exposure to JCTH-4 and TAM</i>	75
Discussion	77
Acknowledgements.....	85
References	86
CHAPTER 3: Selective Cytotoxicity Against Human Osteosarcoma Cells by a Novel Synthetic C-1 Analogue of 7-deoxypancratistatin is Potentiated by Curcumin	93
List of Abbreviations	94
Summary	95

Introduction.....	96
Materials and Methods	100
<i>Cell Culture</i>	100
<i>Cell Treatment</i>	101
<i>Nuclear Staining</i>	101
<i>Annexin V Binding Assay</i>	102
<i>WST-1 Assay for Cell Viability</i>	102
<i>Tetramethylrhodamine Methyl Ester (TMRM) Staining</i>	103
<i>Mitochondrial Isolation</i>	103
<i>Amplex Red Assay</i>	104
<i>Treatment of Isolated Mitochondria & Evaluation of Apoptogenic Factor Release</i>	104
<i>Cellular Lysate Preparation</i>	105
<i>Western Blot Analyses</i>	105
<i>Monodansylcadaverine (MDC) Staining</i>	106
<i>Propidium Iodide (PI) Staining</i>	106
Results	107
<i>JCTH-4 causes selective cytotoxicity in OS cells in a time and dose-dependent manner</i>	107
<i>CC potentiates the cytotoxicity of JCTH-4 selectively in OS cells</i>	107
<i>JCTH-4 alone & in combination with CC induces apoptosis in OS cells</i>	111
<i>JCTH-4 alone and in combination with CC targets OS cell mitochondria</i>	116
<i>JCTH-4 selectively induces autophagy alone and with CC in OS cells</i>	123
Discussion	127
Author Contributions	134
Acknowledgements.....	134
Funding.....	134
References.....	135
CHAPTER 4: Structure Activity Relationship Analysis of Synthetic Analogues of Pancreatistatin: Anti-cancer Activity is Dependent on Functional Mitochondrial Complex II and III	143
List of Abbreviations	144
Summary	146

Introduction.....	147
Materials and Methods	150
<i>Cell Culture</i>	150
<i>Isolation and Culture of Peripheral Blood Mononuclear cells (PBMCs)</i>	154
<i>Chemicals and Cell Treatment</i>	155
<i>WST-1 Assay for Cell Viability</i>	156
<i>Cell Death Analysis: Annexin V Binding Assay & Propidium Iodide (PI) Staining</i> ..	156
<i>Quantitation of Reactive Oxygen Species (ROS)</i>	157
<i>Mitochondrial Isolation</i>	159
<i>Treatment of Isolated Mitochondria & Evaluation of Apoptogenic Factor Release</i> . 159	
<i>Western Blot Analyses</i>	160
<i>Oxygen Consumption Quantitation</i>	161
<i>Three-Dimensional Spheroid Culture and Assays</i>	161
<i>In Vivo Xenograft Models</i>	163
<i>Statistical Analysis</i>	163
Results	164
<i>PST Analogues have Selective and Potent Anti-Cancer Activity with Efficacy Surpassing Standard Chemotherapeutics and Natural PST</i>	164
<i>PST Analogues Induce Apoptosis Selectively in Cancer Cells</i>	169
<i>PST Analogues Cause Mitochondrial Dysfunction and Activate the Intrinsic Pathway of Apoptosis in Cancer Cells</i>	172
<i>PST Analogues Decrease Oxygen Consumption Capabilities of Cancer Cells</i>	176
<i>PST Analogue-Induced Apoptosis is Dependent on Functional Complex II and III of the Mitochondrial Electron Transport Chain</i>	178
<i>PST Analogues Selectively Induce Apoptosis in 3D Spheroid Models of Cancer</i> ..	181
<i>PST Analogues Decrease Growth of Tumors in Xenograft Mouse Models</i>	185
Discussion	188
Author Contributions	192
Acknowledgements.....	192
References	193
Supplemental Materials.....	199

CHAPTER 5: Exploiting Mitochondrial & Oxidative Vulnerabilities with a Synthetic Analogue of Pancratistatin in Combination with Piperlongumine for Cancer Therapy	228
List of Abbreviations	229
Summary	230
Introduction.....	231
Materials and Methods	233
<i>Cell Culture</i>	233
<i>Isolation and Culture of Peripheral Blood Mononuclear cells (PBMCs)</i>	235
<i>Cell Treatment</i>	236
<i>WST-1 Assay for Cell Viability</i>	236
<i>Cell Death Analysis: Annexin V Binding Assay & Propidium Iodide (PI) Staining</i> ..	237
<i>Tetramethylrhodamine Methyl Ester (TMRM) Staining</i>	238
<i>Oxygen Consumption Quantitation</i>	238
<i>Mitochondrial Isolation</i>	239
<i>Treatment of Isolated Mitochondria & Evaluation of Apoptogenic Factor Release</i> . 240	
<i>Western Blot Analyses</i>	240
<i>Quantitation of Reactive Oxygen Species (ROS)</i>	241
<i>Statistical Analysis</i>	242
Results	243
<i>SVTH-6 Selectively Induces Cytotoxicity in Cancer Cells with Greater Efficacy than JCTH-4</i>	243
<i>PL Enhances Cytotoxicity in Selectively in Cancer Cells</i>	245
<i>Selective Induction of Cell Death in Cancer Cells by SVTH-6 is Enhanced with PL</i> 247	
<i>PL Selectively Enhances Mitochondrial Membrane Potential (MMP) Dissipation by SVTH-6 in Cancer Cells</i>	249
<i>PL Enhances Mitochondrial Dysfunction by SVTH-6</i>	251
<i>Enhancement of SVTH-6 Anti-Cancer Activity by PL is Dependent on Oxidative Stress</i>	254
Discussion	256
Author Contributions	260
Acknowledgements	260
Grant Support	260

References	261
CHAPTER 6: General Discussion	267
List of Abbreviations	268
Conclusion.....	277
References	278
Appendices	281
Vita Auctoris	365

List of Figures

CHAPTER 1

Figure 1.1. Summary of Extrinsic and Intrinsic Apoptosis	6
Figure 1.2. Structure of Pancreatistatin (PST) and Narciclasine with the Proposed Minimum Anti-Cancer Pharmacophore	21
Figure 1.3. Structure of 7-deoxyPST and PST Analogues	24

CHAPTER 2

Figure 2.1. PST induces apoptosis in CRC cells and structural comparison to its synthetic 7-deoxy analogues	57
Figure 2.2. JCTH-4 induces apoptosis in CRC cells	58
Figure 2.3. JCTH-4 decreases viability of CRC cells in a time and dose-dependent manner	59
Figure 2.4. TAM enhances apoptosis-inducing activity of JCTH-4 selectively in CRC cells	61
Figure 2.5. TAM enhances viability decrease in CRC cells by JCTH-4	62
Figure 2.6. JCTH-4 induces phosphatidylserine externalization alone and in combination with TAM in CRC cells	63
Figure 2.7. JCTH-4 and TAM dissipate MMP in CRC cells	65
Figure 2.8. JCTH-4 and TAM increase ROS generation in isolated mitochondria from CRC cells	67
Figure 2.9. JCTH-4 and TAM cause release of apoptogenic factor Cyto c from isolated mitochondria in CRC cells	69
Figure 2.10. JCTH-4 induces apoptosis in CRC cells independent of caspases	71
Figure 2.11. JCTH-4 and TAM induce autophagy in CRC cells	74
Figure 2.12. Initial JCTH-4 treatment reduces resilience of CRC cells after drug removal	76

CHAPTER 3

Figure 3.1. Comparison of chemical structures	108
Figure 3.2. JCTH-4 causes selective cytotoxicity in OS cells in a time and dose-dependent manner	109
Figure 3.3. CC potentiates the cytotoxicity of JCTH-4 selectively in OS cells	110

Figure 3.4. JCTH-4 alone and in combination with CC yields apoptotic morphology in OS cells	112
Figure 3.5. JCTH-4 and CC do not yield apoptotic morphology in HOb and NFF cells	113
Figure 3.6. JCTH-4 alone and in combination with CC induces phosphatidylserine externalization in OS cells	114
Figure 3.7. JCTH-4 alone and with CC does not induce phosphatidylserine externalization in HOb and NFF cells	115
Figure 3.8. JCTH-4 dissipates MMP alone and in combination with CC in OS cells	117
Figure 3.9. JCTH-4 and CC do not dissipate MMP in HOb and NFF cells	118
Figure 3.10. JCTH-4 directly causes mitochondrial ROS production and release of apoptogenic factors independent of caspases	121
Figure 3.11. JCTH-4 induces autophagy in OS cells alone and with CC	125
Figure 3.12. JCTH-4 and CC do not induce autophagy in Hob and NFF cells	126

CHAPTER 4

Figure 4.1. Structure of PST and PST Analogues	166
Figure 4.2. PST Analogues have Selective and Potent Anti-Cancer Activity with Efficacy Surpassing Standard Chemotherapeutics and Natural PST	167
Figure 4.3. PST Analogues Induce Apoptosis Selectively in Cancer Cells	170
Figure 4.4. PST Analogues Cause Mitochondrial Dysfunction and Activate the Intrinsic Pathway of Apoptosis in Cancer Cells	174
Figure 4.5. PST Analogues Decrease Oxygen Consumption Capabilities of Cancer Cells	177
Figure 4.6. PST Analogue-Induced Apoptosis is Dependent on Functional Complex II and III of the Mitochondrial Electron Transport Chain	179
Figure 4.7. PST Analogues Selectively Induce Apoptosis in 3D Spheroid Models of Cancer	183
Figure 4.8. PST Analogues Decrease Growth of Tumors in Xenograft Mouse Models	186
Supplemental Figure S4.1A. PST Analogues & PST Decrease Viability of MV-4-11 Leukemia Cells in a Time and Dose Dependent Manner	200

Supplemental Figure S4.1B. Taxol Decreases Viability of MV-4-11 Leukemia Cells	201
Supplemental Figure S4.1C. PST Analogues & PST Decrease Viability of E6-1 Leukemia Cells in a Time and Dose Dependent Manner	202
Supplemental Figure S4.1D. PST Analogues & PST Decrease Viability of U-937 Leukemia Cells in a Dose Dependent Manner	203
Supplemental Figure S4.1E. PST Analogues Decrease Viability of MDA-MB-231 Triple Negative Breast Cancer Cells in a Dose Dependent Manner with Greater Efficacy than Taxol and Doxorubicin	204
Supplemental Figure S4.1F. PST Analogues & PST Decrease Viability of MDA-MB-468 Triple Negative Breast Cancer Cells in a Time and Dose Dependent Manner	205
Supplemental Figure S4.1G. Taxol and Doxorubicin Decrease Viability of MDA-MB-468 Triple Negative Breast Cancer Cells with Less Efficacy than PST Analogues	206
Supplemental Figure S4.1H. PST Analogues & PST Decrease Viability of SUM 149 Breast Cancer Cells in a Time and Dose Dependent Manner	207
Supplemental Figure S4.1I. PST Analogues & PST Decrease Viability of HCT 116 Colorectal Carcinoma Cells in a Time and Dose Dependent Manner	208
Supplemental Figure S4.1J. PST Analogues Decrease Viability of BxPC-3 Pancreatic Adenocarcinoma Cells in a Time and Dose Dependent Manner with Greater Efficacy than Gemcitabine (GEM) and Taxol	209
Supplemental Figure S4.1K. PST Analogues Decrease Viability of PANC-1 Pancreatic Cancer Cells in a Time and Dose Dependent Manner with Greater Efficacy than Gemcitabine (GEM)	210
Supplemental Figure S4.1L. PST Analogues Decrease Viability of Saos-2 Osteosarcoma Cells in a Time and Dose Dependent Manner	211
Supplemental Figure S4.1M. PST Analogues Decrease Viability of U-2 OS Osteosarcoma Cells in a Time and Dose Dependent Manner	212
Supplemental Figure S4.1N. PST Analogues & PST Decrease Viability of U-87 MG Glioblastoma Cells in a Time and Dose Dependent Manner with Greater Efficacy than Taxol	213

Supplemental Figure S4.1O. PST Analogues Decrease Viability of G-361 Malignant Melanoma Cells in a Time and Dose Dependent Manner	214
Supplemental Figure S4.1P. PST Analogues Decrease Viability of OVCAR-3 Ovarian Adenocarcinoma Cells in a Time and Dose Dependent Manner	215
Supplemental Figure S4.1Q. PST Analogues Decrease Viability of NCI-H23 Non-Small Cell Lung Cancer Cells in a Time and Dose Dependent Manner with Greater Efficacy than Cisplatin and Gemcitabine	216
Supplemental Figure S4.1R. PST Analogues Decrease Viability of A549 Non-Small Cell Lung Cancer Cells in a Dose Dependent Manner	217
Supplemental Figure S4.1S. PST Analogues & PST Decrease Viability of MCF7 Breast Cancer Cells in a Time and Dose Dependent Manner	218
Supplemental Figure S4.1T. PST Analogues Decrease Viability of DU-145 Prostate Carcinoma Cells in a Dose Dependent Manner	219
Supplemental Figure S4.1U. PST Analogues & PST have Minimal Toxicity on AG09309 Normal Human Fibroblasts	220
Supplemental Figure S4.1V. PST Analogues & PST have Minimal Toxicity on CCD-18Co Normal Colon Fibroblasts	221
Supplemental Figure S4.2. PST Analogues & PST Induce Apoptosis Selectively in Cancer Cells: Minimal Induction of Apoptosis was Induced in Non-Cancerous Peripheral Blood Mononuclear Cells	222
Supplemental Figure S4.3A. PST Analogues & PST Cause Mitochondrial Membrane Potential (MMP) Collapse in a Time Dependent Manner in MV-4-11 Leukemia Cells	223
Supplemental Figure S4.3B. PST Analogues & PST Cause Mitochondrial Membrane Potential (MMP) Collapse in a Time Dependent Manner in E6-1 Leukemia Cells	224
Supplemental Figure S4.4. PST Analogues Induce Apoptosis in MV-4-11 Leukemia Cells in a Partial Caspase-Dependent Manner	225
Supplemental Figure S4.5. PST Analogue-Induced Apoptosis is not Dependent on Functional Complex I of the Mitochondrial Electron Transport Chain	226
Supplemental Figure S4.6. PST Analogues Do not Evidently Affect Tubulin Polymerization	227

CHAPTER 5

Figure 5.1. SVTH-6 Selectively Induces Cytotoxicity in Cancer Cells with Greater Efficacy than JCTH-4	244
Figure 5.2. PL Enhances Cytotoxicity in Selectively in Cancer Cells	246
Figure 5.3. Selective Induction of Cell Death in Cancer Cells by SVTH-6 is Enhanced with PL	248
Figure 5.4. PL Selectively Enhances Mitochondrial Membrane Potential (MMP) Dissipation by SVTH-6 in Cancer Cells	250
Figure 5.5. PL Enhances Mitochondrial Dysfunction by SVTH-6	253
Figure 5.6. Enhancement of SVTH-6 Anti-Cancer Activity by PL is Dependent on Oxidative Stress	255

CHAPTER 6

Figure 6.1. Structure of PST and Synthetic PST Analogues	270
--	-----

List of Appendices

APPENDIX A

Induction of Apoptosis and Autophagy in Human Pancreatic Cancer Cells
by a Novel Synthetic C-1 Analogue of 7-deoxypancratistatin 281

APPENDIX B

Enhancement of Apoptotic and Autophagic Induction by a Novel
Synthetic C-1 Analogue of 7-deoxypancratistatin in Human Breast
Adenocarcinoma and Neuroblastoma Cells with Tamoxifen 316

APPENDIX C

Copyright Transfer Agreement Forms 356

CHAPTER 1: General Introduction

List of Abbreviations

7-deoxyPST	7-deoxypancratistatin
AIF	apoptosis inducing factor
AK2	adenylate kinase 2
ANT	adenine nucleotide translocase
Apaf1	apoptotic peptidase activating factor 1
BH	Bcl-2 homology
CAD	caspase-activated DNase
Cyto c	cytochrome c
DCA	dichloroacetate
DIABLO	direct IAP binding protein with low pI
DISC	death-inducing signalling complex
EndoG	endonuclease G
ETC	electron transport chain
FADD	Fas associated death domain
GSTP1	glutathione S-transferase pi 1
IAP	inhibitor of apoptosis
ICAD	inhibitor of caspase-activated DNase
MMP	mitochondrial membrane potential
MnSOD	manganese-containing superoxide dismutase
PDH	pyruvate dehydrogenase
PDK	pyruvate dehydrogenase kinase
PST	pancratistatin

PTP	permeability transition pore
ROS	reactive oxygen species
SAR	structure activity relationship
SMAC	second mitochondrial activator of caspases
tBid	truncated Bid
VDAC	voltage-dependent anion channel

Cancer

Cancer is a disease characterized by uncontrolled growth and proliferation of cells of the affected organism, which in turn can disrupt normal functioning of tissues and organs (Fearon 1997). In 2012, it was a leading cause of death in the world claiming 8.2 million lives with an estimated 14.1 million new cases; most common cancers diagnosed include lung with 1.82 million cases, breast with 1.67 million, and colorectal with 1.36 million (Ferlay et al. 2014).

Mounting evidence suggests that tumorigenesis, or the development of cancer, is a process of successive accumulation of genetic alterations that results in progressive transformation of cells to a neoplastic phenotype (Renan 1993; FOULDS 1954; Bergers et al. 1998). Undergoing Darwinian evolution, advantageous genetic modifications for growth and survival in cells are selected and propagated. Selected genetic changes disrupt regulatory circuits that normally regulate cell homeostasis and proliferation and give rise to acquired capabilities, which are proposed to be mutually observed in most and possibly all types of cancer (Hanahan & Weinberg 2000). These hallmarks of cancer include: self-sufficiency in growth signals, evasion of growth suppressors, sustained angiogenesis, infinite replicative potential, tissue invasion and metastasis, reprogramming of energy metabolism, escape from immune destruction, and resistance to apoptosis (Hanahan & Weinberg 2000; Hanahan & Weinberg 2011). This dissertation will heavily focus on apoptosis evasion, and explore various tactics to overcome defects in cell death programming in cancer cells.

Apoptosis

Apoptosis or type I programmed cell death is a naturally occurring physiological phenomenon of the body (Green & Reed 1998). This process is characterized by membrane blebbing, chromatin condensation, DNA fragmentation, and the formation of membrane bound cell fragments called apoptotic bodies (Kerr et al. 1972; Fink & Cookson 2005). Furthermore, the characteristic flipping of phosphatidylserine from the inner to outer leaflet of the plasma membrane during apoptosis facilitates recognition and subsequent engulfment of apoptotic bodies by phagocytes (Fadok et al. 1998). Thus, apoptosis is a mechanism that allows cells to perish in a controlled manner without affecting cells in neighbouring environments (Kerr et al. 1972; Wyllie et al. 1980). In contrast, necrosis is a form of cell death characterized by cell swelling, plasma membrane rupture, and lysis that can lead to inflammation (Fink & Cookson 2005).

Extrinsic and Intrinsic Apoptosis

The two main modalities of apoptosis include the extrinsic and intrinsic pathways, which are distinguished by the location of initiation; the extrinsic pathway requires an external stimulus while the intrinsic pathway is triggered by an intracellular stress (Fulda & Debatin 2006). Extrinsic and intrinsic apoptosis are summarized in **Figure 1.1**. These two pathways can involve a family of cysteine proteases known as caspases.

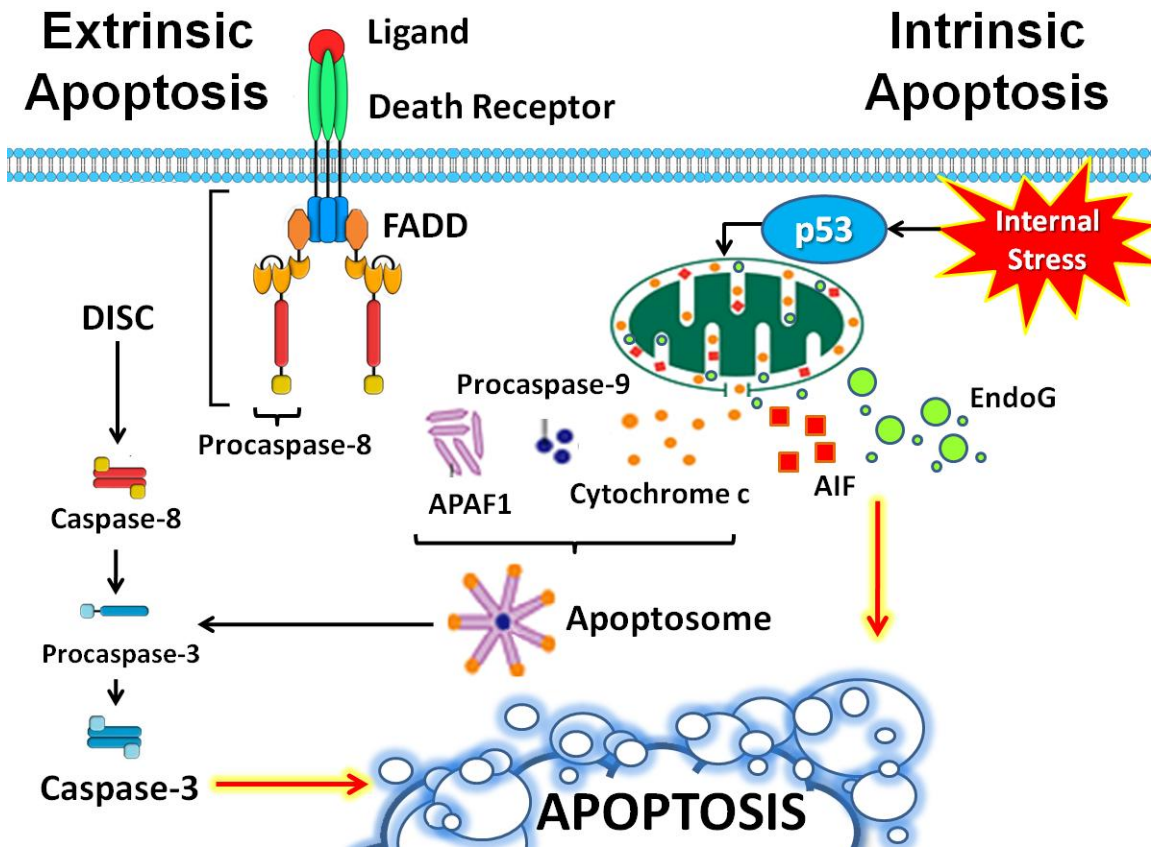


Figure 1.1 Summary of Extrinsic and Intrinsic Apoptosis

When a death-promoting stimulus is absent, these proteases exist as inactive zymogens. Upon activation of apoptosis, these precursors are proteolytically cleaved to their active forms (Degterev et al. 2003). Caspases can be further classified as initiator or executioner caspases. Initiator caspases, which include caspase-2, -8, -9, and -10, are autoproteolytically cleaved upon activation of apoptosis by an external or intracellular stimulus and relay this apoptotic signal to executioner caspases. Executioner caspases include caspase-3, -6, and -7, which are cleaved and activated by initiator caspases. Once active, executioner caspases cleave a multitude of proteins involved in various cellular functions, including structural stability and survival, to exert their lethal effects on cells (Fischer et al. 2003). One such protein is inhibitor of caspase-activated DNase (ICAD), which inhibits caspase-activated DNase (CAD). Upon executioner caspase cleavage of ICAD, CAD is no longer inhibited and free to translocate to the nucleus, where it fragments DNA (Enari et al. 1998).

The extrinsic pathway of apoptosis is a receptor mediated process in which a death ligand binds to its corresponding death receptor. A number of death receptors exist and include CD95/Fas/Apo1, TNFR1, TNFR2, DR3/Wsl-1/Tramp, DR4/TRAIL-R1, DR5/TRAIL-R2/TRICK2/Killer, and DR6 (Degterev et al. 2003). Upon ligand binding, the receptor oligomerizes and associates with proteins in the cytosol to form the death-inducing signalling complex (DISC) (Ashkenazi & Dixit 1998). This complex is composed of the intracellular domain of the death receptor, the Fas associated death domain (FADD) adaptor protein, and procaspase-8/10. Once assembled, procaspase-8/10 is cleaved to caspase-

8/10. Caspase-8/10 activates caspase-3, -6, and/or -7, which then execute apoptosis. Caspase-8/10 can also cleave the protein Bid, yielding truncated Bid (tBid), which promotes oligomerization of pro-apoptotic Bax protein and mitochondrial membrane potential collapse and subsequent apoptotic execution (Kim et al. 2009; Roucou et al. 2002). Thus, there is crosstalk between the extrinsic and intrinsic pathway of apoptosis.

In contrast to the extrinsic pathway of apoptosis, the intrinsic pathway is elicited by internal stress, such as DNA damage and oxidative stress (Fulda & Debatin 2006). Following this initial stress, mitochondrial permeabilization is induced, causing apoptogenic factor release from the mitochondrial intermembrane space to the cytosol. This release can subsequently lead to direct or indirect execution of apoptosis (Debatin et al. 2002).

Apoptogenic Factors

The apoptogenic factor cytochrome c (Cyto c) normally plays an active role in mitochondrial oxidative phosphorylation, facilitating the transfer of electrons between complex III and IV of the electron transport chain (Ow et al. 2008). However, once released into the cytosol, it assembles with apoptotic peptidase activating factor 1 (Apaf1) and procaspase-9, forming the apoptosome complex. The formation of this complex promotes the cleavage of procaspase-9 into active caspase-9 (Li et al. 1997), which subsequently activates caspase-3/6/7 (Enari et al. 1998). In contrast to this caspase-dependent induction of apoptosis, which indirectly triggers apoptosis through the successive activation of

initiator and executioner caspases, the apoptogenic factors apoptosis inducing factor (AIF) and endonuclease G (EndoG) can translocate to the nucleus to fragment DNA and execute apoptosis (Earnshaw 1999).

Additional apoptogenic factors are also housed and released upon mitochondrial membrane permeabilization. Second mitochondrial activator of caspases (SMAC)/direct IAP binding protein with low pI (DIABLO) release into the cytosol promotes Cyto c mediated apoptosis by binding and inhibiting inhibitor of apoptosis (IAP) proteins (Srinivasula et al. 2001). One such protein is XIAP, which acts to inhibit caspase-3, -7, and -9 (Scott et al. 2005; Srinivasula et al. 2001). HtrA/Omi serves as a chaperon and serine protease in the mitochondrial intermembrane space to degrade or facilitate proper folding of mitochondrial proteins (Vande Walle et al. 2008). Like SMAC/DIABLO, the serine protease HtrA2/Omi abolishes function of IAP proteins once released from the mitochondria, but through proteolytic degradation as opposed to allosteric inhibition (Yang et al. 2003; Srinivasula et al. 2003). Adenylate kinase 2 (AK2) acts to catalyze the interconversion of adenine nucleotides and maintain cellular energy homeostasis by relaying AMP levels to metabolic sensors (Dzeja & Terzic 2009). Upon release from the mitochondria, AK2 was found to form a complex with FADD and caspase-10, leading to activation of this initiator caspase and subsequent execution of apoptosis (Lee et al. 2007). Thus, the intrinsic pathway of apoptosis can facilitate crosstalk to the extrinsic pathway upon mitochondrial membrane permeabilization.

The Bcl-2 Family of Proteins

Mitochondrial outer membrane permeabilization is governed by the Bcl-2 family of proteins. Members of this family share at least one or more of the four Bcl-2 homology (BH) domains, which include BH1, BH2, BH3 and BH4, and can be either anti-apoptotic or pro-apoptotic by discouraging or promoting mitochondrial outer membrane permeabilization, respectively (Strasser 2005; Youle & Strasser 2008). BH1 and BH2 are present in all anti-apoptotic proteins, which include Bcl-2, Bcl-XL, Bcl-W, A1, Mcl-1 and Boo/Diva. The BH3 domain allows these proteins to dimerize with other members of the Bcl-2 family and is crucial for pro-apoptotic activity. Thus, this domain is present in all pro-apoptotic members of the Bcl-2 family of proteins, which include Bax, Bok, Bcl-X_s, Bak, Bcl-G_L, Bfk, Bad, Bik, Bid, Hrk, Bim, Noxa, Puma, and Bmf (Strasser 2005; Youle & Strasser 2008). The overall proportion of pro-apoptotic Bcl-2 family proteins to anti-apoptotic Bcl-2 family proteins present within the cell will dictate the stability of the mitochondrial outer membrane and cell fate (Green & Reed 1998; Tait & Green 2010). An increase in expression of pro-apoptotic Bcl-2 proteins by a death stimulus can be facilitated by the p53 tumor suppressor, which has been shown to transcriptionally activate Bax, Puma, Noxa, and Bid directly (Hemann & Lowe 2006). With insufficient anti-apoptotic proteins present to suppress the activity of pro-apoptotic proteins, the balance of Bcl-2 family of proteins is tipped in favor of apoptosis and mitochondrial outer membrane permeabilization occurs.

Mitochondrial Membrane Permeabilization

Two different mechanisms for the permeabilization of the mitochondrial outer membrane have been presented (Bouchier-Hayes et al. 2005). One involves the formation of pores composed of pro-apoptotic Bcl-2 family proteins on the mitochondrial outer membrane that allow cytotoxic proteins to be expelled from the mitochondrial intermembrane space (Kuwana et al. 2002). However, evidence supporting this mechanism is derived from cell-free system experiments that lack the intricacies of *in vitro* and *in vivo* models.

Alternatively, mitochondria can be permeabilized via the permeability transition pore (PTP) which spans the inner and outer mitochondrial membranes (Brenner & Grimm 2006). The three principle proteins of the permeability transition pore are voltage-dependent anion channel (VDAC) in the mitochondrial outer membrane, adenine nucleotide translocase (ANT) in the inner mitochondrial membrane, and cyclophilin D in the matrix (Kroemer et al. 2007). When the gate keeper protein cyclophilin D associates with ANT, it promotes PTP formation and opening, allowing an influx of water and solutes into the mitochondrial matrix (Schinzel et al. 2005; Bernardi 1999). Consequences of this influx include mitochondrial swelling, mitochondrial outer membrane rupture, release of apoptogenic factors from the mitochondrial intermembrane space, collapse of mitochondrial membrane potential (MMP), and uncoupling of oxidative phosphorylation (Bouchier-Hayes et al. 2005). Bax and Bak have been shown to facilitate this process and the release of apoptogenic factors by associating with VDAC (Shimizu et al. 1999; Narita et al. 1998). However, this

promotion of PTP opening can be prevented by the glycolytic enzyme, hexokinase, which has been demonstrated to associate with VDAC and prevent Bax binding to VDAC (Pastorino et al. 2002).

Interestingly, an isoform of hexokinase, hexokinase II, is overexpressed in a variety of tumor cells, which acts to satisfy the energetic needs of these highly glycolytic cells. In addition to fueling energy production, hexokinase II also plays a role in apoptosis evasion in cancer cells by binding to VDAC, and thus, preventing pro-apoptotic Bcl-2 proteins from interacting with VDAC and subsequent PTP opening (Pedersen et al. 2002). Consequently, inhibition of hexokinase II may provide therapeutic benefit as seen with the hexokinase II inhibitor 3-bromopyruvate *in vitro*; this inhibitor triggered hexokinase II dissociation from the mitochondria, mitochondrial release of AIF, and apoptosis (Chen et al. 2009). Like the overexpression of hexokinase II, a multitude of cellular modifications have been observed in cancer cells, which function to circumvent apoptosis programming and fuel proliferation in cancer cells. In the next few sections, some of these distinct features in cancer cells will be explored as well as potential opportunities for therapeutic intervention.

Evasion of Apoptosis by Cancer Cells

Apoptosis can occur physiologically during embryogenesis or as a safeguard against DNA damage (Kerr et al. 1972; Wyllie et al. 1980). Under such normal circumstances, this process is tightly regulated. However, apoptosis and its associated programming can be pathologically altered in various disease

states (Brown & Attardi 2005). As mentioned previously, a hallmark or acquired trait of cancer cells is their ability to evade apoptosis (Hanahan & Weinberg 2000). As with other acquired advantages of cancer cells, the ability to cheat death is the result of various genetic alterations through mutations or epigenetic modifications (Berdasco & Esteller 2010). Through these changes, neoplastic cells evolve a number of tactics to survive. The loss of TP53 tumor suppressor function is the most common method observed in cancer cells.

The p53 Tumor Suppressor

The *TP53* gene, which encodes the p53 protein, has been reported to be mutated or deleted in over 50 percent of human tumors (Hollstein et al. 1991). The p53 protein serves as a transcription factor for many genes responsible for DNA repair, cell cycle arrest, and apoptosis in response to a number of cellular stresses (Zilfou & Lowe 2009). In absence of cellular stress, inactivity of p53 is maintained by MDM2, which inhibits p53 transcriptional activity and marks p53 for degradation via ubiquitination (Toledo & Wahl 2006).

In response to hypoxia, oncogene activation, or DNA damage, p53 can promote apoptosis via transactivation of pro-apoptotic proteins such as Bax, Puma, and Noxa or induce senescence by transactivation of the p21 protein (Zilfou & Lowe 2009). p53 also acts as a transcription factor for extrinsic apoptosis death receptors 4 and 5, and thus, it can promote this cell death pathway (Ashkenazi & Dixit 1998). However, if such p53 safeguard mechanisms fail, potentially harmful mutations can persist and propagate, potentiating the

development of cancer. Therefore, it is not surprising that mutations in p53 are the most common type of mutation in human cancers, and if p53 is functional, MDM2 is commonly overexpressed to abolish its death promoting functions (Hollstein et al. 1991; Toledo & Wahl 2006).

As p53 plays vital roles in initiating apoptosis, functional reactivation of mutant p53 presents as an attractive approach to cancer therapy. Mutant p53 rescue has been explored by pharmacological manipulation via small molecules with some success *in vitro* and *in vivo* (Bullock & Fersht 2001; Bykov et al. 2009; Bykov & Wiman 2014). One lead compound, APR-246, was found to restore wildtype conformation in mutant p53, induce apoptosis in cancer cells, and inhibit the growth of tumors in mouse models (Bykov et al. 2002). As such, APR-246 was advanced to a Phase I/II clinical trial with promising findings (Lehmann et al. 2012); p53 target gene expression, cell cycle arrest, and apoptosis was observed in tumor cells from treated patients. Moreover, in cancers with wildtype p53 and overexpressed MDM2, small molecule inhibition of MDM2 has been explored with preclinical success (Zhao et al. 2015; Shangary & Wang 2009).

Metabolic Reprogramming in Cancer Cells

A distinct metabolic phenotype is observed in cancer cells, in which glycolysis dominates as the main source of energy production rather than ATP production in mitochondria, a phenomenon known as the Warburg effect (Warburg, 1956). In turn, this glycolytic phenotype and alteration of mitochondria provides a proliferative advantage and an acquired resistance to apoptosis

(DeBerardinis et al. 2008; Gogvadze et al. 2008; Gogvadze et al. 2010; Plas & Thompson 2002; Vander Heiden et al. 2009; Pastorino et al. 2002; Chen et al. 2010; Green & Kroemer 2004; Casellas et al. 2002). Therefore, exploitation of these distinct features in cancer cells may provide novel strategies for cancer therapy.

As with hexokinase II, cancer cells have elevated levels of various proteins that function to promote glycolysis and/or discourage mitochondrial oxidative phosphorylation. As a result, this decreases the likelihood of oxidative stress-induced apoptosis by limiting use of the electron transport chain, a prominent generator of reactive oxygen species (Rohlena et al. 2013). Thus, reversal of this shift in metabolic phenotype could be an effective therapeutic tactic. Pyruvate dehydrogenase (PDH) is a mitochondrial gate-keeping enzyme, which converts pyruvate to acetyl-CoA, permitting it to enter the Krebs cycle. PDH kinase (PDK) inhibits PDH and subsequent glucose oxidation in the mitochondria via phosphorylation. Common events involved in cancer progression, including loss of p53 (Contractor & Harris 2012) and hypoxia-inducible factor 1 α (HIF1 α) activation (Kim et al. 2006), can result in increased PDK expression. Thus, this aberrant expression of PDK presents itself as a potentially lucrative target in cancer cells. The small molecule dichloroacetate (DCA) is a well known inhibitor of PDK and has been used for many years as a therapeutic for lactic acidosis associated with inherited mitochondrial diseases (Bowker-Kinley et al. 1998; Knoechel et al. 2006; Stacpoole 1989). Interestingly, DCA-mediated inhibition of PDK has been shown to shift the metabolism of

pyruvate from lactate generation and glycolysis to mitochondria-based glucose oxidation (Bonnet et al. 2007). This shift in metabolic phenotype towards oxidative phosphorylation was accompanied by decreases in MMP, increases in mitochondrial H₂O₂, and activation of voltage-gated K⁺ channels in cancer cells. These cellular events lead to apoptosis induction and decreased proliferation of cancer cells *in vitro* as well as inhibition of tumor growth *in vivo*, in absence of any apparent toxicity (Bonnet et al. 2007). Pre-clinical and clinical work has shown that DCA alone may be effective against glioblastoma multiforme (Bonnet et al. 2007; Michelakis et al. 2010). Furthermore, as DCA releases cancer cells from an apoptosis resistant state, it may serve as a potent sensitizer of cancer cells to other chemotherapeutics. Despite these findings, effective *in vitro* concentrations of DCA are high and may not translate to a feasible dosage for patient consumption as a monotherapy (Bonnet et al. 2007).

Reactive Oxygen Species (ROS) Scavengers & Generators

It has been shown that cancer cells have higher basal levels of ROS (Szatrowski & Nathan 1991; Trachootham et al. 2006) and that high concentrations of ROS can be a driving force behind tumor progression (Petros et al. 2005). In the development of cancer, mutations of genes encoding mitochondrial electron transport chain (ETC) components can yield an increase in ROS generation (Wallace 2005). Disruptions in the ETC can lead to the improper transfer of a single electron to an O₂ molecule, forming a superoxide radical. Superoxide radicals are quickly converted to H₂O₂, by superoxide

dismutase, which can in turn diffuse to the nucleus and cause DNA damage and exacerbate genomic instability in cancer cells (Petros et al. 2005). However, when in excess, ROS levels can lead to DNA, protein, and cell membrane damage, ultimately resulting in cell death. In response to higher ROS levels, malignancies have been shown to overexpress ROS scavengers, including thioredoxin reductase-1 (Yoo et al. 2006), manganese-containing superoxide dismutase (MnSOD) (Hu et al. 2005) and glutathione S-transferase pi 1 (GSTP1) (Raj et al. 2011). This suggests an increased dependency on antioxidative enzymes by cancer cells to survive. Thus, agents targeting ROS scavengers, as with the GSPT1 targeting compound piperlongumine (Raj et al. 2011), or increasing ROS levels directly with various mitochondrial targeting agents may allow for selective cancer targeting (Ralph et al. 2006). Furthermore, a combination of complementary chemotherapeutics, such as those targeting ROS scavengers and those raising ROS levels, may be an effective therapeutic strategy (Schumacker 2006). This selective killing of cancer cells with small molecules targeting the cellular ROS stress response has been dubbed "oxycution" and is an emerging field in cancer therapeutics (Burgess 2011; Raj et al. 2011). Mitochondria, in the context of cancer, will be the subject of the following section, as they are the main generators of ROS.

Cancer Cell Mitochondria and Mitocans

Cancer mitochondria feature several distinct differences, in comparison to non-transformed cells, which may permit for cancer specific targeting (Gogvadze et al. 2008; Chen et al. 2010). The glycolytic phenotype of cancer cells creates an acidic cytosolic environment, contributing to mitochondria hyperpolarization. Invasiveness and apoptotic resistance has been associated with hyperpolarization of mitochondria (Heerdt et al. 2006). This feature may allow selective targeting of cancer cells. Anti-cancer agents may be devised such that they are processed into a positively charged molecule that can be selectively taken up into the highly negative internal environment of the mitochondrial matrix, which is the result of hyperpolarization. Similar to hexokinase II, various antiapoptotic proteins of the Bcl-2 family of proteins are highly expressed in cancer cells, which discourage mitochondrial membrane permeabilization (Green & Kroemer 2004; Casellas et al. 2002; Mathupala et al. 1997). Furthermore, as cancer cells are more susceptible to ROS insult, targeting ETC components could be an effective therapeutic tactic (Rohlena et al. 2013). Collectively, these cancer cell mitochondria-specific features provide a basis for targeting cancer cell mitochondria, and thus, cancer cells selectively.

Compounds that specifically target cancer cell mitochondria to induce mitochondrial dysfunction and apoptosis have been classified as mitocans (Chen et al. 2010; Ralph et al. 2006). These comprise of ETC inhibitors, mitochondrial PTP activators, mimetics of pro-apoptotic Bcl-2 proteins, and inhibitors of anti-apoptotic Bcl-2 proteins (Rohlena et al. 2013; Yip & Reed 2008; Adams & Cory

2007). These compounds are generally well tolerated by non-cancerous cells and are effective anti-cancer agents, as a monotherapy or as chemosensitizers (Neuzil et al. 2013).

Vitamin E Analogues

With growing interest in mitocans as selective anti-cancer agents, vitamin E analogues have been studied intensively. In particular, α -Tocopheryl succinate is able to selectively induce apoptosis in cancer cells by targeting mitochondria as shown in both *in vitro* and *in vivo* models (Zhao et al. 2009). This anti-cancer activity has been attributed to its ability to target complex II of the mitochondrial ETC at the ubiquinone binding site, causing ROS generation and mitochondrial dysfunction (Dong et al. 2008; Dong et al. 2009). Liposomal-based formulations and vitamin E analogues are being developed to optimize its therapeutic benefits (Dong et al. 2009; Neuzil et al.; Zhao et al. 2009).

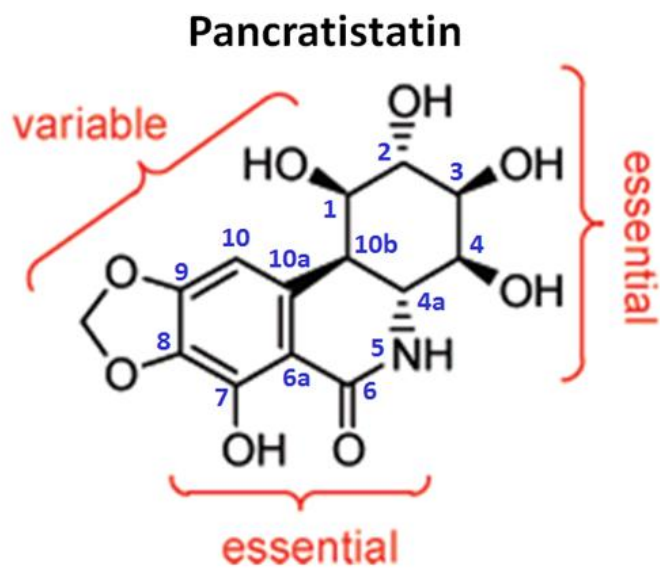
Taxol

Taxol, a common tubulin stabilizing chemotherapeutic isolated from the bark of the Pacific yew tree, was also found to target the mitochondria by interacting with the anti-apoptotic protein Bcl-2 (Ferlini et al. 2009). Furthermore, additional studies using isolated mitochondria demonstrated the ability of Taxol to promote free radical formation and mitochondrial membrane permeabilization, as indicated by the release of Cyto c (Varbiro et al. 2001). However, despite the ability of Taxol to target mitochondria, its side effects produced by its tubulin

targeting actions still remain problematic (Ferlini et al. 2009; Jordan & Wilson 2004). Using this drug at as a chemosensitizer at lower doses, taking advantage of its mitochondria targeting abilities, could limit its harmful effects at higher doses (Ferlini et al. 2009).

Pancreatistatin and Narciclasine

The Amaryllidaceae family of plants has been used in traditional medicine for the treatment of various diseases including cancer (Kornienko & Evidente 2008). One such plant is the *Hymenocallis littoralis* plant. To identify, characterize, and scientifically validate compounds responsible for these health benefits, components from the *Hymenocallis littoralis* plant were extracted and analyzed. Consequently, the natural compound pancreatistatin (PST) (**Figure 1.2**), was first extracted and characterized in 1984 from this plant (Pettit et al. 1984; Pettit et al. 2004). Our laboratory has shown PST to induce apoptosis in numerous cancer types including leukemia, breast cancer, human neuroblastoma, colorectal cancer, glioblastoma, prostate cancer, and melanoma cells without adverse effects to normal cells (Kekre et al. 2005; McLachlan et al. 2005; Siedlakowski et al. 2008; Griffin et al. 2010; Griffin, Karnik, et al. 2011; Griffin, McNulty, et al. 2011; Chatterjee et al. 2010). PST treatment was shown to target cancer cell mitochondria; it caused dissipation of MMP, ROS generation at early time points, and induction of apoptogenic factor release (McLachlan et al. 2005; Siedlakowski et al. 2008; Griffin, Karnik, et al. 2011).



Narciclasine

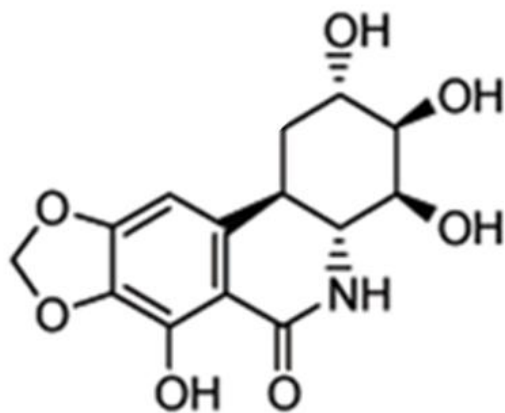


Figure 1.2. Structure of Pancreatistatin (PST) and Narciclasine with the Proposed Minimum Anti-Cancer Pharmacophore

Additionally, a synergistic anti-cancer effect was observed when PST was utilized with tamoxifen in human breast cancer cells, with no effect on normal breast fibroblast cells (Siedlakowski et al. 2008).

Tamoxifen is commonly used to treat estrogen receptor positive breast cancers (Baum 2005). It is understood that tamoxifen antagonizes the estrogen receptor to elicit its anti-cancer effects. However, other studies have provided evidence of additional targeting by tamoxifen autonomous of the estrogen receptor (Mandlekar & Kong 2001; Moreira et al. 2006). In particular, it has been demonstrated that tamoxifen interacts with Complex I of the mitochondrial respiratory chain at the flavin mononucleotide site (Moreira et al. 2006). The anti-cancer synergism with PST was found to be a result of mitochondrial targeting irrespective of the estrogen receptor (Siedlakowski et al. 2008). Similar findings were found in melanoma cells, as tamoxifen was demonstrated to sensitize the mitochondria of these cancer cells to dysfunction and permeabilization by PST (Chatterjee et al. 2010).

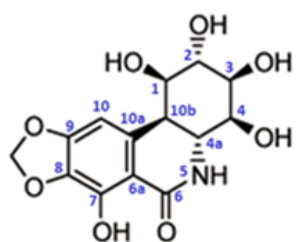
Another Amaryllidaceae alkaloid, narciclasine (**Figure 1.2**), is extracted from the *Narcissus tazetta* plant, a species of daffodil and a known modulator of plant growth (Kornienko & Evidente 2008). It is very similar in structure compared to PST, only lacking the hydroxyl group at the C-1 position. Narciclasine exhibits anti-cancer properties comparable to PST. Similarly, narciclasine has been shown to activate the intrinsic pathway of apoptosis, dependent on Cyto c release and caspase-9 activation in MCF7 breast cancer cells (Dumont et al. 2007). In contrast, the pro-apoptotic effects of narciclasine in PC-3 prostate

carcinoma cells was dependent on Fas and DR4 death receptor-mediated activation of caspase-8 (Dumont et al. 2007).

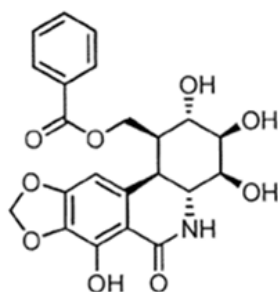
Synthetic Analogues of Pancratistatin

Despite having potent activity against a wide range of cancers, preclinical work on both PST and narciclasine has been hindered by the low availability of these compounds from their natural source. To circumvent this issue, various analogues of PST have been synthesized and subjected to structure activity relationship (SAR) analyses (Griffin et al. 2007; McNulty et al. 2008). Consequently, these studies have assisted in elucidating the minimum anti-cancer pharmacophore (**Figure 1.2**). These analogues, however, featured poorer anti-cancer activity when compared to natural PST.

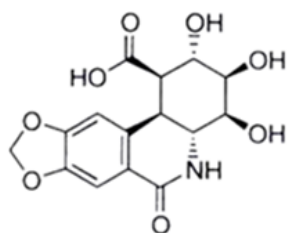
More recently, 7-deoxypancratistatin (7-deoxyPST) analogues were synthesized and screened for anti-cancer activity (Collins et al. 2010); these included JCTH-1, JCTH-2, JCTH-3, and JCTH-4 (**Figure 1.3**). Our preliminary work has shown JCTH-4 to have comparable anti-cancer activity compared to natural PST while JCTH-3 had limited activity (Collins et al. 2010). JCTH-1 and -2, however, had very minimal anti-cancer activity. This was the first time a PST analogue with the C-7 hydroxyl group absent was found to have substantial anti-cancer activity. Subsequently, additional PST analogues were designed and synthesized in an effort to find chemical modifications to maximize anti-cancer activity.



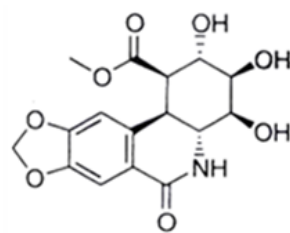
Pancratistatin (PST)



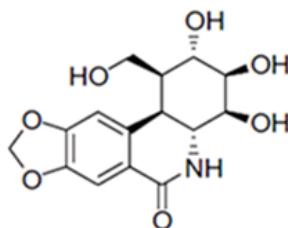
SVTH-7



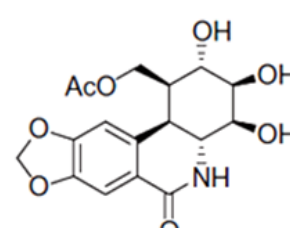
JCTH-1



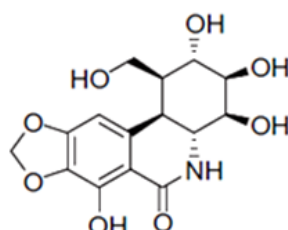
JCTH-2



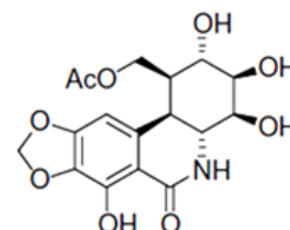
JCTH-3



JCTH-4



SVTH-5



SVTH-6

7-deoxyPST Analogues

Figure 1.3. Structure of 7-deoxyPST and PST Analogues

Analogues with the full proposed anti-cancer pharmacophore of PST and related alkaloids were made, which incorporated the hydroxyl group at the C-7 position (Vshyvenko et al. 2011). These included SVTH-5 and -6, the C-7 hydroxylated equivalents of JCTH-3 and -4, respectively, and the novel analogue SVTH-7 (**Figure 3**). This dissertation will collectively evaluate and characterize the anti-cancer activity of these novel 7-deoxyPST and PST analogues to assess their therapeutic potential.

Objectives

The evaluation of anti-cancer activity of synthetic 7-deoxyPST and PST analogues will be completed in this body of work, which include JCTH-1, JCTH-2, JCTH-3, JCTH-4, SVTH-5, SVTH-6, and SVTH-7. SAR analyses and characterization of anti-cancer activity will be carried out as outlined by the objectives listed below:

1. Evaluate 7-deoxyPST and PST analogues for selective anti-cancer activity in various two- and three-dimensional culture models of cancerous and non-cancerous cells
2. Evaluate the anti-cancer activity of these analogues *in vivo*
3. Characterize the mechanism of selective anti-cancer activity exhibited by these 7-deoxyPST and PST analogues
4. Evaluate the efficacy of these analogues in combination with other anti-cancer agents

The outcomes of this study will potentially identify novel compounds with therapeutic potential alone and in combination with other anti-cancer agents. Moreover, distinct features between cancer and non-cancerous cells may be identified and characterized. Such findings would provide a basis for better understanding cancer etiology that can be exploited to improve or design new therapeutic strategies.

References

- Adams, J.M. & Cory, S., 2007. The Bcl-2 apoptotic switch in cancer development and therapy. *Oncogene*, 26(9), pp.1324–37.
- Ashkenazi, A. & Dixit, V.M., 1998. Death receptors: signaling and modulation. *Science (New York, N.Y.)*, 281(5381), pp.1305–8.
- Baum, M., 2005. Adjuvant endocrine therapy in postmenopausal women with early breast cancer: where are we now? *European journal of cancer (Oxford, England : 1990)*, 41(12), pp.1667–77.
- Berdasco, M. & Esteller, M., 2010. Aberrant epigenetic landscape in cancer: how cellular identity goes awry. *Developmental cell*, 19(5), pp.698–711.
- Bergers, G., Hanahan, D. & Coussens, L.M., 1998. Angiogenesis and apoptosis are cellular parameters of neoplastic progression in transgenic mouse models of tumorigenesis. *The International journal of developmental biology*, 42(7), pp.995–1002.
- Bernardi, P., 1999. Mitochondrial Transport of Cations: Channels, Exchangers, and Permeability Transition. *Physiol Rev*, 79(4), pp.1127–1155.
- Bonnet, S. et al., 2007. A mitochondria-K⁺ channel axis is suppressed in cancer and its normalization promotes apoptosis and inhibits cancer growth. *Cancer cell*, 11(1), pp.37–51.
- Bouchier-Hayes, L., Lartigue, L. & Newmeyer, D.D., 2005. Mitochondria: pharmacological manipulation of cell death. *The Journal of clinical investigation*, 115(10), pp.2640–7.
- Bowker-Kinley, M.M. et al., 1998. Evidence for existence of tissue-specific

- regulation of the mammalian pyruvate dehydrogenase complex. *The Biochemical journal*, 329 (Pt 1, pp.191–6.
- Brenner, C. & Grimm, S., 2006. The permeability transition pore complex in cancer cell death. *Oncogene*, 25(34), pp.4744–56.
- Brown, J.M. & Attardi, L.D., 2005. The role of apoptosis in cancer development and treatment response. *Nature reviews. Cancer*, 5(3), pp.231–7.
- Bullock, A.N. & Fersht, A.R., 2001. Rescuing the function of mutant p53. *Nature reviews. Cancer*, 1(1), pp.68–76.
- Burgess, D.J., 2011. Therapy: selective oxycution? *Nature reviews. Cancer*, 11(9), pp.622–3.
- Bykov, V.J.N. et al., 2009. Mutant p53 rescue and modulation of p53 redox state. *Cell cycle (Georgetown, Tex.)*, 8(16), pp.2509–17.
- Bykov, V.J.N. et al., 2002. Restoration of the tumor suppressor function to mutant p53 by a low-molecular-weight compound. *Nature medicine*, 8(3), pp.282–8.
- Bykov, V.J.N. & Wiman, K.G., 2014. Mutant p53 reactivation by small molecules makes its way to the clinic. *FEBS letters*, 588(16), pp.2622–7.
- Casellas, P., Galiegue, S. & Basile, A.S., 2002. Peripheral benzodiazepine receptors and mitochondrial function. *Neurochemistry international*, 40(6), pp.475–86.
- Chatterjee, S.J., McNulty, J. & Pandey, S., 2010. Sensitization of human melanoma cells by tamoxifen to apoptosis induction by pancratistatin, a nongenotoxic natural compound. *Melanoma research*.
- Chen, G. et al., 2010. Preferential killing of cancer cells with mitochondrial

- dysfunction by natural compounds. *Mitochondrion*, 10(6), pp.614–25.
- Chen, Z. et al., 2009. Role of mitochondria-associated hexokinase II in cancer cell death induced by 3-bromopyruvate. *Biochimica et biophysica acta*, 1787(5), pp.553–60.
- Collins, J. et al., 2010. Chemoenzymatic synthesis of Amaryllidaceae constituents and biological evaluation of their C-1 analogues. The next generation synthesis of 7-deoxypancratistatin and trans-dihydrolycoricidine. *The Journal of organic chemistry*, 75(9), pp.3069–84.
- Contractor, T. & Harris, C.R., 2012. p53 negatively regulates transcription of the pyruvate dehydrogenase kinase Pdk2. *Cancer research*, 72(2), pp.560–7.
- Debatin, K.-M., Poncet, D. & Kroemer, G., 2002. Chemotherapy: targeting the mitochondrial cell death pathway. *Oncogene*, 21(57), pp.8786–803.
- DeBerardinis, R.J. et al., 2008. The biology of cancer: metabolic reprogramming fuels cell growth and proliferation. *Cell metabolism*, 7(1), pp.11–20.
- Degtarev, A., Boyce, M. & Yuan, J., 2003. A decade of caspases. *Oncogene*, 22(53), pp.8543–67.
- Dong, L.-F. et al., 2008. Alpha-tocopheryl succinate induces apoptosis by targeting ubiquinone-binding sites in mitochondrial respiratory complex II. *Oncogene*, 27(31), pp.4324–35.
- Dong, L.-F. et al., 2009. Suppression of tumor growth in vivo by the mitocan alpha-tocopheryl succinate requires respiratory complex II. *Clinical cancer research: an official journal of the American Association for Cancer Research*, 15(5), pp.1593–600.

- Dumont, P. et al., 2007. The Amaryllidaceae isocarbostryl narciclasine induces apoptosis by activation of the death receptor and/or mitochondrial pathways in cancer cells but not in normal fibroblasts. *Neoplasia (New York, N.Y.)*, 9(9), pp.766–76.
- Dzeja, P. & Terzic, A., 2009. Adenylate kinase and AMP signaling networks: metabolic monitoring, signal communication and body energy sensing. *International journal of molecular sciences*, 10(4), pp.1729–72.
- Earnshaw, W.C., 1999. Apoptosis. A cellular poison cupboard. *Nature*, 397(6718), pp.387, 389.
- Enari, M. et al., 1998. A caspase-activated DNase that degrades DNA during apoptosis, and its inhibitor ICAD. *Nature*, 391(6662), pp.43–50.
- Fadok, V.A. et al., 1998. The role of phosphatidylserine in recognition of apoptotic cells by phagocytes. *Cell death and differentiation*, 5(7), pp.551–62.
- Fearon, E.R., 1997. Human cancer syndromes: clues to the origin and nature of cancer. *Science (New York, N.Y.)*, 278(5340), pp.1043–50.
- Ferlay, J. et al., 2014. Cancer incidence and mortality worldwide: sources, methods and major patterns in GLOBOCAN 2012. *International journal of cancer. Journal international du cancer*, 136(5), pp.E359–86.
- Ferlini, C. et al., 2009. Paclitaxel directly binds to Bcl-2 and functionally mimics activity of Nur77. *Cancer research*, 69(17), pp.6906–14.
- Fink, S.L. & Cookson, B.T., 2005. Apoptosis, pyroptosis, and necrosis: mechanistic description of dead and dying eukaryotic cells. *Infection and*

- immunity*, 73(4), pp.1907–16.
- Fischer, U., Jänicke, R.U. & Schulze-Osthoff, K., 2003. Many cuts to ruin: a comprehensive update of caspase substrates. *Cell death and differentiation*, 10(1), pp.76–100.
- FOULDS, L., 1954. The experimental study of tumor progression: a review. *Cancer research*, 14(5), pp.327–39.
- Fulda, S. & Debatin, K.-M., 2006. Extrinsic versus intrinsic apoptosis pathways in anticancer chemotherapy. *Oncogene*, 25(34), pp.4798–811.
- Gogvadze, V., Orrenius, S. & Zhivotovsky, B., 2008. Mitochondria in cancer cells: what is so special about them? *Trends in cell biology*, 18(4), pp.165–73.
- Gogvadze, V., Zhivotovsky, B. & Orrenius, S., 2010. The Warburg effect and mitochondrial stability in cancer cells. *Molecular aspects of medicine*, 31(1), pp.60–74.
- Green, D.R. & Kroemer, G., 2004. The pathophysiology of mitochondrial cell death. *Science (New York, N.Y.)*, 305(5684), pp.626–9.
- Green, D.R. & Reed, J.C., 1998. Mitochondria and apoptosis. *Science (New York, N.Y.)*, 281(5381), pp.1309–12.
- Griffin, C. et al., 2010. Pancratistatin induces apoptosis in clinical leukemia samples with minimal effect on non-cancerous peripheral blood mononuclear cells. *Cancer cell international*, 10, p.6.
- Griffin, C., Karnik, A., et al., 2011. Pancratistatin selectively targets cancer cell mitochondria and reduces growth of human colon tumor xenografts. *Molecular cancer therapeutics*, 10(1), pp.57–68.

- Griffin, C. et al., 2007. Selective cytotoxicity of pancratistatin-related natural Amaryllidaceae alkaloids: evaluation of the activity of two new compounds. *Cancer cell international*, 7, p.10.
- Griffin, C., McNulty, J. & Pandey, S., 2011. Pancratistatin induces apoptosis and autophagy in metastatic prostate cancer cells. *International journal of oncology*, 38(6), pp.1549–56.
- Hanahan, D. & Weinberg, R.A., 2011. Hallmarks of cancer: the next generation. *Cell*, 144(5), pp.646–74.
- Hanahan, D. & Weinberg, R.A., 2000. The hallmarks of cancer. *Cell*, 100(1), pp.57–70.
- Heerdt, B.G., Houston, M.A. & Augenlicht, L.H., 2006. Growth properties of colonic tumor cells are a function of the intrinsic mitochondrial membrane potential. *Cancer research*, 66(3), pp.1591–6.
- Vander Heiden, M.G., Cantley, L.C. & Thompson, C.B., 2009. Understanding the Warburg effect: the metabolic requirements of cell proliferation. *Science (New York, N.Y.)*, 324(5930), pp.1029–33.
- Hemann, M.T. & Lowe, S.W., 2006. The p53-Bcl-2 connection. *Cell death and differentiation*, 13(8), pp.1256–9.
- Hollstein, M. et al., 1991. p53 mutations in human cancers. *Science (New York, N.Y.)*, 253(5015), pp.49–53.
- Hu, Y. et al., 2005. Mitochondrial manganese-superoxide dismutase expression in ovarian cancer: role in cell proliferation and response to oxidative stress. *The Journal of biological chemistry*, 280(47), pp.39485–92.

- Jordan, M.A. & Wilson, L., 2004. Microtubules as a target for anticancer drugs. *Nature Reviews Cancer*, 4(4), pp.253–265.
- Kekre, N. et al., 2005. Pancreatistatin causes early activation of caspase-3 and the flipping of phosphatidyl serine followed by rapid apoptosis specifically in human lymphoma cells. *Cancer chemotherapy and pharmacology*, 56(1), pp.29–38.
- Kerr, J.F., Wyllie, A.H. & Currie, A.R., 1972. Apoptosis: a basic biological phenomenon with wide-ranging implications in tissue kinetics. *British journal of cancer*, 26(4), pp.239–57.
- Kim, H. et al., 2009. Stepwise activation of BAX and BAK by tBID, BIM, and PUMA initiates mitochondrial apoptosis. *Molecular cell*, 36(3), pp.487–99.
- Kim, J. et al., 2006. HIF-1-mediated expression of pyruvate dehydrogenase kinase: a metabolic switch required for cellular adaptation to hypoxia. *Cell metabolism*, 3(3), pp.177–85.
- Knoechel, T.R. et al., 2006. Regulatory roles of the N-terminal domain based on crystal structures of human pyruvate dehydrogenase kinase 2 containing physiological and synthetic ligands. *Biochemistry*, 45(2), pp.402–15.
- Kornienko, A. & Evidente, A., 2008. Chemistry, biology, and medicinal potential of narciclasine and its congeners. *Chemical reviews*, 108(6), pp.1982–2014.
- Kroemer, G., Galluzzi, L. & Brenner, C., 2007. Mitochondrial membrane permeabilization in cell death. *Physiological reviews*, 87(1), pp.99–163.
- Kuwana, T. et al., 2002. Bid, Bax, and lipids cooperate to form supramolecular openings in the outer mitochondrial membrane. *Cell*, 111(3), pp.331–42.

- Lee, H.-J. et al., 2007. AK2 activates a novel apoptotic pathway through formation of a complex with FADD and caspase-10. *Nature cell biology*, 9(11), pp.1303–10.
- Lehmann, S. et al., 2012. Targeting p53 in vivo: a first-in-human study with p53-targeting compound APR-246 in refractory hematologic malignancies and prostate cancer. *Journal of clinical oncology: official journal of the American Society of Clinical Oncology*, 30(29), pp.3633–9.
- Li, P. et al., 1997. Cytochrome c and dATP-dependent formation of Apaf-1/caspase-9 complex initiates an apoptotic protease cascade. *Cell*, 91(4), pp.479–89.
- Mandlekar, S. & Kong, A.N., 2001. Mechanisms of tamoxifen-induced apoptosis. *Apoptosis: an international journal on programmed cell death*, 6(6), pp.469–77.
- Mathupala, S.P., Rempel, A. & Pedersen, P.L., 1997. Aberrant glycolytic metabolism of cancer cells: a remarkable coordination of genetic, transcriptional, post-translational, and mutational events that lead to a critical role for type II hexokinase. *Journal of bioenergetics and biomembranes*, 29(4), pp.339–43.
- McLachlan, A. et al., 2005. Pancratistatin: a natural anti-cancer compound that targets mitochondria specifically in cancer cells to induce apoptosis. *Apoptosis: an international journal on programmed cell death*, 10(3), pp.619–30.
- McNulty, J. et al., 2008. synthesis and biological evaluation of fully functionalized

- seco-pancratistatin analogues. *Journal of natural products*, 71(3), pp.357–63.
- Michelakis, E.D. et al., 2010. Metabolic modulation of glioblastoma with dichloroacetate. *Science translational medicine*, 2(31), p.31ra34.
- Moreira, P.I. et al., 2006. Tamoxifen and estradiol interact with the flavin mononucleotide site of complex I leading to mitochondrial failure. *The Journal of biological chemistry*, 281(15), pp.10143–52.
- Narita, M. et al., 1998. Bax interacts with the permeability transition pore to induce permeability transition and cytochrome c release in isolated mitochondria. *Proceedings of the National Academy of Sciences of the United States of America*, 95(25), pp.14681–6.
- Neuzil, J. et al., 2013. Classification of mitocans, anti-cancer drugs acting on mitochondria. *Mitochondrion*, 13(3), pp.199–208.
- Neuzil, J. et al., Vitamin E analogues as a novel group of mitocans: anti-cancer agents that act by targeting mitochondria. *Molecular aspects of medicine*, 28(5-6), pp.607–45.
- Ow, Y.-L.P. et al., 2008. Cytochrome c: functions beyond respiration. *Nature reviews. Molecular cell biology*, 9(7), pp.532–42.
- Pastorino, J.G., Shulga, N. & Hoek, J.B., 2002. Mitochondrial binding of hexokinase II inhibits Bax-induced cytochrome c release and apoptosis. *The Journal of biological chemistry*, 277(9), pp.7610–8.
- Pedersen, P.L. et al., 2002. Mitochondrial bound type II hexokinase: a key player in the growth and survival of many cancers and an ideal prospect for

- therapeutic intervention. *Biochimica et biophysica acta*, 1555(1-3), pp.14–20.
- Petros, J.A. et al., 2005. mtDNA mutations increase tumorigenicity in prostate cancer. *Proceedings of the National Academy of Sciences of the United States of America*, 102(3), pp.719–24.
- Pettit, G. et al., 1984. Isolation and structure of pancratistatin. *Journal of the Chemical Society, Chemical Communications*, (24).
- Pettit, G.R., Melody, N. & Herald, D.L., 2004. Antineoplastic agents. 511. Direct phosphorylation of phenpanstatin and pancratistatin. *Journal of natural products*, 67(3), pp.322–7.
- Plas, D.R. & Thompson, C.B., 2002. Cell metabolism in the regulation of programmed cell death. *Trends in endocrinology and metabolism: TEM*, 13(2), pp.75–8.
- Raj, L. et al., 2011. Selective killing of cancer cells by a small molecule targeting the stress response to ROS. *Nature*, 475(7355), pp.231–4.
- Ralph, S.J. et al., 2006. Mitocans: mitochondrial targeted anti-cancer drugs as improved therapies and related patent documents. *Recent patents on anti-cancer drug discovery*, 1(3), pp.327–46.
- Renan, M.J., 1993. How many mutations are required for tumorigenesis? Implications from human cancer data. *Molecular carcinogenesis*, 7(3), pp.139–46.
- Rohlana, J., Dong, L.-F. & Neuzil, J., 2013. Targeting the mitochondrial electron transport chain complexes for the induction of apoptosis and cancer treatment. *Current pharmaceutical biotechnology*, 14(3), pp.377–89.

- Roucou, X. et al., 2002. Bax oligomerization in mitochondrial membranes requires tBid (caspase-8-cleaved Bid) and a mitochondrial protein. *The Biochemical journal*, 368(Pt 3), pp.915–21.
- Schinzel, A.C. et al., 2005. Cyclophilin D is a component of mitochondrial permeability transition and mediates neuronal cell death after focal cerebral ischemia. *Proceedings of the National Academy of Sciences of the United States of America*, 102(34), pp.12005–10.
- Schumacker, P.T., 2006. Reactive oxygen species in cancer cells: live by the sword, die by the sword. *Cancer cell*, 10(3), pp.175–6.
- Scott, F.L. et al., 2005. XIAP inhibits caspase-3 and -7 using two binding sites: evolutionarily conserved mechanism of IAPs. *The EMBO journal*, 24(3), pp.645–55.
- Shangary, S. & Wang, S., 2009. Small-molecule inhibitors of the MDM2-p53 protein-protein interaction to reactivate p53 function: a novel approach for cancer therapy. *Annual review of pharmacology and toxicology*, 49, pp.223–41.
- Shimizu, S., Narita, M. & Tsujimoto, Y., 1999. Bcl-2 family proteins regulate the release of apoptogenic cytochrome c by the mitochondrial channel VDAC. *Nature*, 399(6735), pp.483–7.
- Siedlakowski, P. et al., 2008. Synergy of Pancreatistatin and Tamoxifen on breast cancer cells in inducing apoptosis by targeting mitochondria. *Cancer biology & therapy*, 7(3), pp.376–84.
- Srinivasula, S.M. et al., 2001. A conserved XIAP-interaction motif in caspase-9

- and Smac/DIABLO regulates caspase activity and apoptosis. *Nature*, 410(6824), pp.112–6.
- Srinivasula, S.M. et al., 2003. Inhibitor of apoptosis proteins are substrates for the mitochondrial serine protease Omi/HtrA2. *The Journal of biological chemistry*, 278(34), pp.31469–72.
- Stacpoole, P.W., 1989. The pharmacology of dichloroacetate. *Metabolism: clinical and experimental*, 38(11), pp.1124–44.
- Strasser, A., 2005. The role of BH3-only proteins in the immune system. *Nature reviews. Immunology*, 5(3), pp.189–200.
- Szatrowski, T.P. & Nathan, C.F., 1991. Production of large amounts of hydrogen peroxide by human tumor cells. *Cancer research*, 51(3), pp.794–8.
- Tait, S.W.G. & Green, D.R., 2010. Mitochondria and cell death: outer membrane permeabilization and beyond. *Nature reviews. Molecular cell biology*, 11(9), pp.621–32.
- Toledo, F. & Wahl, G.M., 2006. Regulating the p53 pathway: in vitro hypotheses, in vivo veritas. *Nature reviews. Cancer*, 6(12), pp.909–23.
- Trachootham, D. et al., 2006. Selective killing of oncogenically transformed cells through a ROS-mediated mechanism by beta-phenylethyl isothiocyanate. *Cancer cell*, 10(3), pp.241–52.
- Varbiro, G. et al., 2001. Direct effect of Taxol on free radical formation and mitochondrial permeability transition. *Free radical biology & medicine*, 31(4), pp.548–58.
- Vshyvenko, S. et al., 2011. Synthesis of C-1 homologues of pancratistatin and

- their preliminary biological evaluation. *Bioorganic & medicinal chemistry letters*, 21(16), pp.4750–2.
- Wallace, D.C., 2005. A mitochondrial paradigm of metabolic and degenerative diseases, aging, and cancer: a dawn for evolutionary medicine. *Annual review of genetics*, 39, pp.359–407.
- Vande Walle, L., Lamkanfi, M. & Vandenabeele, P., 2008. The mitochondrial serine protease HtrA2/Omi: an overview. *Cell death and differentiation*, 15(3), pp.453–60.
- Warburg, O., 1956. On the origin of cancer cells. *Science (New York, N.Y.)*, 123(3191), pp.309–14.
- Wyllie, A.H., Kerr, J.F. & Currie, A.R., 1980. Cell death: the significance of apoptosis. *International review of cytology*, 68, pp.251–306.
- Yang, Q.-H. et al., 2003. Omi/HtrA2 catalytic cleavage of inhibitor of apoptosis (IAP) irreversibly inactivates IAPs and facilitates caspase activity in apoptosis. *Genes & development*, 17(12), pp.1487–96.
- Yip, K.W. & Reed, J.C., 2008. Bcl-2 family proteins and cancer. *Oncogene*, 27(50), pp.6398–406.
- Yoo, M.-H. et al., 2006. Thioredoxin reductase 1 deficiency reverses tumor phenotype and tumorigenicity of lung carcinoma cells. *The Journal of biological chemistry*, 281(19), pp.13005–8.
- Youle, R.J. & Strasser, A., 2008. The BCL-2 protein family: opposing activities that mediate cell death. *Nature reviews. Molecular cell biology*, 9(1), pp.47–59.

- Zhao, Y. et al., 2015. Small-molecule inhibitors of the MDM2-p53 protein-protein interaction (MDM2 Inhibitors) in clinical trials for cancer treatment. *Journal of medicinal chemistry*, 58(3), pp.1038–52.
- Zhao, Y., Neuzil, J. & Wu, K., 2009. Vitamin E analogues as mitochondria-targeting compounds: from the bench to the bedside? *Molecular nutrition & food research*, 53(1), pp.129–39.
- Zilfou, J.T. & Lowe, S.W., 2009. Tumor suppressive functions of p53. *Cold Spring Harbor perspectives in biology*, 1(5), p.a001883.

**CHAPTER 2: A Novel Synthetic C1 Analogue of 7-deoxypancratistatin
Induces Apoptosis in p53 Positive and Negative Human Colorectal Cancer
Cells by Targeting the Mitochondria: Enhancement of Activity by
Tamoxifen**

Dennis Ma¹, Phillip Tremblay¹, Kevinjeet Mahngar¹, Pardis Akbari-Asl¹, Jonathan Collins², Tomas Hudlicky², James McNulty³, and Siyaram Pandey^{1*}

^{1*}Department of Chemistry and Biochemistry, University of Windsor,
401 Sunset Avenue, Windsor, Ontario N9B 3P4, Canada
Phone: +519-253-3000, ext. 3701
spandey@uwindsor.ca

²Chemistry Department and Centre for Biotechnology, Brock University, 500
Glenridge Avenue, St. Catharines, Ontario L2S 3A1, Canada
thudlicky@brocku.ca

³Department of Chemistry, McMaster University, 1280 Main Street West,
Hamilton, Ontario L8S 4M1, Canada
jmcnult@mcmaster.ca

List of Abbreviations

ANT	adenine nucleotide translocase
CK	creatine kinase
CRC	colorectal cancer
CypD	cyclophilin D
Cyto c	cytochrome c
ER	estrogen receptor
IC ₅₀	half-maximal inhibitory concentration
JCTH-1	JC-TH-acid-1
JCTH-4	JC-TH-acetate-4
HK	hexokinase
LC3	microtubule-associated protein 1 light chain 3
MDC	monodansylcadaverine
MMP	mitochondrial membrane potential
MRC	mitochondrial respiratory chain
mtDNA	mitochondrial DNA
NFF	normal human fetal fibroblast
PBR	peripheral benzodiazepine receptor
PQ	paraquat
PST	pancratistatin
PTP	permeability transition pore
RFU	relative fluorescence units
ROS	reactive oxygen species

SDHA	succinate dehydrogenase subunit A
TAM	tamoxifen
TMRM	tetramethylrhodamine methyl ester
VDAC	voltage-dependent anion channel

Summary

The natural compound Pancreatistatin (PST), isolated from the *Hymenocallis littoralis* plant, specifically induces apoptosis in many cancer cell lines. Unlike many other chemotherapeutics, PST is not genotoxic and has minimal adverse effects on non-cancerous cells. However, its availability for preclinical and clinical work is limited due to its low availability in its natural source and difficulties in its chemical synthesis. Several synthetic analogues of 7-deoxypancratistatin with different modifications at C1 were synthesized and screened for apoptosis inducing activity in human colorectal cancer (CRC) cells. We found that a C1 acetoxymethyl derivative of 7-deoxypancratistatin, JC-TH-acetate-4 (JCTH-4), was effective in inducing apoptosis in both p53 positive (HCT-116) and p53 negative (HT-29) human CRC cell lines, demonstrating similar efficacy to that of natural PST. JCTH-4 was able to decrease mitochondrial membrane potential (MMP), increase levels of reactive oxygen species in isolated mitochondria, cause release of the apoptogenic factor cytochrome c (Cyto c) from isolated mitochondria, and induce autophagy in HCT-116 and HT-29 cells. Interestingly, when JCTH-4 was administered with tamoxifen (TAM), there was an enhanced effect in apoptosis induction, reactive oxygen species (ROS) production and Cyto c release by isolated mitochondria, and autophagic induction by CRC cells. Minimal toxicity was exhibited by a normal human fetal fibroblast (NFF) and a normal colon fibroblast (CCD-18Co) cell line. Hence, JCTH-4 is a novel compound capable of selectively inducing

apoptosis and autophagy in CRC cells alone and in combination with TAM and may serve as a safer and more effective alternative to current cancer therapies.

Introduction

Globally, colorectal cancer (CRC) accounts for 9.4 % of all newly diagnosed cancers (Parkin et al. 2005). In 2009, CRC was the third most common cancer responsible for 49,920 deaths in the USA (Murphy & Ryan 2010). Current treatments include surgery, radiotherapy, and chemotherapy. Most chemotherapeutics however, are genotoxic in nature and cause adverse effects in non-cancerous cells. More recent efforts have achieved improved rates of survival with metastatic CRC, using combination therapy of various drugs, such as administration of oxaliplatin or irinotecan with flouoruracil (de Gramont et al. 2000; Douillard et al. 2000; Maindrault-Goebel et al. 1999; André et al. 1999). Despite these efforts, CRC remains as one of the most prominent and aggressive forms of cancer.

Many cancers develop as a result of defects in the apoptosis or programmed cell death pathway (Borst & Rottenberg 2004). In the intrinsic pathway of apoptosis, various pro-apoptotic proteins act to permeabilize the mitochondria, dissipate mitochondrial membrane potential (MMP), and cause release of apoptogenic factors, such as cytochrome c (Cyto c), from the mitochondrial intermembrane space into the cytosol (Earnshaw 1999). Once in the cytosol, apoptogenic factors can directly or indirectly execute apoptosis. As most cancers possess malfunctions in this pathway, much effort has been put into restoring or selectively activating this pathway for cancer therapy.

Pancratistatin (PST), a natural compound from the *Hymenocallis littoralis* plant, specifically induces apoptosis in numerous cancer cell lines (Kekre et al.

2005; McLachlan et al. 2005). Contrasting with many chemotherapeutic agents, PST is non-genotoxic and does not exhibit adverse effects in non-cancerous cells (Kekre et al. 2005; McLachlan et al. 2005). Nonetheless, the availability of PST for preclinical and clinical work is limited as it is only present in its natural source in very low quantities and there have been great difficulties associated with its chemical synthesis. We have synthesized and tested several synthetic derivatives of 7-deoxypancratistatin and have found a C1 acetoxymethyl derivative, JC-TH-acetate-4 (JCTH-4), which has similar efficacy and selective apoptosis inducing activity to that of PST (Collins et al. 2010).

Tamoxifen (TAM) is commonly administered to estrogen receptor (ER) positive breast cancer patients (Baum 2005). In such cases, TAM binds the ER to induce apoptosis by preventing estrogen binding, which normally activates pro-survival signalling pathways. However, other studies have provided evidence of estrogen receptor independent mechanisms of apoptotic induction by TAM (Mandlekar & Kong 2001; Moreira et al. 2006). More specifically, TAM has been shown to interact with the flavin mononucleotide site of Complex I of the mitochondrial respiratory chain (MRC) (Moreira et al. 2006). Interestingly, our past work also indicates PST to act on a mitochondrial target (McLachlan et al. 2005). We have previously exploited this mitochondrial targeting and demonstrated a sensitization by TAM to PST-induced apoptosis in ER positive and negative breast cancer and melanoma cell lines (Siedlakowski et al. 2008; Chatterjee et al. 2010). Another recent report has also shown enhancement of cytotoxic effects of nelfinavir, an HIV drug, by TAM in an ER independent manner

in breast cancer cells (Brüning et al. 2010). As TAM has exhibited capabilities in enhancing the cytotoxicity of certain anti-cancer agents in cancer cells, we wanted to evaluate the combinatory effects of TAM and JCTH-4.

This study analyzes the combinatory treatment of TAM and JCTH-4 in both p53 positive HCT-116 and p53 negative HT-29 human CRC cell lines. Our results show JCTH-4 to be effective in inducing apoptosis and autophagy in both cell lines through mitochondrial targeting. Interestingly, when JCTH-4 was administered with TAM, there was an enhancement in the aforementioned effects in both cell lines. Minimal toxicity by JCTH-4 alone and with TAM was exhibited in a normal human fetal fibroblast (NFF) and a normal colon fibroblast (CCD-18Co) cell line. Thus, this study presents a therapeutic window in combination therapy using a novel synthetic analogue of PST with a clinically available drug to rival current cancer therapies.

Materials and Methods

Cell Culture

The human CRC cells lines HT-29 and HCT 116 (ATCC, CCL-218 & CCL-247, Manassas, VA, USA) were grown and cultured with McCoy's Medium 5a (Gibco BRL, VWR, Mississauga, ON, Canada) supplemented with 2 mM L-glutamine, 10 % fetal bovine serum (FBS) and 10 mg/ml gentamicin (Gibco BRL, VWR, Mississauga, ON, Canada). The apparently normal human fetal fibroblast (NFF) cell line (Coriell Institute for Medical Research, AG04431B, Camden, NJ, USA) was grown in Dulbecco's Modified Eagle's Medium, High Glucose (Thermo Scientific, Waltham, MA, USA) supplemented with 15 % (v/v) FBS and 10 mg/mL gentamycin (Gibco BRL, VWR, Mississauga, ON, Canada). The normal colon fibroblast (CCD-18Co) cell line (ATCC, CRL-1459, Manassas, VA, USA) was cultured with Eagle's Minimal Essential Medium supplemented with 10 % (v/v) FBS and 10 mg/mL gentamycin (Gibco BRL, VWR, Mississauga, ON, Canada). All cells were grown at 37° C and 5 % CO₂.

Cell Treatment

Cells were grown to 60–70 % confluence and treated with pancratistatin (PST), tamoxifen (TAM) citrate salt (Sigma-Aldrich, T9262, Mississauga, ON, Canada), JC-TH-acetate-4 (JCTH-4), JC-TH-acid-1 (JCTH-1), and other synthetic 7-deoxypancratistatin analogues at the indicated concentrations and time points. The C-1 analogues were produced by chemoenzymatic synthesis from bromobenzene as previously described (Collins et al. 2010).

Nuclear Staining

Following treatment and incubation with the aforementioned drugs, nuclei were stained with Hoechst 33342 dye (Molecular Probes, Eugene, OR, USA). Post drug treatment and incubation, cells were incubated with 10 μ M Hoechst 33342 dye for 5 minutes. Images were captured at 400x magnification on a Leica DM IRB inverted fluorescence microscope (Wetzlar, Germany).

Annexin V Binding Assay

Subsequent to drug treatment and incubation, the Annexin V binding assay was performed to confirm apoptotic induction. Post drug treatment and incubation, cells were washed twice using phosphate buffer saline (PBS) and resuspended and incubated in Annexin V binding buffer (10 mM HEPES, 10 mM NaOH, 140 mM NaCl, 1 mM CaCl₂, pH 7.6) with Annexin V AlexaFluor-488 (1:50) (Sigma-Aldrich, Mississauga, ON, Canada) for 15 minutes. Images were captured at 400x magnification on a Leica DM IRB inverted fluorescence microscope (Wetzlar, Germany).

WST-1 Assay for Cell Viability

The WST-1 based colorimetric assay for cell viability, an indicator of active cell metabolism, was conducted according to the manufacturer's protocol (Roche Applied Science, Indianapolis, IN, USA). 96-well clear bottom tissue culture plates were seeded with approximately 2.0×10^3 HT-29 or HCT 116 cells/well, 5.0×10^3 NFF cells/well, or 4.0×10^3 CCD-18Co cells/well and treated with

JCTH-4 and TAM at the indicated concentrations and durations. Subsequent to drug treatment and incubation, the WST-1 reagent, which is cleaved to formazan by cellular enzymes, was added to each well and incubated for 4 hours at 37° C. The metabolic product formazan was quantified by taking absorbance readings at 450 nm on a Wallac Victor³™ 1420 Multilabel Counter (PerkinElmer, Woodbridge, ON, Canada). Absorbance readings were expressed as percentages of the untreated control groups.

Tetramethylrhodamine Methyl Ester (TMRM) Staining

Tetramethylrhodamine methyl ester (TMRM) (Gibco BRL, VWR, Mississauga, ON, Canada) was used to detect MMP. Cells were grown on coverslips and treated with the indicated doses of drugs for the indicated durations. Following drug incubation, cells were incubated with 200 nM TMRM for 45 minutes at 37° C. Images were captured at 400x magnification on a Leica DM IRB inverted fluorescence microscope (Wetzlar, Germany).

Mitochondrial Isolation

Mitochondria were isolated from untreated HT-29 and HCT 116 cells as per a previously published protocol (Siedlakowski et al. 2008). In brief, cells were washed two times with cold PBS and resuspended in hypotonic buffer (1 mM EDTA, 5 mM Tris-HCl, 210 mM mannitol, 70 mM sucrose, 10 µM Leu-pep and Pep-A, 100 µM PMSF). Cells were homogenized manually and subsequently centrifuged at 600 x g for 5 minutes at 4° C. The resulting supernatant was

centrifuged at 15,000 x g for 15 minutes at 4° C. Subsequently, the cytosolic supernatant was discarded and the mitochondrial pellet was resuspended in cold reaction buffer (2.5 mM malate, 10 mM succinate, 10 µM Leu-pep and Pep-A, 100 µM PMSF in PBS).

Amplex Red Assay

The levels of ROS produced were quantified with Amplex Red (Molecular Probes, Eugene, OR, USA). Equal amounts of isolated mitochondria suspended in cold reaction buffer were loaded into an opaque 96-well plate (20 µg of protein/well) with the indicated concentrations of drugs. Paraquat (PQ) (Sigma-Aldrich, Mississauga, ON, Canada) was used as a positive control at 250 µM. In each well, Amplex Red reagent was added to a final concentration of 50 µM and horseradish peroxidase (HRP) (Sigma-Aldrich, Mississauga, ON, Canada) was added in the ratio of 6 U/200 µL. Plates were read at Ex. 560 nm and Em. 590 nm on a spectrofluorometer (SpectraMax Gemini XS, Molecular Devices, Sunnyvale, CA, USA) in 10 minute intervals for 4 hours. Fluorescence readings were expressed as relative fluorescence units (RFU).

Cellular Lysate Preparation

CRC cells were treated for 72 hours with the indicated concentrations of JCTH-4 and TAM. Treated cells were mechanically homogenized in cold hypotonic buffer (10 mM Tris HCl at pH 7.2, 5 mM KCl, 1 mM MgCl₂, 1 mM EGTA, 1% Triton-X-100; 10 μM Leu-pep and Pep-A, 100 μM PMSF). Cell lysates were stored at -20° C until use.

Western Blot Analyses

Protein samples (mitochondrial pellets, post mitochondrial supernatants, or cell lysates) were subjected to SDS-PAGE. Electrophoresed samples were transferred to a nitrocellulose membrane and were blocked with a 5% w/v milk TBST (Tris-Buffered Saline Tween-20) solution for 1 hour. Membranes were probed with an anti-cytochrome c antibody (1:1000) (Abcam, ab13575, Cambridge, MA, USA), an anti-succinate dehydrogenase subunit A antibody (1:1000) (Santa Cruz Biotechnology, Inc., sc-59687, Paso Robles, CA, USA), an anti-LC3 antibody (1:500) (Novus Biologicals, NB100-2220, Littleton, CO, USA), or an anti-β-Actin antibody (1:1000) overnight at 4° C. Subsequently, membranes were subjected to one 15 minute and two 5 minute washes in TBST and were incubated with an anti-mouse (1:2000) or an anti-rabbit (1:2000) horseradish peroxidase-conjugated secondary antibody (1:2000) (Abcam, ab6728, ab6802, Cambridge, MA, USA) for 1 hour at 25° C. Following three consecutive 5 minute washes in TBST, bands were visualized with enhanced chemiluminescence

reagent (Sigma-Aldrich, CPS160, Mississauga, ON, Canada). Densitometry analyses were performed using ImageJ software.

Z-VAD-FMK Caspase Inhibition

To determine the dependence of caspases in apoptosis induction, the broad spectrum caspase inhibitor Z-VAD-FMK was used. Approximately 2.0×10^3 HCT 116 cells were seeded in 96-well clear bottom tissue culture plates. After 24 hours, cells were treated with 1 μ M JCTH-4 alone and with 25 μ M and 50 μ M Z-VAD-FMK. Following 72 hours, the WST-1 reagent was added to each well and incubated for 4 hours at 37° C. Plates were read at 450 nm on a Wallac Victor³™ 1420 Multilabel Counter (PerkinElmer, Woodbridge, ON, Canada). Absorbance readings were expressed as a percentage of untreated control cell groups.

Monodansylcadaverine (MDC) Staining

Monodansylcadaverine (MDC) (Sigma-Aldrich, Mississauga, ON, Canada) staining was used to detect autophagic vacuoles. Cells were grown on coverslips and treated with the indicated doses of drugs for the indicated durations. Following drug incubation, cells were incubated with 0.1 mM MDC for 15 min. Images were captured at 400x magnification on a Leica DM IRB inverted fluorescence microscope (Wetzlar, Germany).

Long-term Analysis on Growth Rate

To evaluate the long term effects of JCTH-4 and TAM on growth rate, cells were treated for 72 hours at the indicated concentrations of drugs. Following drug incubation, cells were trypsinized and 2 plates per experimental group were seeded with approximately 5.0×10^5 live cells, quantified with Trypan Blue exclusion dye, in drug-free media. Subsequently, cells were trypsinized and the number of live cells was quantified using Trypan Blue exclusion dye after 48 and 96 hours using 1 plate of cells per time point per experimental group.

Results

JCTH-4 Effectively Induces Apoptosis in Human CRC Cells

Natural PST (**Figure 2.1A**) has been shown to induce apoptosis selectively in cancer cells (Siedlakowski et al. 2008; Chatterjee et al. 2010; Griffin et al. 2011). As there are insufficient quantities of PST available for preclinical and clinical work, various synthetic analogues of PST were synthesized and screened for similar specific apoptosis inducing activity on both p53 positive HCT-116 and p53 negative HT-29 human CRC cell lines. As seen with Hoechst dye, 1 μ M natural PST after 96 hours yielded condensed, brightly stained nuclei accompanied by apoptotic bodies, indicative of apoptosis in HT-29 and HCT 116 cells (**Figure 2.1B**). Interestingly, one of the synthetic compounds, JCTH-4, induced apoptosis with comparable efficacy to that of PST in both cell lines, while many other synthetic analogues (data not shown) of PST such as JCTH-1 did not (**Figure 2.2A & B**).

The effect of JCTH-4 on both the HT-29 and HCT 116 cell lines was quantified using a WST-1 based colorimetric assay for cell viability, an indicator of active cell metabolism. JCTH-4 was able to reduce cell viability in both cell lines in a time and dose dependent manner and exhibited approximate half-maximal inhibitory concentration (IC_{50}) values of 1 μ M and 0.25 μ M in HT-29 and HCT 116 cells respectively after 96 hours (**Figure 2.3A & B**). Notably, JCTH-4 demonstrated selectivity to CRC cell lines as non-cancerous normal human fetal fibroblasts (NFF) and normal colon fibroblasts (CCD-18Co) were significantly less sensitive compared to both CRC cells lines after 72 hours (**Figure 2.3C**).

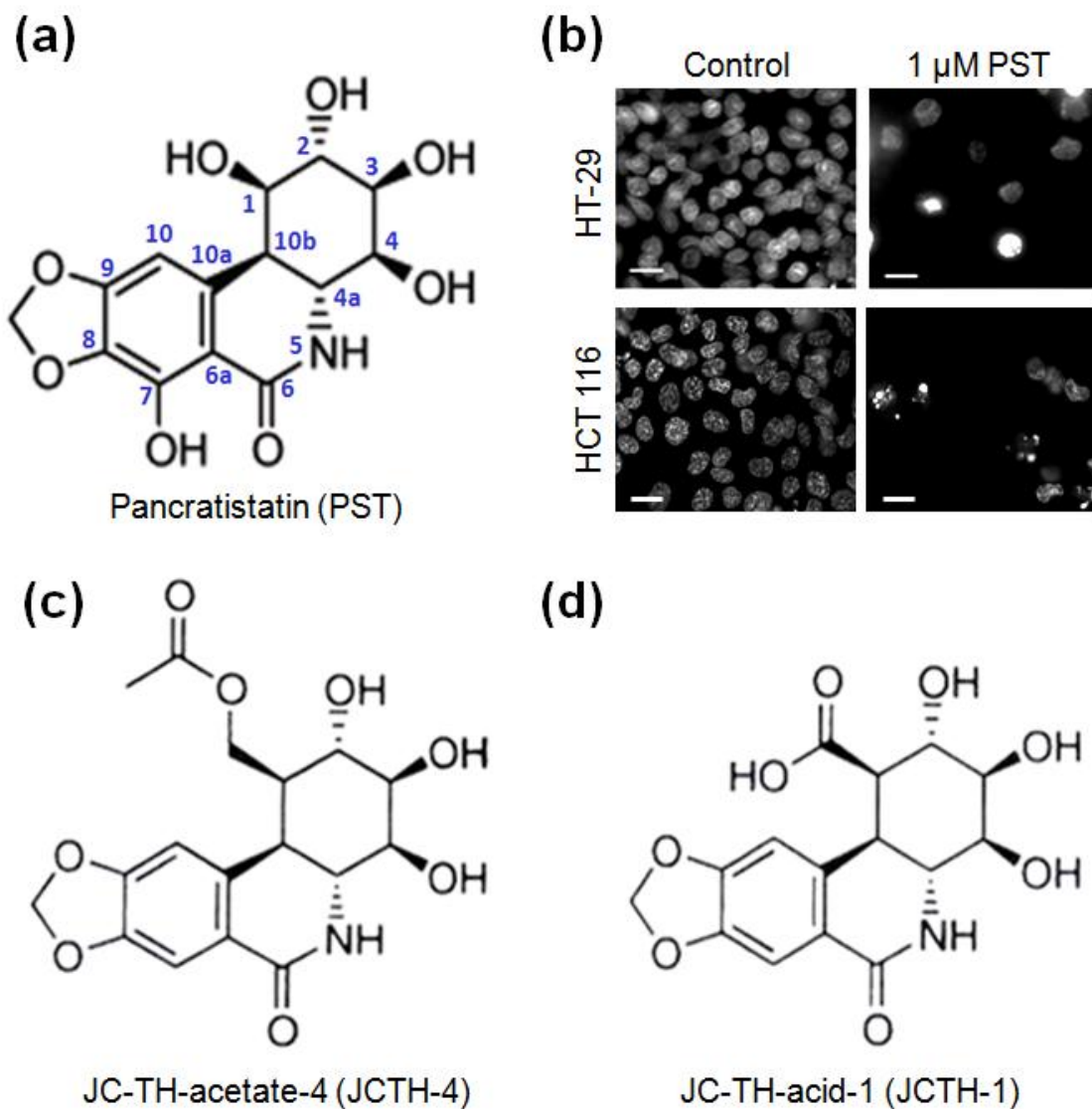


Figure 2.1. PST induces apoptosis in CRC cells and structural comparison to its synthetic 7-deoxy analogues. (A) Chemical structure of pancratistatin (PST). **(B)** Nuclear morphology of HCT 116 and HT-29 cells stained with Hoechst dye treated with 1 μ M PST and the solvent control (Me_2SO) after 96 hours. Scale bar= 15 μ m. **(C)** Chemical structure of JC-TH-acetate-4 (JCTH-4). **(D)** Chemical structure of JC-TH-acid-1 (JCTH-1).

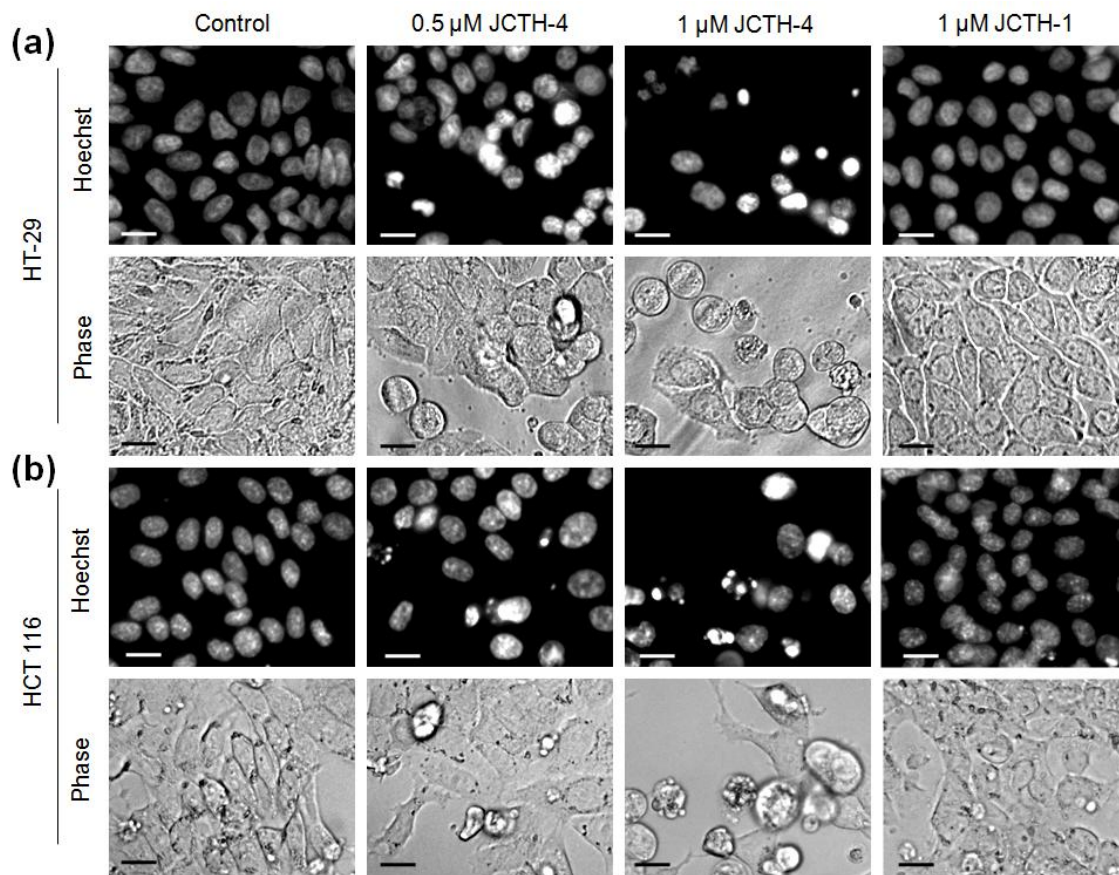


Figure 2.2. JCTH-4 induces apoptosis in CRC cells. Nuclear morphology of (A) HT-29 and (B) HCT 116 cells stained with Hoechst dye treated with the indicated concentrations of JCTH-1 and JCTH-4 after 96 hours. Control groups were treated with solvent (Me_2SO). Scale bar= 15 μ m.

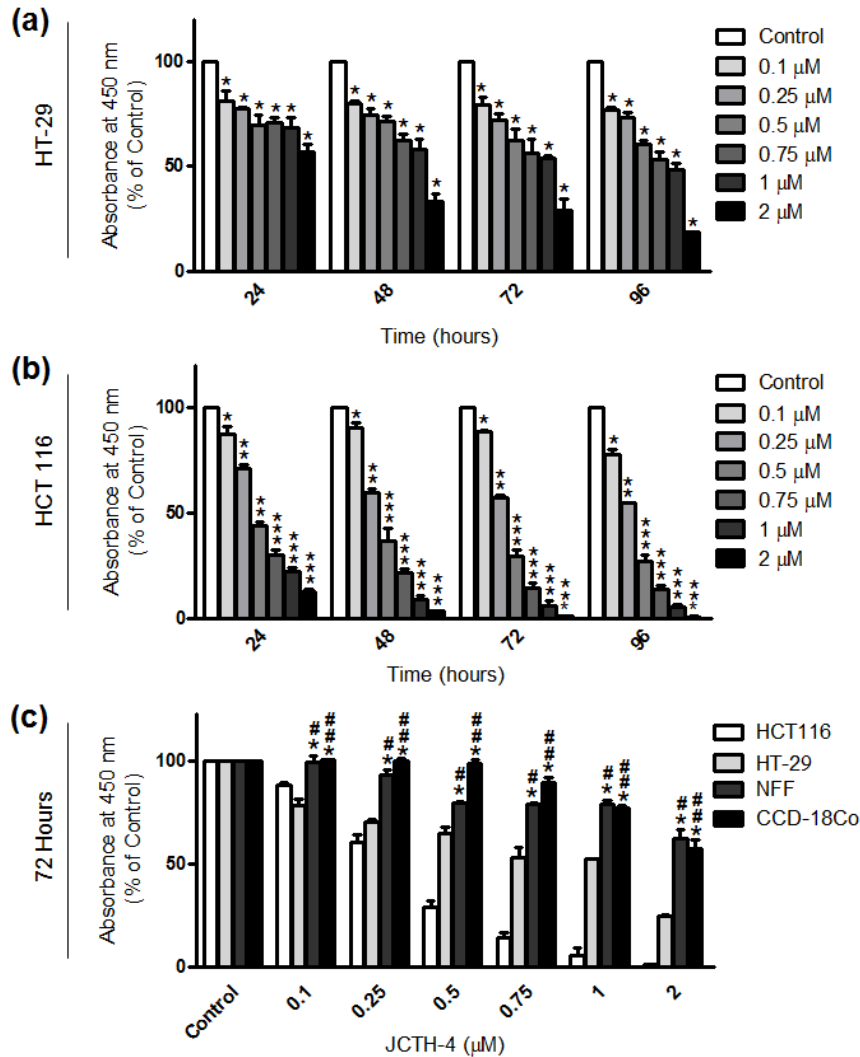


Figure 2.3. JCTH-4 decreases viability of CRC cells in a time and dose-dependent manner. (A) 96-well plates were seeded with HT-29 cells and treated with JCTH-4 at concentrations ranging from 0.1 μ M to 2 μ M for 24, 48, 72, and 96 hours. Subsequent to drug treatment and incubation, the WST-1 reagent was added to each well, absorbance readings were taken at 450 nm, and expressed as a percentage of the control (Me₂SO). Statistics were performed using GraphPad Prism version 5.0. Values are expressed as mean \pm SD from quadruplicates of 3 experiments. * p <0.005 versus control. (B) As performed with HT-29 cells, the WST-1 reagent was used to access viability of HCT 116 cells with the same concentrations of JCTH-4 and durations as previously described. Values are expressed as mean \pm SD from quadruplicates of 3 independent experiments. * p <0.05, ** p <0.005, *** p <0.0005 versus control. (C) The WST-1 reagent was used to evaluate viability of NFF and CCD-18Co cells with the aforementioned concentrations of JCTH-4 after 72 hours. Values are expressed as mean \pm SD from quadruplicates of 3 independent experiments. Viability of HT-29 and HCT 116 cells presented correspond to 72 hours of treatment with JCTH-4. * p <0.01 versus HT-29; # p <0.01, ## p <0.005 versus HCT 116.

TAM Enhances the Apoptotic Efficacy of JCTH-4 in CRC Cells

We have previously shown PST and TAM to synergistically induce apoptosis in ER positive and negative breast cancer and melanoma cells (Siedlakowski et al. 2008; Chatterjee et al. 2010). To investigate the potential of JCTH-4 to replicate the combinatorial effects of PST and TAM, we treated HT-29 and HCT 116 cells with JCTH-4 and TAM. Enhanced induction of apoptosis of JCTH-4 was observed when treated with TAM as exhibited by Hoechst staining (**Figure 2.4A & B**). No evident apoptosis induction was exhibited in CCD-18Co cells by JCTH-4 alone and in combination with TAM (**Figure 2.4C**).

The WST-1 based colorimetric assay was used to quantify cell viability. This confirmed a greater decrease in viability of HCT 116 cells using 0.5 μ M JCTH-4 with 5 μ M and 10 μ M TAM compared to 0.5 μ M JCTH-4 alone, and a more prominent decrease in viability using 1 μ M JCTH-4 with 10 μ M TAM compared to 1 μ M JCTH-4 alone after 72 hours (**Figure 2.5A**). After 72 hours, the 1 μ M JCTH-4 and 10 μ M TAM combinational treatment was significantly less toxic to NFF (**Figure 2.5B**) and CCD-18Co (**Figure 2.5C**) cells.

Phosphatidylserine externalization, a biochemical marker of apoptosis, was detected by Annexin V binding to confirm apoptotic induction. JCTH-4 caused phosphatidylserine externalization indicated by the green fluorescence, confirming the induction of apoptosis (**Figure 2.6A & B**). Such apoptotic induction was not exhibited in NFF cells (**Figure 2.6C**). Thus, combinational treatment of JCTH-4 and TAM demonstrates cytotoxic selectivity towards CRC cell lines.

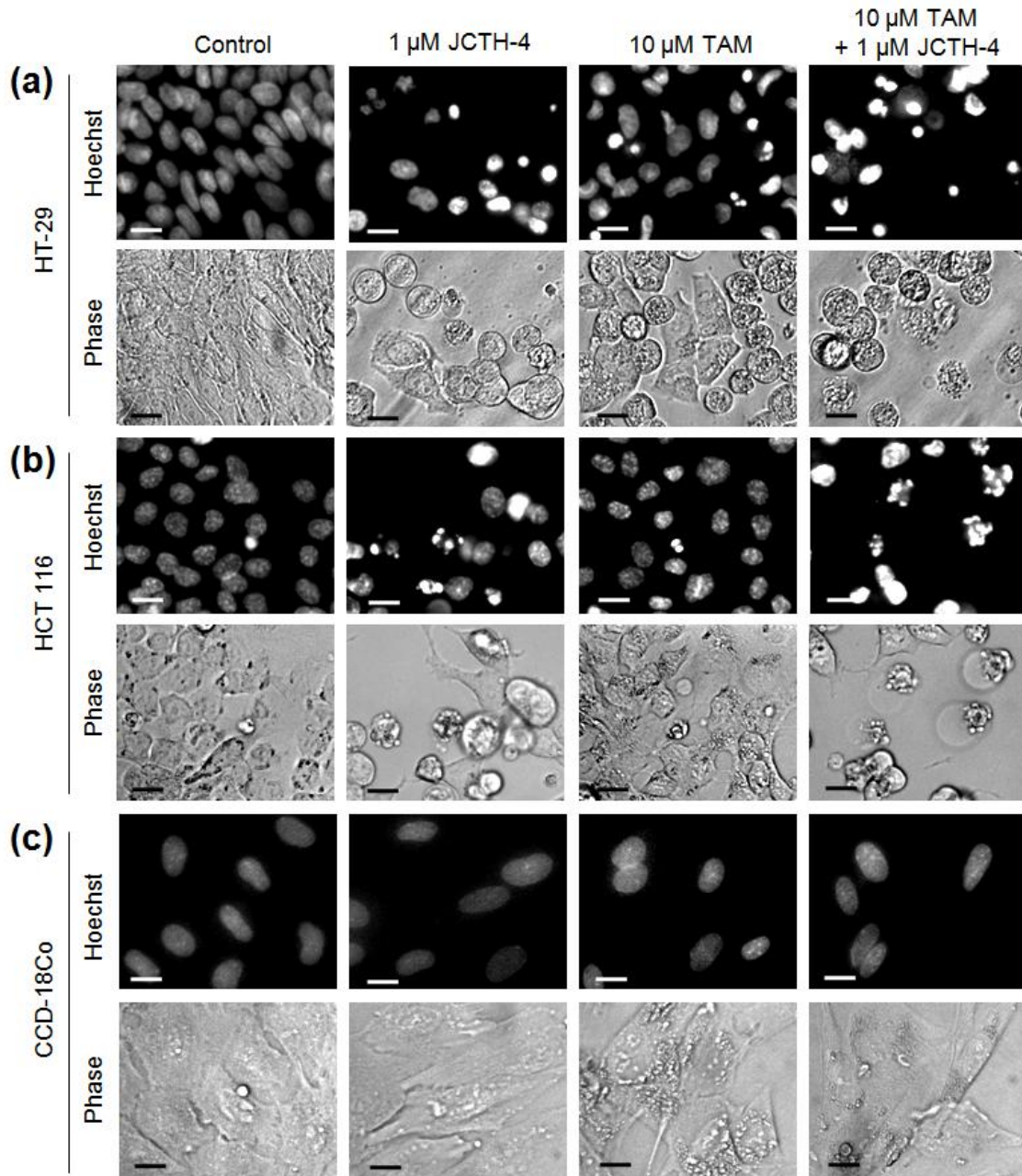


Figure 2.4. TAM enhances apoptosis-inducing activity of JCTH-4 selectively in CRC cells. Nuclear morphology of **(A)** HT-29, **(B)** HCT 116, and **(C)** CCD-18Co cells treated with the indicated concentrations of TAM and JCTH-4 for 96 hours stained with Hoechst dye. Control groups were treated with solvent (Me_2SO). Scale bar= 15 μm .

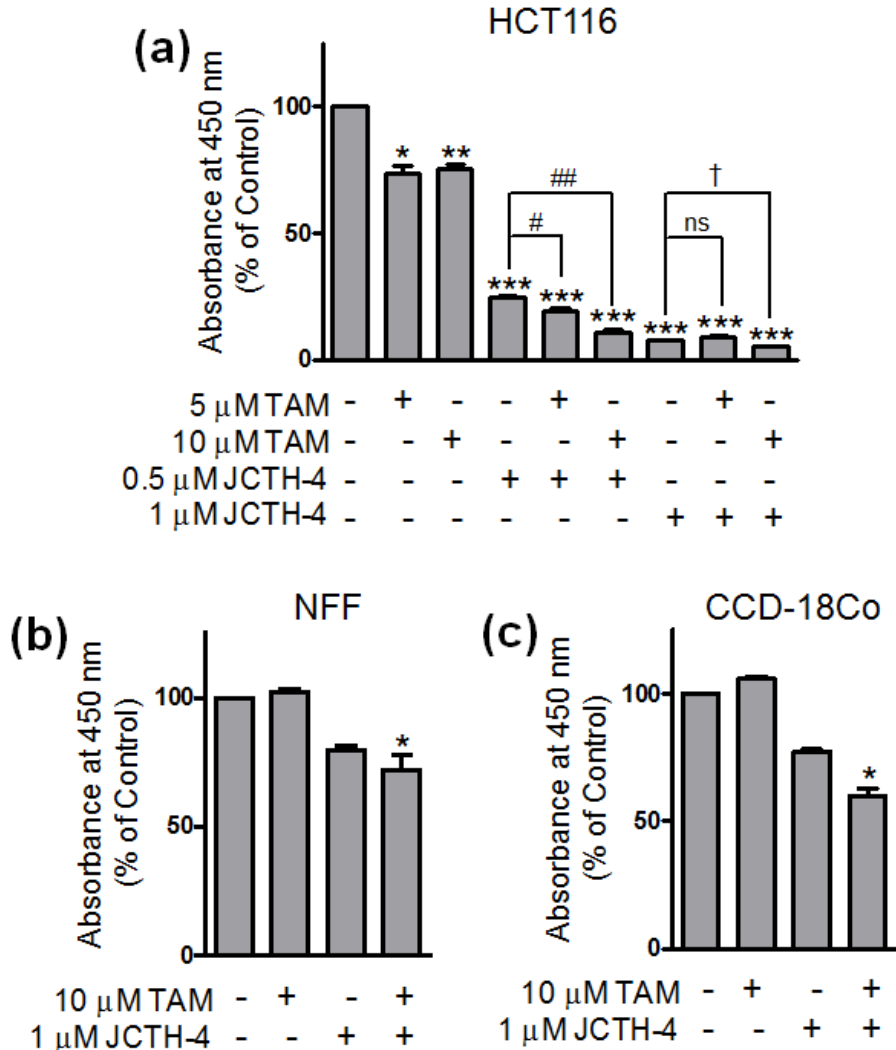


Figure 2.5 TAM enhances viability decrease in CRC cells by JCTH-4. (A) As previously described, the WST-1 reagent was used to measure viability of HCT 116 cells treated with the indicated concentrations of TAM and JCTH-4 for 72 hours. Absorbance readings were taken at 450 nm and expressed as a percentage of the control (Me₂SO). Statistics were performed using GraphPad Prism version 5.0. Values are expressed as mean \pm SD from quadruplicates of 3 independent experiments. * p <0.05, ** p <0.005, *** p <0.0001 versus control; # p <0.05, ## p <0.005 versus 0.5 μ M JCTH-4; † p <0.05 versus 1 μ M JCTH-4. **(B)** The WST-1 reagent was used to measure viability of NFF cells treated with the indicated concentrations of TAM of JCTH-4 for 72 hours. Values are expressed as mean \pm SD from quadruplicates of 3 independent experiments. * p <0.005 versus 10 μ M TAM + 1 μ M JCTH-4 combinational treatment on HCT 116 cells (Figure 5A). **(C)** The WST-1 reagent was used to measure viability of CCD-18Co cells treated with the indicated concentrations of TAM of JCTH-4 for 72 hours. Values are expressed as mean \pm SD from quadruplicates of 3 independent experiments. * p <0.005 versus 10 μ M TAM + 1 μ M JCTH-4 combinational treatment on HCT 116 cells (Figure 5A).

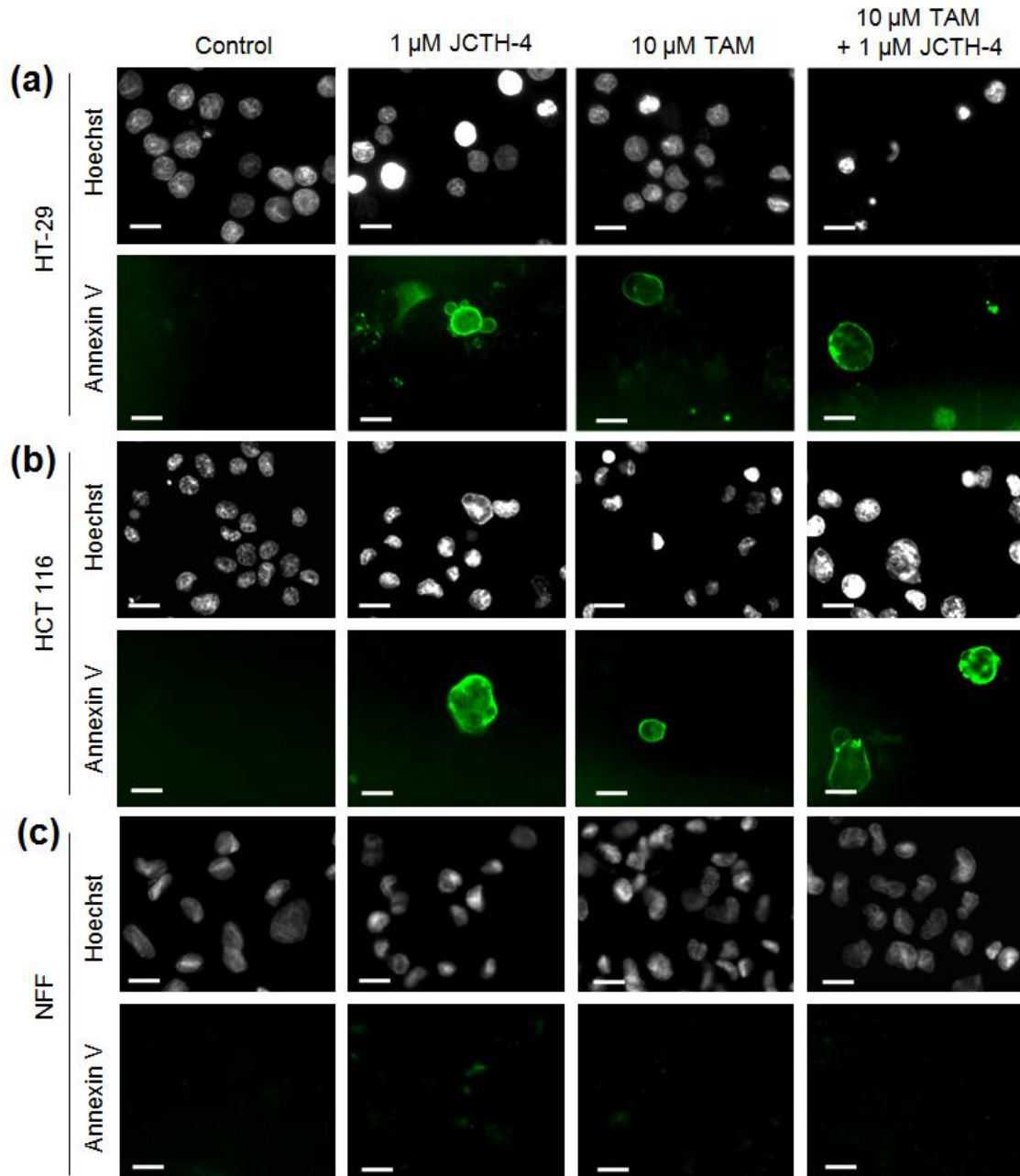


Figure 2.6. JCTH-4 induces phosphatidylserine externalization alone and in combination with TAM in CRC cells. Annexin V binding to externalized phosphatidylserine was monitored to confirm apoptotic induction in **(A)** HT-29, **(B)** HCT 116, and **(C)** NFF cells treated with JCTH-4 and TAM for 72 hours at the indicated concentrations. Control groups were treated with solvent (Me_2SO). Images were taken at 400x magnification on a fluorescent microscope. Scale bar= 15 μm .

JCTH-4 and TAM Target the Mitochondria in HT-29 and HCT 116 Cells

Although TAM is well characterized as an ER antagonist in the treatment of ER positive breast cancers, there have been studies which indicate that TAM can induce apoptosis independently of the estrogen receptor via mitochondrial targeting (Moreira et al. 2006). Moreover, we have previously provided evidence supporting the mitochondria as a target of PST and have shown TAM to strengthen the ability of PST to dissipate MMP and increase in ROS production (Siedlakowski et al. 2008; Chatterjee et al. 2010).

To assess the ability of JCTH-4 to dissipate MMP both alone and in combination with TAM, HT-29 and HCT 116 cells were treated for 96 hours and stained with tetramethylrhodamine methyl ester (TMRM). Both 1 μ M JCTH-4 and 10 μ M TAM alone were able to dissipate MMP in both cell lines indicated by the decrease in positive TMRM staining; however, when used together, there was a greater dissipation in MMP (**Figure 2.7A & B**). No evident dissipation in MMP was observed in CCD-18Co cells by JCTH-4 and TAM alone and in combination (**Figure 2.7C**).

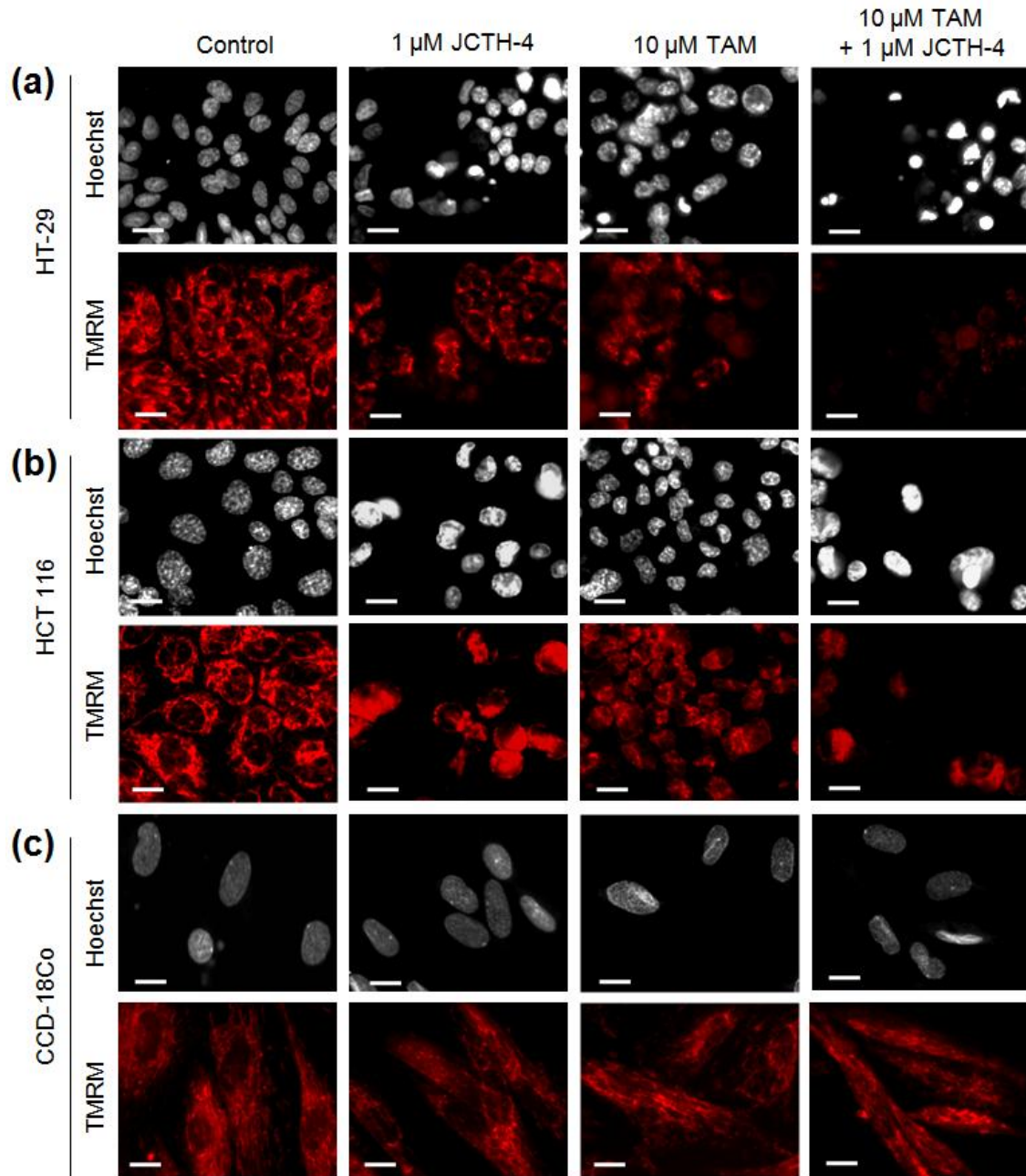


Figure 2.7. JCTH-4 and TAM dissipate MMP in CRC cells. (A) HT-29, (B) HCT 116, and (C) CCD-18Co cells were grown on coverslips and treated with the indicated concentrations of drugs for 96 hours and subsequently stained with TMRM to detect MMP. Control groups were treated with solvent (Me_2SO). Images were captured at 400x magnification on a fluorescence microscope. Scale bar= 15 μ m.

Increases in reactive oxygen species (ROS) production in mitochondria have been associated with both the cause and effect of mitochondrial membrane permeabilization, and the release of apoptogenic factors (Madesh & Hajnóczy 2001; Simon et al. 2000; Batandier et al. 2004). To assess the ability of JCTH-4 and TAM to increase generation of ROS in mitochondria directly, isolated mitochondria from HT-29 and HCT 116 cells were treated with 1 μ M JCTH-4 and 10 μ M TAM alone and in combination. ROS generation was monitored with Amplex Red dye over 4 hours in 10 minute intervals. Paraquat (PQ), a known inducer of mitochondrial ROS generation, was used as a positive control at 250 μ M (Cochemé & Murphy 2008). In both cell lines, JCTH-4 and TAM alone caused a significant increase in ROS production compared to control and with the combinational treatment the increase was significantly greater than either JCTH-4 or TAM alone in HT-29 and HCT 116 cells (**Figure 2.8A & B**).

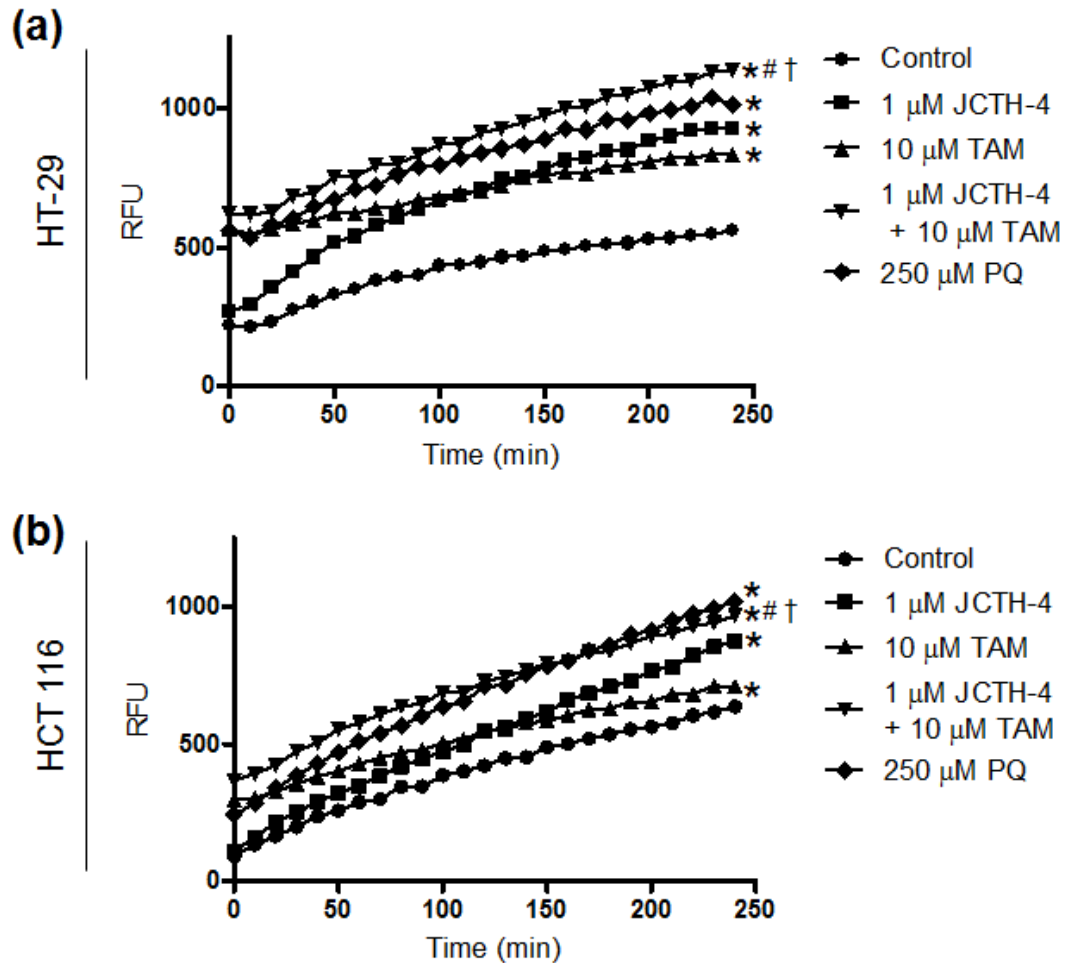


Figure 2.8. JCTH-4 and TAM increase ROS generation in isolated mitochondria from CRC cells. Isolated mitochondria from **(A)** HT-29 and **(B)** HCT 116 cells were treated directly with JCTH-4 and TAM at the indicated concentrations and ROS was measured with Amplex Red substrate in presence of horseradish peroxidase (HRP). The control groups were treated with solvent (Me_2SO). Paraquat (PQ) was used at 250 μM as a positive control in both cell lines. Fluorescence readings were taken in 10 minute intervals for 4 hours at Ex. 560 nm and Em. 590 nm and expressed as relative fluorescence units (RFU). Statistics were performed using GraphPad Prism version 5.0. Image is representative of 3 independent experiments demonstrating similar trends. Values are expressed as mean \pm SD of quadruplicates of 1 independent experiment. * $p < 0.05$ versus control; # $p < 0.05$ versus 1 μM JCTH-4; † $p < 0.05$ against 10 μM TAM.

The release of apoptogenic factors such as Cyto c from the mitochondria following mitochondrial membrane permeabilization is important for apoptosis signalling and execution (Green & Reed 1998). To assess the ability of both JCTH-4 and TAM to directly trigger release of Cyto c, isolated mitochondria from HT-29 cells were treated with the indicated concentrations of JCTH-4 and TAM for 2 hours. Post treatment, the samples were centrifuged and western blot analyses were performed for Cyto c on the supernatants and succinate dehydrogenase subunit A (SDHA) on the mitochondrial pellets. Both JCTH-4 and TAM alone were able to cause release of Cyto c but the effect was greatly enhanced with the combinatorial treatment, significantly releasing more Cyto c than both treatments alone (**Figure 2.9**). Collectively these results are supportive of a mitochondrial target for both JCTH-4 and TAM.

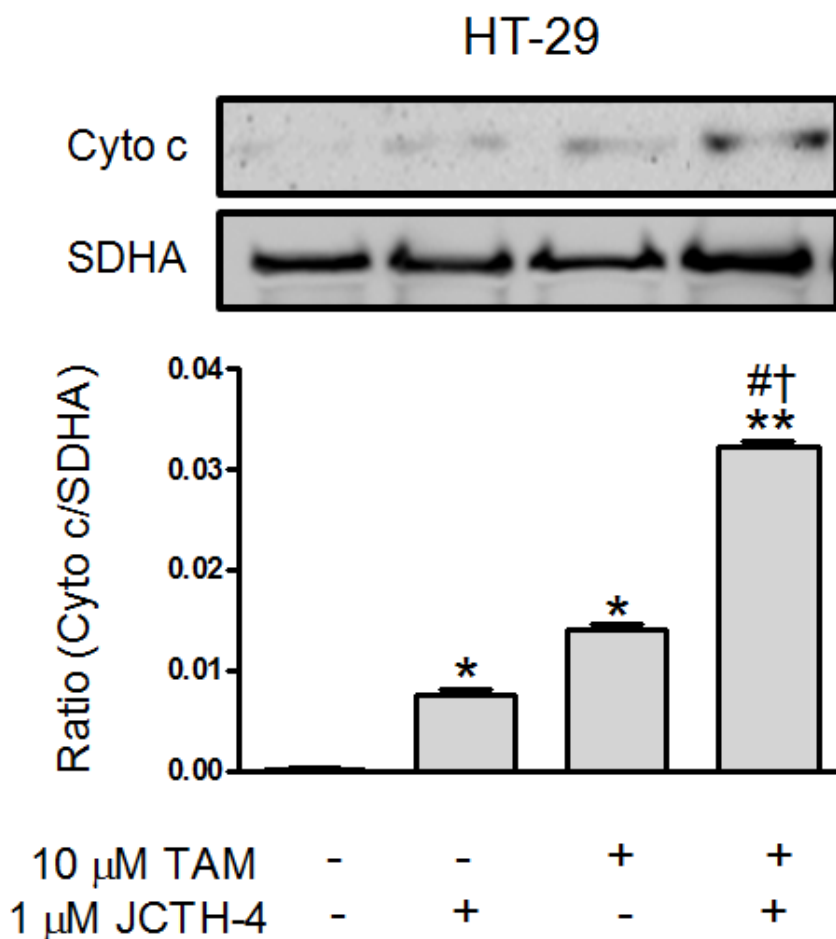


Figure 2.9. JCTH-4 and TAM cause release of apoptogenic factor Cyto c from isolated mitochondria in CRC cells. Isolated mitochondrial from HT-29 cells were directly treated with JCTH-4 and TAM at the indicated concentrations for 2 hours. The control group was treated with solvent (Me_2SO). Following drug incubation, samples were resuspended and centrifuged $15,000 \times g$ for 15 minutes at 4°C . Subsequently, western blot analyses were performed for Cyto c on the resultant supernatants and SDHA on the resultant mitochondrial pellets resuspended in reaction buffer. Densitometric analyses were performed using ImageJ software. Statistics were performed using GraphPad Prism version 5.0. Values are expressed as mean \pm SD. * $p < 0.005$, ** $p < 0.0005$ versus control; # $p < 0.005$ versus 1 μM JCTH-4; † $p < 0.0005$ versus 10 μM TAM.

JCTH-4 Induces Apoptosis in a Caspase-Independent Manner

Caspases are proteases well known for their participation in apoptosis signalling (Stennicke & Salvesen 1999). However, there are other pathways which are independent of these proteases. To determine the dependence on caspases in JCTH-4 induced apoptosis, HCT 116 cells were treated with JCTH-4 alone and in combination with the broad spectrum caspase inhibitor Z-VAD-FMK at 25 μ M and 50 μ M. Using the WST-1 based colorimetric assay to assess cell viability, there was no statistically significant difference observed in cell viability between the JCTH-4 treatment alone and the JCTH-4 treatment in combination with Z-VAD-FMK at both 25 μ M and 50 μ M, indicative of caspase independence in JCTH-4 induced apoptosis (**Figure 2.10**).

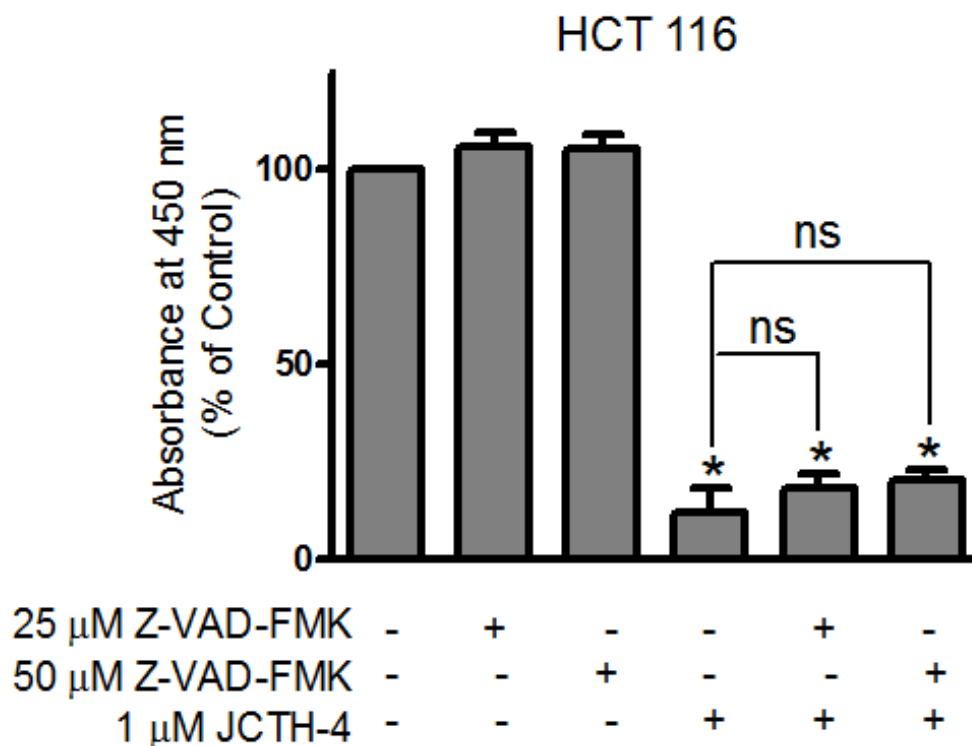


Figure 2.10. JCTH-4 induces apoptosis in CRC cells independent of caspases. To determine the dependence on caspases in the induction of apoptosis by JCTH-4, HCT 116 cells were treated with JCTH-4 alone and in combination with the broad spectrum caspase inhibitor Z-VAD-FMK at the indicated concentrations. After 72 hours, the WST-1 reagent was used to evaluate cell viability as previously described. Absorbance readings were taken at 450 nm and expressed as a percentage of the control (Me_2SO). Statistics were performed using GraphPad Prism version 5.0. Values are expressed as mean \pm SD from quadruplicates of 3 independent experiments. * $p < 0.005$ versus control.

JCTH-4 Induces Autophagy in HT-29 and HCT 116 Cells

Autophagy, a process in which cells break down their own constituents, can be induced by various forms of cellular stress such as hypoxia, reactive oxygen species, protein aggregates, nutrient deprivation, growth factor deprivation, damaged organelles, and mutant proteins (Kroemer et al. 2010). During this process, cytosolic material is taken up by autophagosomes, which are double-membraned vesicles that fuse to lysosomes to form autolysosomes. Subsequent to autolysosome formation, intra-autophagosomal contents are broken down by lysosomal enzymes (Kroemer et al. 2010). To access the induction of autophagy, HT-29 and HCT 116 cells were treated with 1 μ M JCTH-4 and 10 μ M TAM alone and in combination for 72 hours and stained with monodansylcadaverine (MDC) (**Figure 2.11A & B**). Bright punctate MDC staining was observed in JCTH-4 and in TAM treated HT-29 and HCT 116 cells, indicative of autophagosomes. Interestingly, the combinatory treatment yielded the greatest induction of autophagosome formation, as indicated by the high intensity punctate MDC staining. However, after 72 hours of treatment of CCD-18Co cells, minimal MDC staining was observed with JCTH-4, and bright punctate staining was observed with TAM (**Figure 2.11C**). With the combinational treatment of JCTH-4 and TAM, CCD-18Co cells exhibited MDC staining intensity similar to that of TAM alone.

Upon autophagic induction, microtubule-associated protein 1 light chain 3 (LC3) localized in the cytosol, LC3-I, is conjugated to phosphatidylethanolamine, resulting in the lipidated protein LC3-II that is recruited to autophagosomal

membranes (Kroemer et al. 2010). Consequently, detection of LC3-II has been used as a marker of autophagic induction. To confirm the induction of autophagy, western blot analyses were performed using an anti-LC3 antibody on cell lysates from HT-29 and HCT 116 cells treated with the indicated concentrations of JCTH-4 and TAM for 72 hours. Results confirmed that JCTH-4 induced autophagy in both CRC cell lines (**Figure 2.11D & E**). Furthermore, the addition of TAM to JCTH-4 treatment enhanced the conversion of LC3-I to LC3-II. Therefore, these results indicate that JCTH-4 alone and in combination with TAM, triggers autophagic induction in CRC cell lines.

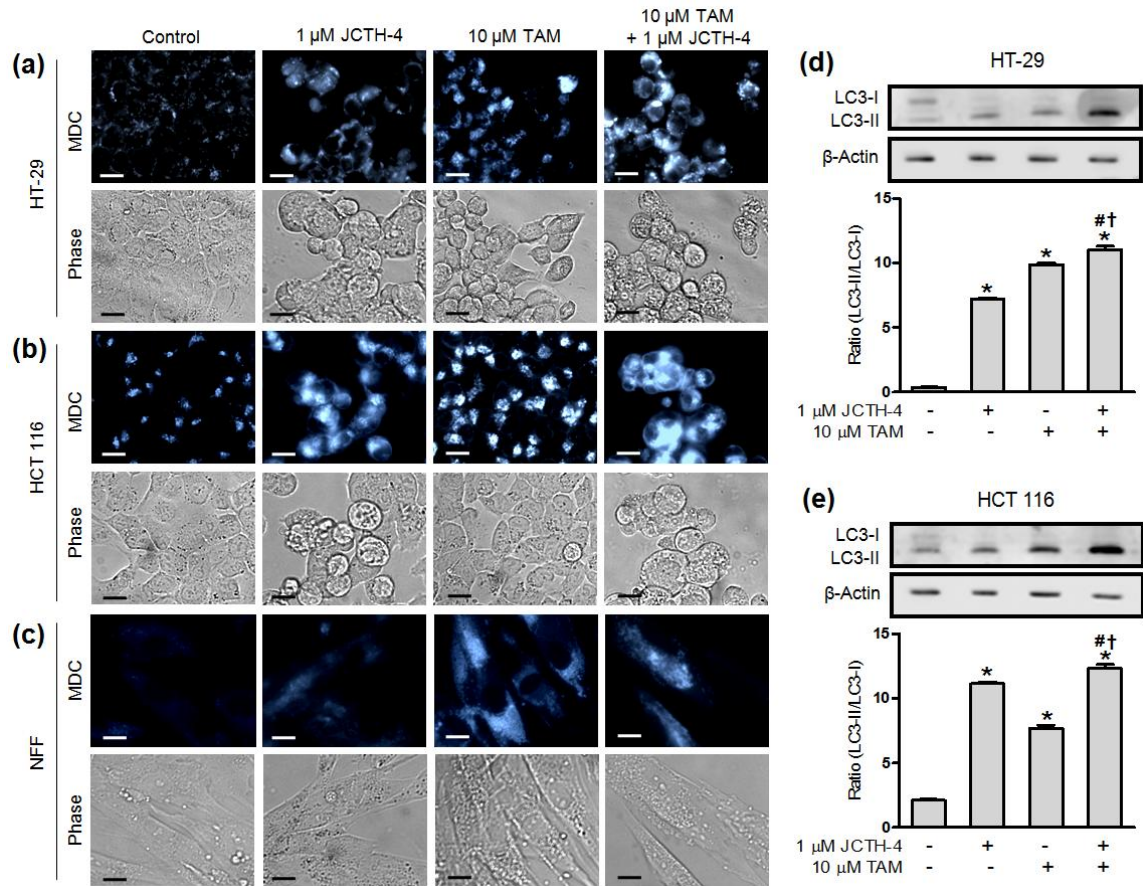


Figure 2.11. JCTH-4 and TAM induce autophagy in CRC cells. Cells were grown on coverslips and treated with JCTH-4 and TAM at the indicated concentrations. The control group was treated with solvent (Me_2SO). After 72 hours, **(A)** HT-29, **(B)** HCT 116, and **(C)** NFF cells were stained with MDC to detect autophagic vacuoles. Images were captured at 400x magnification on a fluorescence microscope. Scale bar= 15 μm . Western blot analyses were performed for LC3-II and β -Actin on cell lysates of CRC cells treated for 72 hours with the indicated concentrations of JCTH-4 and TAM. Densitometric analyses were performed using ImageJ software. Statistics were performed using GraphPad Prism version 5.0. Values are expressed as mean \pm SD. **(D)** HT-29: * $p < 0.0005$ versus control; # $p < 0.005$ versus 1 μM JCTH-4; † $p < 0.005$ versus 10 μM TAM. **(E)** HCT 116: * $p < 0.0005$ versus control; # $p < 0.05$ versus 1 μM JCTH-4; † $p < 0.005$ versus 10 μM TAM.

Long-Term Effect on Human CRC Cells Post Exposure to JCTH-4 and TAM

CRC is notorious for its aggressive nature, thus, the resilience of HT-29 and HCT 116 cells after exposure to 1 μM JCTH-4 and 10 μM TAM alone and in combination was examined. After the HT-29 and HCT 116 cells were initially exposed to the aforementioned treatments for 72 hours, approximately 5.0×10^5 live cells were seeded in drug-free media and the number of live cells was monitored over an additional 96 hours using Trypan Blue exclusion dye. As determined by quantifying the number of live cells, the cells initially treated with 1 μM JCTH-4 exhibited a significantly smaller growth rate in both the HT-29 and HCT 116 cells in drug-free media compared to the control group (**Figure 2.12A & B**). The growth rate following drug removal after initial treatment was synergistically reduced in the combination treatment group compared to both 1 μM JCTH-4 and 10 μM TAM alone in HT-29 and HCT 116 cells; however, the initial treatment of 10 μM TAM alone caused an increase in the growth rate in HCT 116 cells and had no significant effect on the growth rate in HT-29 cells after media replacement (**Figure 2.12A & B**).

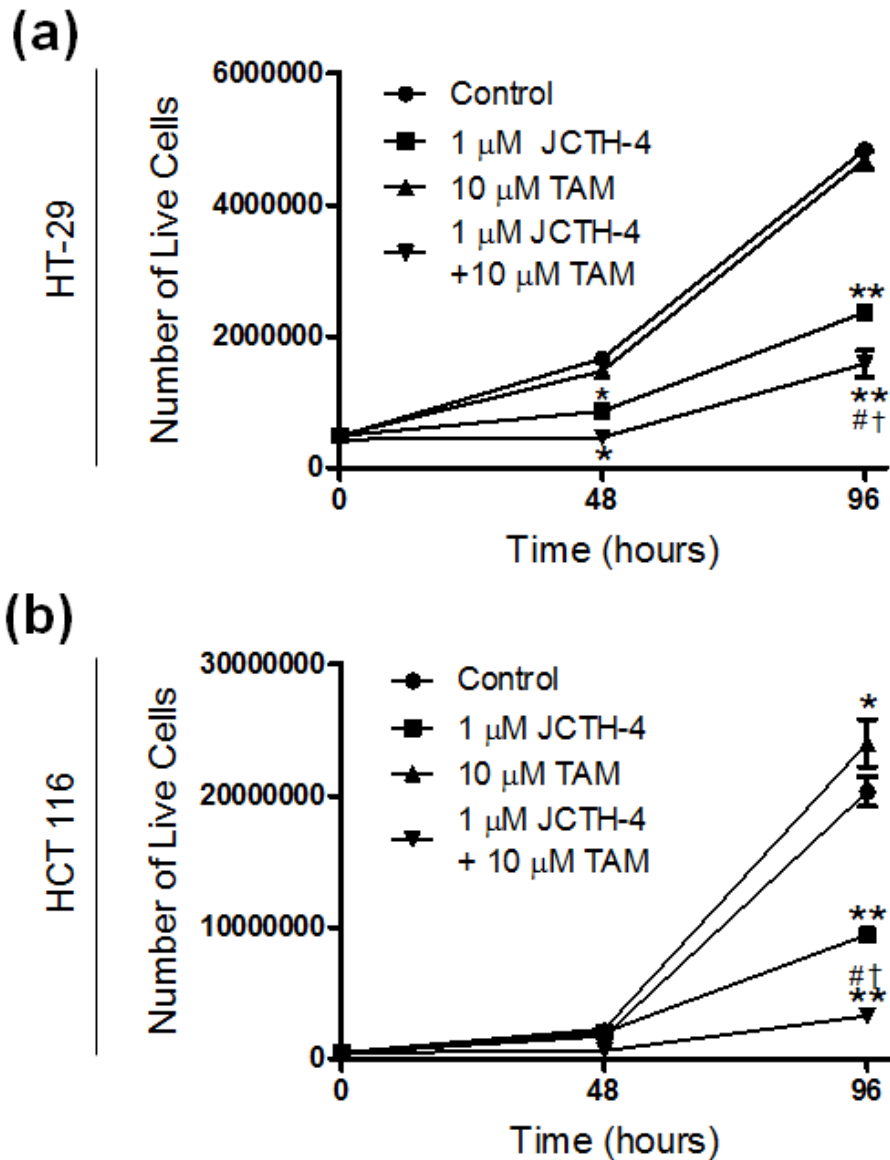


Figure 2.12. Initial JCTH-4 treatment reduces resilience of CRC cells after drug removal. (A) Subsequent to 72 hours of treatment with JCTH-4 and TAM at the indicated concentrations, approximately 5.0×10^5 live HT-29 cells were seeded in drug-free media and the number of live cells were counted after 48 and 96 hours using Trypan Blue exclusion dye. Statistics were performed using GraphPad Prism version 5.0. Values are expressed as mean \pm SD ($n=3$). * $p<0.005$, ** $p<0.0005$ versus control (Me_2SO); # $p<0.05$ versus 1 μM JCTH-4; † $p<0.05$ versus 10 μM TAM. **(B)** The aforementioned procedure was performed with HCT 116 cells. Statistics were performed using GraphPad Prism version 5.0. Values are expressed as mean \pm SD ($n=3$). ** $p<0.01$, ** $p<0.005$ versus control (Me_2SO); # $p<0.05$ versus 1 μM JCTH-4; † $p<0.05$ versus 10 μM TAM.

Discussion

There has been great difficulty in synthesizing PST (**Figure 2.1A**). Many synthetic analogues of PST have been synthesized but demonstrated minimal anti-cancer activity (McNulty et al. 2008). For the first time, we have demonstrated substantial cancer specific apoptosis inducing activity using a novel synthetic derivative of PST, JCTH-4, with comparable efficacy to that of PST, in both p53 positive HCT-116 and p53 negative HT-29 human CRC cell lines. In both CRC cell lines, this C1 acetoxymethyl derivative of 7-deoxypancratistatin was able to effectively induce apoptosis at 1 μ M (**Figure 2.2A & B**). NFF and CCD-18Co cells were significantly less sensitive to JCTH-4 than the CRC cells both alone (**Figure 2.3C**) and in combination with TAM (**Figure 2.5A-C**). Moreover, JCTH-4 alone and in combination with TAM did not yield any evident induction of apoptosis in NFF cells observed by Hoechst and Annexin V assays (**Figure 2.6C**).

The various synthetic analogues of 7-deoxypancratistatin tested in this report are identical in structure with the exception of a varying functional group at C1 (**Figure 2.1C & D**). Specific anti-cancer activity was found only in JCTH-4 and not in the other synthetic analogues, such as JCTH-1. This suggests a critically specific binding of JCTH-4 to some particular protein domain or enzymatic pocket of a key cellular protein by the functional group at C1. Furthermore, this study demonstrates an active compound in the PST series lacking the C7 hydroxyl group, previously reported to mildly contribute to apoptotic activity, demonstrating the unimportance of this group to the structural minimum pharmacophore for

cancer specific cytotoxicity (McNulty et al. 2008). The minimum pharmacophore essential for specific anti-cancer activity suggests a specific target and mode of action of JCTH-4, as opposed to the non-specific binding to various cellular targets exhibited by many current chemotherapeutics. This report provides evidence of specific mitochondrial targeting.

The classification of mitocans collectively includes anti-cancer agents which directly or indirectly target mitochondrial functioning (Chen et al. 2010). Both PST and JCTH-4 fall under this classification. Our previous reports provide evidence of mitochondrial targeting by PST (McLachlan et al. 2005; Siedlakowski et al. 2008). Similarly, this report presents data indicative of mitochondrial targeting by JCTH-4 in CRC cell lines. JCTH-4 was able to dissipate MMP (**Figure 2.7A & B**), increase generation of reactive oxygen species in isolated mitochondria (**Figure 2.8A & B**), and cause release the apoptogenic factor Cyto c from isolated mitochondria (**Figure 2.9**) in both HCT-116 and HT-29 cells. Furthermore, the broad spectrum caspase inhibitor Z-VAD-FMK was unable to prevent JCTH-4-induced apoptosis (**Figure 2.10**). This supports the action of JCTH-4 at the level of mitochondrial destabilization, upstream of executioner caspase activation, to cause release of various apoptogenic factors involved in both caspase dependent and independent pathways of apoptotic induction.

As the Bcl-2 family of proteins serves crucial regulatory roles in apoptosis, there has been a growing interest in the development of small molecules capable of directly binding to and modifying the activity of Bcl-2 proteins, such as the pro-apoptotic protein Bax (Leber et al. 2010). However, we have evidence to rule out

such direct binding to Bax specifically by PST and JCTH-4. We have previously stably transfected and expressed anti-Bax single-domain antibodies (sdAbs) in human neuroblastoma cells (SH-SY5Y) capable of blocking Bax function (Gueorguieva et al. 2006). These sdAbs however, were unable to prevent PST-induced apoptosis in the SH-SY5Y cells (Griffin et al. 2011). Moreover, the tumor suppressor p53 functions as a transcription factor for the pro-apoptotic proteins Bax, Noxa, and PUMA and also indirectly activates Bim, which all act to permeabilize the mitochondrial membrane to induce apoptosis (Miyashita & Reed 1995; Oda et al. 2000; Nakano & Vousden 2001; Puthalakath & Strasser 2002). In many aggressive cancers however, p53 is often mutated giving rise to resistance to many chemotherapeutics. Interestingly, both PST and JCTH-4 effectively induced apoptosis in both p53 positive and p53 negative human CRC cell lines. This suggests these compounds are capable of bypassing malfunctions in p53 and in a manner independent of p53 downstream proteins such as Bax.

In treating ER positive breast cancer, TAM is well known as an ER antagonist. In such circumstances, TAM interferes with estrogen binding to the ER which inhibits various signalling cascades resulting in apoptosis. The ER receptor was also found to be expressed in CRC. The CRC cell lines HT-29 and HCT 116 are both positive for ER beta and in HT-29 cells in particular, previous work has proven TAM to be effective in inhibiting cell proliferation and inducing apoptosis (Fang et al. 2009; Janakiram et al. 2009). Independent of the ER, former studies have suggested TAM to act on the Complex I of the electron

transport chain at the flavin mononucleotide site. Accordingly, we have demonstrated TAM to increase ROS generation (**Figure 2.8A & B**) and cause release of Cyto c (**Figure 2.9**) in isolated mitochondria from both HT-29 and HCT 116 cells. As a proof-of-concept of mitochondrial targeting in both TAM and JCTH-4, combinatory treatment with these compounds yielded greater increase in ROS production (**Figure 2.8A & B**) and greater release of Cyto c (**Figure 2.9**) in isolated mitochondria from HT-29 and HCT 116 cells than either of these compounds alone. Consequently, the enhanced mitochondrial targeting in these cell lines is most likely responsible for the greater apoptotic induction (**Figure 2.4A & B**) and MMP dissipation (**Figure 2.7A & B**) with the combinatory treatment of TAM with JCTH-4. Furthermore, when these treatments were removed after 72 hours of incubation, the HT-29 and HCT 116 cells initially treated with both 1 μ M JCTH-4 and 10 μ M TAM exhibited a synergistically reduced growth rate compared to both 1 μ M JCTH-4 and 10 μ M TAM alone in drug-free media (**Figure 2.12A & B**). Notably, the CRC cells initially treated with 1 μ M JCTH-4 alone grew much slower than the control group in drug-free media. However, 10 μ M TAM alone had no significant effect on growth rate post-drug incubation in HT-29 cells and caused an increase in growth rate in HCT 116 cells after drug removal. Although previous work has shown TAM to exert moderate cytotoxicity against CRC cells at higher doses, TAM treatment alone at 10 μ M appears to be ineffective and potentially detrimental in treating CRC unless utilized with JCTH-4 (Fang et al. 2009).

Consistent with the findings in this report, our previous work has shown TAM to sensitize ER positive and negative breast cancer and melanoma cell lines to PST-induced cell death via mitochondrial targeting independent of estrogen receptors (Siedlakowski et al. 2008; Chatterjee et al. 2010). As we have shown specific mitochondrial targeting in cancer cells with PST and JCTH-4, there are numerous factors that may render cancer cells vulnerable to such targeting. Most cancer cells rely predominantly on glycolysis as the main source of energy production regardless of the abundance of oxygen present in the surrounding environment (Warburg, 1956). Furthermore, studies have proven cancer cells to exhibit higher levels of ROS which have been attributed to mitochondrial DNA (mtDNA) mutations in multiple types of cancers (Szatrowski & Nathan 1991; Carew et al. 2003; Indo et al.; Ishikawa et al. 2008). MRC complexes are encoded in mtDNA, and thus, mutations in these genes could give rise to errors in electron transport and subsequent electron leakage and superoxide generation (Adam-Vizi & Chinopoulos 2006; Brandon et al. 2006). Moreover, cancer cells possess elevated mitochondrial transmembrane potential, which can act to supplement the generation of ROS by the MRC (Chen et al. 2010). Increased levels of ROS have also been linked to the establishment of aggressive and advanced malignancies (Patel et al. 2007; Kumar et al. 2008). However, if the levels of ROS surpass the antioxidant capabilities of the cell, cytotoxicity and cell death may result (Fruehauf & Meyskens 2007). Thus, it is possible for cancer cells to be more sensitive to compounds that abolish cellular antioxidant activity or promote ROS production.

The permeability transition pore (PTP) is a complex spanning the mitochondrial membranes and is proposed to be composed of multiple proteins including adenine nucleotide translocase (ANT), voltage-dependent anion channel (VDAC), and cyclophilin D (CypD). Under normal physiological conditions, small molecules are permitted in and out of the mitochondria via the PTP to maintain mitochondrial homeostasis. In the presence of apoptotic stimuli, the PTP can give rise to dissipation of MMP, ATP depletion, and expulsion of apoptogenic factors resulting in apoptosis (Berridge et al. 2009). Proteins associated with the PTP, which play roles in regulation of its opening, are peripheral benzodiazepine receptor (PBR), creatine kinase (CK), and hexokinase (HK) (Halestrap 2009). In various types of cancer, PBR, HKII, and CK have all been reported to be over-expressed (Corsi et al. 2008; Meffert et al. 2005; Palmieri et al. 2009). Additionally, ANT, VDAC, and CypD are more abundant in malignant tissues (Kim et al. 2006; Pedersen 2008; Chen et al. 2009). Consequently, these mitochondrial abnormalities may serve as specific targets that can be exploited by PST and JCTH-4 to specifically induce apoptosis in cancer cells.

Autophagy exists as a stress response, allowing cells to survive under harsh environments (Kroemer et al. 2010). However, extensive degradation of intracellular contents by this process can lead to autophagic cell death (Dalby et al. 2010). Recently, induction of autophagy has been implicated in both killing cancer cells, via autophagic cell death, as well as protecting cancer cells against chemotherapy (Dalby et al. 2010). Interestingly, TAM has been shown to induce

autophagy in various cancer cell types (Dalby et al. 2010). We found strong autophagic induction in CRC (**Figure 2.11A, B, D, E**) and NFF (**Figure 2.11C**) cells treated with TAM but found minimal cell death (**Figure 2.11A-C**). This may indicate that autophagic induction by TAM is a protective response in CRC and NFF cells. We also observed that JCTH-4 induced autophagy in CRC cells (**Figure 2.11A, B, D, E**) with significant induction of apoptosis (**Figure 2.6A & B**). Activation of autophagy in NFF cells however, appeared to be very minimal by JCTH-4 (**Figure 2.11C**). As described previously, JCTH-4 causes mitochondrial dysfunction that leads to apoptosis; however, in response to mitochondrial dysfunction and oxidative stress, these CRC cells may trigger autophagy as a default mechanism. When JCTH-4 and TAM are used together, there was an enhanced induction of autophagy in CRC cells (**Figure 2.11A, B, D, E**). More interestingly, the protective autophagic response induced by TAM becomes lethal in the presence of JCTH-4, causing autophagic/apoptotic cell death (**Figure 2.4 A & B, 2.5A, 2.6A & B, 2.11A, B, D, E**). However, since mitochondria are permeabilized, the CRC cells ultimately undergo apoptosis. Such pathological autophagic processes were not observed in the NFF cell line as shown with MDC and bright field pictures (**Figure 2.11C**). As TAM has been established to target complex I of the MRC, it can be hypothesized that such targeting can lead to the generation of oxidative stress which is insufficient to destabilize the mitochondria but sufficient to produce a protective autophagic response (Moreira et al. 2006). Nevertheless, such oxidative stress generated by TAM may act to sensitize cancer cell mitochondria to JCTH-4-induced dysfunction and permeabilization,

ultimately yielding apoptosis. As both TAM and JCTH-4 are able to generate oxidative stress (**Figure 2.8A & B**), the combinatorial production of such stress by both compounds may give rise to extensive activation of the autophagic pathway to ultimately yield a detrimental response.

In conclusion, we present a novel derivative of PST, JCTH-4, created by de novo synthesis, capable of specifically inducing apoptosis in human CRC cell lines via mitochondrial targeting. As a synthetic derivative of PST demonstrating similar efficacy and specificity towards cancer cells has been discovered, previous limitations on PST, including its low availability in its natural source and difficulties in its chemical synthesis, have been overcome. Moreover, TAM was able to enhance the efficacy of JCTH-4 and induce a pathological autophagic response in CRC cells in the presence of JCTH-4. Therefore, the novel synthetic compound JCTH-4 may serve as a safer and more effective alternative, both alone and in combination with TAM, to the chemotherapeutics currently available.

Acknowledgements

This work has been supported by the Knights of Columbus Chapter 9671 (Windsor, Ontario), NSERC, and a CIHR Frederick Banting and Charles Best Canada Graduate Scholarship awarded to Dennis Ma. Thank you to Carly Griffin for providing the pancratistatin results presented in this manuscript. We would also like to thank Colleen Mailloux for the critical review of this manuscript.

References

- Adam-Vizi, V. & Chinopoulos, C., 2006. Bioenergetics and the formation of mitochondrial reactive oxygen species. *Trends in pharmacological sciences*, 27(12), pp.639–45.
- André, T. et al., 1999. CPT-11 (irinotecan) addition to bimonthly, high-dose leucovorin and bolus and continuous-infusion 5-fluorouracil (FOLFIRI) for pretreated metastatic colorectal cancer. GERCOR. *European journal of cancer (Oxford, England : 1990)*, 35(9), pp.1343–7.
- Batandier, C., Lerverve, X. & Fontaine, E., 2004. Opening of the mitochondrial permeability transition pore induces reactive oxygen species production at the level of the respiratory chain complex I. *The Journal of biological chemistry*, 279(17), pp.17197–204.
- Baum, M., 2005. Adjuvant endocrine therapy in postmenopausal women with early breast cancer: where are we now? *European journal of cancer (Oxford, England : 1990)*, 41(12), pp.1667–77.
- Berridge, M. V, Herst, P.M. & Lawen, A., 2009. Targeting mitochondrial permeability in cancer drug development. *Molecular nutrition & food research*, 53(1), pp.76–86.
- Borst, P. & Rottenberg, S., 2004. Cancer cell death by programmed necrosis? *Drug resistance updates: reviews and commentaries in antimicrobial and anticancer chemotherapy*, 7(6), pp.321–4.
- Brandon, M., Baldi, P. & Wallace, D.C., 2006. Mitochondrial mutations in cancer. *Oncogene*, 25(34), pp.4647–62.

- Brüning, A. et al., 2010. Tamoxifen enhances the cytotoxic effects of nelfinavir in breast cancer cells. *Breast cancer research : BCR*, 12(4), p.R45.
- Carew, J.S. et al., 2003. Mitochondrial DNA mutations in primary leukemia cells after chemotherapy: clinical significance and therapeutic implications. *Leukemia*, 17(8), pp.1437–47.
- Chatterjee, S.J., McNulty, J. & Pandey, S., 2010. Sensitization of human melanoma cells by tamoxifen to apoptosis induction by pancratistatin, a nongenotoxic natural compound. *Melanoma research*.
- Chen, G. et al., 2009. Different redox states in malignant and nonmalignant esophageal epithelial cells and differential cytotoxic responses to bile acid and honokiol. *Antioxidants & redox signaling*, 11(5), pp.1083–95.
- Chen, G. et al., 2010. Preferential killing of cancer cells with mitochondrial dysfunction by natural compounds. *Mitochondrion*, 10(6), pp.614–25.
- Cochemé, H.M. & Murphy, M.P., 2008. Complex I is the major site of mitochondrial superoxide production by paraquat. *The Journal of biological chemistry*, 283(4), pp.1786–98.
- Collins, J. et al., 2010. Chemoenzymatic synthesis of Amaryllidaceae constituents and biological evaluation of their C-1 analogues. The next generation synthesis of 7-deoxypancratistatin and trans-dihydrolycoricidine. *The Journal of organic chemistry*, 75(9), pp.3069–84.
- Corsi, L., Geminiani, E. & Baraldi, M., 2008. Peripheral benzodiazepine receptor (PBR) new insight in cell proliferation and cell differentiation review. *Current clinical pharmacology*, 3(1), pp.38–45.

- Dalby, K.N. et al., 2010. Targeting the prodeath and prosurvival functions of autophagy as novel therapeutic strategies in cancer. *Autophagy*, 6(3), pp.322–9.
- Douillard, J.Y. et al., 2000. Irinotecan combined with fluorouracil compared with fluorouracil alone as first-line treatment for metastatic colorectal cancer: a multicentre randomised trial. *Lancet (London, England)*, 355(9209), pp.1041–7.
- Earnshaw, W.C., 1999. Apoptosis. A cellular poison cupboard. *Nature*, 397(6718), pp.387, 389.
- Fang, Y.-J. et al., 2009. MMP7 expression regulated by endocrine therapy in ERbeta-positive colon cancer cells. *Journal of experimental & clinical cancer research : CR*, 28, p.132.
- Fruehauf, J.P. & Meyskens, F.L., 2007. Reactive oxygen species: a breath of life or death? *Clinical cancer research : an official journal of the American Association for Cancer Research*, 13(3), pp.789–94.
- de Gramont, A. et al., 2000. Leucovorin and fluorouracil with or without oxaliplatin as first-line treatment in advanced colorectal cancer. *Journal of clinical oncology : official journal of the American Society of Clinical Oncology*, 18(16), pp.2938–47.
- Green, D.R. & Reed, J.C., 1998. Mitochondria and apoptosis. *Science (New York, N.Y.)*, 281(5381), pp.1309–12.
- Griffin, C. et al., 2011. Pancratistatin selectively targets cancer cell mitochondria and reduces growth of human colon tumor xenografts. *Molecular cancer*

- therapeutics*, 10(1), pp.57–68.
- Gueorguieva, D. et al., 2006. Identification of single-domain, Bax-specific intrabodies that confer resistance to mammalian cells against oxidative-stress-induced apoptosis. *FASEB journal: official publication of the Federation of American Societies for Experimental Biology*, 20(14), pp.2636–8.
- Halestrap, A.P., 2009. What is the mitochondrial permeability transition pore? *Journal of molecular and cellular cardiology*, 46(6), pp.821–31.
- Indo, H.P. et al., Evidence of ROS generation by mitochondria in cells with impaired electron transport chain and mitochondrial DNA damage. *Mitochondrion*, 7(1-2), pp.106–18.
- Ishikawa, K. et al., 2008. ROS-generating mitochondrial DNA mutations can regulate tumor cell metastasis. *Science (New York, N.Y.)*, 320(5876), pp.661–4.
- Janakiram, N.B., Steele, V.E. & Rao, C. V, 2009. Estrogen receptor-beta as a potential target for colon cancer prevention: chemoprevention of azoxymethane-induced colon carcinogenesis by raloxifene in F344 rats. *Cancer prevention research (Philadelphia, Pa.)*, 2(1), pp.52–9.
- Kekre, N. et al., 2005. Pancreatistatin causes early activation of caspase-3 and the flipping of phosphatidyl serine followed by rapid apoptosis specifically in human lymphoma cells. *Cancer chemotherapy and pharmacology*, 56(1), pp.29–38.
- Kim, G.J., Chandrasekaran, K. & Morgan, W.F., 2006. Mitochondrial dysfunction,

- persistently elevated levels of reactive oxygen species and radiation-induced genomic instability: a review. *Mutagenesis*, 21(6), pp.361–7.
- Kroemer, G., Mariño, G. & Levine, B., 2010. Autophagy and the integrated stress response. *Molecular cell*, 40(2), pp.280–93.
- Kumar, B. et al., 2008. Oxidative stress is inherent in prostate cancer cells and is required for aggressive phenotype. *Cancer research*, 68(6), pp.1777–85.
- Leber, B. et al., 2010. Drugs targeting Bcl-2 family members as an emerging strategy in cancer. *Expert reviews in molecular medicine*, 12, p.e28.
- Madesh, M. & Hajnóczky, G., 2001. VDAC-dependent permeabilization of the outer mitochondrial membrane by superoxide induces rapid and massive cytochrome c release. *The Journal of cell biology*, 155(6), pp.1003–15.
- Maindrault-Goebel, F. et al., 1999. Oxaliplatin added to the simplified bimonthly leucovorin and 5-fluorouracil regimen as second-line therapy for metastatic colorectal cancer (FOLFOX6). GERCOR. *European journal of cancer (Oxford, England : 1990)*, 35(9), pp.1338–42.
- Mandlekar, S. & Kong, A.N., 2001. Mechanisms of tamoxifen-induced apoptosis. *Apoptosis: an international journal on programmed cell death*, 6(6), pp.469–77.
- McLachlan, A. et al., 2005. Pancratistatin: a natural anti-cancer compound that targets mitochondria specifically in cancer cells to induce apoptosis. *Apoptosis: an international journal on programmed cell death*, 10(3), pp.619–30.
- McNulty, J. et al., 2008. synthesis and biological evaluation of fully functionalized

- seco-pancratistatin analogues. *Journal of natural products*, 71(3), pp.357–63.
- Meffert, G. et al., 2005. Elevated creatine kinase activity in primary hepatocellular carcinoma. *BMC gastroenterology*, 5, p.9.
- Miyashita, T. & Reed, J.C., 1995. Tumor suppressor p53 is a direct transcriptional activator of the human bax gene. *Cell*, 80(2), pp.293–9.
- Moreira, P.I. et al., 2006. Tamoxifen and estradiol interact with the flavin mononucleotide site of complex I leading to mitochondrial failure. *The Journal of biological chemistry*, 281(15), pp.10143–52.
- Murphy, J.E. & Ryan, D.P., 2010. American Society of Clinical Oncology 2010 colorectal update. *Expert review of anticancer therapy*, 10(9), pp.1371–3.
- Nakano, K. & Vousden, K.H., 2001. PUMA, a novel proapoptotic gene, is induced by p53. *Molecular cell*, 7(3), pp.683–94.
- Oda, E. et al., 2000. Noxa, a BH3-only member of the Bcl-2 family and candidate mediator of p53-induced apoptosis. *Science (New York, N.Y.)*, 288(5468), pp.1053–8.
- Palmieri, D. et al., 2009. Analyses of resected human brain metastases of breast cancer reveal the association between up-regulation of hexokinase 2 and poor prognosis. *Molecular cancer research : MCR*, 7(9), pp.1438–45.
- Parkin, D.M. et al., Global cancer statistics, 2002. *CA: a cancer journal for clinicians*, 55(2), pp.74–108.
- Patel, B.P. et al., 2007. Lipid peroxidation, total antioxidant status, and total thiol levels predict overall survival in patients with oral squamous cell carcinoma.

Integrative cancer therapies, 6(4), pp.365–72.

Pedersen, P.L., 2008. Voltage dependent anion channels (VDACs): a brief introduction with a focus on the outer mitochondrial compartment's roles together with hexokinase-2 in the "Warburg effect" in cancer. *Journal of bioenergetics and biomembranes*, 40(3), pp.123–6.

Puthalakath, H. & Strasser, A., 2002. Keeping killers on a tight leash: transcriptional and post-translational control of the pro-apoptotic activity of BH3-only proteins. *Cell death and differentiation*, 9(5), pp.505–12.

Siedlakowski, P. et al., 2008. Synergy of Pancratistatin and Tamoxifen on breast cancer cells in inducing apoptosis by targeting mitochondria. *Cancer biology & therapy*, 7(3), pp.376–84.

Simon, H.U., Haj-Yehia, A. & Levi-Schaffer, F., 2000. Role of reactive oxygen species (ROS) in apoptosis induction. *Apoptosis : an international journal on programmed cell death*, 5(5), pp.415–8.

Stennicke, H.R. & Salvesen, G.S., 1999. Catalytic properties of the caspases. *Cell death and differentiation*, 6(11), pp.1054–9.

Szatrowski, T.P. & Nathan, C.F., 1991. Production of large amounts of hydrogen peroxide by human tumor cells. *Cancer research*, 51(3), pp.794–8.

Warburg, O., 1956. On the origin of cancer cells. *Science (New York, N.Y.)*, 123(3191), pp.309–14.

CHAPTER 3: Selective Cytotoxicity Against Human Osteosarcoma Cells by a Novel Synthetic C-1 Analogue of 7-deoxypancratistatin is Potentiated by Curcumin

Dennis Ma¹, Phillip Tremblay¹, Kevinjeet Mahngar¹, Jonathan Collins², Tomas Hudlicky², and Siyaram Pandey^{1*}

^{1*}Department of Chemistry and Biochemistry, University of Windsor,
401 Sunset Avenue, Windsor, Ontario N9B 3P4, Canada
Phone: +519-253-3000, ext. 3701
spandey@uwindsor.ca

²Chemistry Department and Centre for Biotechnology, Brock University, 500
Glenridge Avenue, St. Catharines, Ontario L2S 3A1, Canada
thudlicky@brocku.ca

List of Abbreviations

AIF	apoptosis inducing factor
CC	curcumin
EndoG	endonuclease G
HO _b	normal human osteoblast
IC ₅₀	half-maximal inhibitory concentration
JCTH-4	JC-TH-acetate-4
LC3	microtubule-associated protein 1 light chain 3
MDC	monodansylcadaverine
MMP	mitochondrial membrane potential
NFF	normal human fetal fibroblast
OS	osteosarcoma
PI	propidium iodide
PQ	paraquat
PST	pancratistatin
RFU	relative fluorescence units
ROS	reactive oxygen species
SDHA	succinate dehydrogenase subunit A
TAM	tamoxifen
TMRM	tetramethylrhodamine methyl ester

Summary

The natural compound pancratistatin (PST) is a non-genotoxic inducer of apoptosis in a variety of cancers. Nonetheless, PST is not readily synthesized and is present in very low quantities in its natural source to be applied clinically. We have previously synthesized and evaluated several synthetic analogues of 7-deoxypancratistatin, and found that JC-TH-acetate-4 (JCTH-4), a C-1 acetoxymethyl analogue, possessed similar apoptosis inducing activity compared to PST. In this study, osteosarcoma (OS) cells (Saos-2, U-2 OS) were substantially susceptible to JCTH-4-induced apoptosis through mitochondrial targeting; JCTH-4 induced collapse of mitochondrial membrane potential (MMP), increased reactive oxygen species (ROS) production in isolated mitochondria, and caused release of apoptosis inducing factor (AIF) and endonuclease G (EndoG) from isolated mitochondria. Furthermore, JCTH-4 selectively induced autophagy in OS cells. Additionally, we investigated the combinatory effect of JCTH-4 with the natural compound curcumin (CC), a compound found in turmeric spice, previously shown to possess antiproliferative properties. CC alone had no observable effect on OS cells. However, when present with JCTH-4, CC was able to enhance the cytotoxicity of JCTH-4 selectively in OS cells. Cytotoxicity by JCTH-4 alone and in combination with CC was not observed in normal human osteoblasts (HOb) and normal human fetal fibroblasts (NFF). Therefore, this report illustrates a new window in combination therapy, utilizing a novel synthetic analogue of PST with the natural compound CC, for the treatment of OS.

Introduction

For many centuries, a plethora of natural products have been used in traditional medicine for the treatment of numerous ailments. One such product includes the *Curcuma longa* herb (Ravindran et al. 2009). Traditionally, this herb has been used to treat anorexia, rheumatism, sinusitis, hepatic disorders, and inflammation (Singh 2007). More recently, a component of this herb, the compound curcumin (CC) also referred to as (1E,6E)-1,7-bis(4-hydroxy-3-methoxyphenyl)-1,6-heptadiene-3,5-dione or diferuloylmethane, has been recognized for its antiproliferative properties in treating cancer (Ravindran et al. 2009). In particular, CC has been shown to regulate expression of genes implicated in cell proliferation, metastasis, chemotherapy resistance, and angiogenesis (Ravindran et al. 2009; Kuttan et al. 1985). The anti-neoplastic properties of CC are exhibited in many types of malignancies including osteosarcoma (OS) (Ravindran et al. 2009; Walters et al. 2008).

OS, a primary malignant bone tumor, is an extremely aggressive form of cancer associated with poor prognosis (Arndt & Crist 1999). It occurs most commonly in the developing bones of children and adolescents and is often accompanied by lung metastases and subsequent respiratory failure (Marina et al. 2004). Current treatment strategies include surgery and radiation therapy with adjuvant chemotherapy with agents such as doxorubicin, cisplatin, methotrexate, etoposide, and ifosfamide at high doses (Marina et al. 2004). Despite the use of these chemotherapeutics, the 5-year survival rate for patients with metastatic OS is only 20% (Marina et al. 2004). Furthermore, toxicity has been associated with

the use of these drugs and chemoresistance frequently develops in this aggressive cancer; thus, more selective and effective chemotherapeutics are needed for OS (Bielack et al. 2002; Baum et al.; Smith et al. 1991; Meistrich et al. 1989; Goorin et al. 1991).

Previously, we have shown the natural compound pancratistatin (PST), isolated from the *Hymenocallis littoralis* plant, to induce cytotoxicity in a number of malignant cell lines at concentrations below 1 μ M and reduce the volume of human prostate and colon tumor xenografts (Kekre et al. 2005; McLachlan et al. 2005; Siedlakowski et al. 2008; Chatterjee et al. 2010; Griffin, Karnik, et al. 2011; Griffin, McNulty, et al. 2011). Contrasting from many approved chemotherapeutics in use, non-cancerous cell lines are markedly less sensitive to PST (Kekre et al. 2005; McLachlan et al. 2005; Siedlakowski et al. 2008; Chatterjee et al. 2010; Griffin, Karnik, et al. 2011; Griffin, McNulty, et al. 2011). PST however, is present in only parts per million quantities in its natural source and there have been many difficulties associated with its chemical synthesis; therefore, the major bottleneck of this compound has been its low availability for preclinical and clinical work. We have recently synthesized and screened 7-deoxypancratistatin derivatives and have identified a C-1 acetoxymethyl analogue, JC-TH-acetate-4 (JCTH-4), with comparable efficacy and specificity to PST against several cancer cell lines (Collins et al. 2010).

Evasion of apoptosis, or type I programmed cell death, as a result of abnormalities in pathways leading to apoptosis plays a major role in the development of cancer; therefore, much effort has been made to manipulate and

restore apoptosis as a way to treat cancer (Borst & Rottenberg 2004; Liu et al. 2011). Apoptosis can be activated in response to a death ligand binding to its corresponding death receptor or in response to an internal stress stimulus such as DNA damage (Reed 2000). In response to such internal stress, various proapoptotic proteins are upregulated and translocated to the mitochondria where they induce mitochondrial membrane permeabilization, collapse of mitochondrial membrane potential (MMP), and release of apoptogenic factors which subsequently execute apoptosis directly or indirectly (Earnshaw 1999). Execution of this pathway yields nuclear and cellular condensation, membrane blebbing, and formation of apoptotic bodies which are phagocytosed by phagocytes or neighbouring cells (Reed 2000). As well as apoptosis, much focus has been put on the implications of other cell death pathways in cancer therapy (Kroemer et al. 2010; Levine 2007).

Autophagy has been recognized as a cellular pro-survival response to various forms of sublethal cellular stress such as DNA damage, deficiencies in growth factors and nutrients, protein aggregates, reactive oxygen species, hypoxia, pathogens, and defective organelles (Kroemer et al. 2010). Once this pathway is activated, cytoplasmic material is sequestered by double-membraned vesicles known as autophagosomes. These autophagosomes fuse with lysosomes to form autolysosomes which degrade the contained cytoplasmic contents (Levine 2007). Extensive activation of autophagy however, can result in a pro-death response leading to autophagic cell death, classified as type II programmed cell death (Gozuacik & Kimchi 2004).

In this report, we demonstrate JCTH-4 to be a potent inducer of apoptosis and autophagy in OS cells (Saos-2, U-2 OS) via mitochondrial targeting. Furthermore, CC was able to potentiate the cytotoxic effects of JCTH-4 in Saos-2 and U-2 OS cells. The normal human fetal fibroblast (NFF) and normal human osteoblast (HOb) cell lines utilized in this study were drastically less sensitive to JCTH-4 alone and in combination with CC, presenting a potential therapeutic window for this aggressive malignancy.

Materials and Methods

Cell Culture

An OS cell line, Saos-2 (American Type Culture Collection, Cat. No. HTB-85, Manassas, VA, USA), was grown in McCoy's 5A Medium Modified (Sigma-Aldrich Canada, Mississauga, ON, Canada) supplemented with 15% (v/v) fetal bovine serum (FBS) standard (Thermo Scientific, Waltham, MA, USA) and 10 mg/mL gentamicin (Gibco BRL, VWR, Mississauga, ON, Canada). An additional OS cell line, U-2 OS (American Type Culture Collection, Cat. No. HTB-96, Manassas, VA, USA), was grown in McCoy's 5A Medium Modified (Sigma-Aldrich Canada, Mississauga, ON, Canada) supplemented with 10% (v/v) FBS standard (Thermo Scientific, Waltham, MA, USA) and 10 mg/mL gentamicin (Gibco BRL, VWR, Mississauga, ON, Canada). Apparently NFF cells (Coriell Institute for Medical Research, Cat. No. AG04431B, Camden, NJ, USA) were cultured in Dulbecco's Modified Eagle's Medium, High Glucose (Thermo Scientific, Waltham, MA, USA) supplemented with 15% (v/v) FBS standard (Thermo Scientific, Waltham, MA, USA) and 10 mg/mL gentamicin (Gibco BRL, VWR, Mississauga, ON, Canada). HOb cells (Cell Applications, Inc., Cat. No. 406-05a, San Diego, CA, USA) were cultured in Osteoblast Growth Medium (Cell Applications, Inc., Cat. No. 417-500, San Diego, CA, USA). All cells were grown at 37° C and 5 % CO₂.

Cell Treatment

After culturing cells to 60–70 % confluence, they were treated with CC (Sigma-Aldrich Canada, Cat. No. C7727, Mississauga, ON, Canada), tamoxifen (TAM) citrate salt (Sigma-Aldrich, Cat. No. T9262, Mississauga, ON, Canada), the broad spectrum caspase inhibitor Z-VAD-FMK (EMD Chemicals, Gibbstown, NJ, USA), and JCTH-4 (((1S, 2S, 3R, 4S, 4aR, 11bR)-2, 3, 4-Trihydroxy-6-oxo-1, 2, 3, 4, 4a, 5, 6, 11b-octahydro-[1,3]dioxolo[4,5-j]phenanthridin-1-yl)methyl Acetate) at the indicated doses and durations. As per a previously published protocol, JCTH-4 was produced by chemoenzymatic synthesis from bromobenzene (Collins et al. 2010). All stock solutions of drugs were made with dimethylsulfoxide (Me₂SO).

Nuclear Staining

Post treatment and incubation with the aforementioned drugs, Hoechst 33342 dye (Molecular Probes, Eugene, OR, USA) was used to stain the nuclei. Cells were incubated with 10 µM Hoechst 33342 dye for 5 minutes and images were taken at 400x magnification on a Leica DM IRB inverted fluorescence microscope (Wetzlar, Germany).

Annexin V Binding Assay

The Annexin V binding assay was performed to verify the induction of apoptosis. Following drug treatment, cells were washed two times using phosphate buffer saline (PBS), resuspended in Annexin V binding buffer (10 mM HEPES, 10 mM NaOH, 140 mM NaCl, 1 mM CaCl₂, pH 7.6), and incubated with Annexin V AlexaFluor-488 (1:50) (Sigma-Aldrich Canada, Mississauga, ON, Canada) for 15 minutes. Micrographs were taken at 400x magnification on a Leica DM IRB inverted fluorescence microscope (Wetzlar, Germany).

WST-1 Assay for Cell Viability

The WST-1 based colorimetric assay was performed according to the manufacturer's protocol (Roche Applied Science, Indianapolis, IN, USA) to quantify cell viability as a function of active cell metabolism. 96-well clear bottom tissue culture plates were seeded with approximately 6.0×10^3 Saos-2 cells/well, 7.5×10^3 U-2 OS cells/well, 5.0×10^3 NFF cells/well, or 4.0×10^3 HOb cells/well and treated with JCTH-4 and CC at the indicated concentrations and for the indicated durations. Following treatment, the WST-1 reagent, which is processed to formazan by cellular enzymes, was added to each well and incubated for 4 hours at 37° C. Absorbance readings were taken at 450 nm on a Wallac Victor³™ 1420 Multilabel Counter (PerkinElmer, Woodbridge, ON, Canada) to quantify the formazan product and were expressed as percentages of the solvent control groups (Me₂SO).

Tetramethylrhodamine Methyl Ester (TMRM) Staining

TMRM (Gibco BRL, VWR, Mississauga, ON, Canada) was used as an indicator for MMP. Cells were grown on coverslips and treated with the indicated concentrations of JCTH-4 and CC for the indicated durations. Subsequent to drug treatment, cells were incubated with 200 nM TMRM for 45 minutes at 37° C. Micrographs were taken at 400x magnification on a Leica DM IRB inverted fluorescence microscope (Wetzlar, Germany).

Mitochondrial Isolation

Mitochondria were isolated from untreated Saos-2 and U-2 OS cells. These cells were washed two times with cold PBS, resuspended in hypotonic buffer (1 mM EDTA, 5 mM Tris-HCl, 210 mM mannitol, 70 mM sucrose, 10 µM Leu-pep, 10 µM Pep-A, and 100 µM PMSF), manually homogenized, and subsequently centrifuged at 600 x g for 5 minutes at 4° C. The supernatant was centrifuged at 15,000 x g for 15 minutes at 4° C. The resulting cytosolic supernatant was discarded and the mitochondrial pellet was resuspended in cold reaction buffer (2.5 mM malate, 10 mM succinate, 10 µM Leu-pep, 10 µM Pep-A, and 100 µM PMSF in PBS).

Amplex Red Assay

Generation of reactive oxygen species (ROS) was quantified with Amplex Red (Molecular Probes, Eugene, OR, USA). Opaque 96-well plates were equally loaded with isolated mitochondria suspended in cold reaction buffer, with 20 µg of protein/well. The Bio-Rad protein assay (Bio-Rad Laboratories, Hercules, CA USA) was used for protein quantification as per manufacturer's protocol. Isolated mitochondria were incubated with the indicated concentrations of drugs, Amplex Red reagent at a final concentration of 50 µM, and horseradish peroxidase (Sigma-Aldrich Canada, Mississauga, ON, Canada) in the ratio of 6 U/200 µL. Paraquat (PQ) (Sigma-Aldrich Canada, Mississauga, ON, Canada) was used as a positive control at 250 µM. Fluorescence readings were acquired after 2 hours of incubation at Ex. 560 nm and Em. 590 nm on a spectrofluorometer (SpectraMax Gemini XS, Molecular Devices, Sunnyvale, CA, USA). Fluorescence readings were expressed as relative fluorescence units (RFU).

Treatment of Isolated Mitochondria & Evaluation of Apoptogenic Factor Release

Mitochondria isolated from Saos-2 and U-2 OS cells were directly treated with JCTH-4 and CC at the indicated concentrations for 2 hours in cold reaction buffer (2.5 mM malate, 10 mM succinate, 10 µM Leu-pep, 10 µM Pep-A, and 100 µM PMSF in PBS). The control group was treated with solvent (Me₂SO). After treatment, mitochondrial samples were vortexed and centrifuged at 15,000 x g for 15 minutes at 4°C. The resultant supernatant and mitochondrial pellet

(resuspended in cold reaction buffer) samples were subjected to western blot analyses to monitor for mitochondrial release or retention of apoptogenic factors.

Cellular Lysate Preparation

Cells were treated for 72 hours with the indicated concentrations of JCTH-4, CC, and TAM, and subsequently homogenized manually in cold hypotonic buffer (10 mM Tris HCl at pH 7.2, 5 mM KCl, 1 mM MgCl₂, 1 mM EGTA, 1% Triton-X-100; 10 μM Leu-pep, 10 μM Pep-A, and 100 μM PMSF). Cell lysates were stored at -20° C until use.

Western Blot Analyses

SDS-PAGE was performed on the protein samples. Electrophoresed proteins were transferred to a nitrocellulose membrane. For 1 hour, membranes were blocked with a 5% w/v milk TBST (Tris-Buffered Saline with Tween-20) solution. The membranes were probed with various primary antibodies overnight at 4° C for microtubule-associated protein1 light chain 3 (LC3) raised in rabbit (1:500) (Novus Biologicals, Cat. No. NB100-2220, Littleton, CO, USA), β-Actin raised in mouse (1:1000) (Santa Cruz Biotechnology, Inc., Cat. No. sc-81178, Paso Robles, CA, USA), apoptosis inducing factor (AIF) raised in rabbit (1:1000) (Abcam, Cat. No. ab1998, Cambridge, MA, USA), endonuclease G (EndoG) raised in rabbit (1:1000) (Abcam, Cat. No. ab9647, Cambridge, MA, USA), and succinate dehydrogenase subunit A (SDHA) raised in mouse (1:1000) (Santa Cruz Biotechnology, Cat. No. sc-59687, Paso Robles, CA, USA). Following

primary antibody incubation, membranes were washed once for 15 minutes and twice for 5 minutes with TBST and were incubated with an anti-mouse (1:2000) or an anti-rabbit (1:2000) horseradish peroxidase-conjugated secondary antibody (Abcam, Cat. No. ab6728 & ab6802, Cambridge, MA, USA) for 1 hour at 25° C. After secondary antibody incubation, the membranes were washed three times for 5 minutes in TBST. Bands were visualized with enhanced chemiluminescence reagent (Sigma-Aldrich Canada, Cat. No. CPS160, Mississauga, ON, Canada) and densitometry analyses were performed using ImageJ software.

Monodansylcadaverine (MDC) Staining

MDC (Sigma-Aldrich Canada, Mississauga, ON, Canada) was used to detect autophagic vacuoles. Cells were grown on coverslips and treated with TAM, JCTH-4, and CC at the indicated concentrations and for the indicated durations. After treatment, cells were incubated with 0.1 mM MDC for 15 minutes. Using a Leica DM IRB inverted fluorescence microscope (Wetzlar, Germany), micrographs were taken at 400x magnification.

Propidium Iodide (PI) Staining

PI (Sigma-Aldrich Canada, Mississauga, ON, Canada) was used to detect cell lysis. Cells were incubated with 1µg/mL PI for 10 minutes and images were taken at 400x magnification on a Leica DM IRB inverted fluorescence microscope (Wetzlar, Germany).

Results

JCTH-4 causes selective cytotoxicity in OS cells in a time and dose-dependent manner

As we have previously found PST (**Figure 3.1A**) to be effective in producing cytotoxicity selectively in various cancer cell lines, we evaluated the activity of JCTH-4 (**Figure 3.1B**) in the OS cell lines Saos-2 and U-2 OS using the WST-1 based colorimetric assay for cell viability. JCTH-4 decreased cell viability in a time and dose dependent manner and had a half-maximal inhibitory concentration (IC_{50}) value of 0.25 μ M after 48 hours in both Saos-2 and U-2 OS cells (**Figure 3.2A & B**). Importantly, JCTH-4 was selective to OS cells as HOb and NFF cells were drastically less sensitive to this compound (**Figure 3.2C**).

CC potentiates the cytotoxicity of JCTH-4 selectively in OS cells

The natural compound CC has been shown to possess anti-cancer properties as well as the ability to enhance the efficacy of various chemotherapeutics (Patel & Majumdar 2009; Epelbaum et al. 2010). Thus, we evaluated the combinatorial effects of CC and JCTH-4 in OS cells. CC alone at 5 μ M had no significant effect on Saos-2 (96 hours) and U-2 OS cells (72 hours); however, when used in combination, CC was able to selectively potentiate the effect of JCTH-4 in these OS cell lines as HOb and NFF cells were markedly less sensitive to this combinatorial insult (**Figure 3.3A-D**).

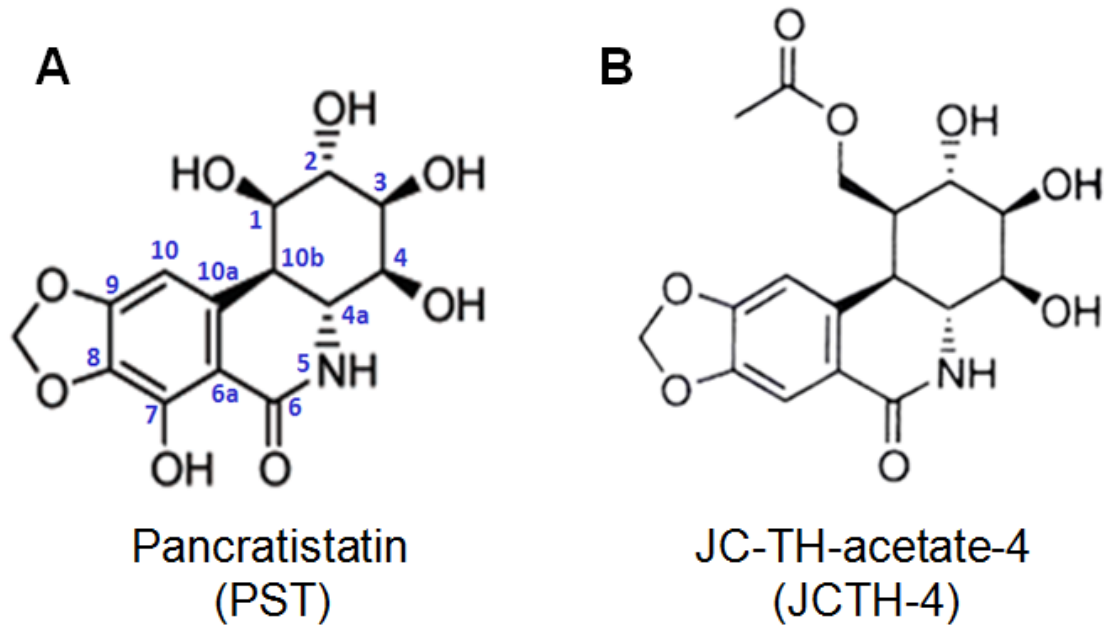


Figure 3.1. Comparison of chemical structures. Structures of **(A)** Pancratistatin (PST) and **(B)** JC-TH-acetate-4 (JCTH-4).

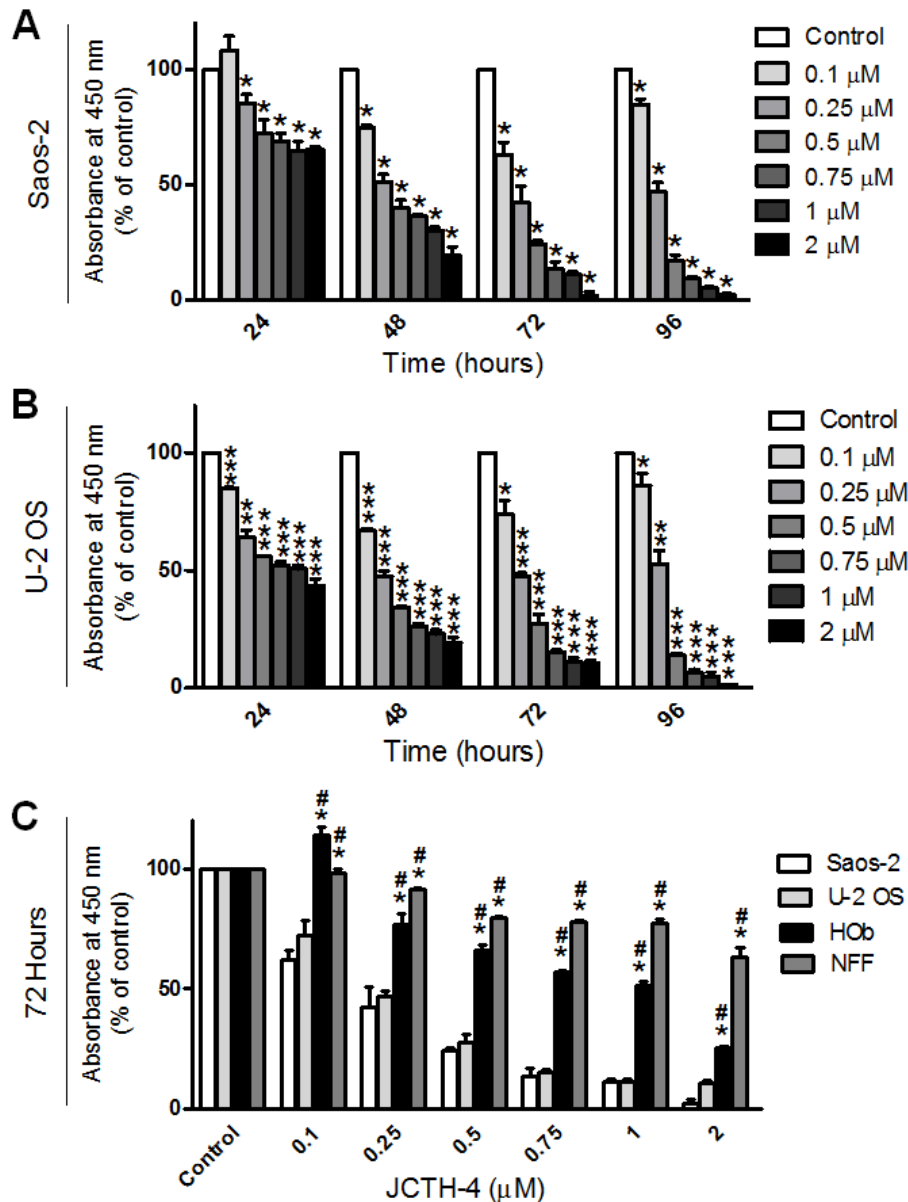


Figure 3.2. JCTH-4 causes selective cytotoxicity in OS cells in a time and dose-dependent manner. Effect of JCTH-4 on cellular viability of OS cells was determined by the WST-1 based colorimetric assay. **(A)** Saos-2 and **(B)** U-2 OS cells were treated with JCTH-4 and the WST-1 reagent was used to quantify cell viability. Absorbance was read at 450 nm and expressed as a percent of the control (Me₂SO). Values are expressed as mean \pm SD from quadruplicates of 3 independent experiments. * p <0.05, ** p <0.01, *** p <0.001 versus solvent control (Me₂SO). **(C)** Effect on cellular viability of HOb and NFF cells treated with JCTH-4 compared to Saos-2 and U-2 OS cells after 72 hours. The WST-1 reagent was used to quantify cellular viability. Absorbance was read at 450 nm and expressed as a percent of the solvent control (Me₂SO). Values are expressed as mean \pm SD from quadruplicates of 3 independent experiments. * p <0.005 versus Saos-2 cells; # p <0.005 versus U-2 OS cells.

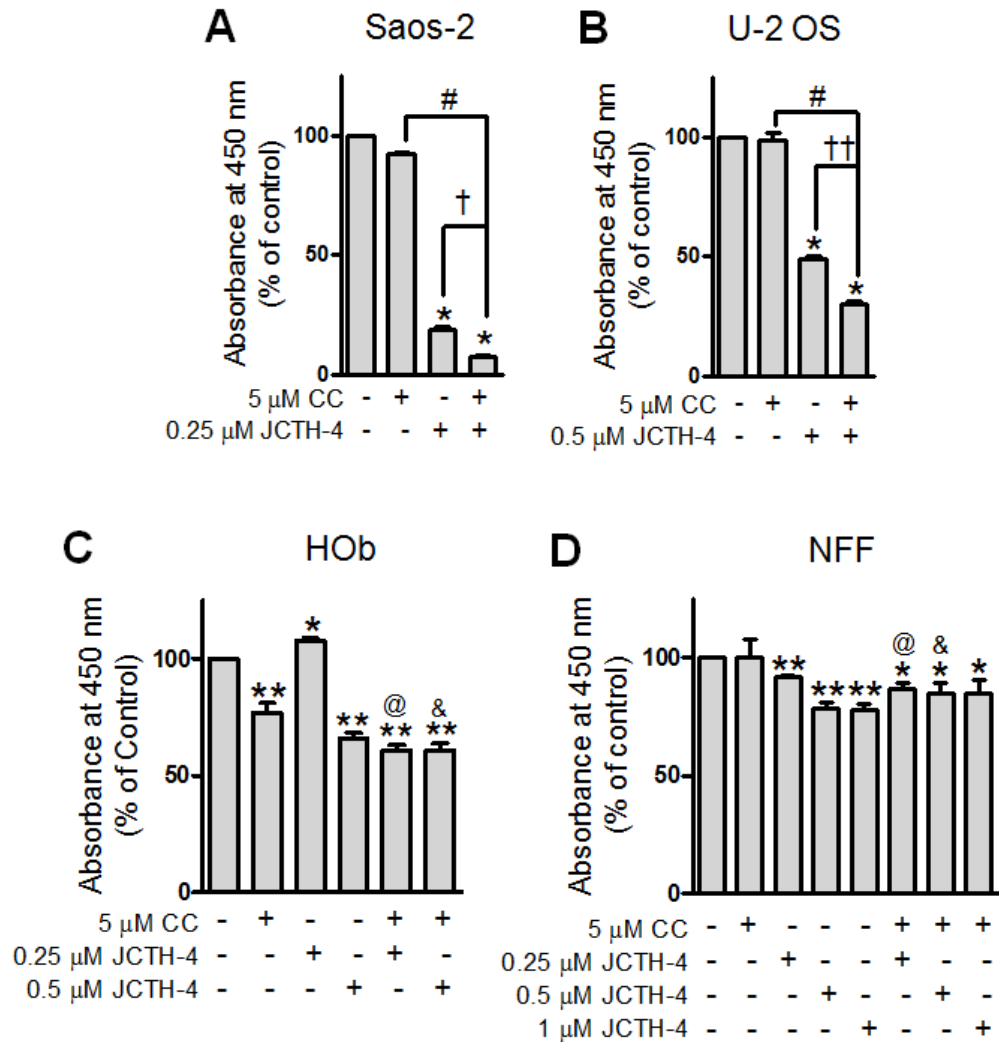


Figure 3.3. CC potentiates the cytotoxicity of JCTH-4 selectively in OS cells. Effect of JCTH-4 & CC in combination on cellular viability of OS cells was determined by the WST-1 based colorimetric assay. **(A)** Saos-2 (96 hours), **(B)** U-2 OS (72 hours), **(C)** HOb (72 hours), and **(D)** NFF (72 hours) cells were treated with JCTH-4 and CC and the WST-1 reagent was used to quantify cellular viability. Absorbance was read at 450 nm and expressed as a percent of the solvent control (Me_2SO). Values are expressed as mean \pm SD from quadruplicates of 3 independent experiments. * p <0.05, ** p <0.01, versus solvent control (Me_2SO); † p <0.001 versus 0.25 μ M JCTH-4; †† p <0.01 versus 0.5 μ M JCTH-4; # p <0.001 versus 5 μ M CC; @ p <0.001 versus 0.25 μ M JCTH-4 + 5 μ M CC treatment with Saos-2 cells (Figure 3A); & p <0.01 versus 0.5 μ M JCTH-4 + 5 μ M CC treatment with U-2 OS cells (Figure 3B).

JCTH-4 alone & in combination with CC induces apoptosis in OS cells

Nuclear and cellular morphology was monitored in Saos-2 and U-2 OS cells treated with JCTH-4 and CC at the indicated concentrations for 96 and 72 hours respectively. As depicted by Hoechst staining, JCTH-4 produced brightly stained, condensed nuclei, and apoptotic bodies while corresponding phase micrographs revealed cell condensation and blebbing in a dose dependent manner; such features are indicative of apoptosis (**Figure 3.4A & B**). This morphology was not present in OS cells treated with 5 μ M CC alone (**Figure 3.4A & B**); however, the frequency of these morphological changes induced by JCTH-4 was enhanced when used with 5 μ M CC (**Figure 3.4A & B**). All of the aforementioned treatments did not produce apoptotic morphology in both HOb and NFF cells (**Figure 3.5A & B**). Selective induction of apoptosis by JCTH-4 alone and in combination with CC in OS cells was confirmed by Annexin V binding to externalized phosphatidylserine, a marker for apoptosis, indicated by green fluorescence (**Figure 3.6 & 3.7**) (Zhang et al. 1997).

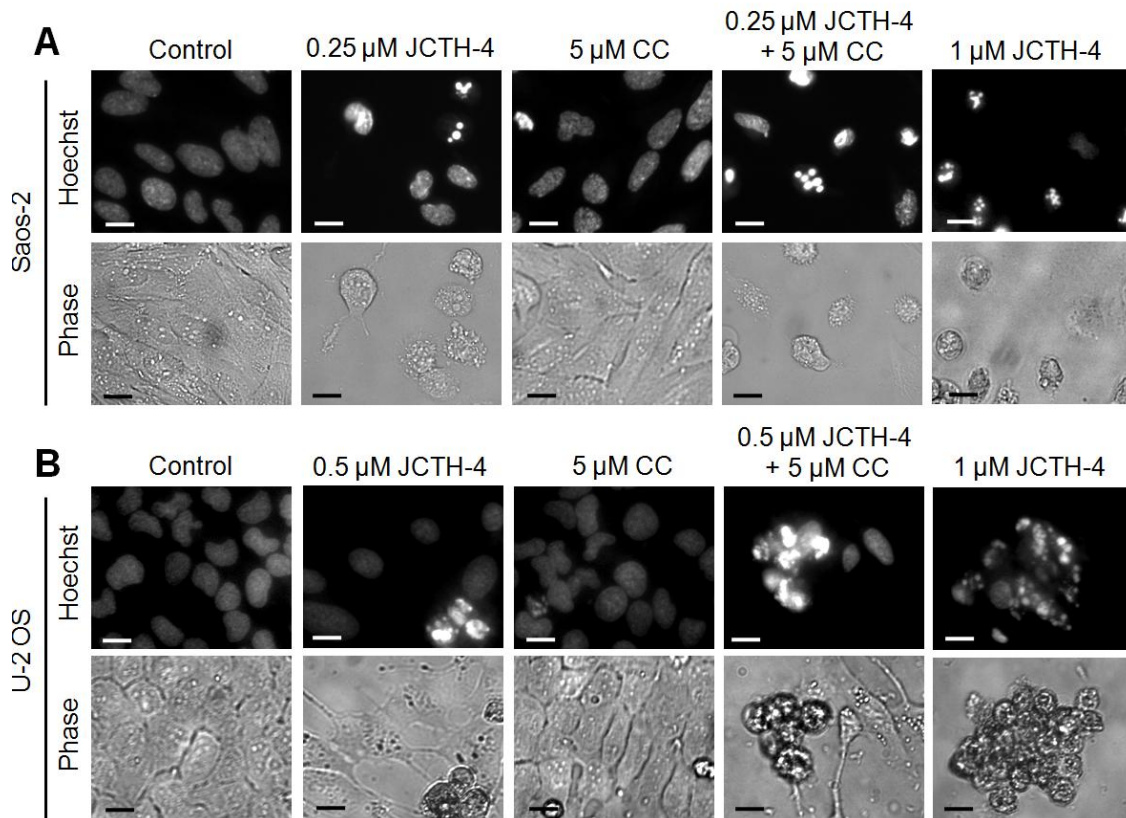


Figure 3.4. JCTH-4 alone and in combination with CC yields apoptotic morphology in OS cells. Nuclear and cellular morphology of **(A)** Saos-2 cells after 96 hours of treatment and **(B)** U-2 OS cells after 72 hours of treatment. Cells were treated with JCTH-4, CC, and solvent control (Me_2SO). Post treatment, the cells were stained with Hoechst 33342 dye. Corresponding phase micrographs are shown below the Hoechst micrographs. Apoptotic morphology is evident in cells with bright and condensed nuclei accompanied by apoptotic bodies, as well as cell shrinkage and blebbing. Images were taken at 400x magnification on a fluorescent microscope. Scale bar = 15 μm .

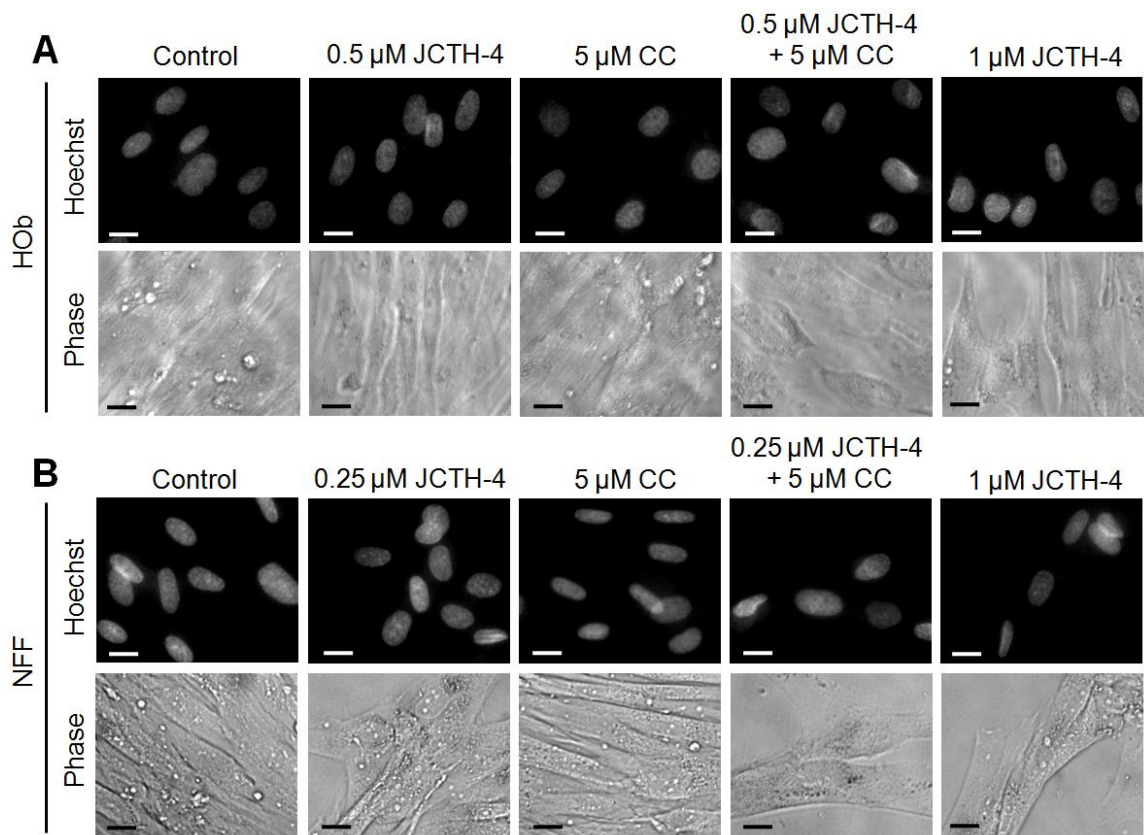


Figure 3.5. JCTH-4 and CC do not yield apoptotic morphology in HOb and NFF cells. Nuclear and cellular morphology of **(A)** HOb and **(B)** NFF cells after 72 hours of treatment. Cells were treated with JCTH-4, CC, and solvent control (Me_2SO). Post treatment, the cells were stained with Hoechst 33342 dye. Corresponding phase micrographs are shown below the Hoechst micrographs. Apoptotic morphology is evident in cells with bright and condensed nuclei accompanied by apoptotic bodies, as well as cell shrinkage and blebbing. Images were taken at 400x magnification on a fluorescent microscope. Scale bar = 15 μm .

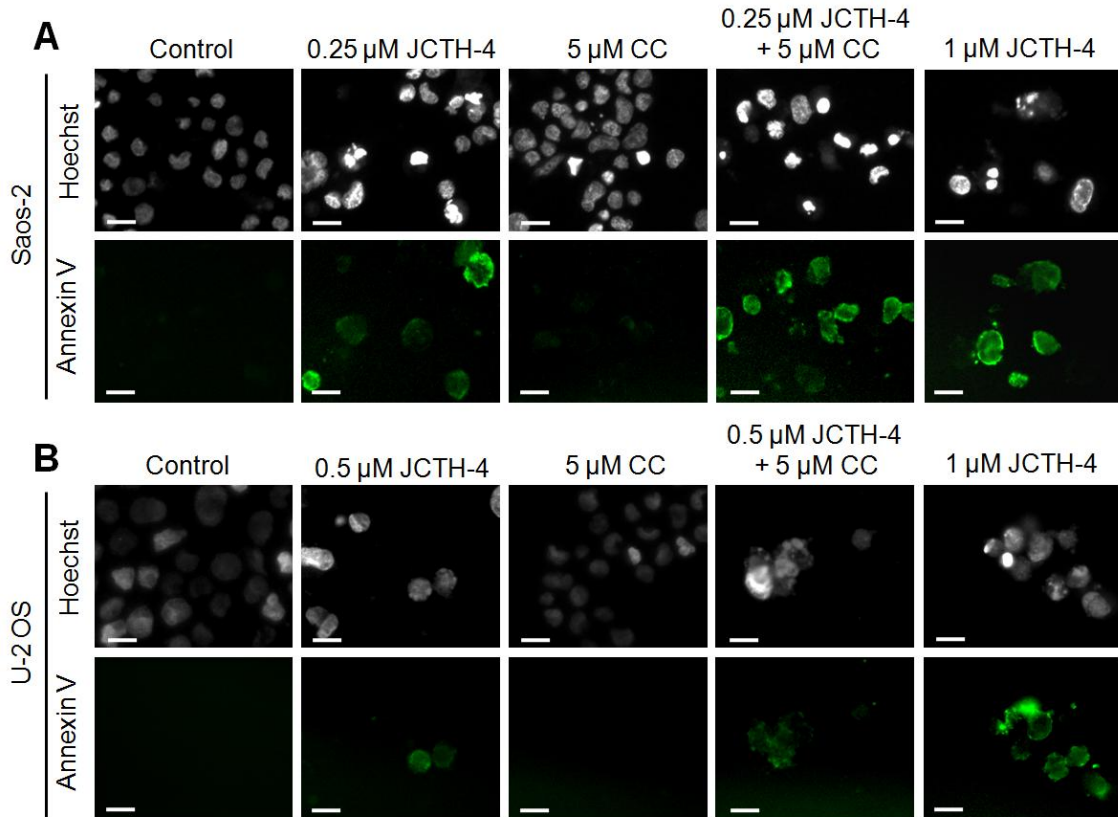


Figure 3.6. JCTH-4 alone and in combination with CC induces phosphatidylserine externalization in OS cells. Annexin V binding to externalized phosphatidylserine was monitored to confirm induction of apoptosis in **(A)** Saos-2 cells after 96 hours of treatment and **(B)** U-2 OS cells after 72 hours of treatment with the indicated concentrations of JCTH-4, CC, and solvent control (Me_2SO). Cells were also stained with Hoechst dye. Images were taken at 400x magnification on a fluorescent microscope. Green fluorescence is indicative of Annexin V binding to externalized phosphatidylserine of the plasma membrane. Scale bar = 15 μm .

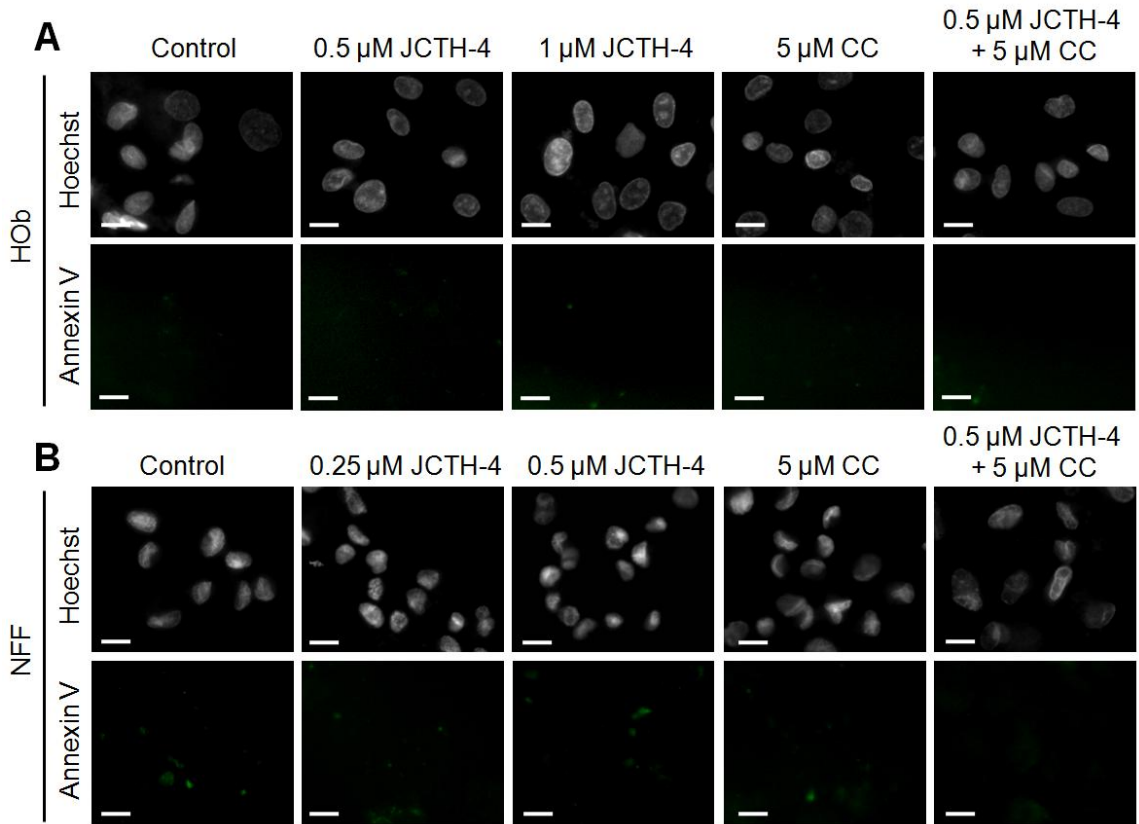


Figure 3.7. JCTH-4 alone and with CC does not induce phosphatidylserine externalization in HOb and NFF cells. Annexin V binding to externalized phosphatidylserine was monitored to confirm that apoptosis was not induced in **(A)** HOb and **(B)** NFF cells after 72 hours of treatment. Cells were treated with the indicated concentrations of JCTH-4, CC and solvent control (Me_2SO). Cells were also stained with Hoechst dye. Images were taken at 400x magnification on a fluorescent microscope. Green fluorescence is indicative of Annexin V binding to externalized phosphatidylserine of the plasma membrane. Scale bar = 15 μ m.

JCTH-4 alone and in combination with CC targets OS cell mitochondria

In preceding studies, PST has been found to exert its effects by way of mitochondrial targeting; thus, mechanistic studies were performed to verify such targeting by JCTH-4 in OS cells (McLachlan et al. 2005; Siedlakowski et al. 2008; Chatterjee et al. 2010; Griffin, Karnik, et al. 2011). Saos-2 and U-2 cells were treated for 96 and 72 hours respectively with JCTH-4 and CC at the indicated concentrations and stained with Hoechst dye and TMRM, an indicator of intact MMP and impermeabilized mitochondrial membrane, depicted by red fluorescence. Greatest dissipation of MMP was seen in OS cells treated with 1 μ M JCTH-4 (**Figure 3.8A & B**). Dissipation of MMP was also seen with lower doses of JCTH-4; this dissipation by JCTH-4 was enhanced with the addition of 5 μ M CC, which had no observable effect on MMP its own (**Figure 3.8A & B**). Additionally, none of these treatments yielded MMP dissipation in HOb and NFF cells (**Figure 3.9A & B**).

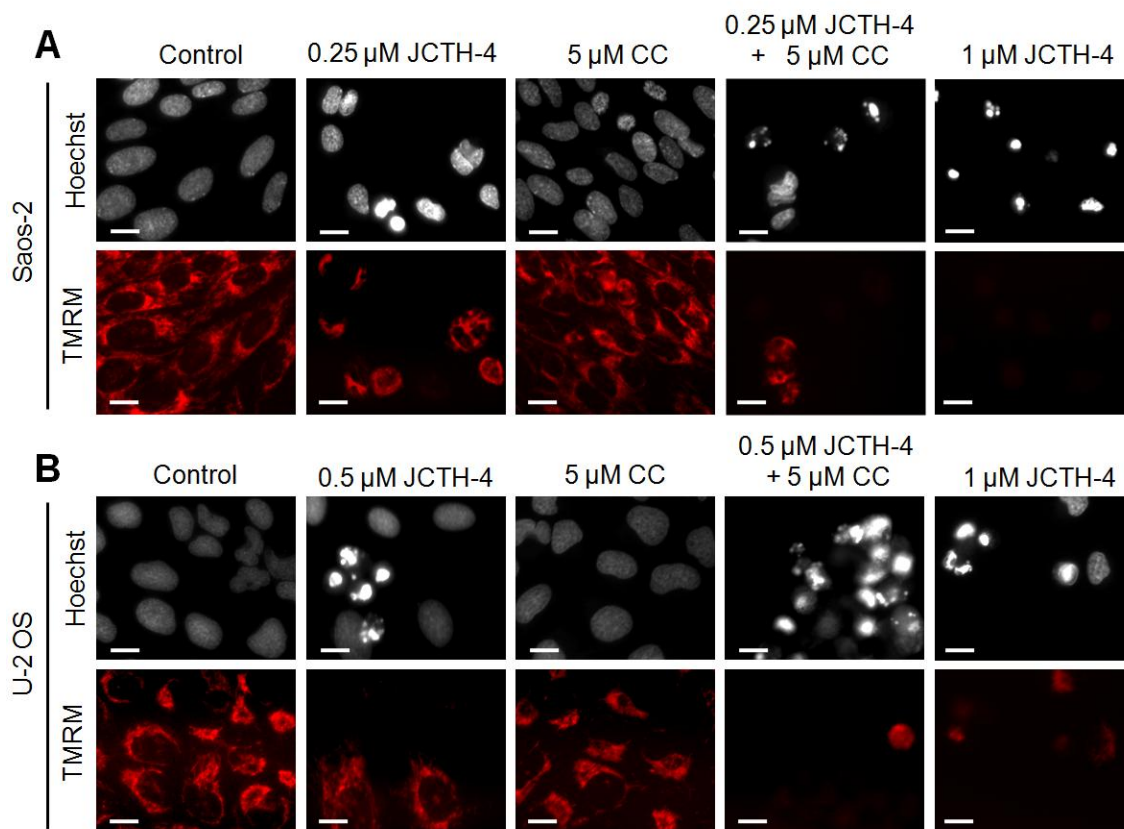


Figure 3.8. JCTH-4 dissipates MMP alone and in combination with CC in OS cells. Effect of JCTH-4 and CC on MMP in **(A)** Saos-2 cells after 96 hours of treatment and **(B)** U-2 OS cells after 72 hours of treatment was examined by TMRM staining. Cells were grown on coverslips, treated with the indicated concentrations of JCTH-4, CC, and solvent control (Me_2SO) and stained with TMRM and Hoechst dye. Images were taken at 400x magnification on a fluorescent microscope. Red fluorescent punctuate marks are indicative of mitochondria with intact MMP. Scale bar = 15 μ m.

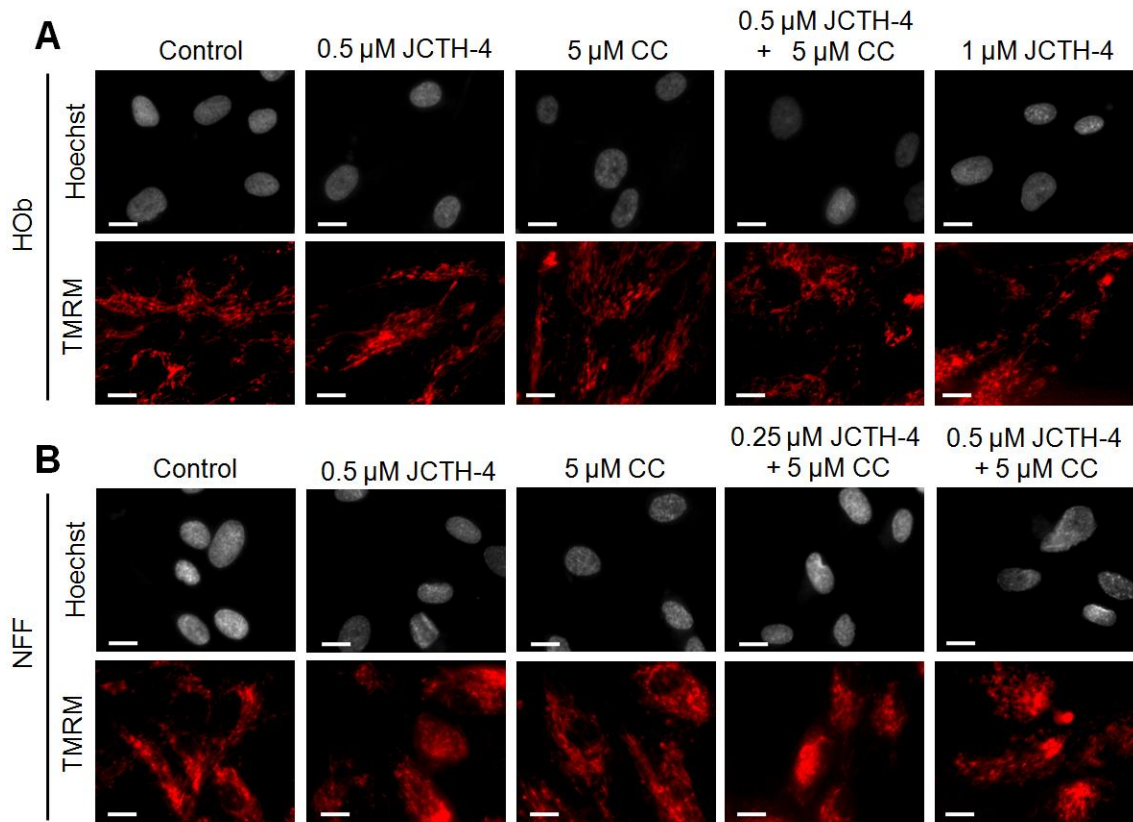


Figure 3.9. JCTH-4 and CC do not dissipate MMP in HOB and NFF cells. Effect of JCTH-4 and CC on MMP in **(A)** HOB and **(B)** NFF cells after 72 hours of treatment was examined by TMRM staining. Cells were grown on coverslips, treated with the indicated concentrations of JCTH-4, CC, and solvent control (Me_2SO), and stained with TMRM and Hoechst dye. Images were taken at 400x magnification on a fluorescent microscope. Red fluorescent punctuate marks are indicative of mitochondria with intact MMP. Scale bar = 15 μm .

Oxidative stress produced in the mitochondria has been associated with the dysfunction of this organelle; in particular, mitochondrial permeabilization and apoptogenic factor release have both been linked to increases in ROS production (Madesh & Hajnóczy 2001; Simon et al. 2000; Batandier et al. 2004; Cochemé & Murphy 2008). After apoptogenic factors are released into the cytosol from the mitochondria, some can execute apoptosis by translocating to the nucleus or participating in cytosolic downstream pathways (Earnshaw 1999). To evaluate the ability of JCTH-4 to induce the generation of ROS directly in mitochondria of OS cells, mitochondria were isolated from Saos-2 and U-2 OS cells, treated directly with various doses of JCTH-4 and CC for 2 hours, and analyzed for ROS production with Amplex Red. JCTH-4 alone at several concentrations caused an increase in ROS production in OS cells which was further enhanced by the addition of 5 μ M CC (**Figure 3.10A & B**). 5 μ M CC alone also increased ROS generation in isolated OS cell mitochondria (Figure 10A,B) PQ, known to cause ROS production in mitochondria, was used as a positive control (Cochemé & Murphy 2008). Furthermore, isolated mitochondria of OS cells treated with JCTH-4 alone or with CC for 2 hours were monitored for the release of apoptogenic factors. Post treatment, mitochondrial samples were resuspended and centrifuged; resultant post mitochondrial supernatants and mitochondrial pellets were monitored by western blot analyses for the release and retention of apoptogenic factors respectively. By analyzing the resultant mitochondrial pellet samples of U-2 OS cells, isolated U-2 OS cell mitochondria treated with JCTH-4 retained less of the apoptogenic factor AIF (**Figure 3.10C**). JCTH-4 also caused

the release of the apoptogenic factor EndoG in a dose dependent manner from these U-2 OS mitochondria, deduced by the analysis of the post mitochondrial supernatants (**Figure 3.10C**). Similarly, JCTH-4 and 5 μ M CC alone caused the release of AIF from isolated mitochondria of Saos-2 cells; however, combinatorial treatment yielded the greatest release of AIF (**Figure 3.10D**).

The execution of apoptosis by released apoptogenic factors from the mitochondria can be achieved with the activation of proteins known as caspases, a family of cysteine proteases, or directly by the apoptogenic factor (Earnshaw 1999; Kroemer et al. 2010). To determine the dependence of caspases in JCTH-4-induced apoptosis, the broad spectrum caspase inhibitor Z-VAD-FMK was used at various doses in combination with JCTH-4. However, as determined through the WST-1 based colorimetric assay for cell viability, this inhibitor was not able to protect Saos-2 cells from JCTH-4 insult (**Figure 3.10E**). Thus, JCTH-4 exerts its cytotoxicity against OS cells in a manner independent of caspase activation.

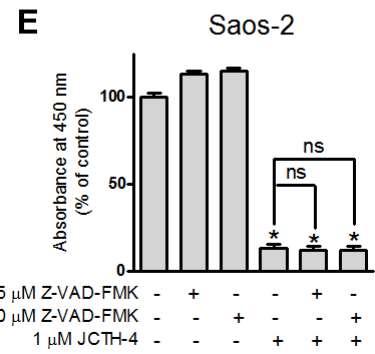
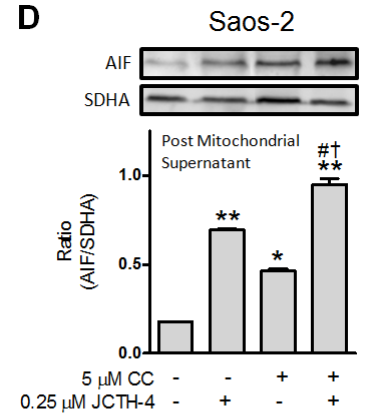
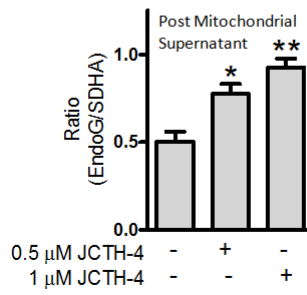
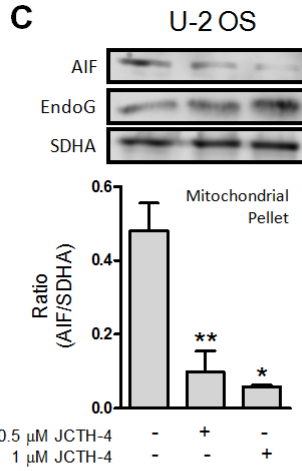
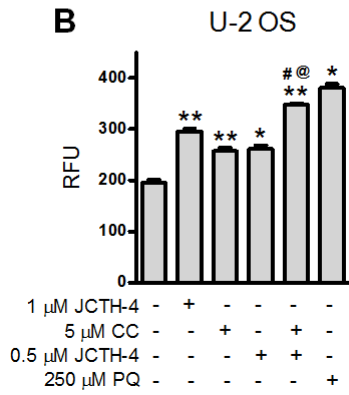
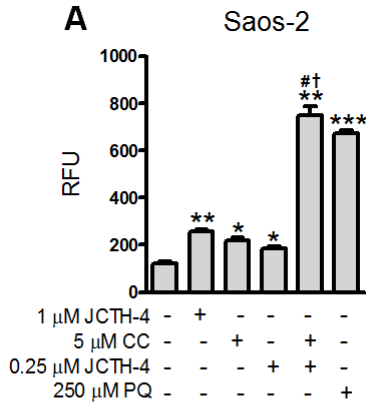


Figure 3.10. JCTH-4 directly causes mitochondrial ROS production and release of apoptogenic factors independent of caspases. (A) Saos-2 and **(B)** U-2 OS isolated mitochondria were treated directly with JCTH-4, CC, PQ, and solvent control (Me₂SO), and incubated with Amplex Red and horseradish peroxidase for 2 hours. Subsequently, fluorescence readings were taken at Ex. 560 nm and Em. 590 nm and expressed as relative fluorescence units (RFU). Statistics were performed using GraphPad Prism version 5.0. Image is representative of 3 independent experiments demonstrating similar trends. Values are expressed as mean ± SD of quadruplicates of 1 independent experiment. **p*<0.05, ***p*<0.01, ****p*<0.001 versus solvent control (Me₂SO); †*p*<0.01 versus 0.25 μM JCTH-4; @*p*<0.01 versus 0.5 μM JCTH-4; #*p*<0.01 versus 5 μM CC. Isolated mitochondria samples treated directly with JCTH-4, CC, and solvent control (Me₂SO) for 2 hours were also centrifuged, producing mitochondrial pellets and post mitochondrial supernatants which were examined for retention and release of apoptogenic factors respectively via western blot analyses; **(C)** Retention of AIF and release of EndoG by U-2 OS cell mitochondria and **(D)** release of AIF by Saos-2 cell mitochondria was monitored. Mitochondrial pellets were probed for SDHA to serve as loading controls. Densitometric analyses were performed using ImageJ software and statistics were calculated using GraphPad Prism version 5.0. Image is representative of 3 independent experiments demonstrating similar trends. Values are expressed as mean ± SD of triplicates of one independent experiment. **p*<0.01, ***p*<0.001 versus solvent control (Me₂SO); †*p*<0.01 versus 0.25 μM JCTH-4; #*p*<0.01 versus 5 μM CC. **(E)** Saos-2 cells were treated with broad spectrum caspase inhibitor Z-VAD-FMK with and without JCTH-4 for 72 hours. WST-1 reagent was used to quantify cell viability. Absorbance was read at 450 nm and expressed as a percent of solvent control (Me₂SO). Values are expressed as mean ± SD from quadruplicates of 3 independent experiments. **p*<0.001 versus solvent control (Me₂SO); ns = not significant.

JCTH-4 selectively induces autophagy alone and with CC in OS cells

Various studies have reported chemotherapeutics to trigger both pro-death and pro-survival autophagy (Dalby et al. 2010). Moreover, because JCTH-4 produced oxidative stress, a known autophagy inducer, we monitored OS cells for autophagic induction following treatment with JCTH-4 and CC. As illustrated MDC staining, OS cells treated with various doses of JCTH-4 produced blue punctate staining, indicative of autophagic vacuoles (**Figure 3.11A & B**). Such staining was also seen with the combinatorial treatment of 0.25 μ M JCTH-4 and 5 μ M CC, but not with 5 μ M CC treatment alone (**Figure 3.11A & B**). Corresponding phase and PI images show cell shrinkage and blebbing with JCTH-4 treatment alone and in combination, but not with CC alone, while only combination treatment gave some positive PI staining (**Figure 3.11A & B**).

During autophagy, LC3 situated in the cytosol, referred to as LC3-I, is converted to LC3-II, a lipidated form of LC3 that is recruited to autophagosomal membranes (Kabeya et al. 2000). To confirm the induction of autophagy in OS cells, western blot analyses were carried out on cell lysates of Saos-2 cells treated with the indicated concentrations of JCTH-4 and CC for 72 hours to monitor the conversion of LC3-I to LC3-II. TAM, a known inducer of autophagy, was used as a positive control. This conversion was enhanced with JCTH-4 at various concentrations (**Figure 3.11C**). With the treatment of 5 μ M CC alone, LC3-II conversion decreased, and when used with 0.25 μ M JCTH-4, the effect was not significantly different from 0.25 μ M JCTH-4 alone (**Figure 3.11C**). In HOb and NFF cells, autophagic induction was only seen in the TAM positive

control groups but not in cells treated with JCTH-4 and CC alone and in combination (**Figure 3.12A & B**). Therefore, JCTH-4 selectively induces autophagy in OS cells.

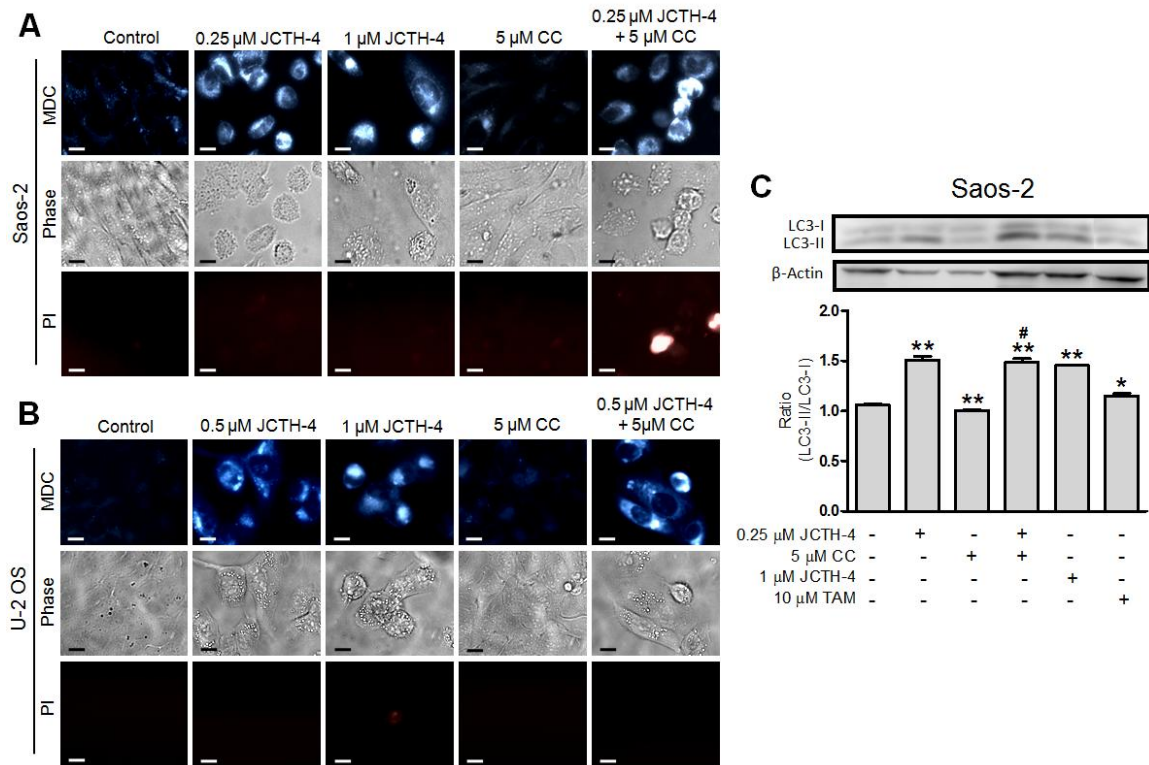


Figure 3.11. JCTH-4 induces autophagy in OS cells alone and with CC. The presence of autophagic vacuoles in **(A)** Saos-2 after 96 hours of treatment and **(B)** U-2 OS cells after 72 hours of treatment with JCTH-4, CC, and solvent control (Me_2SO) was determined by MDC staining. Bright blue punctate marks are indicative of autophagic vacuoles. Corresponding phase and PI micrographs are shown below the MDC images. Scale bar = 15 μm . **(C)** Cell lysates of Saos-2 cells treated with JCTH-4, CC, TAM as positive control, and solvent control (Me_2SO) for 72 hours were examined for the conversion of LC3-I to LC3-II by western blot analyses. β -actin was probed to serve as a loading control. Densitometric analyses were done using ImageJ software and statistics were calculated using GraphPad Prism version 5.0. Image is representative of 3 independent experiments demonstrating similar trends. Values are expressed as mean \pm SD of triplicates of one independent experiment. * p <0.05, ** p <0.01 versus solvent control (Me_2SO); # p <0.01 versus 5 μM CC.

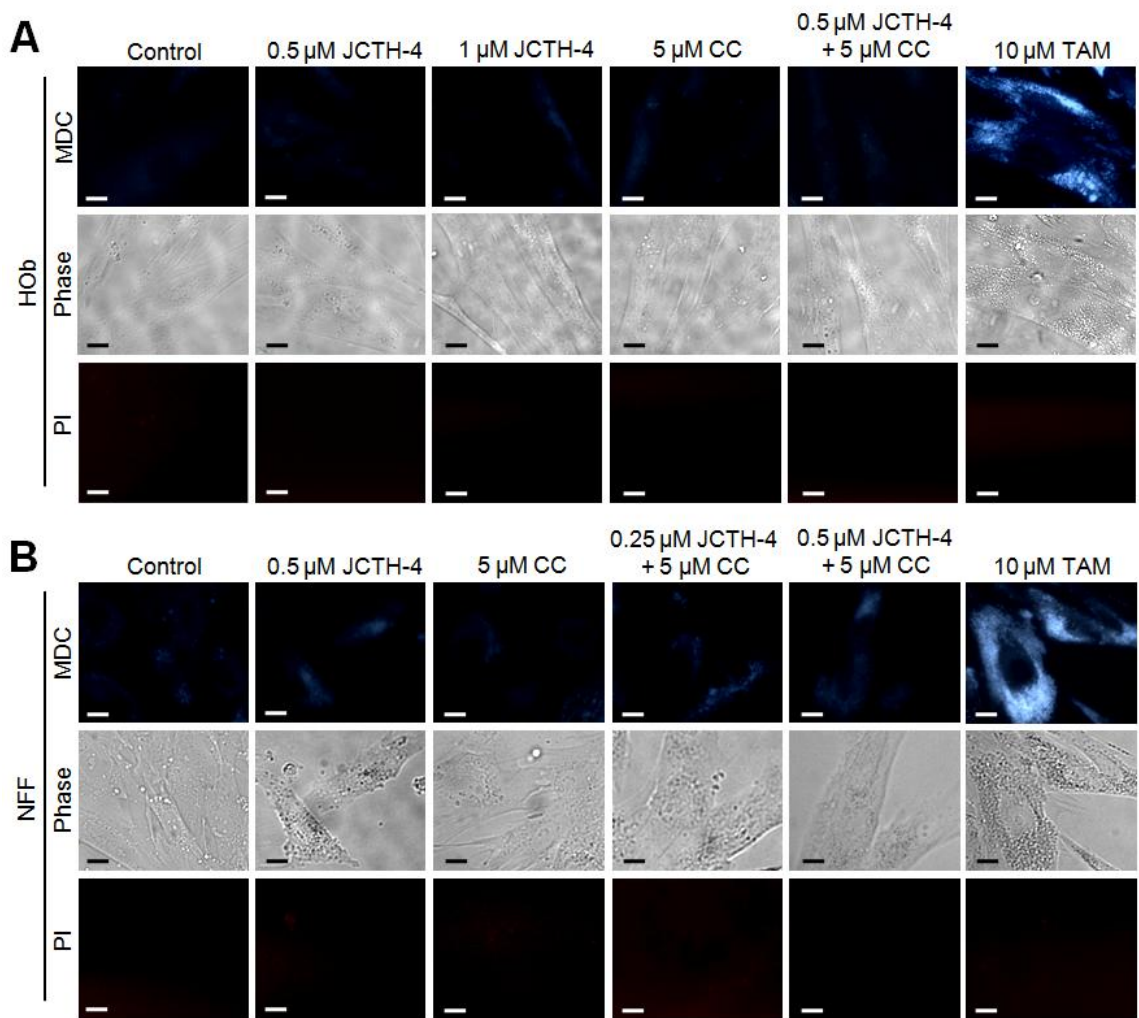


Figure 3.12. JCTH-4 and CC do not induce autophagy in Hob and NFF cells. MDC staining was used to detect the presence of autophagic vacuoles in **(A)** Hob and **(B)** NFF cells after 72 hours of treatment with JCTH-4, CC, and solvent control (Me_2SO) at the indicated concentrations. Bright blue punctate marks are indicative of autophagic vacuoles. Corresponding phase and PI micrographs are shown below the MDC images. Scale bar = 15 μ m.

Discussion

In this study, we demonstrate JCTH-4 to be a highly potent agent against OS cells. More specifically, JCTH-4 exerts its cytotoxicity against OS by way of apoptotic induction; OS cells treated with JCTH-4 exhibited cell shrinkage, blebbing, nuclear condensation, apoptotic body formation, phosphatidylserine externalization, and MMP dissipation (**Figure 3.4, 3.6, 3.8**). OS cells treated with JCTH-4 alone were negative for PI staining, a plasma membrane impermeable DNA stain, suggesting these cells were not dying by necrosis, a form of cell death characterized by lysis of the plasma membrane (**Figure 3.11A & B**) (Pollack & Leeuwenburgh 2001). However, some PI positive staining was present in the combination treatment with CC, which could be a result of the permeabilization of cell membranes of late apoptotic cells (**Figure 3.11A & B**) (Gregory & Devitt 2004). Considerable toxicity to non-malignant tissue has been associated with a majority of the chemotherapeutics used for OS (Singal & Iliskovic 1998; Ta et al. 2006; Flombaum & Meyers 1999; Gurjal et al. 1999; Loebstein & Koren 1998). However, HOb cells, a normal non-cancerous equivalent to the OS cells used in this study, as well as NFF cells exhibited markedly decreased sensitivity and did not show evident signs of apoptotic induction with JCTH-4 treatment (**Figure 3.2C, 3.5, 3.7, 3.9**); therefore, JCTH-4 is selective towards OS cells and may prove to be a safer alternative for OS treatment to the current chemotherapeutics in use. Such selectivity suggests a specific target in cancer cells.

Previously, we have provided supporting evidence suggesting that PST targets cancer cell mitochondria (McLachlan et al. 2005; Griffin, Karnik, et al. 2011). Complementing this data, we report similar results with JCTH-4. In addition to the JCTH-4-induced collapse of MMP in OS cells, observations made after direct JCTH-4-insult to isolated OS mitochondria strongly suggest this specific apoptotic activity to be attributed to mitochondrial targeting; with regards to isolated mitochondria from OS cells, JCTH-4 caused an increase in ROS generation and the release of apoptogenic factors (**Figure 3.10**). Likewise, PST selectively dissipated MMP with whole cell treatment and caused ROS production in isolated cancer cell mitochondria and not in non-cancerous cell mitochondria (McLachlan et al. 2005; Siedlakowski et al. 2008). Additionally, the tumor suppressor p53, which causes the expression of proapoptotic proteins that permeabilize the mitochondria in response to different forms of intracellular stress, proved to be of little importance in JCTH-4-induced apoptosis (Zilfou & Lowe 2009); Saos-2 cells, which do not express p53, and U-2 OS cells, with wildtype p53, were equally very sensitive to JCTH-4 insult (**Figure 3.2A & B, 3.4**) (Masuda et al. 1987; Navaraj et al. 2005). This circumvention in p53 activity strengthens the argument for a mitochondrial target as all p53 cellular events upstream of mitochondrial permeabilization have been proven to be insignificant in JCTH-4-induced cytotoxicity. As well as taking part in apoptosis pathways involved with the mitochondria, caspases are also utilized in apoptosis pathways independent of the mitochondria (Degterev et al. 2003). Akin to PST, we have found caspases to be nonessential in JCTH-4-induced apoptosis (**Figure 3.10E**),

and that AIF and EndoG, two apoptogenic factors involved in caspase-independent pathways of apoptosis, are released from the mitochondria by direct JCTH-4 insult (**Figure 3.10C & D**); thus, caspase signalling upstream of mitochondrial membrane permeabilization and independent of mitochondria are not vital for the induction of apoptosis by JCTH-4, thereby further supporting the notion of a mitochondrial target by JCTH-4 (Griffin, Karnik, et al. 2011; Earnshaw 1999; Degterev et al. 2003; Susin et al. 1999; Li et al. 2001). It is this targeting of the mitochondria that may provide the means to cancer selectivity by JCTH-4.

Cancer cells possess many distinct characteristics, such as marked differences in their mitochondria and energy metabolism, which may be exploited for cancer selective therapy (Gogvadze et al. 2008; Chen et al. 2010). Cancer cells possess a distinct metabolic phenotype, a phenomenon referred to as the Warburg effect, in which levels of aerobic glycolysis are elevated; thus, these cells have high glucose uptake and through the production of lactate, produce an acidic microenvironment (Warburg 1956; Gambhir 2002; Gatenby & Gillies 2004). Consequently, this glycolytic shift confers a proliferative advantage and an acquired resistance to apoptosis in cancer cells; intermediates of glycolysis provide a vast source of resources needed for nucleotide and lipid synthesis and alterations of the outer mitochondrial membrane have rendered it less susceptible to permeabilization (DeBerardinis et al. 2008; Gogvadze et al. 2010; Plas & Thompson 2002). Therefore, a promising strategy in cancer therapy would be to divert cancer cell metabolism away from glycolysis, which was demonstrated by other efforts via the promotion of oxidative phosphorylation

(Bonnet et al. 2007). Such a strategy may be employed by JCTH-4. A major factor promoting the resistance to apoptosis as a result of this metabolic shift is the glycolytic enzyme hexokinase; its association to the outer mitochondrial membrane has been shown to discourage mitochondrial membrane permeabilization (Vander Heiden et al. 2009; Pastorino et al. 2002). Cancer cells have also been reported to highly express antiapoptotic members of the Bcl-2 family of proteins, all of which inhibit mitochondrial outer membrane permeabilization (Green & Kroemer 2004; Casellas et al. 2002). Thus, JCTH-4 may act by targeting these proteins.

Traditional medicines have long used natural products in treating various disorders. Modern science is now rediscovering many of these products and their potential in rectifying numerous pathological conditions (Griffin, Karnik, et al. 2011; Chatterjee et al. 2011). The natural compound CC, used to treat an array of ailments, has been recognized to possess potent activity against numerous cancers, including OS (Walters et al. 2008; Ravindran et al. 2009). As determined by the WST-1 colorimetric assay, other reports have established IC_{50} values of 17.2 μ M and 21.6 μ M in Saos-2 and U-2 OS cells respectively after 72 hours (Walters et al. 2008). By similar means, we found 5 μ M CC to have very little to no effect on these cell lines (**Figure 3.3A & B**). However, when used with JCTH-4, CC was found to potentiate the cytotoxic effects of JCTH-4 in both Saos-2 and U-2 OS cells with HO_b and NFF cells being markedly less sensitive to this combinatorial treatment (**Figure 3.3A-D**). Like JCTH-4 treatment alone, this combinatorial treatment exerts its cytotoxicity against OS cells selectively

through induction of apoptosis (**Figure 3.4-3.7**). Although whole cell treatment of OS cells with 5 μ M CC did not appear to effect viability of mitochondria (**Figure 3.8**), direct insult to isolated OS mitochondria induced ROS production and release of AIF (**Figure 3.10A, B, D**); such discrepancies between whole cell and direct mitochondrial treatment may be attributed to low solubility or uptake of CC (Kurien et al. 2007). In accordance with our findings, although at higher doses, other studies report whole cell treatment with CC to induce ROS production and AIF release from mitochondria (Thayyullathil et al. 2008; Rashmi et al. 2005). Interestingly, direct treatment of CC on OS mitochondria enhanced ROS production and AIF release (**Figure 3.10A, B, D**). CC is known to bind and target numerous proteins; however, these findings suggest CC binds either one of these known targets and/or an unknown protein, both associated to the mitochondria (Ravindran et al. 2009; Aggarwal et al. 2007). As JCTH-4 is shown to elicit its cancer selective effects via mitochondrial targeting, such targeting by CC may be responsible for sensitizing OS cells to JCTH-4-induced apoptosis.

Dual roles, both pro-death and pro-survival, have been implicated in autophagic induction elicited by chemotherapeutic insult (Dalby et al. 2010). JCTH-4 was found to induce autophagy at doses between 0.25 μ M and 1 μ M while 5 μ M CC yielded no observable autophagic response in OS cells (**Figure 3.11**). The autophagic response produced by the combination treatment of 5 μ M CC and 0.25 μ M JCTH-4 was not significantly different from the response elicited by the 0.25 μ M JCTH-4 treatment alone; this may indicate the enhancement in activity of JCTH-4 by CC to be a result of targeting the apoptosis pathway rather

than that of autophagy by CC. Previous work has shown CC alone to induce autophagy, although at much higher doses used in this study; inconsistencies between these findings and that of this report again may be attributed to the low solubility and uptake of CC (Kurien et al. 2007; Aoki et al. 2007). JCTH-4 treatment yielded autophagic induction which was accompanied by significant cytotoxicity and cell death, as depicted in the corresponding phase images and previous figures (**Figure 3.2A & B, 3.3A & B, 3.4, 3.6, 3.11A & B**); this may indicate JCTH-induced autophagy to be a detrimental response in OS cells. Such induction was not evident in HOb and NFF cells (**Figure 3.13**); therefore, autophagic induction by JCTH-4 is selective towards OS cells. As established in this report, JCTH-4 causes mitochondrial ROS production and mitochondrial dysfunction. Oxidative stress is a known inducer of autophagy and thus, JCTH-4 may trigger autophagy as a default mechanism (Kroemer et al. 2010). Regardless, because JCTH-4 permeabilizes OS cell mitochondria, these cells ultimately die from apoptosis.

Recapitulating the findings of this report, JCTH-4, was found to effectively induce apoptosis and autophagy in OS cells with evidence suggesting this to be a result of mitochondria targeting. Additionally, the natural compound CC was able to potentiate these cytotoxic effects induced by JCTH-4 against OS cells. Importantly, JCTH-4 treatment alone and in combination proved to be selective towards OS cells as non-cancerous cells were markedly less sensitive and did not show evident signs of apoptotic and autophagic induction. Thus, we present

a promising novel strategy, combining the novel synthetic compound JCTH-4 and the natural compound CC for the treatment of OS.

Author Contributions

Conceived and designed the experiments: DM SP. Performed the experiments: DM PT KM JC TH. Analyzed the data: DM SP. Synthesized and provided JCTH-4 used in this study: JC TH. Wrote the paper: DM PT KM SP.

Acknowledgements

Thank you to Cynthia Tran for her initial work on this project and Manika Gupta for the critical review of this manuscript.

Funding

Funding of this work has been provided as a generous gift by the Knights of Columbus Chapter 9671 (Windsor, Ontario). This work has also been supported by a CIHR Frederick Banting and Charles Best Canada Graduate Scholarship awarded to Dennis Ma. The funders had no role in study design, data collection and analysis, decision to publish, or preparation of the manuscript.

References

- Aggarwal, B.B. et al., 2007. Curcumin: the Indian solid gold. *Advances in experimental medicine and biology*, 595, pp.1–75.
- Aoki, H. et al., 2007. Evidence that curcumin suppresses the growth of malignant gliomas in vitro and in vivo through induction of autophagy: role of Akt and extracellular signal-regulated kinase signaling pathways. *Molecular pharmacology*, 72(1), pp.29–39.
- Arndt, C.A. & Crist, W.M., 1999. Common musculoskeletal tumors of childhood and adolescence. *The New England journal of medicine*, 341(5), pp.342–52.
- Batandier, C., Leverage, X. & Fontaine, E., 2004. Opening of the mitochondrial permeability transition pore induces reactive oxygen species production at the level of the respiratory chain complex I. *The Journal of biological chemistry*, 279(17), pp.17197–204.
- Baum, E.S. et al., Phase II trial cisplatin in refractory childhood cancer: Children's Cancer Study Group Report. *Cancer treatment reports*, 65(9-10), pp.815–22.
- Bielack, S.S. et al., 2002. Prognostic factors in high-grade osteosarcoma of the extremities or trunk: an analysis of 1,702 patients treated on neoadjuvant cooperative osteosarcoma study group protocols. *Journal of clinical oncology : official journal of the American Society of Clinical Oncology*, 20(3), pp.776–90.
- Bonnet, S. et al., 2007. A mitochondria-K⁺ channel axis is suppressed in cancer and its normalization promotes apoptosis and inhibits cancer growth. *Cancer cell*, 11(1), pp.37–51.

- Borst, P. & Rottenberg, S., 2004. Cancer cell death by programmed necrosis? *Drug resistance updates: reviews and commentaries in antimicrobial and anticancer chemotherapy*, 7(6), pp.321–4.
- Casellas, P., Galiegue, S. & Basile, A.S., 2002. Peripheral benzodiazepine receptors and mitochondrial function. *Neurochemistry international*, 40(6), pp.475–86.
- Chatterjee, S.J. et al., 2011. The efficacy of dandelion root extract in inducing apoptosis in drug-resistant human melanoma cells. *Evidence-based complementary and alternative medicine: eCAM*, 2011, p.129045.
- Chatterjee, S.J., McNulty, J. & Pandey, S., 2010. Sensitization of human melanoma cells by tamoxifen to apoptosis induction by pancratistatin, a nongenotoxic natural compound. *Melanoma research*.
- Chen, G. et al., 2010. Preferential killing of cancer cells with mitochondrial dysfunction by natural compounds. *Mitochondrion*, 10(6), pp.614–25.
- Cochemé, H.M. & Murphy, M.P., 2008. Complex I is the major site of mitochondrial superoxide production by paraquat. *The Journal of biological chemistry*, 283(4), pp.1786–98.
- Collins, J. et al., 2010. Chemoenzymatic synthesis of Amaryllidaceae constituents and biological evaluation of their C-1 analogues. The next generation synthesis of 7-deoxypancratistatin and trans-dihydrolycoricidine. *The Journal of organic chemistry*, 75(9), pp.3069–84.
- Dalby, K.N. et al., 2010. Targeting the prodeath and prosurvival functions of autophagy as novel therapeutic strategies in cancer. *Autophagy*, 6(3),

pp.322–9.

- DeBerardinis, R.J. et al., 2008. The biology of cancer: metabolic reprogramming fuels cell growth and proliferation. *Cell metabolism*, 7(1), pp.11–20.
- Degterev, A., Boyce, M. & Yuan, J., 2003. A decade of caspases. *Oncogene*, 22(53), pp.8543–67.
- Earnshaw, W.C., 1999. Apoptosis. A cellular poison cupboard. *Nature*, 397(6718), pp.387, 389.
- Epelbaum, R. et al., 2010. Curcumin and gemcitabine in patients with advanced pancreatic cancer. *Nutrition and cancer*, 62(8), pp.1137–41.
- Flombaum, C.D. & Meyers, P.A., 1999. High-dose leucovorin as sole therapy for methotrexate toxicity. *Journal of clinical oncology: official journal of the American Society of Clinical Oncology*, 17(5), pp.1589–94.
- Gambhir, S.S., 2002. Molecular imaging of cancer with positron emission tomography. *Nature reviews. Cancer*, 2(9), pp.683–93.
- Gatenby, R.A. & Gillies, R.J., 2004. Why do cancers have high aerobic glycolysis? *Nature reviews. Cancer*, 4(11), pp.891–9.
- Gogvadze, V., Orrenius, S. & Zhivotovsky, B., 2008. Mitochondria in cancer cells: what is so special about them? *Trends in cell biology*, 18(4), pp.165–73.
- Gogvadze, V., Zhivotovsky, B. & Orrenius, S., 2010. The Warburg effect and mitochondrial stability in cancer cells. *Molecular aspects of medicine*, 31(1), pp.60–74.
- Goorin, A.M. et al., 1991. Changing pattern of pulmonary metastases with adjuvant chemotherapy in patients with osteosarcoma: results from the

- multiinstitutional osteosarcoma study. *Journal of clinical oncology: official journal of the American Society of Clinical Oncology*, 9(4), pp.600–5.
- Gozuacik, D. & Kimchi, A., 2004. Autophagy as a cell death and tumor suppressor mechanism. *Oncogene*, 23(16), pp.2891–906.
- Green, D.R. & Kroemer, G., 2004. The pathophysiology of mitochondrial cell death. *Science (New York, N.Y.)*, 305(5684), pp.626–9.
- Gregory, C.D. & Devitt, A., 2004. The macrophage and the apoptotic cell: an innate immune interaction viewed simplistically? *Immunology*, 113(1), pp.1–14.
- Griffin, C., Karnik, A., et al., 2011. Pancratistatin selectively targets cancer cell mitochondria and reduces growth of human colon tumor xenografts. *Molecular cancer therapeutics*, 10(1), pp.57–68.
- Griffin, C., McNulty, J. & Pandey, S., 2011. Pancratistatin induces apoptosis and autophagy in metastatic prostate cancer cells. *International journal of oncology*, 38(6), pp.1549–56.
- Gurjal, A. et al., 1999. Etoposide-induced pulmonary toxicity. *Lung cancer (Amsterdam, Netherlands)*, 26(2), pp.109–12.
- Vander Heiden, M.G., Cantley, L.C. & Thompson, C.B., 2009. Understanding the Warburg effect: the metabolic requirements of cell proliferation. *Science (New York, N.Y.)*, 324(5930), pp.1029–33.
- Kabeya, Y. et al., 2000. LC3, a mammalian homologue of yeast Apg8p, is localized in autophagosome membranes after processing. *The EMBO journal*, 19(21), pp.5720–8.

- Kekre, N. et al., 2005. Pancratistatin causes early activation of caspase-3 and the flipping of phosphatidyl serine followed by rapid apoptosis specifically in human lymphoma cells. *Cancer chemotherapy and pharmacology*, 56(1), pp.29–38.
- Kroemer, G., Mariño, G. & Levine, B., 2010. Autophagy and the integrated stress response. *Molecular cell*, 40(2), pp.280–93.
- Kurien, B.T. et al., 2007. Improving the solubility and pharmacological efficacy of curcumin by heat treatment. *Assay and drug development technologies*, 5(4), pp.567–76.
- Kuttan, R. et al., 1985. Potential anticancer activity of turmeric (*Curcuma longa*). *Cancer letters*, 29(2), pp.197–202.
- Levine, B., 2007. Cell biology: autophagy and cancer. *Nature*, 446(7137), pp.745–7.
- Li, L.Y., Luo, X. & Wang, X., 2001. Endonuclease G is an apoptotic DNase when released from mitochondria. *Nature*, 412(6842), pp.95–9.
- Liu, J. et al., 2011. Targeting apoptotic and autophagic pathways for cancer therapeutics. *Cancer letters*, 300(2), pp.105–14.
- Loebstein, R. & Koren, G., 1998. Ifosfamide-induced nephrotoxicity in children: critical review of predictive risk factors. *Pediatrics*, 101(6), p.E8.
- Madesh, M. & Hajnóczky, G., 2001. VDAC-dependent permeabilization of the outer mitochondrial membrane by superoxide induces rapid and massive cytochrome c release. *The Journal of cell biology*, 155(6), pp.1003–15.
- Marina, N. et al., 2004. Biology and therapeutic advances for pediatric

- osteosarcoma. *The oncologist*, 9(4), pp.422–41.
- Masuda, H. et al., 1987. Rearrangement of the p53 gene in human osteogenic sarcomas. *Proceedings of the National Academy of Sciences of the United States of America*, 84(21), pp.7716–9.
- McLachlan, A. et al., 2005. Pancratistatin: a natural anti-cancer compound that targets mitochondria specifically in cancer cells to induce apoptosis. *Apoptosis: an international journal on programmed cell death*, 10(3), pp.619–30.
- Meistrich, M.L. et al., 1989. Recovery of sperm production after chemotherapy for osteosarcoma. *Cancer*, 63(11), pp.2115–23.
- Navaraj, A., Mori, T. & El-Deiry, W.S., 2005. Cooperation between BRCA1 and p53 in repair of cyclobutane pyrimidine dimers. *Cancer biology & therapy*, 4(12), pp.1409–14.
- Pastorino, J.G., Shulga, N. & Hoek, J.B., 2002. Mitochondrial binding of hexokinase II inhibits Bax-induced cytochrome c release and apoptosis. *The Journal of biological chemistry*, 277(9), pp.7610–8.
- Patel, B.B. & Majumdar, A.P.N., 2009. Synergistic role of curcumin with current therapeutics in colorectal cancer: minireview. *Nutrition and cancer*, 61(6), pp.842–6.
- Plas, D.R. & Thompson, C.B., 2002. Cell metabolism in the regulation of programmed cell death. *Trends in endocrinology and metabolism: TEM*, 13(2), pp.75–8.
- Pollack, M. & Leeuwenburgh, C., 2001. Apoptosis and aging: role of the

- mitochondria. *The journals of gerontology. Series A, Biological sciences and medical sciences*, 56(11), pp.B475–82.
- Rashmi, R., Kumar, S. & Karunagaran, D., 2005. Human colon cancer cells lacking Bax resist curcumin-induced apoptosis and Bax requirement is dispensable with ectopic expression of Smac or downregulation of Bcl-XL. *Carcinogenesis*, 26(4), pp.713–23.
- Ravindran, J., Prasad, S. & Aggarwal, B.B., 2009. Curcumin and cancer cells: how many ways can curry kill tumor cells selectively? *The AAPS journal*, 11(3), pp.495–510.
- Reed, J.C., 2000. Mechanisms of apoptosis. *The American journal of pathology*, 157(5), pp.1415–30.
- Siedlakowski, P. et al., 2008. Synergy of Pancreatistatin and Tamoxifen on breast cancer cells in inducing apoptosis by targeting mitochondria. *Cancer biology & therapy*, 7(3), pp.376–84.
- Simon, H.U., Haj-Yehia, A. & Levi-Schaffer, F., 2000. Role of reactive oxygen species (ROS) in apoptosis induction. *Apoptosis : an international journal on programmed cell death*, 5(5), pp.415–8.
- Singal, P.K. & Iliskovic, N., 1998. Doxorubicin-induced cardiomyopathy. *The New England journal of medicine*, 339(13), pp.900–5.
- Singh, S., 2007. From exotic spice to modern drug? *Cell*, 130(5), pp.765–8.
- Smith, M.A. et al., 1991. Influence of doxorubicin dose intensity on response and outcome for patients with osteogenic sarcoma and Ewing's sarcoma. *Journal of the National Cancer Institute*, 83(20), pp.1460–70.

- Susin, S.A. et al., 1999. Molecular characterization of mitochondrial apoptosis-inducing factor. *Nature*, 397(6718), pp.441–6.
- Ta, L.E. et al., 2006. Neurotoxicity of oxaliplatin and cisplatin for dorsal root ganglion neurons correlates with platinum-DNA binding. *Neurotoxicology*, 27(6), pp.992–1002.
- Thayyullathil, F. et al., 2008. Rapid reactive oxygen species (ROS) generation induced by curcumin leads to caspase-dependent and -independent apoptosis in L929 cells. *Free radical biology & medicine*, 45(10), pp.1403–12.
- Walters, D.K. et al., 2008. Cytotoxic effects of curcumin on osteosarcoma cell lines. *Investigational new drugs*, 26(4), pp.289–97.
- Warburg, O., 1956. On the origin of cancer cells. *Science (New York, N.Y.)*, 123(3191), pp.309–14.
- Zhang, G. et al., 1997. Early detection of apoptosis using a fluorescent conjugate of annexin V. *BioTechniques*, 23(3), pp.525–31.
- Zilfou, J.T. & Lowe, S.W., 2009. Tumor suppressive functions of p53. *Cold Spring Harbor perspectives in biology*, 1(5), p.a001883.

CHAPTER 4: Structure Activity Relationship Analysis of Synthetic Analogues of Pancratistatin: Anti-cancer Activity is Dependent on Functional Mitochondrial Complex II and III

Dennis Ma¹, Daniel Tarade¹, Tyler Gilbert¹, Christopher Pignanelli¹, Fadi Mansour¹, Scott Adams¹, Colin Curran¹, Alexander Dowhayko¹, Megan Noel¹, Melissa Cowell¹, Sergey Vshyvenko², Tomas Hudlicky², James McNulty³, and Siyaram Pandey^{1*}

^{1*}Department of Chemistry and Biochemistry, University of Windsor,
401 Sunset Avenue, Windsor, Ontario N9B 3P4, Canada
Phone: +519-253-3000, ext. 3701
spandey@uwindsor.ca

²Chemistry Department and Centre for Biotechnology, Brock University, 500
Glenridge Avenue, St. Catharines, Ontario L2S 3A1, Canada
thudlicky@brocku.ca

³Department of Chemistry, McMaster University, 1280 Main Street West,
Hamilton, Ontario L8S 4M1, Canada
jmcnult@mcmaster.ca

List of Abbreviations

7-deoxyPST 7-deoxypancratistatin

AMA	Antimycin A
BMX	basement membrane extract
Casp-3	Caspase-3
Casp-9	Caspase-9
Cyto c	cytochrome c
DCF	2', 7'-dichlorofluorescein
DIC	differential interference contrast
DOX	Doxorubicin
ETC	electron transport chain
GEM	Gemcitabine
H ₂ DCFDA	2', 7'-dichlorofluorescein diacetate
IC ₅₀	half-maximal inhibitory concentration
PBMCs	peripheral blood mononuclear cells
PL	piperlongumine
Pro-Casp-3	Pro-Caspase-3
Pro-Casp-9	Pro-Caspase-9
PI	propidium iodide
PST	pancratistatin PST
ROS	reactive oxygen species
ROT	rotenone
STS	Staurosporine

SDH	succinate dehydrogenase
TMRM	Tetramethylrhodamine Methyl Ester
TNBC	Triple negative breast cancer
TTFA	Thenoyltrifluoroacetone

Summary

Enhanced mitochondrial stability and a decreased dependence on mitochondrial oxidative phosphorylation for energy production confer both an acquired resistance to apoptosis and a proliferative advantage in cancer cells. Thus, exploiting these dissimilarities could strategically be employed for therapy. The natural compound pancratistatin (PST), has been shown to selectively induce apoptosis in a variety of cancer cell types by mitochondrial targeting. However, its low availability in nature and complexities in its chemical synthesis have hindered its clinical advancement. To overcome these limiting factors, we synthesized a number of PST analogues with the complete anti-cancer pharmacophore of PST and related alkaloids. A medium throughput screen was completed on 18 cancer cell lines and non-cancerous cells. PST analogues SVTH-7, -6, and -5 demonstrated potent anti-cancer activity with greater efficacy than natural PST, 7-deoxyPST analogues, and several standard chemotherapeutics. They were efficient in disrupting mitochondrial function, activating the intrinsic pathway of apoptosis in both monolayer and spheroid culture, and reducing growth of tumor xenografts *in vivo*. Interestingly, the pro-apoptotic effects of SVTH-7 on cancer cells and mitochondria were abrogated with the inhibition of mitochondrial complex II, and to a slightly lesser extent complex III, signifying mitochondrial or metabolic vulnerabilities may be exploited by this PST analogue. Therefore, this work provides a scaffold for characterizing distinct mitochondrial and metabolic features of cancer cells and reveals several lead compounds with high therapeutic potential.

Introduction

Mitochondria serve many cellular functions including energy production via oxidative phosphorylation. Additionally, this organelle plays a pivotal role in apoptosis, a cellular suicide program, by housing apoptogenic factors that act to the detriment of the cell once released into the cytoplasm (Tait & Green 2010). Unlike the extrinsic pathway of apoptosis which requires an external stimulus, the intrinsic pathway is elicited by internal stress, such as DNA damage and oxidative stress (Fulda & Debatin 2006). Following intracellular stress, mitochondrial permeabilization is induced, causing apoptogenic factor release, and subsequent execution of apoptosis. This process can occur physiologically, during embryogenesis or as a safeguard against DNA damage, or can be pathologically altered in various disease states (Brown & Attardi 2005). Cancer cells divert most of their means of energy production to glycolysis and away from mitochondrial oxidative phosphorylation (Vander Heiden et al. 2009). This reallocation in cellular energetics, in addition to the upregulation of anti-apoptotic proteins, provides additional stability to mitochondria and, consequently, an acquired resistance to apoptosis (DeBerardinis et al. 2008; Gogvadze et al. 2010; Plas & Thompson 2002). Thus, targeting the differences in energy metabolism and cancer cell mitochondria could serve as potential strategies for cancer therapy.

Mitocans are a class of compounds that have recently emerged and are defined as drugs that specifically target cancer cell mitochondria to induce mitochondrial dysfunction and activation of mitochondrial mediated apoptosis

pathways (Chen et al. 2010; Ralph et al. 2006). These include, but are not limited to, electron transport chain (ETC) blockers, activators of the permeability transition pore of the mitochondria, pro-apoptotic Bcl-2 protein mimetics, and anti-apoptotic Bcl-2 protein inhibitors (Rohlena et al. 2013; Yip & Reed 2008; Adams & Cory 2007). Mitocans have been shown to be generally well tolerated by non-cancerous cells and effective anti-cancer agents, alone or in combination to enhance the activity of other cancer therapies (Neuzil et al. 2013).

We have previously discovered one such compound, pancratistatin (PST), an Amaryllidaceae alkaloid isolated from the *Hymenocallis littoralis* plant, that selectively induces apoptosis in numerous cancer cell types by mitochondrial targeting (Kekre et al. 2005; McLachlan et al. 2005; Siedlakowski et al. 2008; Chatterjee et al. 2010; Griffin et al. 2010; Griffin, McNulty, et al. 2011; Griffin, Karnik, et al. 2011). However, further development of PST has been hindered by its low availability in the *Hymenocallis littoralis* species and complications in its chemical synthesis. Circumventing these bottlenecks, we have synthesized a number of PST analogues that possess the proposed anti-cancer pharmacophore of PST and related alkaloids (Vshyvenko et al. 2011).

In this study, anti-cancer activity of these compounds, 7-deoxypancratistatin (7-deoxyPST) analogues, natural PST and common chemotherapeutics was evaluated via a medium throughput screen in 18 cancer cell lines and non-cancerous cells. Several PST analogues, including SVTH-7, -6, and -5 demonstrated selective, potent anti-cancer activity, having greater efficacy than natural PST, their C-7 deoxy counterparts, and most importantly

several standard chemotherapeutics. These analogues were effective in disrupting mitochondrial function and activating the intrinsic pathway of apoptosis. Furthermore, these analogues were able to induce apoptosis of cancer cells grown in three-dimensional spheroid culture selectively and reduce growth of colorectal cancer and glioblastoma tumor xenografts *in vivo*. Interestingly, inhibition of mitochondrial complex II, and to a slightly lesser extent complex III, abolished the mitochondrial pro-apoptotic effects of SVTH-7, confirming that a mitochondrial vulnerability may be exploited by this PST analogue. These findings form a basis for discerning important mitochondrial and metabolic features in cancer cells and present several compounds with high therapeutic potential.

Materials and Methods

Cell Culture

The E6-1 acute T-cell leukemia cell line (American Type Culture Collection, Cat. No. TIB-152, Manassas, VA, USA), was cultured with RPMI-1640 medium (Sigma-Aldrich Canada, Mississauga, ON, Canada) supplemented with 10% (v/v) fetal bovine serum (FBS) standard (Thermo Scientific, Waltham, MA, USA) and 10 mg/mL gentamicin (Gibco BRL, VWR, Mississauga, ON, Canada).

The MV-4-11 Chronic myelomonocytic leukemia cell line (ATCC, Cat. No. CRL-9591, Manassas, VA, USA). was cultured with Iscove's Modified Dulbecco's Medium (ATCC, Cat. No. 30-2005, Manassas, VA, USA) supplemented with 10% (v/v) FBS standard (Thermo Scientific, Waltham, MA, USA) and 10 mg/mL gentamicin (Gibco BRL, VWR, Mississauga, ON, Canada).

The U-937 histiocytic lymphoma cell line (ATCC, Cat. No. CRL-1593.2, Manassas, VA, USA). was cultured with Iscove's Modified Dulbecco's Medium (ATCC, Cat. No. 30-2005, Manassas, VA, USA) supplemented with 10% (v/v) FBS standard (Thermo Scientific, Waltham, MA, USA) and 10 mg/mL gentamicin (Gibco BRL, VWR, Mississauga, ON, Canada).

The MDA-MB-231 and MDA-MB-468 triple negative breast adenocarcinoma cell lines (ATCC, Cat. No. HTB-26 & HTB-132, Manassas, VA, USA) were cultured with Dulbecco's Modified Eagles Medium HAM F12 (Sigma-Aldrich, Mississauga, ON, Canada) supplemented with 10% (v/v) FBS standard (Thermo Scientific, Waltham, MA, USA) and 10 mg/mL gentamicin (Gibco BRL, VWR, Mississauga, ON, Canada).

The SUM149 inflammatory breast cancer cell line (a generous gift from Dr. Stephen Ethier, Wayne State University, Detroit, MI, USA) was cultured in Dulbecco's Modified Eagles Medium HAM F12 (Sigma-Aldrich, Mississauga, ON, Canada) supplemented with 5% (v/v) FBS standard (Thermo Scientific, Waltham, MA, USA), 10 mg/mL gentamicin (Gibco BRL, VWR, Mississauga, ON, Canada), 5 µg/ml insulin (Sigma-Aldrich, Mississauga, ON, Canada), and 1 µg/ml hydrocortisone (Sigma-Aldrich, Mississauga, ON, Canada).

The human colorectal cancer cell lines HT-29 and HCT 116 (ATCC, Cat. No. CCL-218 & CCL-247, Manassas, VA, USA) were cultured with McCoy's Medium 5a (Gibco BRL, VWR, Mississauga, ON, Canada) supplemented with 2 mM L-glutamine, 10% (v/v), FBS (Thermo Scientific, Waltham, MA, USA) and 10 mg/ml gentamicin (Gibco, BRL, VWR, Mississauga, ON, Canada).

The BxPC-3 (ATCC, Cat. No. CRL-1687, Manassas, VA, USA) pancreatic adenocarcinoma cell line was grown in RPMI-1640 medium (Sigma-Aldrich Canada, Mississauga, ON, Canada) supplemented with 10% (v/v) FBS standard (Thermo Scientific, Waltham, MA, USA) and 10 mg/mL gentamicin (Gibco BRL, VWR, Mississauga, ON, Canada).

The PANC-1 (ATCC, Cat. No. CRL-1469, Manassas, VA, USA), epithelioid carcinoma cell line of the pancreas was grown in Dulbecco's Modified Eagle's Medium (Sigma-Aldrich Canada, Mississauga, ON, Canada) supplemented with 10% (v/v) FBS standard (Thermo Scientific, Waltham, MA, USA) and 10 mg/mL gentamicin (Gibco BRL, VWR, Mississauga, ON, Canada).

The osteosarcoma cell lines, U-2 OS and Saos-2 (ATCC, Cat. No. HTB-96 & HTB-85, Manassas, VA, USA), were grown in McCoy's 5A Medium Modified (Sigma-Aldrich Canada, Mississauga, ON, Canada). The U-2 OS medium was supplemented with 10% (v/v) FBS standard (Thermo Scientific, Waltham, MA, USA) and 10 mg/mL gentamicin (Gibco BRL, VWR, Mississauga, ON, Canada). The Saos-2 medium was supplemented with 15% (v/v) FBS standard (Thermo Scientific, Waltham, MA, USA) and 10 mg/mL gentamicin (Gibco BRL, VWR, Mississauga, ON, Canada).

The U-87 MG glioblastoma cell line (ATCC, Cat. No. HTB-14, Manassas, VA, USA) was grown with Eagle's Minimum Essential Medium (Sigma-Aldrich Canada, Mississauga, ON, Canada) supplemented with 10% FBS standard (Thermo Scientific, Waltham, MA, USA) and 10 mg/mL gentamicin (Gibco BRL, VWR, Mississauga, ON, Canada).

The NCI-H23 non-small cell lung cancer cell line (ATCC, Cat. No. CRL-5800, Manassas, VA, USA) was grown and cultured in RPMI-1640 medium (Sigma-Aldrich Canada, Mississauga, ON, Canada) supplemented with 10% (v/v) FBS standard (Thermo Scientific, Waltham, MA, USA) and 10 mg/mL gentamicin (Gibco BRL, VWR, Mississauga, ON, Canada).

The A549 non-small cell lung cancer cell line (ATCC, Cat. No. CRM-CCL-185, Manassas, VA, USA) was grown and cultured in F-12K medium (ATCC, Cat. No. 30-2004, Manassas, VA, USA) supplemented with 10% (v/v) FBS standard (Thermo Scientific, Waltham, MA, USA) and 10 mg/mL gentamicin (Gibco BRL, VWR, Mississauga, ON, Canada).

The OVCAR-3 ovarian adenocarcinoma cell line (ATCC, Cat. No. HTB-161, Manassas, VA, USA) was grown and cultured in RPMI-1640 medium (Sigma-Aldrich Canada, Mississauga, ON, Canada) supplemented with 0.01 mg/mL bovine insulin, 20% (v/v) FBS standard (Thermo Scientific, Waltham, MA, USA) and 10 mg/mL gentamicin (Gibco BRL, VWR, Mississauga, ON, Canada).

The MCF7 human breast adenocarcinoma cell line (ATCC, Cat. No. HTB-22, Manassas, VA, USA) was grown in RPMI-1640 medium (Sigma-Aldrich Canada, Mississauga, ON, Canada) supplemented with 10% FBS standard (Thermo Scientific, Waltham, MA) and 10 mg/mL gentamicin (Gibco BRL, VWR, Mississauga, ON, Canada).

The G-361 malignant melanoma cell line (ATCC, Cat. No. CRL-1424, Manassas, VA, USA), was grown in McCoy's 5A Medium Modified (Sigma-Aldrich Canada, Mississauga, ON, Canada) supplemented with 10% (v/v) FBS standard (Thermo Scientific, Waltham, MA, USA) and 10 mg/mL gentamicin (Gibco BRL, VWR, Mississauga, ON, Canada).

The DU 145 prostate carcinoma cell line (ATCC, Cat. No. HTB-81, Manassas, VA, USA) was grown with Eagle's Minimum Essential Medium (Sigma-Aldrich Canada, Mississauga, ON, Canada) supplemented with 10% FBS standard (Thermo Scientific, Waltham, MA, USA) and 10 mg/mL gentamicin (Gibco BRL, VWR, Mississauga, ON, Canada).

The AG09309 normal human skin fibroblasts (Coriell Institute for Medical Research, Cat. No. AG09309, Camden, NJ, USA) was grown in Dulbecco's Modified Eagle's Medium, High Glucose (Thermo Scientific, Waltham, MA, USA)

supplemented with 15 % (v/v) FBS and 10 mg/mL gentamicin (Gibco BRL, VWR, Mississauga, ON, Canada).

The CCD-18Co normal colon fibroblasts (ATCC, Cat. No. CRL-1459, Manassas, VA, USA) was grown with Eagle's Minimum Essential Medium (Sigma-Aldrich Canada, Mississauga, ON, Canada) supplemented with 10% FBS standard (Thermo Scientific, Waltham, MA, USA) and 10 mg/mL gentamicin (Gibco BRL, VWR, Mississauga, ON, Canada).

The normal-derived colon mucosa (NCM460) cell line (INCELL Corporation, LLC., San Antonio, TX, USA) was grown in INCELL's M3Base™ medium (INCELL Corporation, LLC., Cat. No. M300A500) supplemented with 10 % (v/v) FBS and 10 mg/mL gentamicin (Gibco BRL, VWR, Mississauga, ON, Canada).

All cells were grown in optimal growth conditions of 37°C and 5 % CO₂. Furthermore, all cells were cultured and passaged for less than 6 months and no authentication of cell lines was performed by the author.

Isolation and Culture of Peripheral Blood Mononuclear cells (PBMCs)

Peripheral blood mononuclear cells (PBMCs) were collected and isolated from healthy volunteers. In brief, whole blood was collected in BD Vacutainer®CPT™ Tubes with Sodium Heparin^N (Becton, Dickinson and Company, Cat. No. 362753, Franklin Lakes, NJ, USA) at room temperature. Tubes were immediately inverted 5 times and centrifuged for 30 minutes at room temperature at 1500-1800 x g. The layer of PBMCs under the plasma layer in

each tube was collected, pooled together, resuspended in 50 mL of PBS, and centrifuged at room temperature at 300 x g for 15 minutes. The supernatant was methodically aspirated without disturbing the pellet and PBMCs were resuspended and cultured in RPMI-1640 medium (Sigma-Aldrich Canada, Mississauga, ON, Canada), supplemented with 10% (v/v) FBS standard (Thermo Scientific, Waltham, MA, USA) and 10 mg/mL gentamicin (Gibco BRL, VWR, Mississauga, ON, Canada) at 37 °C and at 5% CO₂. PBMCs from healthy volunteers 1, 2, 3, and 4 (PBMCs V1, PBMCs V2, PBMCs V3, PBMCs V4) were taken from a healthy 28 year old female, a healthy 18 year old male, a healthy 48 year old male, and a healthy 31 year old female respectively.

Chemicals and Cell Treatment

Cells were treated with PST, PST Analogues, Taxol (Sigma-Aldrich Canada, Cat. No. T7402, Mississauga, ON, Canada), Staurosporine (STS) (Sigma-Aldrich Canada, Cat. No. S4400, Mississauga, ON, Canada), Doxorubicin (DOX) (Sigma-Aldrich Canada, Cat. No. D1515, Mississauga, ON, Canada), Gemcitabine (GEM) (Sigma-Aldrich Canada, Cat. No. G6423, Mississauga, ON, Canada), piperlongumine (PL) (INDOFINE Chemical Company, Inc., Cat. No. P-004, Hillsborough, NJ, USA), the broad spectrum caspase inhibitor, Z-VAD-FMK (EMD Chemicals, Gibbstown, NJ, USA), Antimycin A (AMA) (Sigma-Aldrich Canada, Cat. No. A8674, Mississauga, ON, Canada), Thenoyltrifluoroacetone (TTFA) (Sigma-Aldrich Canada, Cat. No. T27006, Mississauga, ON, Canada), and rotenone (ROT) (Sigma-Aldrich

Canada, Cat. No. R8875, Mississauga, ON, Canada) dissolved in DMSO stock solutions. PST analogues were produced by synthesis from bromobenzene (Collins et al. 2010; Vshyvenko et al. 2011).

WST-1 Assay for Cell Viability

The WST-1 based colorimetric assay (Roche Applied Science, Indianapolis, IN, USA) was performed to quantify cell viability via as a function of cellular metabolism. Cells were seeded in 96-well clear bottom tissue culture plates and grown for 24 hours. Subsequently, cells were treated with the indicated concentrations of chemicals for the indicated time durations. WST-1 reagent was incubated for 4 hours at 37° C with 5 % CO₂. In actively metabolizing cells, the WST-1 reagent is cleaved by cellular enzymes to produce formazan. The presence of formazan was quantified via absorbance readings at 450 nm on a Wallac Victor³™ 1420 Multilabel Counter (PerkinElmer, Woodbridge, ON, Canada). Absorbance readings were expressed as percentages of the solvent treated control group. Inhibitory dose-response curves (log(inhibitor) vs. response -- Variable slope (four parameters)) were calculated using GraphPad Prism 6.

Cell Death Analysis: Annexin V Binding Assay & Propidium Iodide (PI) Staining

The Annexin V binding assay and propidium iodide staining was done in parallel to monitor the externalization of phosphatidylserine on the outer cellular surface, a marker of early apoptosis, and cell permeabilization, a marker of

necrotic or late apoptotic cell death, respectively. Cells were washed with phosphate buffer saline (PBS) and suspended in Annexin V binding buffer (10 mM HEPES, 140 mM NaCl, 2.5 mM CaCl₂, pH 7.4) with green fluorescent Annexin V AlexaFluor-488 (1:20) (Life Technologies Inc, Cat. No. A13201, Burlington, ON, Canada) and 0.01mg/mL of red fluorescent PI (Life Technologies Inc, Cat. No. P3566, Burlington, ON, Canada) for 15 minutes at 37 °C protected from light. The percentage of early (green), late apoptotic cells (green and red), and necrotic cells (red) were quantified using image-based cytometry with a Tali® Image-Based Cytometer (Life Technologies Inc, Cat. No. T10796, Burlington, ON, Canada). Cells from at least 18 random fields were analyzed using both the green (ex. 458 nm; em. 525/20 nm) and red (ex. 530 nm; em. 585 nm) channels. Fluorescent micrographs were taken at 400x magnification using LAS AF6000 software with a Leica DMI6000 fluorescent microscope (Wetzlar, Germany). Cells monitored with microscopy were counterstained with Hoechst 33342 (Molecular Probes, Eugene, OR, USA) to visualize nuclei using a final concentration of 10 µM during the 15 minute incubation.

Quantitation of Reactive Oxygen Species (ROS)

The small molecule 2', 7'-dichlorofluorescein diacetate (H₂DCFDA) was used to monitor whole cell ROS generation. H₂DCFDA enters the cell and is deacetylated by esterases and oxidized by ROS to the highly fluorescent 2', 7'-dichlorofluorescein (DCF) (excitation 495 nm; emission 529 nm). Cells were pretreated with 20 µM H₂DCFDA (Sigma-Aldrich Canada, Cat. No. D6883,

Mississauga, ON, Canada) for 30 minutes at 37°C protected from light at 5% CO₂. Cells were treated for the indicated durations, centrifuged at 600 x g for 5 minutes and suspended in PBS. Percentage of DCF positive cells was quantified using the Tali® Image-Based Cytometer (Life Technologies Inc, Cat. No. T10796, Burlington, ON, Canada) using 12 random fields per group with the green channel (excitation 458 nm; emission 525/20 nm).

Tetramethylrhodamine Methyl Ester (TMRM) Detection of Mitochondrial Membrane Potential

Tetramethylrhodamine methyl ester (TMRM) (Gibco BRL, VWR, Mississauga, ON, Canada) was used for detecting mitochondrial membrane potential (MMP), an indicator of healthy intact mitochondria. Treated cells were incubated with 100 nM TMRM in growth medium for 45 minutes at 37° C and 5% CO₂ protected from light. The percentage of TMRM cells was quantified using image-based cytometry with a Tali® Image-Based Cytometer (Life Technologies Inc, Cat. No. T10796, Burlington, ON, Canada). Cells from at least 18 random fields were analyzed using the red channel (ex. 530 nm; em. 585 nm). Fluorescent micrographs were taken at 400x magnification using LAS AF6000 software with a Leica DMI6000 fluorescent microscope (Wetzlar, Germany). Cells monitored with microscopy were counterstained with Hoechst 33342 (Molecular Probes, Eugene, OR, USA) to visualize nuclei using a final concentration of 10 µM during the 45 minute incubation.

Mitochondrial Isolation

To isolate mitochondria, cells were washed once in cold PBS, re-suspended in hypotonic buffer (1 mM EDTA, 5 mM Tris-HCl, 210 mM mannitol, 70 mM sucrose, 10 μ M Leu-pep and Pep-A, 100 μ M PMSF) and subjected to manual homogenization with a glass tissue grinder. Homogenized cells were centrifuged at 600 x g for 5 minutes at 4° C. The supernatant was centrifuged at 15000 x g for 15 minutes at 4° C and the mitochondrial pellet was suspended in cold reaction buffer (2.5 mM malate, 10 mM succinate, 10 μ M Leu-pep and Pep-A, 100 μ M PMSF in PBS).

Treatment of Isolated Mitochondria & Evaluation of Apoptogenic Factor Release

Isolated mitochondria were treated with drugs at the indicated concentrations and incubated for 2 hours in cold reaction buffer (2.5 mM malate, 10 mM succinate, 10 μ M Leu-pep, 10 μ M Pep-A, and 100 μ M PMSF in PBS). Following treatment, mitochondria samples were vortexed and centrifuged at 15,000 x g for 15 minutes at 4°C. Western Blot analysis was performed on the resulting supernatants and mitochondrial pellets suspended in cold reaction buffer to screen for release or retention of apoptogenic factors.

Western Blot Analyses

Protein samples were subjected to SDS-PAGE, transferred onto a PVDF membrane, and blocked with 5% w/v milk or BSA in TBST (Tris-Buffered Saline Tween-20) solution for 1 hour. Membranes were incubated with primary antibodies overnight at 4 °C: anti-caspase-9 antibody (1:1000) raised in rabbit (Cell Signalling, Cat. No. 9502, Danvers, MA, USA), anti-caspase-3 antibody (1:2000) (Novus Biologicals, Cat. No. NB100-56709V2, Littleton, CO, USA), anti- β -actin antibody (1:1000) (Santa Cruz Biotechnology, Inc., Cat. No. sc-81178, Paso Robles, CA, USA), anti-cytochrome c (Cyto c) antibody (1:1000) raised in mice (Abcam, Cat. No. ab13575, Cambridge, MA, USA), anti-succinate dehydrogenase subunit A antibody (1:1000) raised in mice (Santa Cruz Biotechnology, Inc., sc-59687, Paso Robles, CA, USA). Membranes were quickly rinsed twice, washed once for 15 minutes, and then washed twice for 5 minutes in TBST. Membranes were incubated with horseradish peroxidase-conjugated secondary antibodies for 1 hour: goat anti-mouse antibody (1:2000) (Novus Biologicals, Cat. No. NBP2- 30347H, Littleton, CO, USA), goat anti-rabbit antibody (1:2000) (Novus Biologicals, Cat. No. NBP2-30348H, Littleton, CO, USA). Membranes were quickly rinsed twice and washed for three 5 minute washes with TBST. Chemiluminescence reagent (Thermo Fisher Scientific, Cat. No. 34095, Rockford, IL, USA) was used for band visualization. Densitometry analyses were performed using ImageJ software.

Oxygen Consumption Quantitation

The MitoXpress® Xtra - Oxygen Consumption Assay [HS Method] (Luxcel Biosciences Ltd., Cat. No. MX-200, Cork, Ireland) was used to measure mitochondrial function. 1 000 000 cells/well were seeded in a 96-well black clear bottom tissue culture plate and incubated for an hour at 37° C and 5% CO₂. On a heat pack, 10 µL of MitoXpress® reagent was added to each well excluding the blanks, cells were treated with test compounds, the plate was shaken with a plate shaker, and 2 drops of pre-warmed high sensitivity mineral oil was added to each well to seal off the air supply. Bottom read fluorescence measurements were taken at Ex. 380 nm and Em. 650, every 2 minutes for 2 hours at 37 °C using a SpectraMax Gemini XS multi-well plate reader (Molecular Devices, Sunnyvale, CA, USA). Increases in fluorescence are indicative of oxygen consumption. Oxygen consumption rates were determined by calculating the slope of the linear regions of the oxygen consumption curves using GraphPad Prism 6 software.

Three-Dimensional Spheroid Culture and Assays

To establish three dimensional spheroid cultures, tissue culture plates were coated with basement membrane extract (BMX). Prior to coating, 3-D Culture Matrix™ Basement Membrane Extract Reduced Growth Factor (phenol red free) (Trevigen, Inc., Cat No. 3445-005-01, Gaithersburg, MD, USA) was thawed at 4°C overnight. As BMX forms a solid gel at room temperature, clear 96-well tissue culture plates, 35 mm glass bottom tissue culture dishes (MatTek Corporation, Cat No. P35G-0-14-C, Ashland, MA, USA) and pipette tips were

chilled at -20°C overnight prior to use. On ice and in sterile conditions, clear 96-well tissue culture plate wells or the 14 mm diameter microwells of chilled 35 mm glass bottom tissue culture dishes, were coated with 35 μL and 50 μL BMX respectively, with chilled pipette tips and incubated for 10 minutes at 37°C . Approximately 2000 - 4000 and 5000 cells were seeded in clear 96-well plate wells and microwells of glass bottom dishes respectively and grown in medium with 2% (v/v) BMX 48 hours with 5 % CO_2 at 37°C . Following 48 hours of incubation, medium was replaced with fresh medium supplemented with 2% (v/v) BMX and spheroids were treated with test compounds for 72 hours. Spheroids grown in 96-well plates and glass bottom dishes were subjected to the WST-1 Assay and confocal fluorescence microscopy, respectively. Confocal micrographs were taken with an Olympus Fluoview FV1000 confocal microscope (Olympus Corporation, Shinjuku, Tokyo, Japan) using a UPLSAPO 20X, 0.75 numerical aperture dry objective (Olympus Corporation, Shinjuku, Tokyo, Japan). Cells were counterstained with NucRed Live 647 ReadyProbes[®] Reagent (Life Technologies Inc, Cat. No. R37106, Burlington, ON, Canada) to visualize nuclei.

In Vivo Xenograft Models

Immunocompromised CD-1 nu/nu male mice (Charles River Laboratories, Cat. No. 086, Sherbrooke, QC, Canada) were housed in conditions of a 12-hour light/dark cycle, in accordance with the animal care protocols outlined by the University of Windsor Animal Care Committee (AUPP # 14-15). Mice were injected with 2×10^6 HT-29, HCT 116, or U-87 MG cells suspended in 200 μ L of PBS using a 23-gauge needle in the hind flanks of mice. After establishment of palpable tumors (~ 1 week), mice were treated by intratumoral injection (4-6 mice/group) three times a week for five weeks of 3 mg/kg of PST analogues or DMSO in 200 μ L of PBS. Tumors were measured with calipers and volumes were calculated using the ellipsoid formula $\pi/6 \times \text{length} \times \text{width} \times \text{height}$. Changes in body mass were measured with a scale.

Statistical Analysis

Statistics were performed by GraphPad Prism 6 software. A p-value below 0.05 was considered significant. For experiments with single variable measurements, which include quantification of MMP, and whole cell ROS, a One-Way ANOVA (nonparametric) was conducted and each sample's mean was compared to the mean of the DMSO control unless otherwise specified. For experiments that contained multi-variables (e.g. multiple group comparisons), such as the quantification of live and dead cells, Two-Way ANOVA (nonparametric) was used and each sample's mean was compared to the mean of the control (DMSO vehicle) unless otherwise specified.

Results

PST Analogues have Selective and Potent Anti-Cancer Activity with Efficacy

Surpassing Standard Chemotherapeutics and Natural PST

The preclinical advancement of PST has been hindered by its low yield from its natural source and complexities in its chemical synthesis. Previously, we have shown modest to comparable anti-cancer activity of a 7-deoxyPST analogue in comparison to natural PST (Ma et al. 2011; Ma, Tremblay, et al. 2012; Ma, Collins, et al. 2012). Recently, we have synthesized several PST analogues with a C-7 hydroxyl group (**Figure 4.1**), and resultantly, possess the complete proposed pharmacophore attributed to the anticancer activity of PST and related alkaloids (Vshyvenko et al. 2011). A comprehensive screen of anti-cancer activity of these analogues, in parallel with 7-deoxyPST analogues, PST, and common chemotherapeutics, was completed on 18 cancer cell lines as well as non-cancerous cells using the WST-1 colorimetric assay (**Figure 4.2**). Taken as a whole, SVTH-7, followed by SVTH-6 and SVTH-5, had the most potent activity, with SVTH-7 having much greater activity than natural PST while SVTH-6 and -5 possessed comparable or greater efficacy than natural PST with regards to their half-maximal inhibitory concentration (IC_{50}) values. As predicted, SVTH-6 and SVTH-5, which are C-7 hydroxylated forms of JCTH-4 and JCTH-3, respectively, were markedly more effective than their 7-deoxyPST counterparts. Triple negative breast cancer (TNBC) lacks the estrogen, progesterone, and HER2 receptor, and thus, traditional breast cancer therapies including hormone therapy and Herceptin are not effective (Lips et al. 2015). Standard

chemotherapeutics for TNBC include Taxol and Doxorubicin (DOX). Interestingly, SVTH-7, -6, and -5 had lower IC₅₀ values than Taxol and DOX in the TNBC cell lines MDA-MB-231 and MDA-MB-468. SVTH-7 and SVTH-6 were also more effective than Gemcitabine (GEM), the standard chemotherapeutic for notoriously chemoresistant pancreatic cancer (Berlin & Benson 2010), in the BxPC-3 and PANC-1 pancreatic cancer cell lines. Furthermore, JCTH-3 and -4, and SVTH-5, -6, and -7 were more potent than Cisplatin and GEM, having lower IC₅₀ values in the NCI-H23 non-small cell lung cancer cell line, a commonly chemoresistant cancer. Moreover, SVTH-7 and -6 had lower IC₅₀ values than Taxol in MV-4-11 leukemia, U-87 MG glioblastoma, and MCF7 breast adenocarcinoma cells. Notably, the IC₅₀ values of PST and its analogues in the AG09309 and CCD-18Co non-cancerous cells were well above those observed in the cancer cell lines tested, demonstrating a selective therapeutic window. Additional time points, doses and statistical analyses of compounds tested are shown in **Supplemental Figures S4.1A-V**.

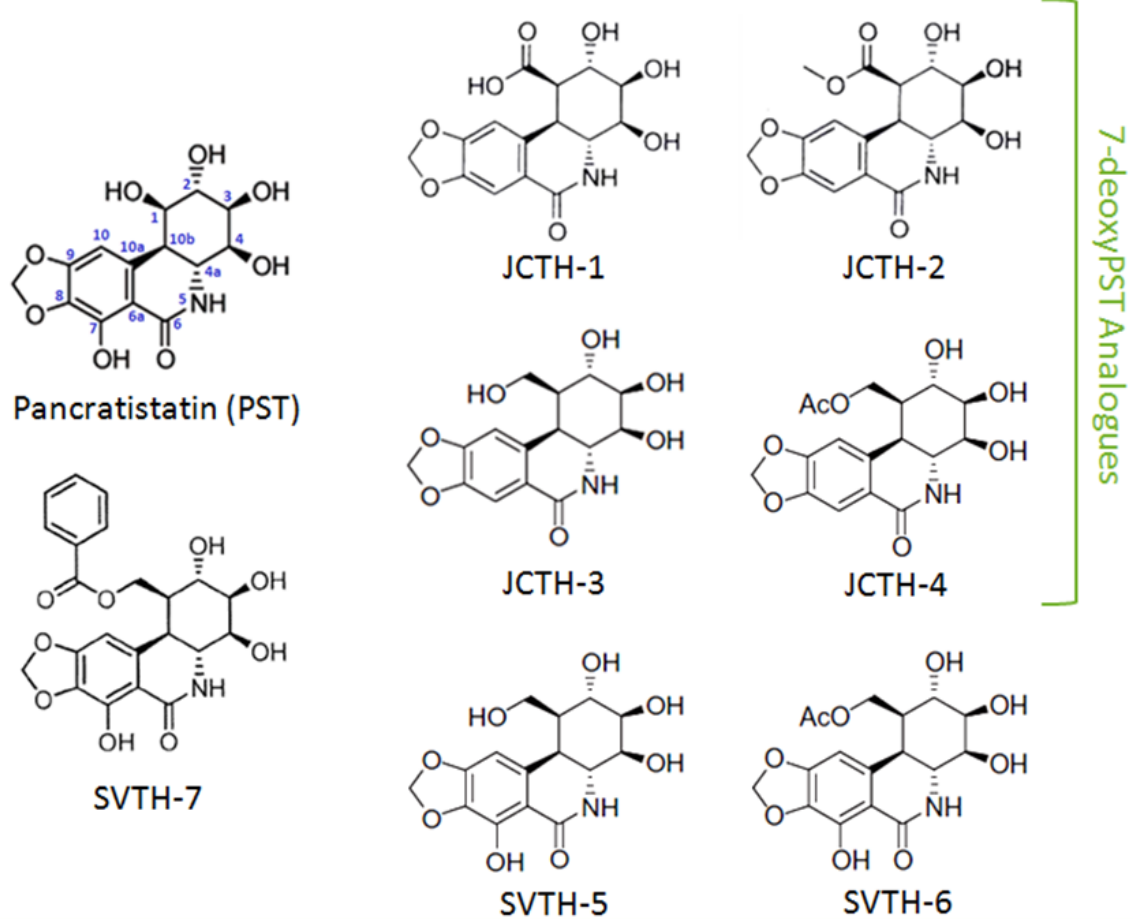


Figure 4.1. Structure of PST and PST Analogues

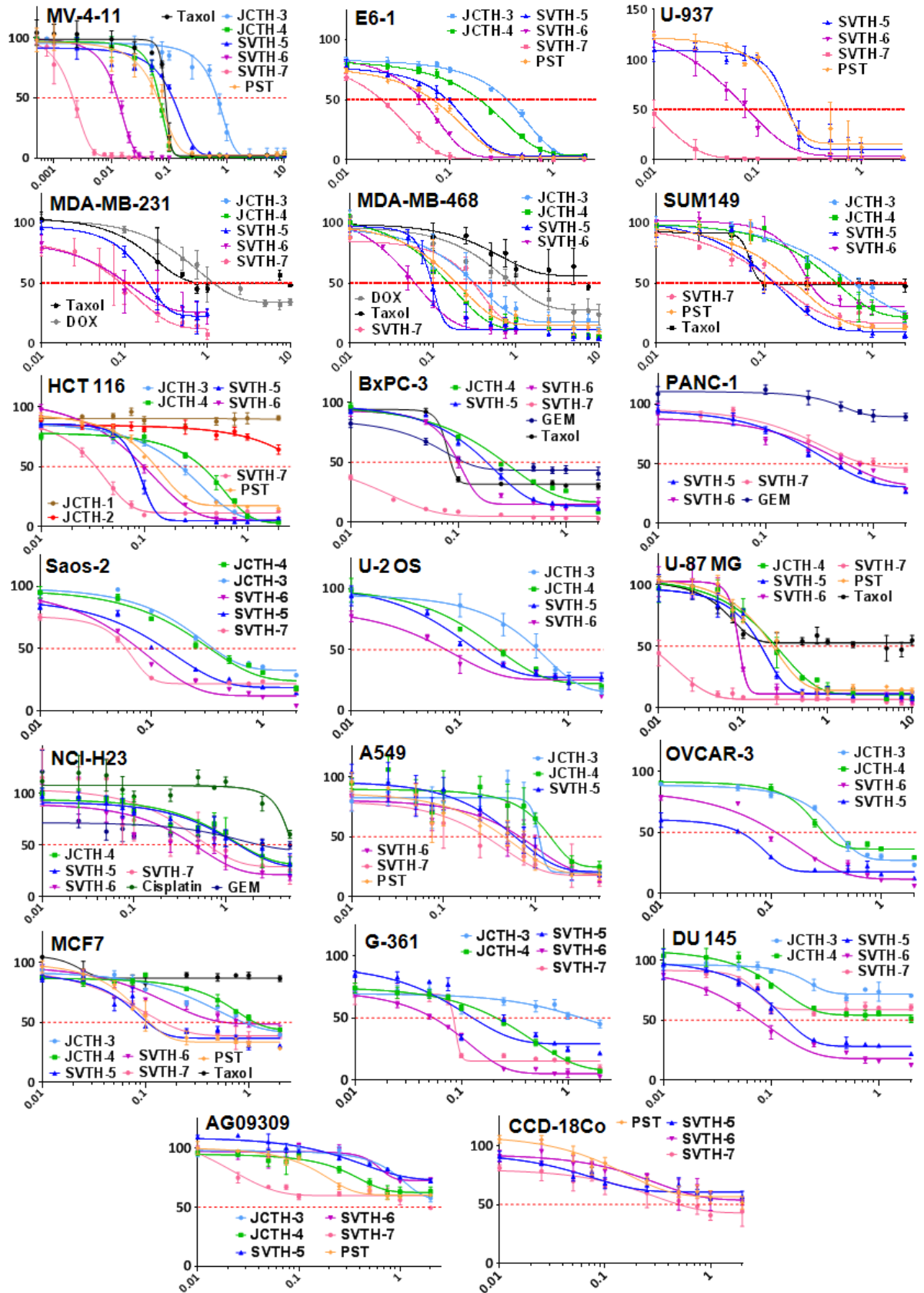


Figure 4.2. PST Analogues have Selective and Potent Anti-Cancer Activity with Efficacy Surpassing Standard Chemotherapeutics and Natural PST.

The WST-1 colorimetric assay was used to screen the anti-cancer activity of PST analogues, PST, Taxol, Doxorubicin (DOX), and Gemcitabine (GEM) in 18 cancer cell lines and non-cancerous cells. After 48 hours of treatment, the absorbance of the processed WST-1 reagent formazan, used to quantify cell viability, was read at 450 nm and expressed as a percent of solvent control (DMSO). Values are expressed as mean \pm SD from quadruplicates of 3 independent experiments. * $p < 0.01$ vs. solvent control (DMSO). X-axis: Concentration (μ M) (using a Log 10 Scale). Y-axis: Absorbance at 450 nm (% of Control).

PST Analogues Induce Apoptosis Selectively in Cancer Cells

To evaluate cell death caused by PST analogues, the Annexin V binding assay and propidium iodide staining was done in parallel to monitor early apoptosis (Fadok et al. 1998), and necrotic or late apoptotic cell death respectively (Poon et al. 2010). PST analogues were effective in inducing apoptosis in the U-937, E6-1, and MV-4-11 blood cancer cell lines (**Figure 4.3A**). SVTH-7, followed by SVTH-6 and SVTH-5 was the most effective in inducing apoptosis compared to natural PST and the 7-deoxyPST analogues. Staurosporine (STS) was used as a positive control for apoptotic induction (Belmokhtar et al. 2001). Non-cancerous cells, including peripheral blood mononuclear cells from healthy volunteers 1 (PBMCs V1) and 2 (PBMCs V2) and AG09309 normal human fibroblasts, were much less sensitive to apoptotic induction. Only SVTH-7 and SVTH-6, at much higher doses required to induce apoptosis in cancer cells, demonstrated mild toxicity (**Figure 4.3B**). Cell death analyses of additional non-cancerous peripheral blood mononuclear cells from other healthy volunteers with similar resilience against PST analogue treatment are depicted in **Supplemental Figure S4.2**. Representative micrographs of E6-1 leukemia cells undergoing apoptosis after 48 hours of PST analogue treatment are shown in **Figure 4.3C**. SVTH-7, -6, and -5 were the most effective at yielding condensed cell morphology, nuclear condensation, and Annexin V (green) and PI (red) fluorescence, which are indicative of apoptotic induction.

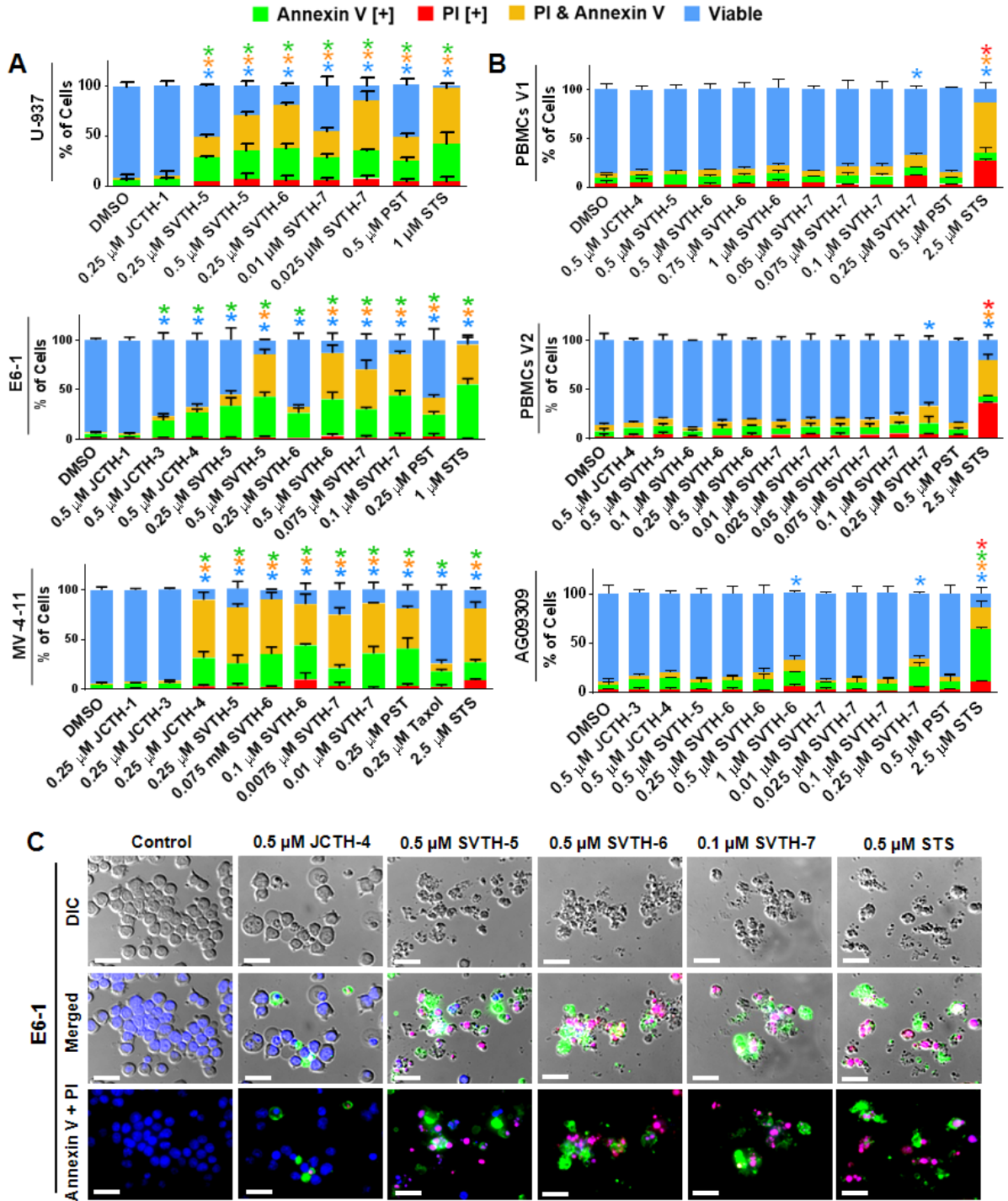


Figure 4.3. PST Analogues Induce Apoptosis Selectively in Cancer Cells. Annexin V binding and PI staining of cells treated for 48 hours was monitored with image-based cytometry. **(A)** U-937, E6-1, and MV-4-11 cancer cell lines. **(B)** Non-cancerous cells: peripheral blood mononuclear cells from volunteer 1 (PBMCs V1) and 2 (PBMCs V2), and AG0309 normal fibroblasts. Values are expressed as mean \pm SD from at least 3 independent experiments. * p <0.01 vs. DMSO control. **(C)** Annexin V binding (green) and PI staining (red) monitored with fluorescent microscopy in E6-1 leukemia cells treated for 48 hours counterstained with Hoechst (cyan). Cell morphology is shown using differential interference contrast (DIC) microscopy. Scale bar = 25 μ m. Micrographs are representative of 3 independent experiments.

PST Analogues Cause Mitochondrial Dysfunction and Activate the Intrinsic Pathway of Apoptosis in Cancer Cells

Mitochondria play a pivotal role in the induction of intrinsic apoptosis. When dysfunctional, these organelles can permeabilize and release apoptogenic factors, leading to the execution of apoptosis (Shi 2001). One of the first events of mitochondrial dysfunction is the generation of reactive oxygen species (ROS) (Lin & Beal 2006). Using H₂DCFDA, an indicator of ROS, PST analogues and PST were shown to increase the production of ROS in MV-4-11 leukemia cells after 3 hours of treatment (**Figure 4.4A**). Piperlongumine (PL) was used as a positive control for ROS generation (Raj et al. 2011). This was followed by dissipation of mitochondrial membrane potential (MMP) at 3 and 6 hours (**Supplemental Figure S4.3A**), with a more pronounced effect at 12 hours (**Figure 4.4B & C**), as shown by a decrease of TMRM red fluorescence. Thus, PST analogues and PST were effective in permeabilizing the mitochondrial membrane, which was not observed in the non-cancerous PBMCs V1 (**Figure 4.4B**). Full time kinetics of TMRM analyses of MV-4-11 and E6-1 leukemia cells treated with PST analogues are depicted in **Supplemental Figures S4.3A & B**.

Following MMP collapse and mitochondrial permeabilization, apoptogenic factors are released and cause subsequent activation of apoptosis. One such factor is cytochrome c (Cyto c), which upon its release from the mitochondria, leads to the conversion of Pro-Caspase-9 (Pro-Casp-9) to Caspase-9 (Casp-9), which in turn cleaves Pro-Caspase-3 (Pro-Casp-3) to Caspase-3 (Casp-3) (Ow et al. 2008). The executioner caspase, Casp-3, exerts its lethal effects by cleaving a

multitude of cellular proteins needed for cellular function, structural stability, and survival (Fischer et al. 2003). After 12 hours, JCTH-4, SVTH-5, -6, and -7 treatment yielded cleavage of Pro-Casp-9 and Pro-Casp-3 in MV-4-11 cells, demonstrating their ability to induce the aforementioned caspase-dependent pathway of apoptosis (**Figure 4.4D**). To confirm the dependence of caspases in PST analogue-induced apoptosis, the Z-VAD-FMK broad-spectrum caspase inhibitor was used (**Figure 4.4E**). Interestingly, this inhibitor was only able to partially rescue E6-1 leukemia cells from PST and PST analogue-induced apoptosis, suggesting caspases and other apoptosis inducers are involved in such cell death. DOX was used as a positive control for Z-VAD-FMK-mediated rescue (Gamen et al. 2000). Similar results were seen with the MV-4-11 leukemia cell line (**Supplemental Figure S4.4**). To determine if PST analogues are able to directly act on cancer cell mitochondria to release Cyto c, mitochondria isolated from MV-4-11 cells were directly treated with PST analogues for 2 hours and the release of Cyto c was monitored (**Figure 4.4F**). Interestingly, such treatment caused release of this apoptogenic factor with the most pronounced effect observed with SVTH-6 and -7. Collectively, these findings suggest that PST analogues are able to act on the mitochondria to induce the intrinsic pathway of apoptosis.

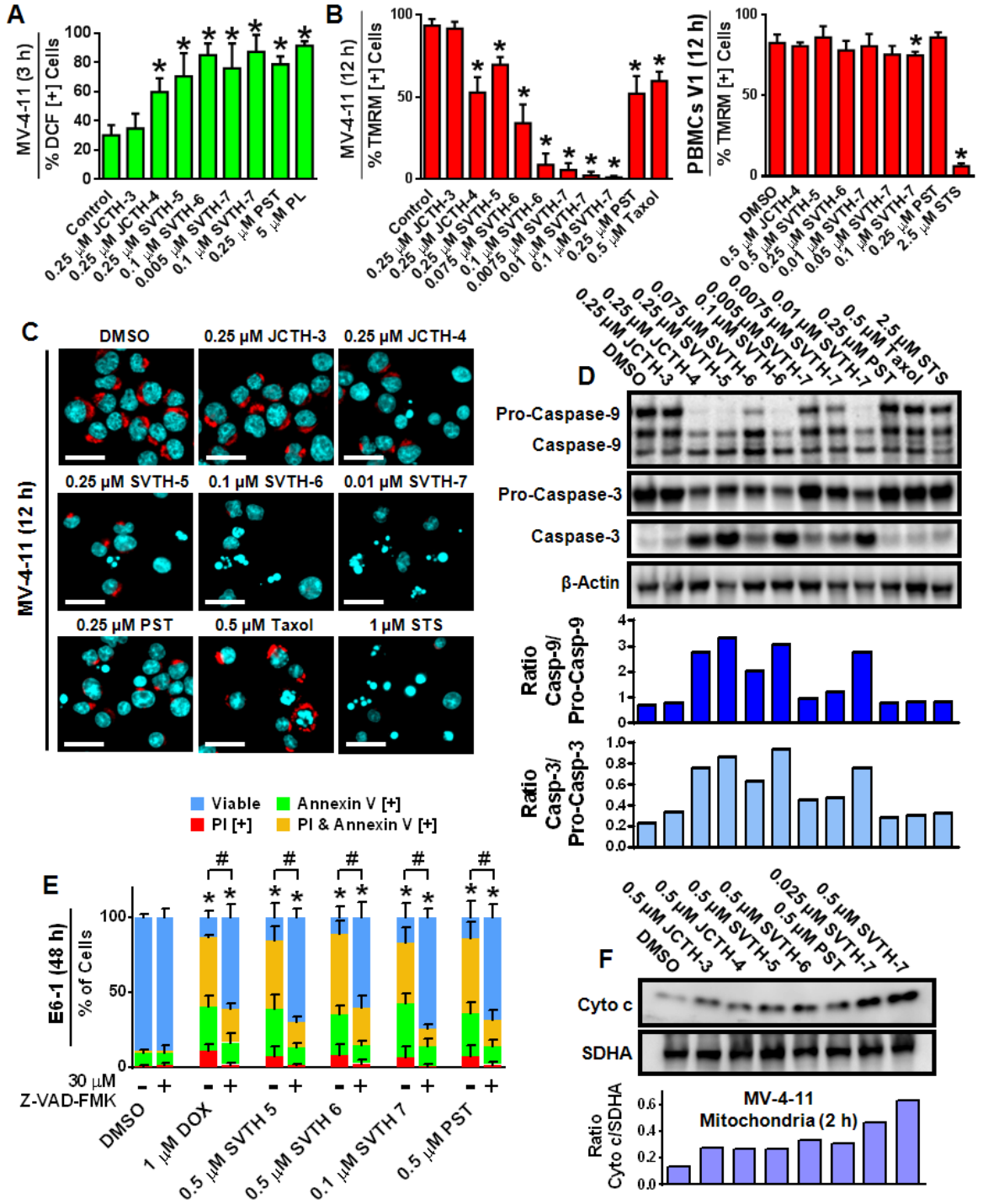


Figure 4.4. PST Analogues Cause Mitochondrial Dysfunction and Activate the Intrinsic Pathway of Apoptosis in Cancer Cells. **(A)** H2DCFDA was used to measure whole cell ROS in MV-4-11 cells treated for 3 hours with image-based cytometry. * $p < 0.01$ vs. DMSO control. **(B)** TMRM was used to monitor MMP in MV-4-11 leukemia cells and non-cancerous peripheral blood mononuclear cells from volunteer 1 (PBMCs V1) with image-based cytometry. * $p < 0.01$ vs. DMSO control. **(C)** TMRM fluorescence microscopy counterstained with Hoechst (cyan). Scale bar = 25 μm . **(D)** Western Blot analyses of caspase cleavage of MV-4-11 cells treated for 12 hours. **(E)** E6-1 leukemia cells were pre-treated with 30 μM Z-VAD-FMK broad spectrum caspase inhibitor for 1 hour and then treated with PST analogues to determine the dependence of caspases in PST analogue-induced apoptosis. Doxorubicin (DOX) was used as a positive control for Z-VAD-FMK mediated rescue. Values are expressed as mean \pm SD from at least 3 independent experiments. * $p < 0.01$ vs. DMSO control (comparison of viable cells only); # $p < 0.001$ vs. respective groups untreated with Z-VAD-FMK (comparison of viable cells only). **(F)** Western Blot analysis of Cyto C release (of post mitochondrial supernatant) from directly treated mitochondria isolated from MV-4-11 cells for 2 hours. SDHA was probed in the mitochondrial pellet samples as a loading control. All quantitative values are expressed as mean \pm SD from at least 3 independent experiments. Micrographs and Western Blots are representative of at least 3 independent experiments demonstrating similar trends.

PST Analogues Decrease Oxygen Consumption Capabilities of Cancer Cells

Oxygen consumption of cells is a direct indicator on mitochondrial function (Brand & Nicholls 2011). To assess the effect of PST analogues on oxygen consumption, the MitoXpress® Xtra - Oxygen Consumption Assay was used **(Figure 4.5)**. SVTH-6, -7, and PST were able to effectively decrease the rate of oxygen consumption in E6-1 leukemia cells. In U-937 lymphoma cells, SVTH-5, -6, and -7 were effective in decreasing oxygen consumption rates. Antimycin A (AMA), a complex III inhibitor of the electron transport chain (ETC), was used as a positive control for oxygen consumption cessation. These results indicate that PST analogues are effective in reducing oxygen consumption and thus, mitochondrial function.

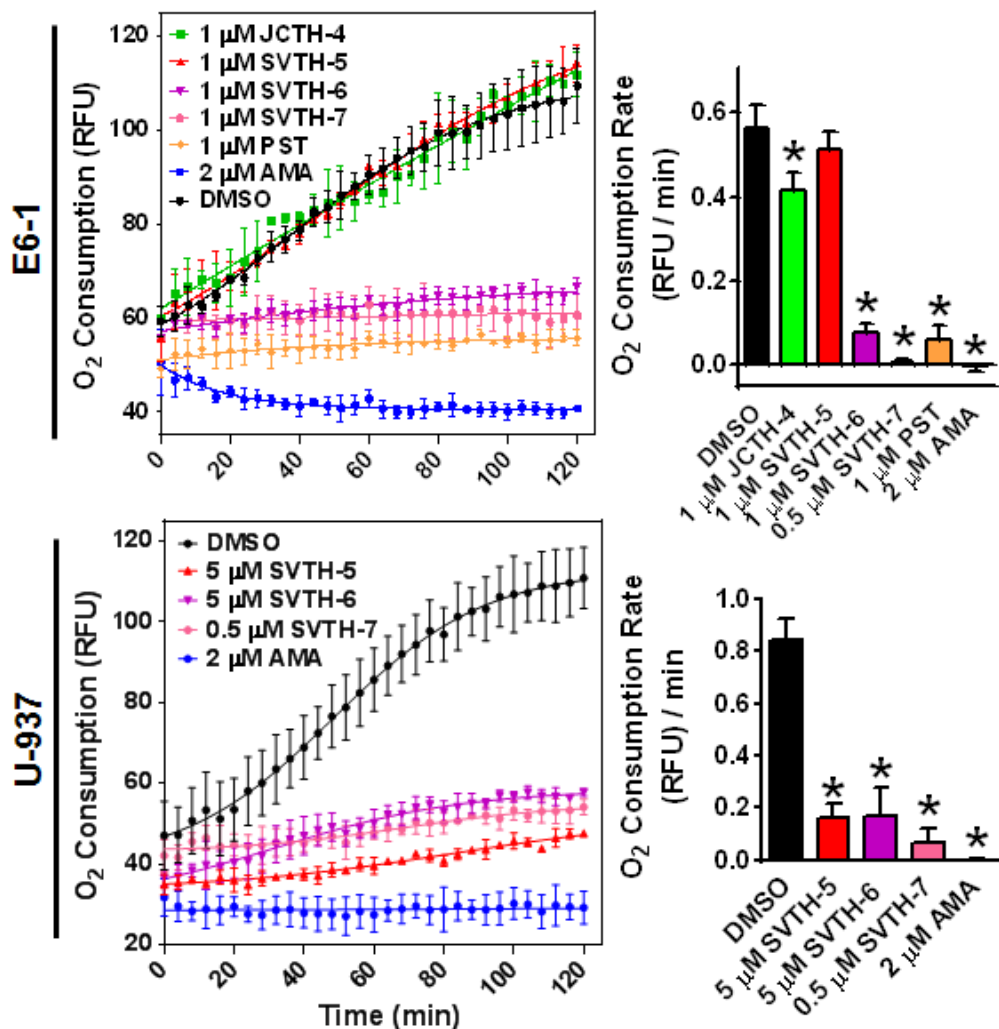


Figure 4.5. PST Analogues Decrease Oxygen Consumption Capabilities of Cancer Cells. The MitoXpress® Xtra - Oxygen Consumption Assay was used to monitor oxygen consumption via fluorescence generation. Cells were treated, and the fluorescent MitoXpress® reagent monitored at Ex. 380 nm and Em. 650, every 2 minutes for 2 hours at 37 °C. Oxygen consumption rates were calculated by measuring the slopes of the linear regions of the oxygen consumption curves. Values are expressed as mean ± SD from at least 3 independent experiments. * $p < 0.001$ vs. DMSO control.

PST Analogue-Induced Apoptosis is Dependent on Functional Complex II and III of the Mitochondrial Electron Transport Chain

As we have shown PST analogues to act on cancer cell mitochondria, we investigated the role of mitochondrial ETC complexes in PST analogue-induced apoptosis using the complex II inhibitor Thenoyltrifluoroacetone (TTFA) and the complex III inhibitor AMA (Chen et al. 2007; Spinazzi et al. 2012). Interestingly, TTFA was able to rescue these cells from SVTH-7 insult as seen at 48 hours, bringing the percentage of dead cells statistically similar to those of the DMSO control treated group (**Figure 4.6A**). Cell salvation by TTFA was specific to SVTH-7 as this inhibitor had no significant effect on Taxol, DOX and STS treatment. A slightly less dramatic rescue was observed with AMA.

Likewise, TTFA was able to protect cancer cell mitochondria from SVTH-7-induced dissipation of MMP at 12 hours and bring the percentage of TMRM positive cells to levels statistically similar to values observed in the DMSO control treated group (**Figure 4.6B**). A similar but less dramatic rescue of MMP was observed with AMA. Prevention of mitochondrial membrane permeabilization by TTFA was specific to SVTH-7 treatment as no significant changes in the percentage of TMRM positive cells was observed with Taxol, DOX, and STS treatment in conjunction with this inhibitor. Interestingly, inhibition of complex I with the inhibitor Rotenone (ROT) (Spinazzi et al. 2012) had no significant effect of SVTH-7 activity (**Supplemental Figure S4.5**). Therefore, these observations imply that functional complex II, and to a lesser extent, complex III are required for SVTH-7 to exert its pro-apoptotic effects in cancer cells.

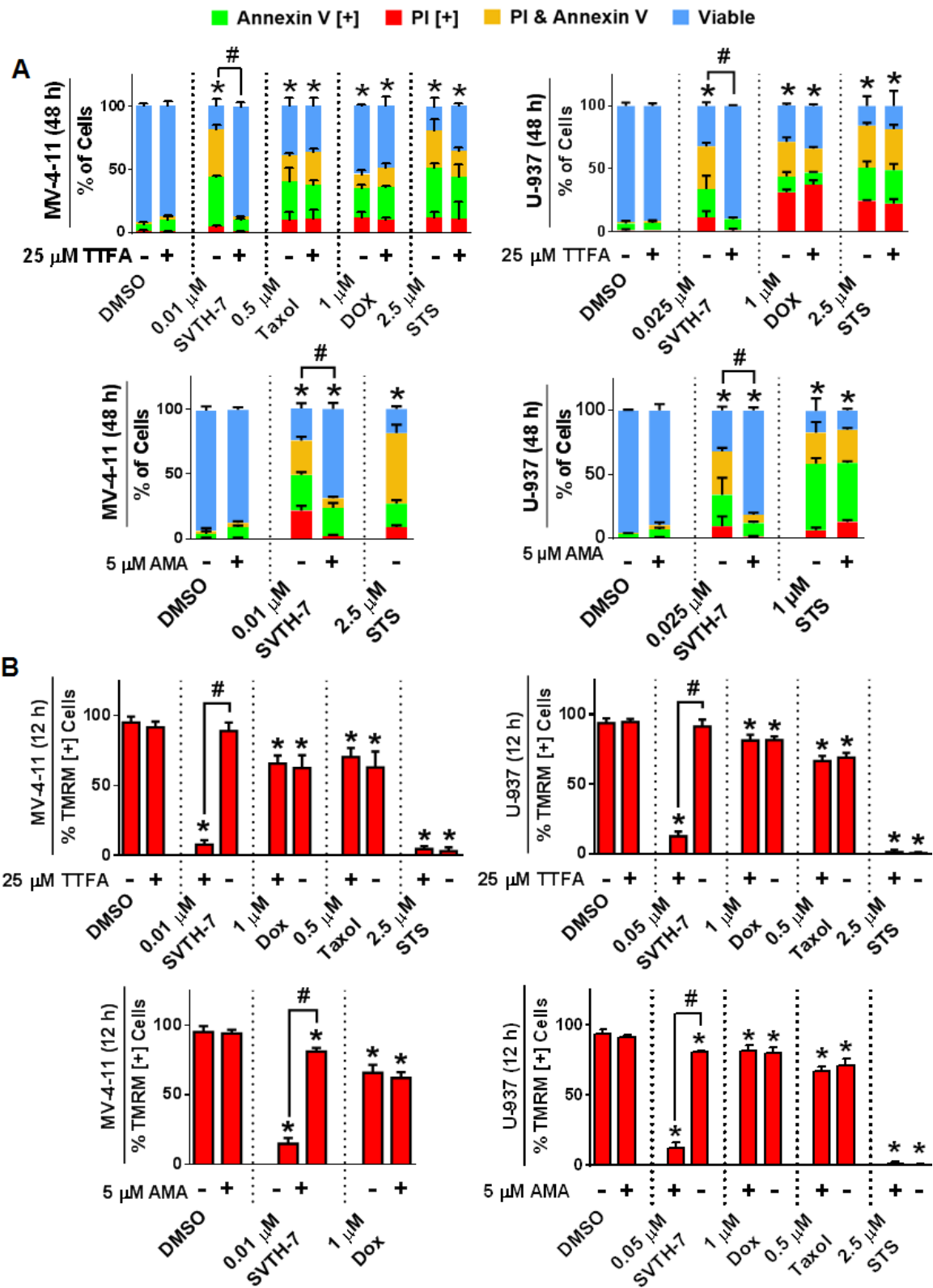


Figure 4.6. PST Analogue-Induced Apoptosis is Dependent on Functional Complex II and III of the Mitochondrial Electron Transport Chain. (A) MV-4-11, and U-937 cancer cells were pre-treated with TTFA complex II inhibitor or antimycin A (AMA) complex III inhibitor for 1 hour and then treated with PST analogues, staurosporine (STS), Doxorubicin (DOX), and Taxol for 48 hours. Annexin V binding (green) and PI staining (PI) (red) was quantified with image based cytometry * $p < 0.01$ vs. DMSO control (comparison of viable cells only); # $p < 0.001$ vs. respective groups without TTFA or AMA (comparison of viable cells only). **(B)** TMRM quantitation of MMP of cells treated as described for 12 hours was performed using image based cytometry. * $p < 0.01$ vs. DMSO control (comparison of viable cells only); # $p < 0.001$ vs. respective groups without TTFA or AMA (comparison of viable cells only). All values are expressed as mean \pm SD from at least 3 independent experiments.

PST Analogues Selectively Induce Apoptosis in 3D Spheroid Models of Cancer

The three-dimensional architecture of tumors has been shown to dictate the responsiveness of cancer cells to chemotherapeutics (Imamura et al. 2015). To evaluate the efficacy of PST analogues in a more architecturally accurate context, cells were grown in three-dimensional spheroid culture on basement membrane extract (BMX) coated surfaces for 48 hours, which provides a scaffold for cells to form three-dimensional structures (Lee et al. 2007), and treated with PST analogues for 72 hours. SVTH-7, -6, -5 and natural PST were the most effective on the HCT 116 colorectal cancer and BxPC-3 pancreatic cancer spheroids as determined by the WST-1 viability assay (**Figure 4.7A**). Interestingly, SVTH-6 and natural PST had comparable anti-cancer activity compared to GEM, the current standard chemotherapeutic for pancreatic cancer (Berlin & Benson 2010), in BxPC-3 spheroids while SVTH-7 had significantly superior activity compared to GEM.

Annexin V binding was monitored in HCT 116 colorectal cancer spheroids (**Figure 4.7B**). Similarly to the STS positive control for apoptosis, HCT 116 cells treated with SVTH-6 and -7 were positive for Annexin V binding, indicated by the green fluorescence. This was accompanied by nuclear condensation and cell shrinkage, as depicted in fluorescence and corresponding differential interference contrast (DIC) micrographs respectively, which are all indicative of apoptosis. Minimal Annexin V binding was present in the solvent DMSO control. In the DIC micrograph of the solvent control, spheroids were dramatically larger and cells exhibited large, round, healthy cellular morphology. NCM460 normal

colon mucosa spheroid cells were dramatically less sensitive to SVTH-6 and -7. Unlike the STS positive control, minimal Annexin V binding was observed in both the solvent control and SVTH-6 and -7 treated cells which exhibited healthy nuclear and cell morphology.

MMP collapse was monitored as another marker of apoptosis (**Figure 4.7C**) (Kroemer et al. 2007). SVTH-6 and -7 were able to dissipate MMP in HCT 116 and BxPC-3 cancer cells in spheroid culture as indicated by the dissipation of red TMRM fluorescence. However, no such dissipation was evident in the NCM460 normal colon mucosa spheroid cells. Together, these results indicate that PST analogues SVTH-6 and -7 are both effective and selective against cancer cells in three-dimensional spheroid culture.

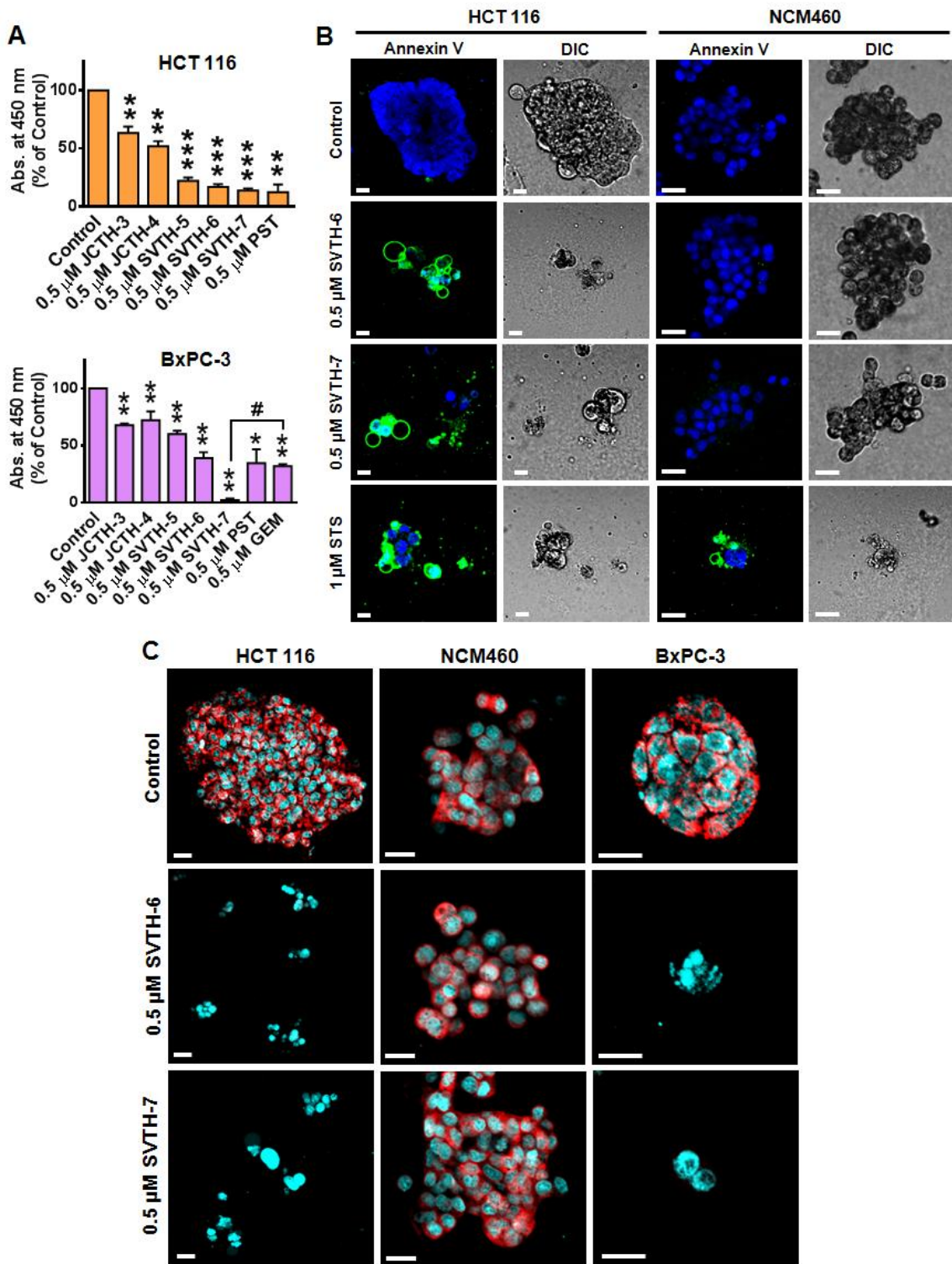


Figure 4.7. PST Analogues Selectively Induce Apoptosis in 3D Spheroid Models of Cancer. Cells were cultured in on basement membrane extract (BMX) to form 3D spheroids, grown for 48 hours, and treated for 72 hours. **(A)** The WST-1 reagent was used to quantify viability. Absorbance was read at 450 nm and expressed as a % of control. Values are expressed as mean \pm SD from triplicates of at least three independent experiments. * $p < 0.05$; ** $p < 0.005$; *** $p < 0.0005$ vs. DMSO control. # $p < 0.001$ vs. 0.5 μ M GEM. **(B)** Confocal microscopy was used to monitor Annexin V binding (green) and **(C)** TMRM fluorescence (red). Cells were counterstained with NucRed Live 647 ReadyProbes® Reagent to visualize nuclei (blue in B, cyan in C). Scale bar = 20 μ m. Micrographs are representative of 3 independent experiments with similar trends.

PST Analogues Decrease Growth of Tumors in Xenograft Mouse Models

To evaluate the anti-cancer activity of PST analogues *in vivo*, cancer cells were subcutaneously injected into the flanks of immunocompromised mice. After palpable tumors were established approximately 1 week after injections, mice were treated with 3 mg/kg of PST analogues intratumorally 3 times a week for approximately 5 weeks. JCTH-4 and SVTH-5 were able to reduce the growth of both HCT 116 and HT-29 colorectal tumor xenografts with SVTH-5 showing greater efficacy (**Figure 4.8A &B**). SVTH-6 was also effective in reducing growth of HT-29 tumors (**Figure 4.8C**). Furthermore, SVTH-6 and -7 were very effective in reducing the growth of HCT 116 colorectal cancer and U-87 MG glioblastoma tumor xenografts as tumor volumes were drastically smaller than the DMSO solvent control treated tumors (**Figure 4.8C**). Mice treated with JCTH-4, SVTH-5, -6, and -7 all increased in mass throughout the studies and did not significantly differ from the masses of mice treated with DMSO solvent control (**Figure 4.8A-C**). These findings demonstrate that PST analogues are able to decrease the growth of tumors *in vivo* and are well tolerated by mice at their effective doses.

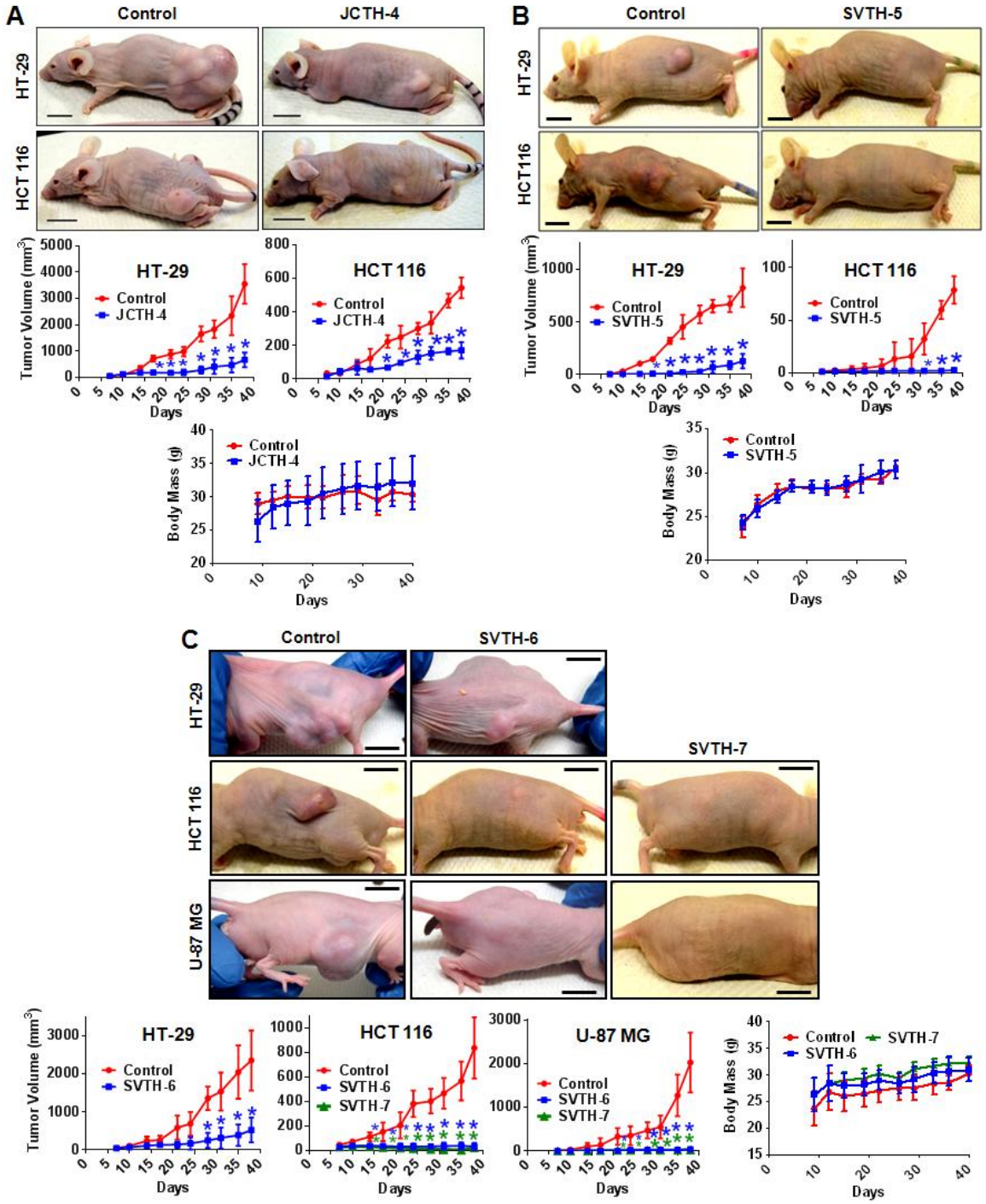


Figure 4.8. PST Analogues Decrease Growth of Tumors in Xenograft Mouse Models. Cancer cells were injected subcutaneously into the flanks of nude mice to establish (day 0). After palpable tumors were detected (approximately 1 week), mice were treated via intratumoral injection with DMSO vehicle control or 3 mg/kg of **(A)** JCTH-4, **(B)** SVTH-5, **(C)** SVTH-6, and SVTH-7 3x/week for approximately 5 weeks. Scale bar for representative tumor sizes at time of sacrifice = 1 cm. Values for tumor volumes and body weights are expressed as mean \pm SD (n=4-6). * $p < 0.05$ vs. control. No significant difference in body masses between control and PST analogue treated mice was observed.

Discussion

In this structure activity relationship analysis, we have discovered that the anti-cancer activity of these alkaloids to be highly dependent on the C-7 hydroxyl group and the functional substitutions on C-1. Several synthetic analogues with the full anti-cancer pharmacophore of PST, including the C-7 hydroxyl group (**refer to Figure 4.1**), were evaluated. Accordingly, SVTH-6 and -5 were more potent against cancer cells compared to their related compounds JCTH-4 and -3, respectively, which lack this functional group. Furthermore, the functional group at C-1 dramatically dictates analogue potency. For example, JCTH-1 and JCTH-2 only different from JCTH-4 in their C-1 functional groups and are nearly devoid of any anti-cancer activity (**Figure 4.2 & 4.3A**). Likewise, SVTH-7 differs only in the group at C-1, when compared to SVTH-6 and -5, and has much greater efficacy against most cancer cell lines tested (**Figure 4.2 & 4.3A**). These findings suggest the C-7 hydroxyl and, more heavily, the C-1 functional groups play a particular role in interaction with the cellular target(s) of interest at specific binding pocket(s). The high anti-cancer activity of SVTH-7 may imply an interaction between the C-1 functional group and a specific hydrophobic pocket, as this analogue possesses a bulky benzene ring at this position.

Very importantly, PST analogues demonstrated potent anti-cancer activity with low therapeutic doses, with minimal effect in normal cells (**Figure 4.2 & 4.3**). In particular, SVTH-7, -6, and -5 demonstrated greater efficacy than the common chemotherapeutics, Taxol, DOX, GEM, and Cisplatin in a multitude of cancer cell types including leukemia, triple negative breast cancer, pancreatic cancer,

glioblastoma, and non-small cell lung cancer (**Figure 4.2**). Additionally, these analogues were both effective and selective in inducing apoptosis in cancer cells grown in three-dimensional culture (**Figure 4.7**), demonstrating their ability to penetrate tumor architecture and induce cell death in cells supported by extracellular matrix. More importantly, these analogues were able to reduce growth of tumors *in vivo* without any apparent toxicity to mice as there was no reduction in body mass or decrease in normal activity (**Figure 4.8**). Thus, these compounds appear to show anti-cancer efficacy indicating that they are stable in physiological systems and could have great potential for anti-cancer therapy in patients.

These analogues do not appear to affect tubulin dynamics (**Supplemental Figure S4.6**), as with the chemotherapeutics Taxol and Colchicine, which would otherwise produce detrimental effects in normal fast dividing cells in the body (Jordan & Wilson 2004). Our findings indicate that this cancer selectivity may be attributed to the ability of these compounds to specifically target cancer cell mitochondria (**Figure 4.4 & 4.5**). Cancer cells have been shown to protect their mitochondria with an abundance of anti-apoptotic proteins, including anti-apoptotic members of the Bcl-2 family of proteins, while downregulating pro-apoptotic proteins (Yip & Reed 2008). Moreover, heavy reliance on glycolysis and having relatively inactive mitochondria limits the generation of ROS by the ETC, further decreasing the likelihood of oxidative stress-induced apoptosis. Inhibiting these anti-apoptotic proteins, mimicking pro-apoptotic proteins, or

targeting ETC complexes could potentially mechanism employed by PST analogues.

Mounting evidence suggests targeting complexes of the ETC to be an effective strategy for targeting cancer cells (Ralph et al. 2006). ETC complex manipulation has been shown to increase ROS, which can promote apoptosis selectively as cancer cells have demonstrated to be more sensitive to oxidative stress (Trachootham et al. 2006; Trachootham et al. 2009). Interestingly, inhibiting ETC complexes II and III abolishes the pro-apoptotic effects of the PST analogue SVTH-7 on cancer cells and their mitochondria, with a slightly more pronounced effect with complex II inhibition (**Figure 4.6**). It may be possible for this PST analogue to directly target these complexes, an interacting partner of these complexes, exploit an unidentified feature of the metabolic state created by these functional complexes, or affect something downstream of these complexes. One such interacting partner of Complex II is TRAP1. This protein has been shown to have an inhibitory effect on complex II, acting as an antioxidant and producing anti-apoptotic effects on tumor cells (Guzzo et al. 2014). Furthermore, succinate dehydrogenase (SDH) or complex II was found to be a mediator of apoptosis, producing ROS for cell death upon intracellular acidification (Lemarie et al. 2011). However, further investigation is required to clarify the role of complex II and III in SVTH-7-mediated apoptosis.

This study comprehensively compares the activity of a number of PST analogues and has shown SVTH-7, followed by SVTH-6 and SVTH-5, to be the most effective against a battery of cancer cell lines, surpassing the anti-cancer

activity of natural PST, 7-deoxyPST analogues, and several chemotherapeutics *in vitro*. These analogues were shown to target cancer cell mitochondria and be selective towards cancer cells in cell and animal models. The requirement of functional complex II and III for SVTH-7 to exert its pro-apoptotic effects in cancer cells points to a potential vulnerability in cancer cells that can be further characterized and exploited to strategically devise new treatment regimes. Therefore, this work provides a scaffold for characterizing distinct mitochondrial and metabolic characteristics in cancer cells that may be used to devise novel therapeutic strategies and highlights several PST analogues with high therapeutic potential.

Author Contributions

Dennis Ma contributed to the conception and design of experiments, execution of experiments, analysis of data, and preparation of the manuscript. Daniel Tarade, Tyler Gilbert, Christopher Pignanelli, Fadi Mansour, Scott Adams, Colin Curran, Alexander Dowhayko, Megan Noel and Melissa Cowell contributed to the execution of experiments and preparation of the manuscript. Sergey Vshyvenko and Tomas Hudlicky synthesized and provided PST analogues for this study. James McNulty provided natural PST for this study. Siyaram Pandey contributed to design of experiments, analysis of data, preparation of the manuscript and obtained funding for the project.

Acknowledgements

Thank you to Phillip Tremblay, Manika Gupta, Ian Tuffley, Sabrina Ma, Kevinjeet Mahngar, Pardis Akbari-Asl, Jashanjit Cheema, Julia Church, Seema Joshi, and Adam Kadri for their initial work and assistance on this project. Thank you to Dr. Siyaram Pandey, Anna Crater-Potter, Krithika Muthukumaran, Colin Curran, Mike Stanesic, and Diego Vazquez for their generous gifts to this project. Funding of this work has been provided as generous donations by the Knights of Columbus Chapter 9671 (Windsor, Ontario) and from Dave and Donna Couvillon in memory of Kevin Couvillon. This work has also been supported by a Vanier Canada Graduate Scholarship, a CIHR Frederick Banting and Charles Best Canada Graduate Scholarship, and an Ontario Graduate Scholarship awarded to Dennis Ma.

References

- Adams, J.M. & Cory, S., 2007. The Bcl-2 apoptotic switch in cancer development and therapy. *Oncogene*, 26(9), pp.1324–37.
- Belmokhtar, C.A., Hillion, J. & Ségal-Bendirdjian, E., 2001. Staurosporine induces apoptosis through both caspase-dependent and caspase-independent mechanisms. *Oncogene*, 20(26), pp.3354–62.
- Berlin, J. & Benson, A.B., 2010. Chemotherapy: Gemcitabine remains the standard of care for pancreatic cancer. *Nature reviews. Clinical oncology*, 7(3), pp.135–7.
- Brand, M.D. & Nicholls, D.G., 2011. Assessing mitochondrial dysfunction in cells. *The Biochemical journal*, 435(2), pp.297–312.
- Brown, J.M. & Attardi, L.D., 2005. The role of apoptosis in cancer development and treatment response. *Nature reviews. Cancer*, 5(3), pp.231–7.
- Chatterjee, S.J., McNulty, J. & Pandey, S., 2010. Sensitization of human melanoma cells by tamoxifen to apoptosis induction by pancratistatin, a nongenotoxic natural compound. *Melanoma research*.
- Chen, G. et al., 2010. Preferential killing of cancer cells with mitochondrial dysfunction by natural compounds. *Mitochondrion*, 10(6), pp.614–25.
- Chen, Y. et al., 2007. Mitochondrial electron-transport-chain inhibitors of complexes I and II induce autophagic cell death mediated by reactive oxygen species. *Journal of cell science*, 120(Pt 23), pp.4155–66.
- Collins, J. et al., 2010. Chemoenzymatic synthesis of Amaryllidaceae constituents and biological evaluation of their C-1 analogues. The next

- generation synthesis of 7-deoxypancratistatin and trans-dihydrolycoricidine. *The Journal of organic chemistry*, 75(9), pp.3069–84.
- DeBerardinis, R.J. et al., 2008. The biology of cancer: metabolic reprogramming fuels cell growth and proliferation. *Cell metabolism*, 7(1), pp.11–20.
- Fadok, V.A. et al., 1998. The role of phosphatidylserine in recognition of apoptotic cells by phagocytes. *Cell death and differentiation*, 5(7), pp.551–62.
- Fischer, U., Jänicke, R.U. & Schulze-Osthoff, K., 2003. Many cuts to ruin: a comprehensive update of caspase substrates. *Cell death and differentiation*, 10(1), pp.76–100.
- Fulda, S. & Debatin, K.-M., 2006. Extrinsic versus intrinsic apoptosis pathways in anticancer chemotherapy. *Oncogene*, 25(34), pp.4798–811.
- Gamen, S. et al., 2000. Doxorubicin treatment activates a Z-VAD-sensitive caspase, which causes deltapسيم loss, caspase-9 activity, and apoptosis in Jurkat cells. *Experimental cell research*, 258(1), pp.223–35.
- Gogvadze, V., Zhivotovsky, B. & Orrenius, S., 2010. The Warburg effect and mitochondrial stability in cancer cells. *Molecular aspects of medicine*, 31(1), pp.60–74.
- Griffin, C. et al., 2010. Pancratistatin induces apoptosis in clinical leukemia samples with minimal effect on non-cancerous peripheral blood mononuclear cells. *Cancer cell international*, 10, p.6.
- Griffin, C., Karnik, A., et al., 2011. Pancratistatin selectively targets cancer cell mitochondria and reduces growth of human colon tumor xenografts.

- Molecular cancer therapeutics*, 10(1), pp.57–68.
- Griffin, C., McNulty, J. & Pandey, S., 2011. Pancreatistatin induces apoptosis and autophagy in metastatic prostate cancer cells. *International journal of oncology*, 38(6), pp.1549–56.
- Guzzo, G. et al., 2014. Inhibition of succinate dehydrogenase by the mitochondrial chaperone TRAP1 has anti-oxidant and anti-apoptotic effects on tumor cells. *Oncotarget*, 5(23), pp.11897–908.
- Vander Heiden, M.G., Cantley, L.C. & Thompson, C.B., 2009. Understanding the Warburg effect: the metabolic requirements of cell proliferation. *Science (New York, N.Y.)*, 324(5930), pp.1029–33.
- Imamura, Y. et al., 2015. Comparison of 2D- and 3D-culture models as drug-testing platforms in breast cancer. *Oncology reports*, 33(4), pp.1837–43.
- Jordan, M.A. & Wilson, L., 2004. Microtubules as a target for anticancer drugs. *Nature Reviews Cancer*, 4(4), pp.253–265.
- Kekre, N. et al., 2005. Pancreatistatin causes early activation of caspase-3 and the flipping of phosphatidyl serine followed by rapid apoptosis specifically in human lymphoma cells. *Cancer chemotherapy and pharmacology*, 56(1), pp.29–38.
- Kroemer, G., Galluzzi, L. & Brenner, C., 2007. Mitochondrial membrane permeabilization in cell death. *Physiological reviews*, 87(1), pp.99–163.
- Lee, G.Y. et al., 2007. Three-dimensional culture models of normal and malignant breast epithelial cells. *Nature methods*, 4(4), pp.359–65.
- Lemarie, A. et al., 2011. Specific disintegration of complex II

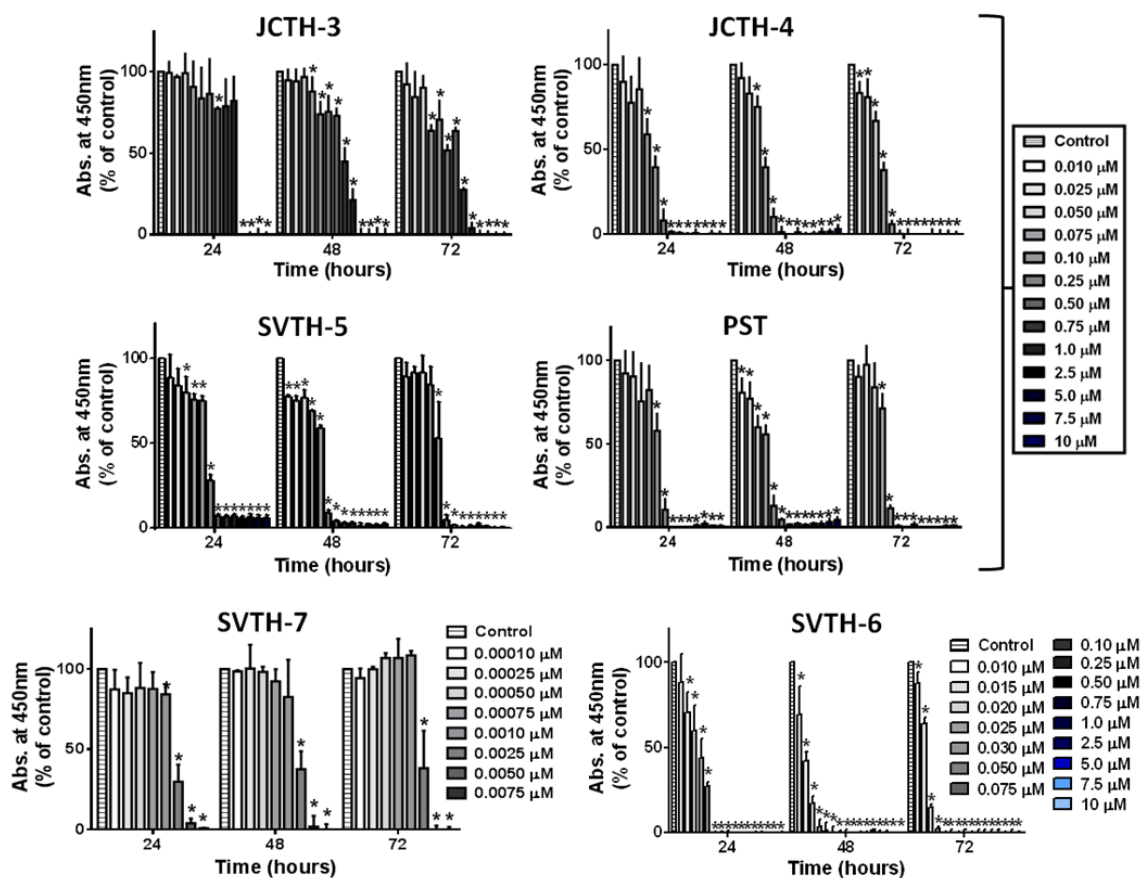
- succinate:ubiquinone oxidoreductase links pH changes to oxidative stress for apoptosis induction. *Cell death and differentiation*, 18(2), pp.338–49.
- Lin, M.T. & Beal, M.F., 2006. Mitochondrial dysfunction and oxidative stress in neurodegenerative diseases. *Nature*, 443(7113), pp.787–95.
- Lips, E.H. et al., 2015. Next generation sequencing of triple negative breast cancer to find predictors for chemotherapy response. *Breast cancer research : BCR*, 17(1), p.134.
- Ma, D., Tremblay, P., et al., 2012. A novel synthetic C-1 analogue of 7-deoxypancratistatin induces apoptosis in p53 positive and negative human colorectal cancer cells by targeting the mitochondria: enhancement of activity by tamoxifen. *Investigational new drugs*, 30(3), pp.1012–27.
- Ma, D., Collins, J., et al., 2012. Enhancement of apoptotic and autophagic induction by a novel synthetic C-1 analogue of 7-deoxypancratistatin in human breast adenocarcinoma and neuroblastoma cells with tamoxifen. *Journal of visualized experiments : JoVE*, (63).
- Ma, D. et al., 2011. Selective cytotoxicity against human osteosarcoma cells by a novel synthetic C-1 analogue of 7-deoxypancratistatin is potentiated by curcumin. *PLoS one*, 6(12), p.e28780.
- McLachlan, A. et al., 2005. Pancratistatin: a natural anti-cancer compound that targets mitochondria specifically in cancer cells to induce apoptosis. *Apoptosis: an international journal on programmed cell death*, 10(3), pp.619–30.
- Neuzil, J. et al., 2013. Classification of mitocans, anti-cancer drugs acting on

- mitochondria. *Mitochondrion*, 13(3), pp.199–208.
- Ow, Y.-L.P. et al., 2008. Cytochrome c: functions beyond respiration. *Nature reviews. Molecular cell biology*, 9(7), pp.532–42.
- Plas, D.R. & Thompson, C.B., 2002. Cell metabolism in the regulation of programmed cell death. *Trends in endocrinology and metabolism: TEM*, 13(2), pp.75–8.
- Poon, I.K.H., Hulett, M.D. & Parish, C.R., 2010. Molecular mechanisms of late apoptotic/necrotic cell clearance. *Cell death and differentiation*, 17(3), pp.381–97.
- Raj, L. et al., 2011. Selective killing of cancer cells by a small molecule targeting the stress response to ROS. *Nature*, 475(7355), pp.231–4.
- Ralph, S.J. et al., 2006. Mitocans: mitochondrial targeted anti-cancer drugs as improved therapies and related patent documents. *Recent patents on anti-cancer drug discovery*, 1(3), pp.327–46.
- Rohlena, J., Dong, L.-F. & Neuzil, J., 2013. Targeting the mitochondrial electron transport chain complexes for the induction of apoptosis and cancer treatment. *Current pharmaceutical biotechnology*, 14(3), pp.377–89.
- Shi, Y., 2001. A structural view of mitochondria-mediated apoptosis. *Nature structural biology*, 8(5), pp.394–401.
- Siedlakowski, P. et al., 2008. Synergy of Pancreatistatin and Tamoxifen on breast cancer cells in inducing apoptosis by targeting mitochondria. *Cancer biology & therapy*, 7(3), pp.376–84.
- Spinazzi, M. et al., 2012. Assessment of mitochondrial respiratory chain

- enzymatic activities on tissues and cultured cells. *Nature protocols*, 7(6), pp.1235–46.
- Tait, S.W.G. & Green, D.R., 2010. Mitochondria and cell death: outer membrane permeabilization and beyond. *Nature reviews. Molecular cell biology*, 11(9), pp.621–32.
- Trachootham, D. et al., 2006. Selective killing of oncogenically transformed cells through a ROS-mediated mechanism by beta-phenylethyl isothiocyanate. *Cancer cell*, 10(3), pp.241–52.
- Trachootham, D., Alexandre, J. & Huang, P., 2009. Targeting cancer cells by ROS-mediated mechanisms: a radical therapeutic approach? *Nature reviews. Drug discovery*, 8(7), pp.579–91.
- Vshyvenko, S. et al., 2011. Synthesis of C-1 homologues of pancratistatin and their preliminary biological evaluation. *Bioorganic & medicinal chemistry letters*, 21(16), pp.4750–2.
- Yip, K.W. & Reed, J.C., 2008. Bcl-2 family proteins and cancer. *Oncogene*, 27(50), pp.6398–406.

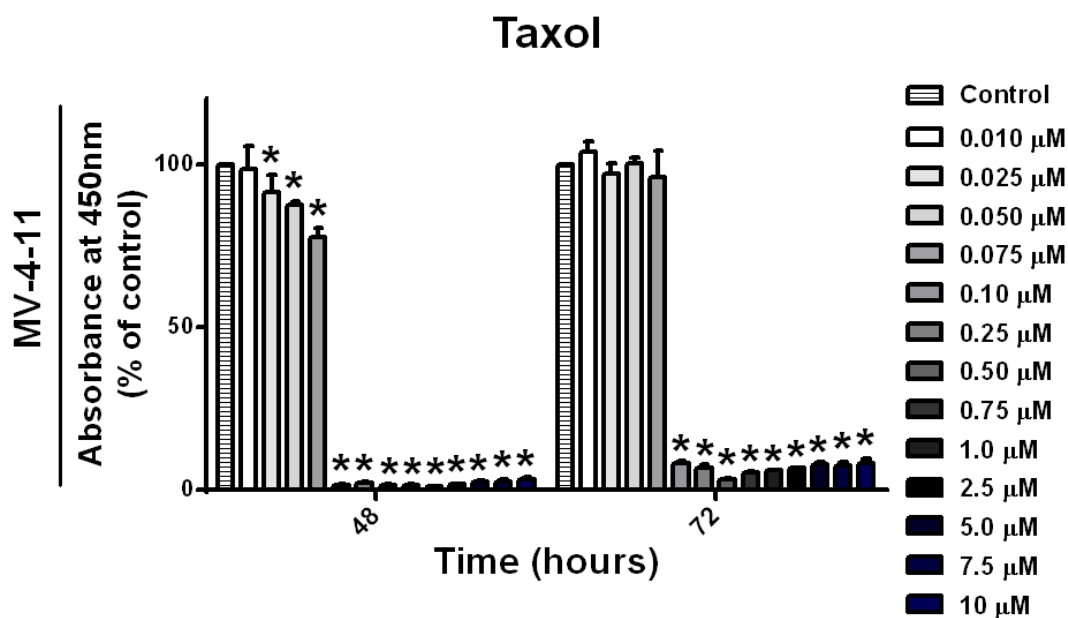
CHAPTER 4
Supplemental Materials

MV-4-11 Biphenotypic B Myelomonocytic Leukemia Cells



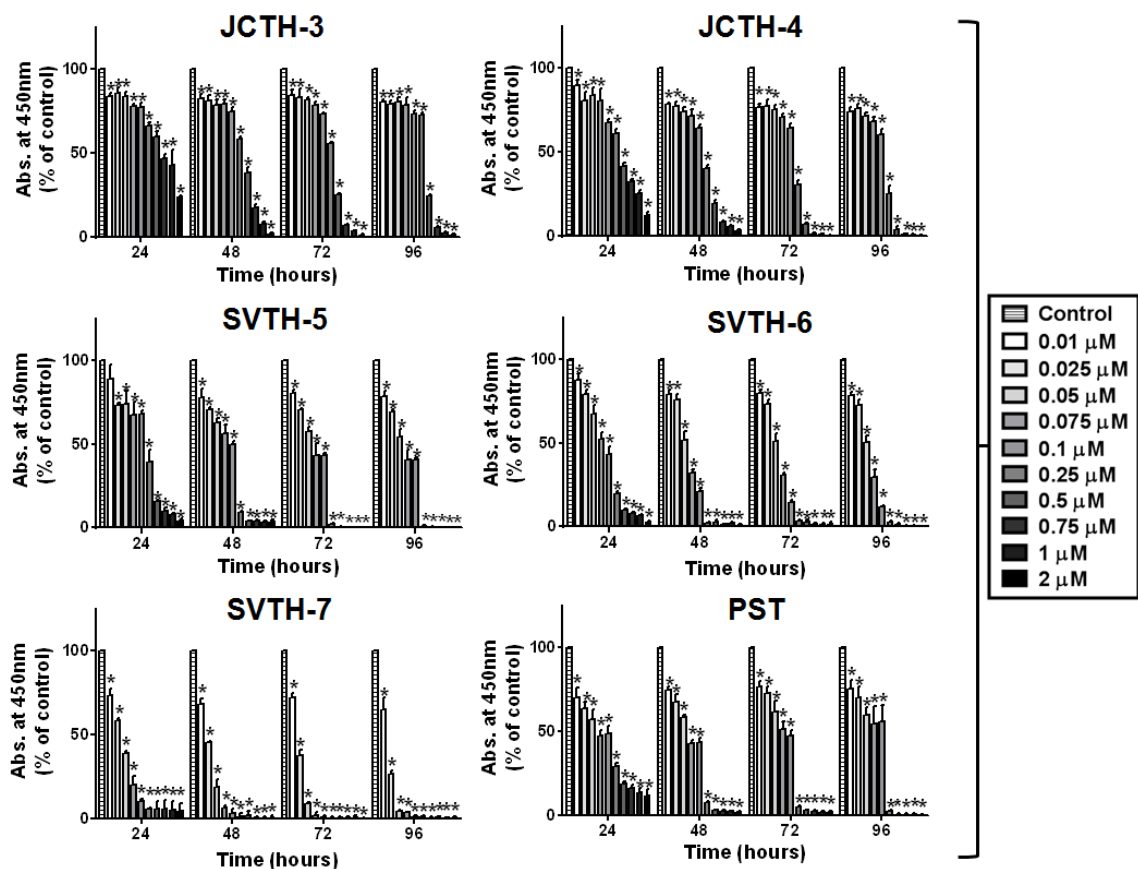
Supplemental Figure S4.1A. PST Analogues & PST Decrease Viability of MV-4-11 Leukemia Cells in a Time and Dose Dependent Manner. The WST-1 colorimetric assay was performed on MV-4-11 cells treated with the indicated concentrations of compounds for the indicated durations. The WST-1 reagent was added and the absorbance of the processed WST-1 reagent formazan, used to quantify cell viability, was read at 450 nm and expressed as a percent of solvent control (DMSO). Values are expressed as mean \pm SD from quadruplicates of 3 independent experiments. $*p < 0.05$ vs. solvent control (DMSO).

MV-4-11 Biphenotypic B Myelomonocytic Leukemia Cells



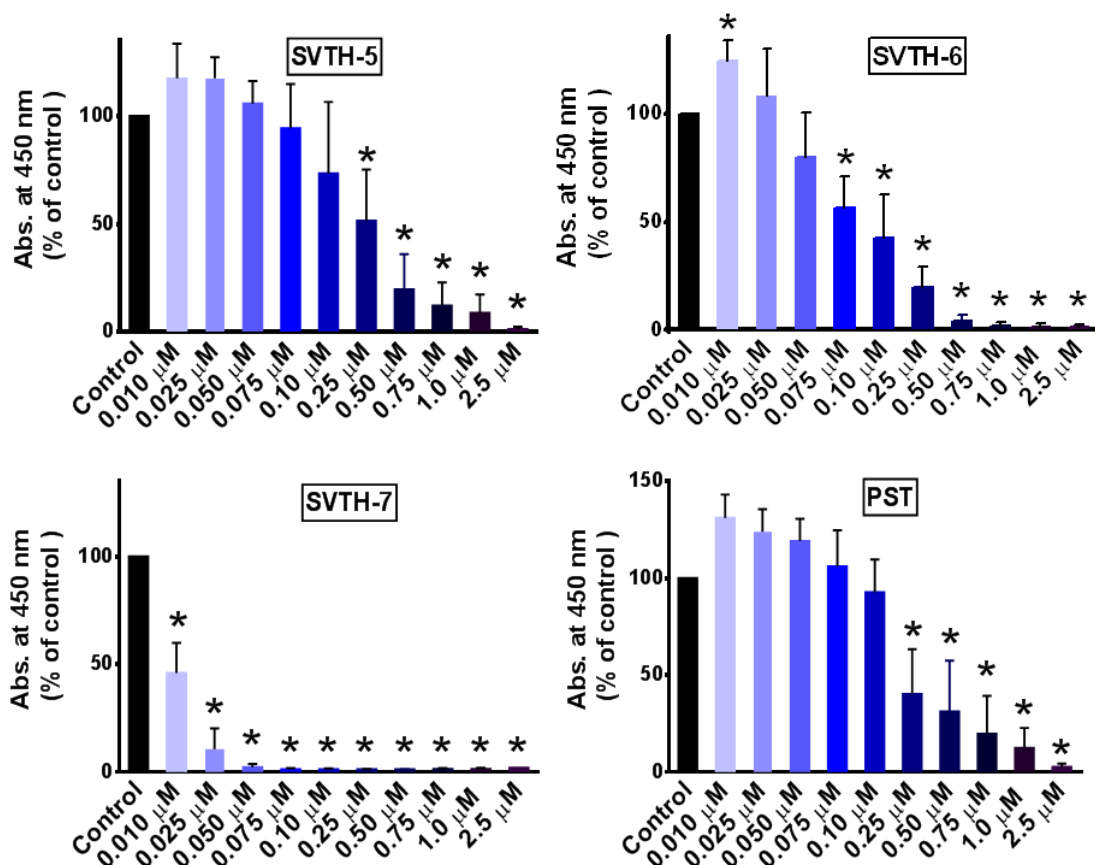
Supplemental Figure S4.1B. Taxol Decreases Viability of MV-4-11 Leukemia Cells. The WST-1 colorimetric assay was performed on MV-4-11 cells treated with the indicated concentrations of Taxol for the indicated durations. The WST-1 reagent was added and the absorbance of the processed WST-1 reagent formazan, used to quantify cell viability, was read at 450 nm and expressed as a percent of solvent control (DMSO). Values are expressed as mean \pm SD from quadruplicates of 3 independent experiments. * $p < 0.05$ vs. solvent control (DMSO).

E6-1 Acute T Cell Leukemia Cells



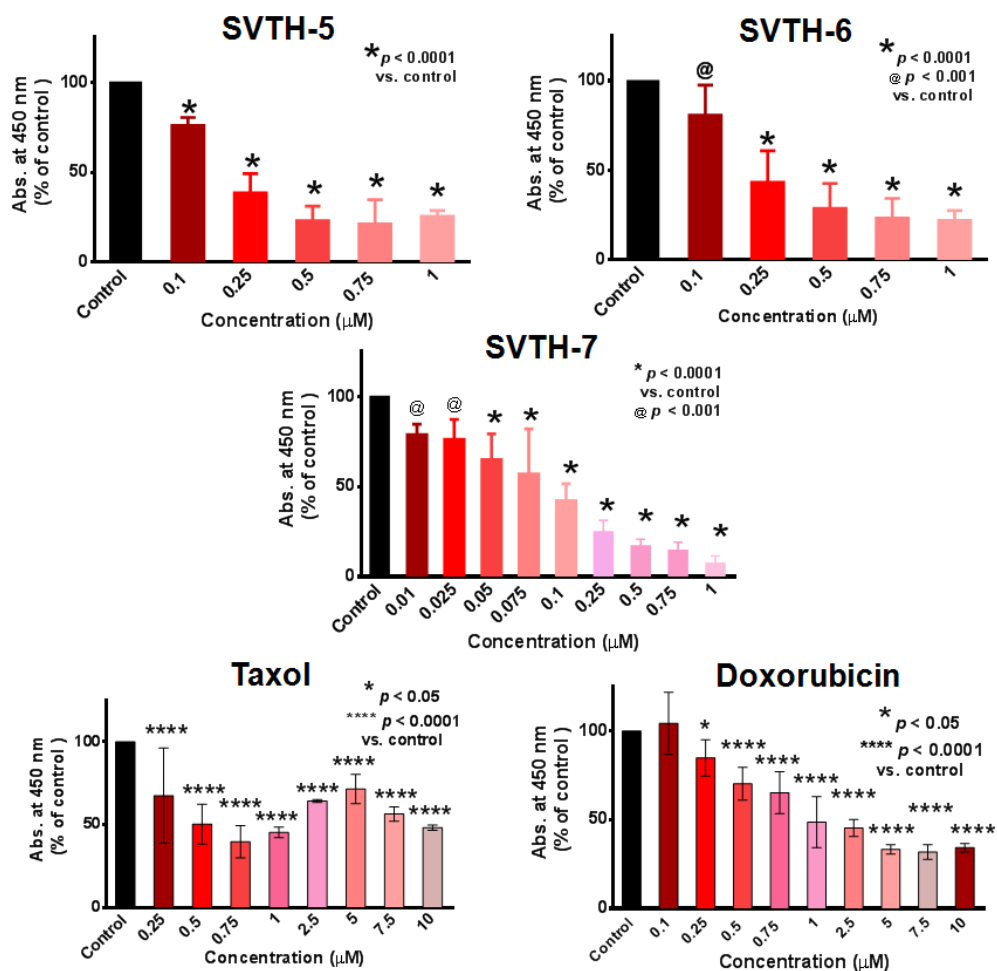
Supplemental Figure S4.1C. PST Analogues & PST Decrease Viability of E6-1 Leukemia Cells in a Time and Dose Dependent Manner. The WST-1 colorimetric assay was performed on E6-1 leukemia cells treated with the indicated concentrations of compounds for the indicated durations. The WST-1 reagent was added and the absorbance of the processed WST-1 reagent formazan, used to quantify cell viability, was read at 450 nm and expressed as a percent of solvent control (DMSO). Values are expressed as mean \pm SD from quadruplicates of 3 independent experiments. * $p < 0.05$ vs. solvent control (DMSO).

U-937 Histiocytic Lymphoma Cells (48 h)



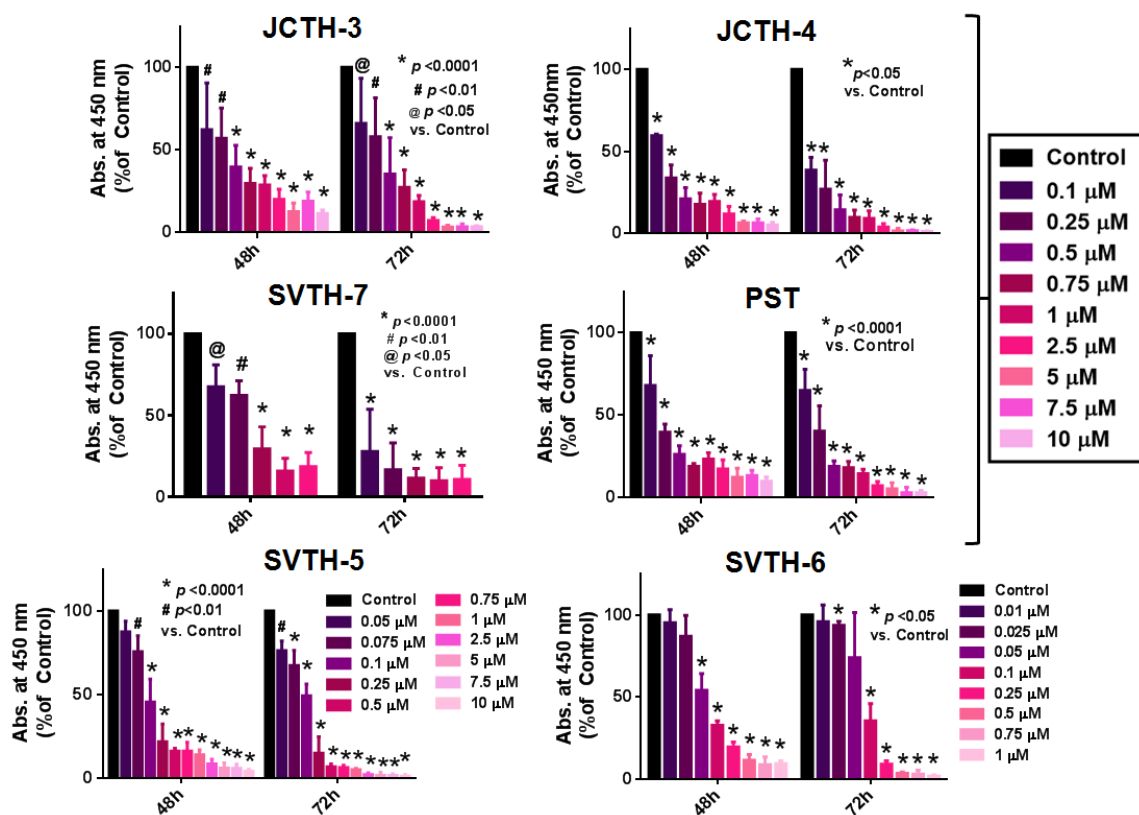
Supplemental Figure S4.1D. PST Analogues & PST Decrease Viability of U-937 Leukemia Cells in a Dose Dependent Manner. The WST-1 colorimetric assay was performed on U-937 lymphoma cells treated with the indicated concentrations of compounds for 48 hours. The WST-1 reagent was added and the absorbance of the processed WST-1 reagent formazan, used to quantify cell viability, was read at 450 nm and expressed as a percent of solvent control (DMSO). Values are expressed as mean \pm SD from quadruplicates of 3 independent experiments. * p <0.05 vs. solvent control (DMSO).

MDA-MB-231 Triple Negative Breast Cancer Cells (48 h)



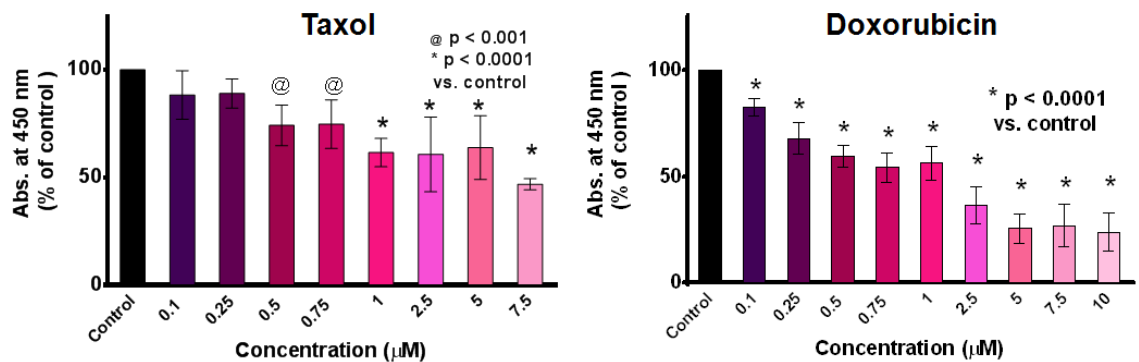
Supplemental Figure S4.1E. PST Analogues Decrease Viability of MDA-MB-231 Triple Negative Breast Cancer Cells in a Dose Dependent Manner with Greater Efficacy than Taxol and Doxorubicin. The WST-1 colorimetric assay was performed on MDA-MB-231 triple negative breast cancer cells treated with the indicated concentrations of compounds for 48 hours. The WST-1 reagent was added and the absorbance of the processed WST-1 reagent formazan, used to quantify cell viability, was read at 450 nm and expressed as a percent of solvent control (DMSO). Values are expressed as mean \pm SD from quadruplicates of 3 independent experiments.

MDA-MB-468 Triple Negative Breast Cancer Cells



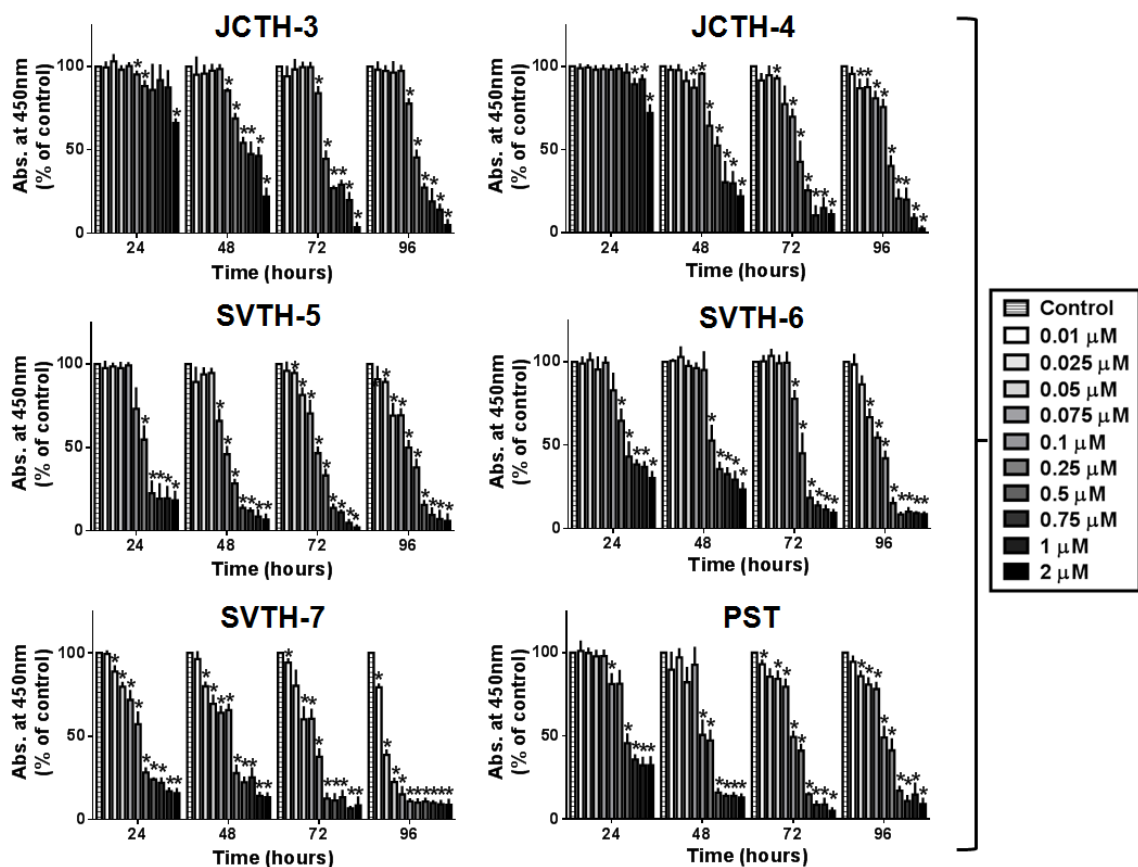
Supplemental Figure S4.1F. PST Analogues & PST Decrease Viability of MDA-MB-468 Triple Negative Breast Cancer Cells in a Time and Dose Dependent Manner. The WST-1 colorimetric assay was performed on MDA-MB-468 triple negative breast cancer cells treated with the indicated concentrations of compounds for the indicated durations. The WST-1 reagent was added and the absorbance of the processed WST-1 reagent formazan, used to quantify cell viability, was read at 450 nm and expressed as a percent of solvent control (DMSO). Values are expressed as mean \pm SD from quadruplicates of 3 independent experiments.

MDA-MB-468 Triple Negative Breast Cancer Cells (48 h)



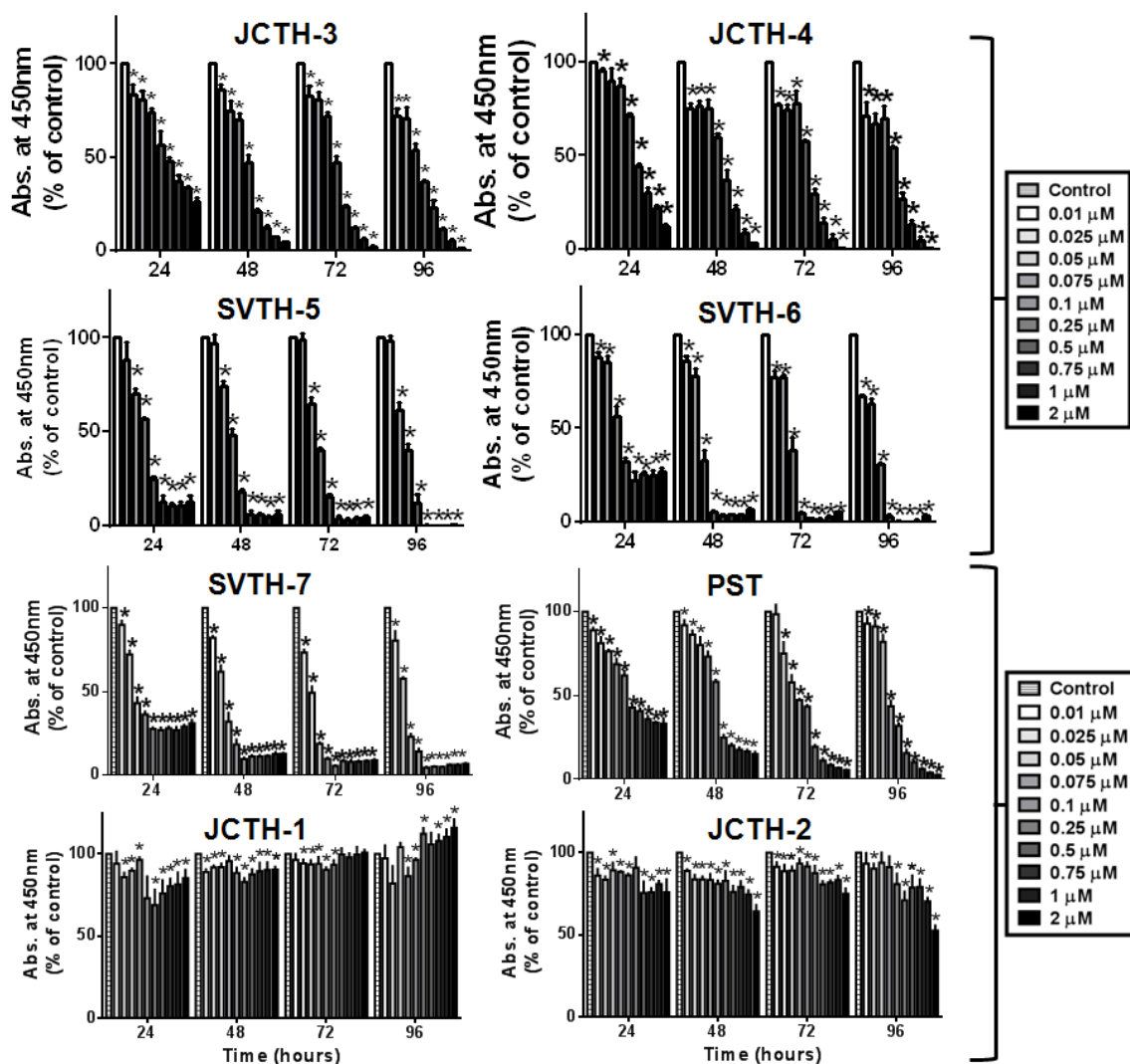
Supplemental Figure S4.1G. Taxol and Doxorubicin Decrease Viability of MDA-MB-468 Triple Negative Breast Cancer Cells with Less Efficacy than PST Analogues. The WST-1 colorimetric assay was performed on MDA-MB-468 triple negative breast cancer cells treated with the indicated concentrations of compounds for 48 hours. The WST-1 reagent was added and the absorbance of the processed WST-1 reagent formazan, used to quantify cell viability, was read at 450 nm and expressed as a percent of solvent control (DMSO). Values are expressed as mean \pm SD from quadruplicates of 3 independent experiments.

SUM 149 Inflammatory Breast Cancer Cells



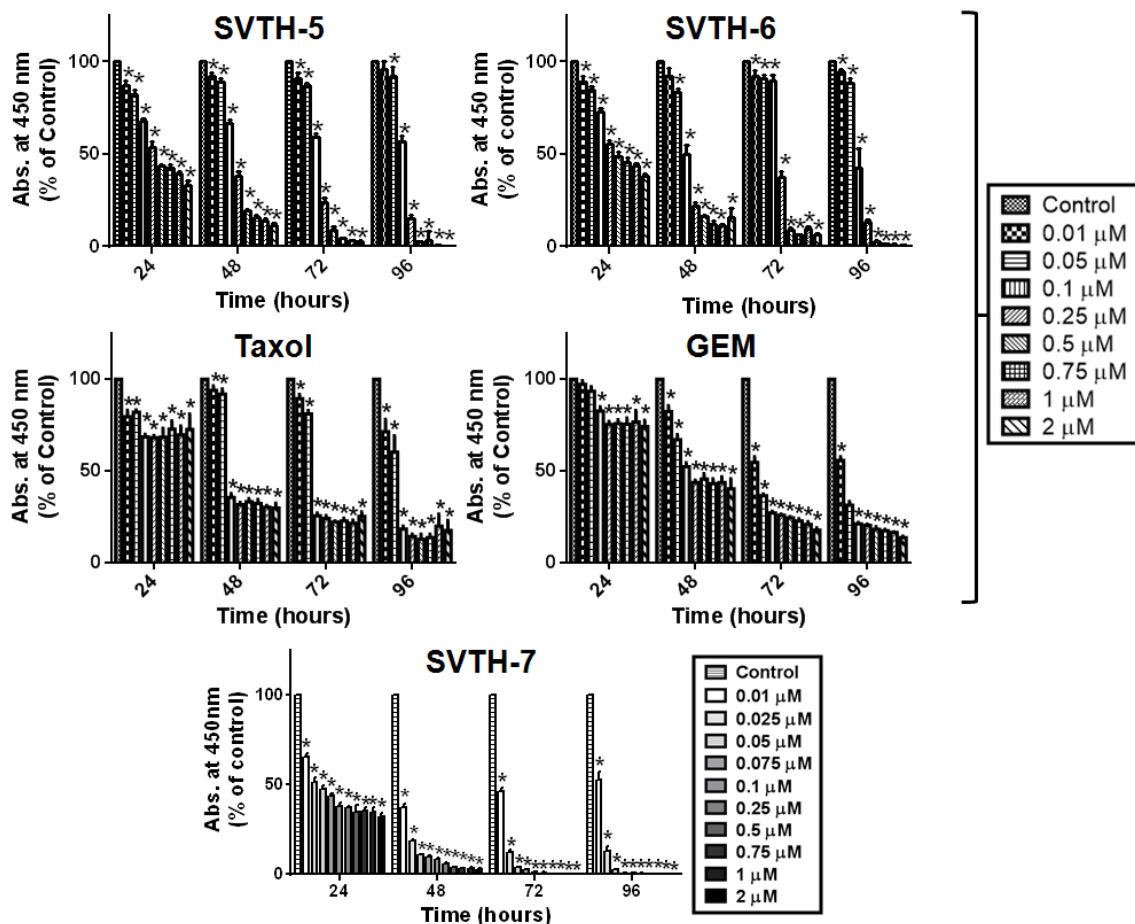
Supplemental Figure S4.1H. PST Analogues & PST Decrease Viability of SUM 149 Breast Cancer Cells in a Time and Dose Dependent Manner. The WST-1 colorimetric assay was performed on SUM 149 breast cancer cells treated with the indicated concentrations of compounds for the indicated durations. The WST-1 reagent was added and the absorbance of the processed WST-1 reagent formazan, used to quantify cell viability, was read at 450 nm and expressed as a percent of solvent control (DMSO). Values are expressed as mean \pm SD from quadruplicates of 3 independent experiments. * $p < 0.05$ vs. solvent control (DMSO).

HCT 116 Colorectal Carcinoma Cells



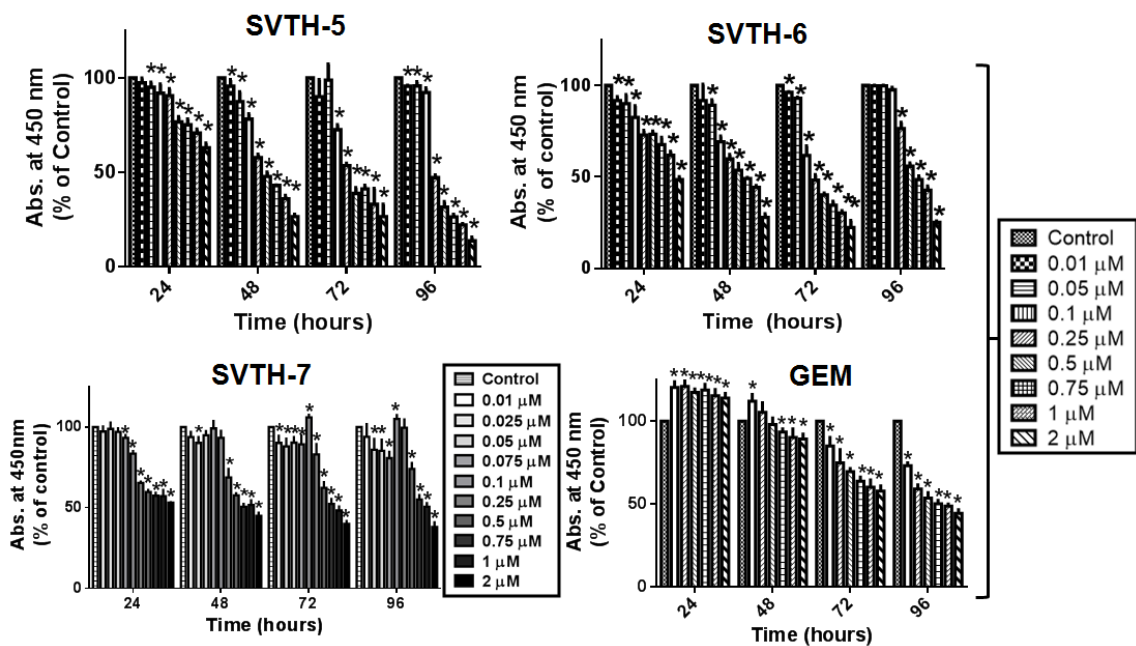
Supplemental Figure S4.11. PST Analogues & PST Decrease Viability of HCT 116 Colorectal Carcinoma Cells in a Time and Dose Dependent Manner. The WST-1 colorimetric assay was performed on HCT 116 colorectal cells treated with the indicated concentrations of compounds for the indicated durations. The WST-1 reagent was added and the absorbance of the processed WST-1 reagent formazan, used to quantify cell viability, was read at 450 nm and expressed as a percent of solvent control (DMSO). Values are expressed as mean \pm SD from quadruplicates of 3 independent experiments. * $p < 0.05$ vs. solvent control (DMSO).

BxPC-3 Pancreatic Adenocarcinoma Cells



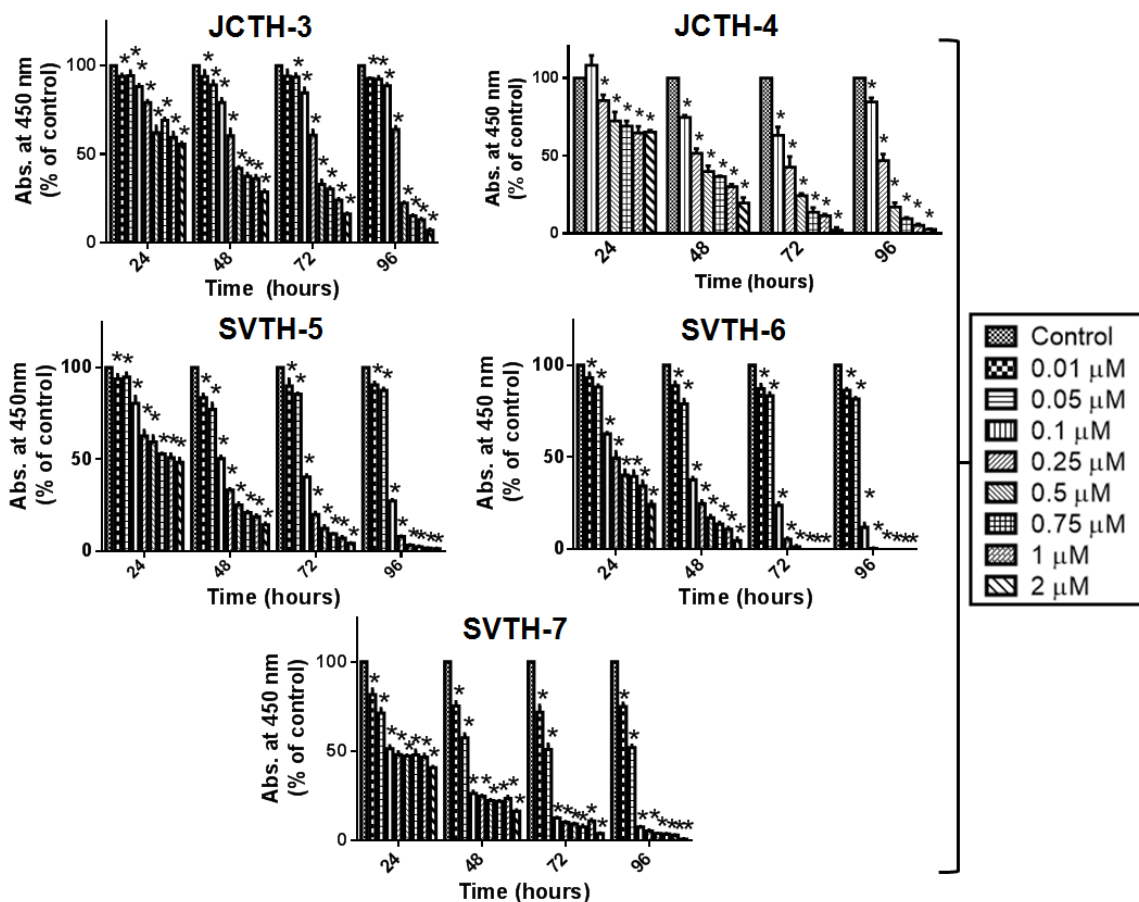
Supplemental Figure S4.1J. PST Analogues Decrease Viability of BxPC-3 Pancreatic Adenocarcinoma Cells in a Time and Dose Dependent Manner with Greater Efficacy than Gemcitabine (GEM) and Taxol. The WST-1 colorimetric assay was performed on BxPC-3 pancreatic adenocarcinoma cells treated with the indicated concentrations of compounds for the indicated durations. The WST-1 reagent was added and the absorbance of the processed WST-1 reagent formazan, used to quantify cell viability, was read at 450 nm and expressed as a percent of solvent control (DMSO). Values are expressed as mean \pm SD from quadruplicates of 3 independent experiments. * $p < 0.05$ vs. solvent control (DMSO).

PANC-1 Pancreatic Epithelioid Carcinoma Cells



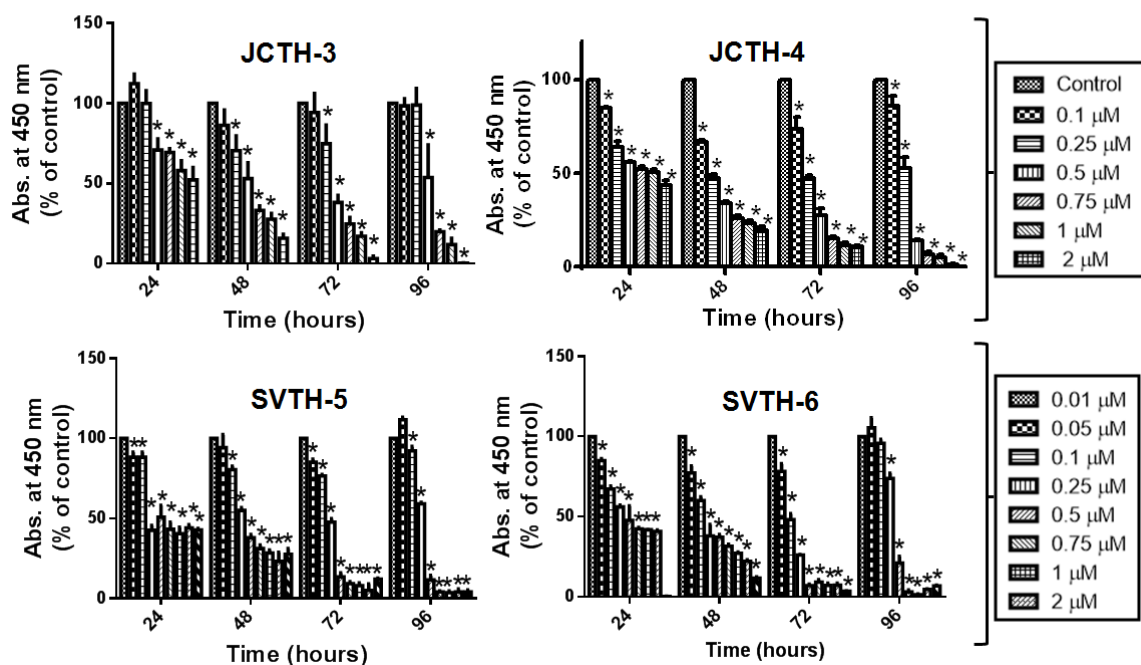
Supplemental Figure S4.1K. PST Analogues Decrease Viability of PANC-1 Pancreatic Cancer Cells in a Time and Dose Dependent Manner with Greater Efficacy than Gemcitabine (GEM). The WST-1 colorimetric assay was performed on PANC-1 pancreatic cancer cells treated with the indicated concentrations of compounds for the indicated durations. The WST-1 reagent was added and the absorbance of the processed WST-1 reagent formazan, used to quantify cell viability, was read at 450 nm and expressed as a percent of solvent control (DMSO). Values are expressed as mean \pm SD from quadruplicates of 3 independent experiments. * $p < 0.05$ vs. solvent control (DMSO).

Saos-2 Osteosarcoma Cells



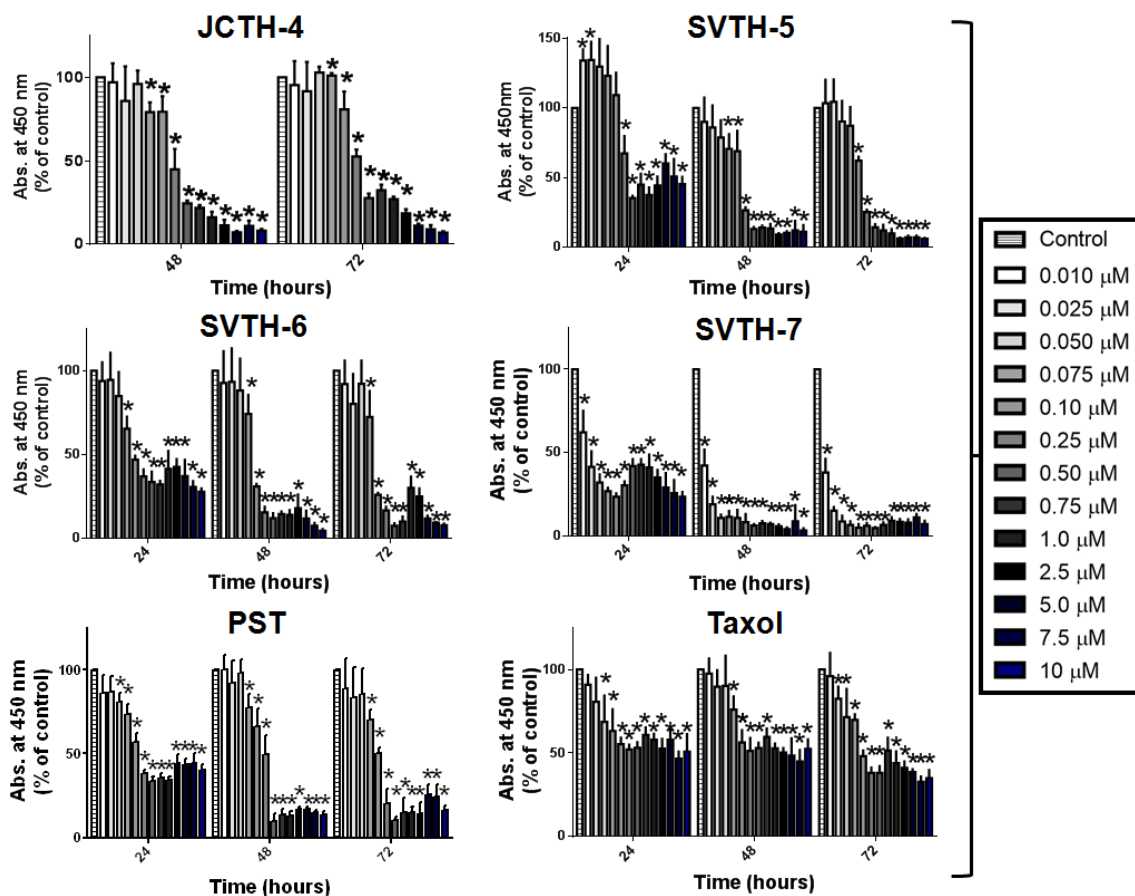
Supplemental Figure S4.1L. PST Analogues Decrease Viability of Saos-2 Osteosarcoma Cells in a Time and Dose Dependent Manner. The WST-1 colorimetric assay was performed on Saos-2 osteosarcoma cells treated with the indicated concentrations of compounds for the indicated durations. The WST-1 reagent was added and the absorbance of the processed WST-1 reagent formazan, used to quantify cell viability, was read at 450 nm and expressed as a percent of solvent control (DMSO). Values are expressed as mean \pm SD from quadruplicates of 3 independent experiments. * p <0.05 vs. solvent control (DMSO).

U-2 OS Osteosarcoma Cells



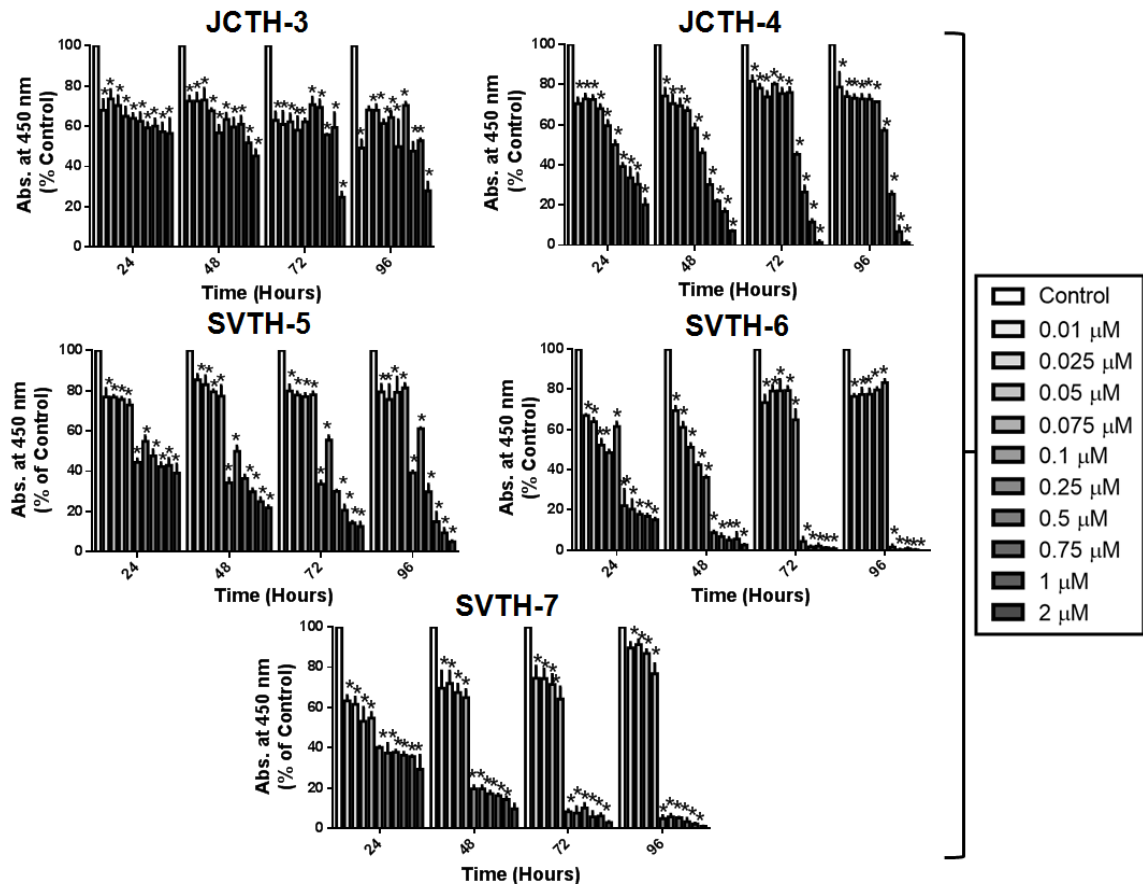
Supplemental Figure S4.1M. PST Analogues Decrease Viability of U-2 OS Osteosarcoma Cells in a Time and Dose Dependent Manner. The WST-1 colorimetric assay was performed on U-2 OS osteosarcoma cells treated with the indicated concentrations of compounds for the indicated durations. The WST-1 reagent was added and the absorbance of the processed WST-1 reagent formazan, used to quantify cell viability, was read at 450 nm and expressed as a percent of solvent control (DMSO). Values are expressed as mean \pm SD from quadruplicates of 3 independent experiments. * $p < 0.05$ vs. solvent control (DMSO).

U-87 MG Glioblastoma Cells



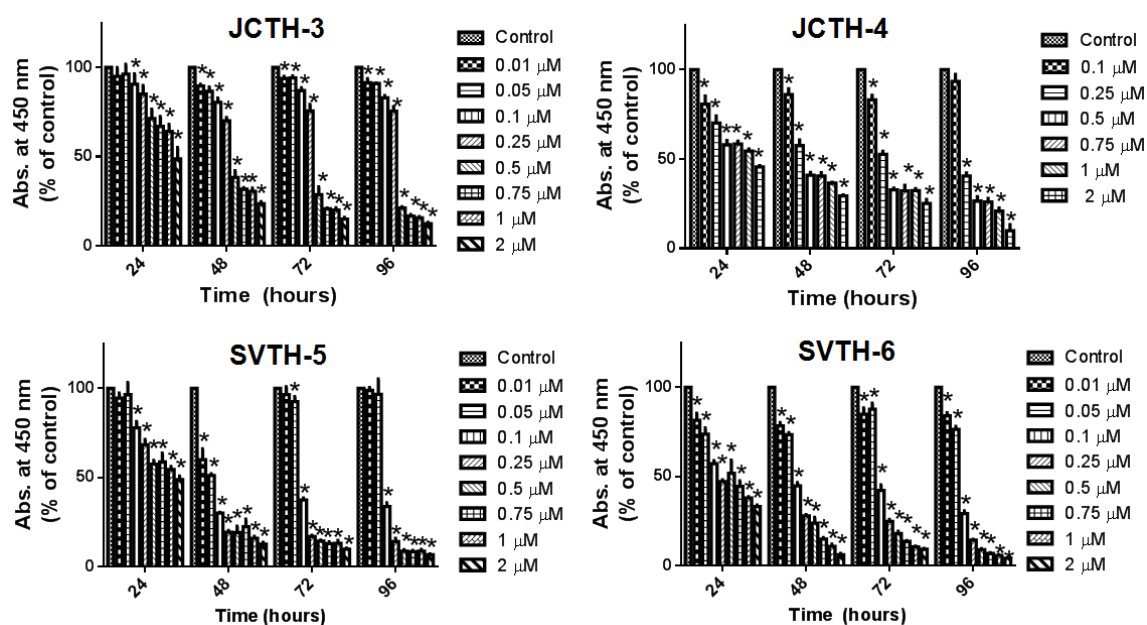
Supplemental Figure S4.1N. PST Analogues & PST Decrease Viability of U-87 MG Glioblastoma Cells in a Time and Dose Dependent Manner with Greater Efficacy than Taxol. The WST-1 colorimetric assay was performed on U-87 MG glioblastoma cells treated with the indicated concentrations of compounds for the indicated durations. The WST-1 reagent was added and the absorbance of the processed WST-1 reagent formazan, used to quantify cell viability, was read at 450 nm and expressed as a percent of solvent control (DMSO). Values are expressed as mean \pm SD from quadruplicates of 3 independent experiments. * $p < 0.05$ vs. solvent control (DMSO).

G-361 Malignant Melanoma Cells



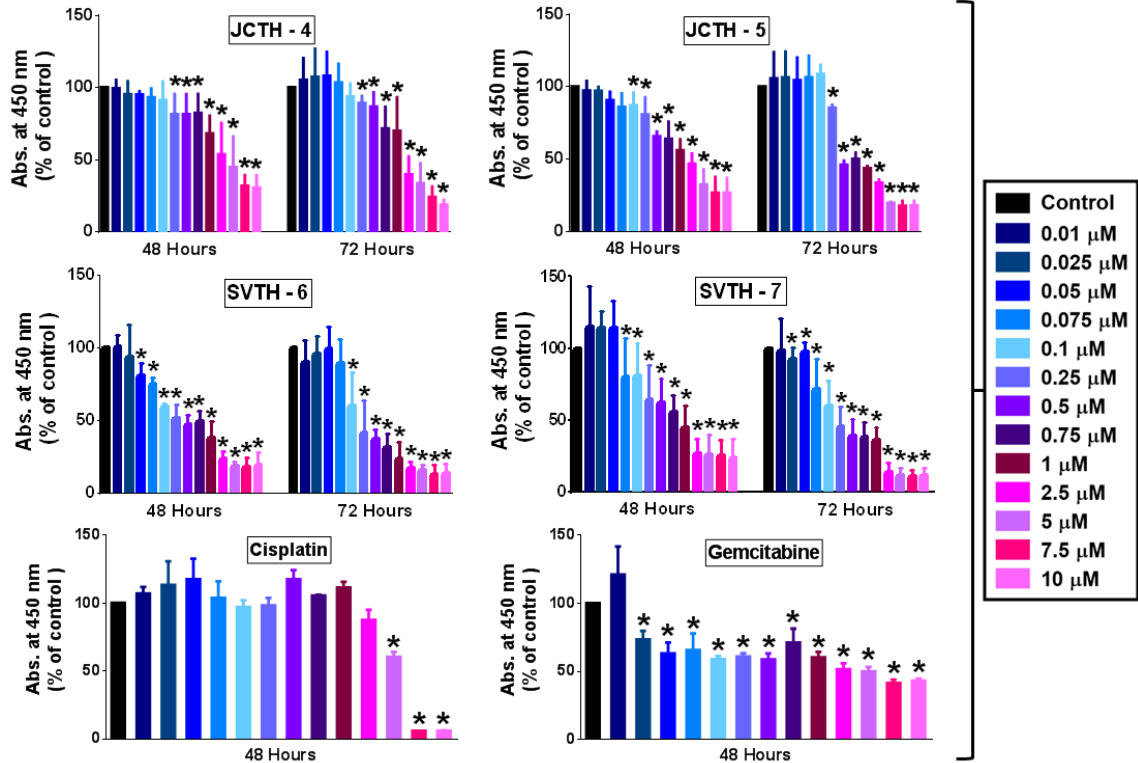
Supplemental Figure S4.10. PST Analogues Decrease Viability of G-361 Malignant Melanoma Cells in a Time and Dose Dependent Manner. The WST-1 colorimetric assay was performed on G-361 malignant melanoma cells treated with the indicated concentrations of compounds for the indicated durations. The WST-1 reagent was added and the absorbance of the processed WST-1 reagent formazan, used to quantify cell viability, was read at 450 nm and expressed as a percent of solvent control (DMSO). Values are expressed as mean \pm SD from quadruplicates of 3 independent experiments. * $p < 0.05$ vs. solvent control (DMSO).

OVCAR-3 Ovarian Adenocarcinoma



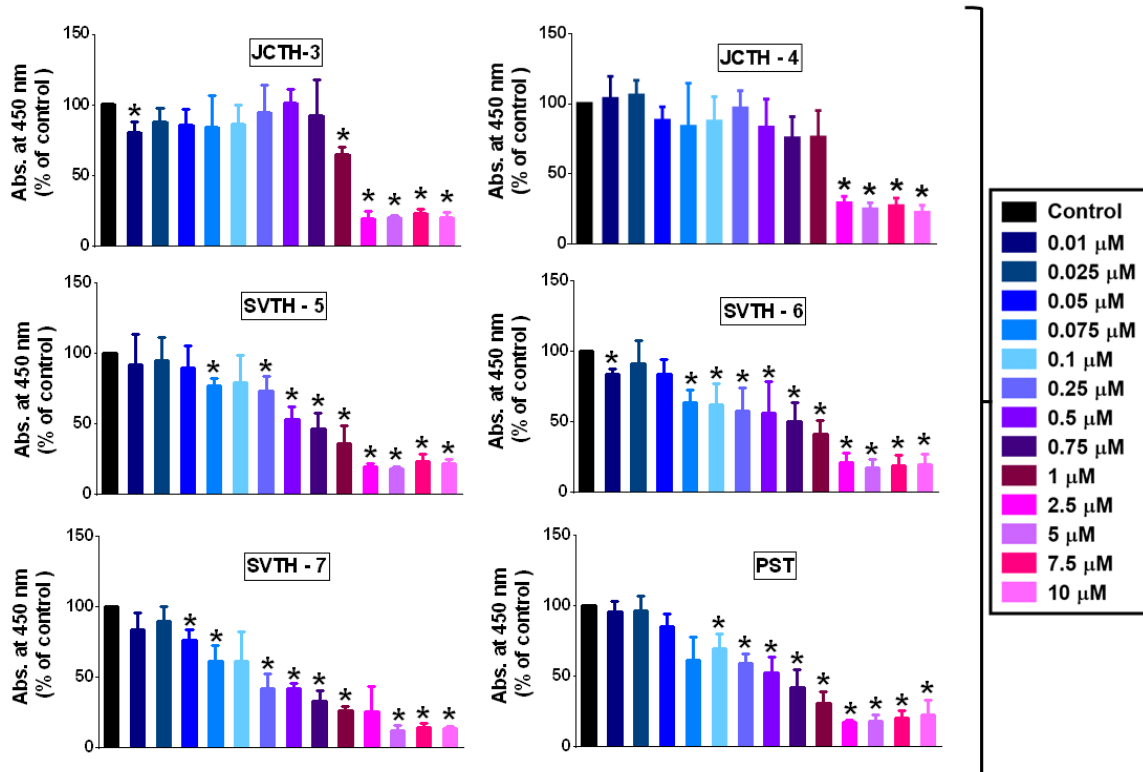
Supplemental Figure S4.1P. PST Analogues Decrease Viability of OVCAR-3 Ovarian Adenocarcinoma Cells in a Time and Dose Dependent Manner. The WST-1 colorimetric assay was performed on OVCAR-3 ovarian adenocarcinoma cells treated with the indicated concentrations of compounds for the indicated durations. The WST-1 reagent was added and the absorbance of the processed WST-1 reagent formazan, used to quantify cell viability, was read at 450 nm and expressed as a percent of solvent control (DMSO). Values are expressed as mean \pm SD from quadruplicates of 3 independent experiments. * $p < 0.05$ vs. solvent control (DMSO).

NCI-H23 Non-Small Cell Lung Carcinoma Cells



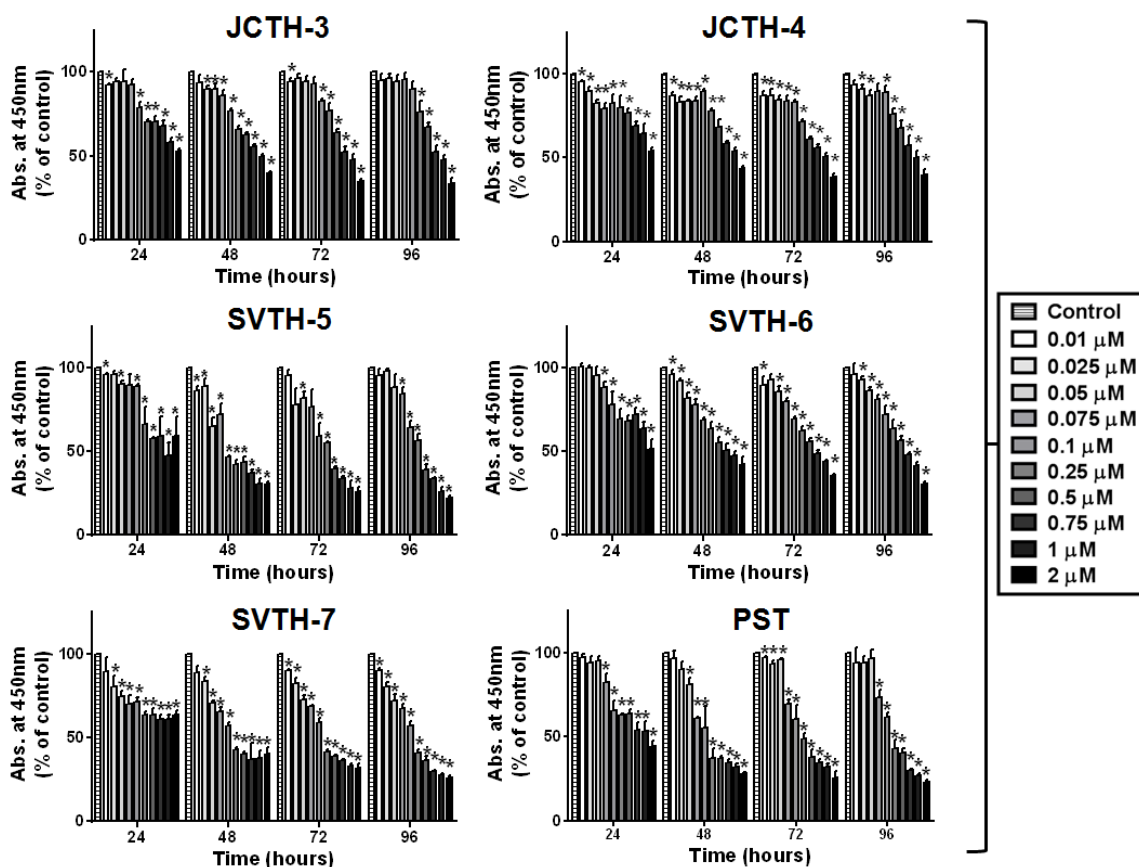
Supplemental Figure S4.1Q. PST Analogues Decrease Viability of NCI-H23 Non-Small Cell Lung Cancer Cells in a Time and Dose Dependent Manner with Greater Efficacy than Cisplatin and Gemcitabine. The WST-1 colorimetric assay was performed on NCI-H23 non-small cell lung cancer cells treated with the indicated concentrations of compounds for the indicated durations. The WST-1 reagent was added and the absorbance of the processed WST-1 reagent formazan, used to quantify cell viability, was read at 450 nm and expressed as a percent of solvent control (DMSO). Values are expressed as mean \pm SD from quadruplicates of 3 independent experiments. * $p < 0.05$ vs. solvent control (DMSO).

A549 Non-Small Cell Lung Carcinoma Cells (48 h)



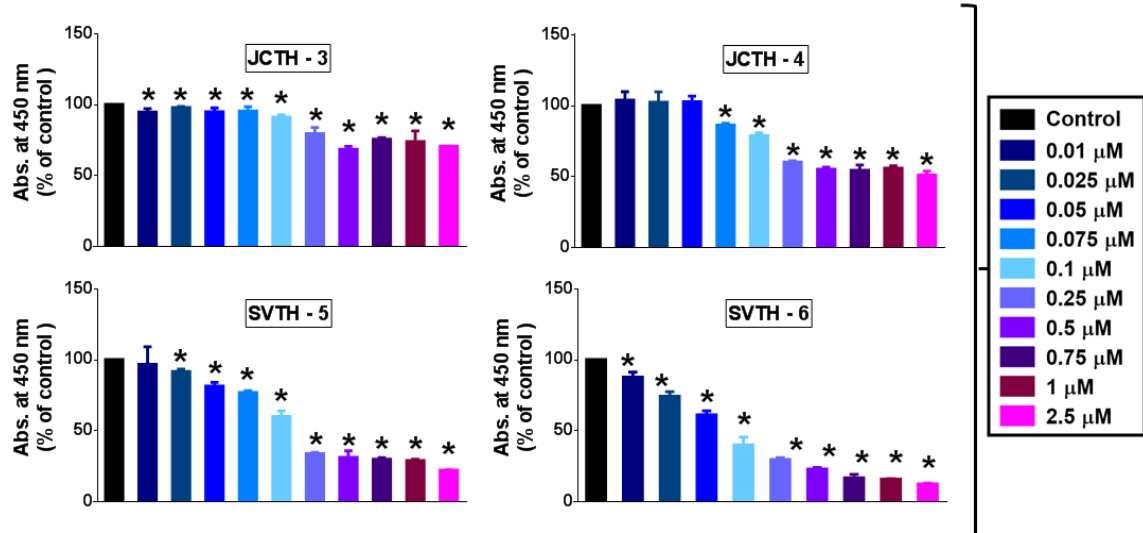
Supplemental Figure S4.1R. PST Analogues Decrease Viability of A549 Non-Small Cell Lung Cancer Cells in a Dose Dependent Manner. The WST-1 colorimetric assay was performed on A549 non-small cell lung cancer cells treated with the indicated concentrations of compounds for 48 hours. The WST-1 reagent was added and the absorbance of the processed WST-1 reagent formazan, used to quantify cell viability, was read at 450 nm and expressed as a percent of solvent control (DMSO). Values are expressed as mean \pm SD from quadruplicates of 3 independent experiments. * p <0.05 vs. solvent control (DMSO).

MCF7 Breast Cancer Cells



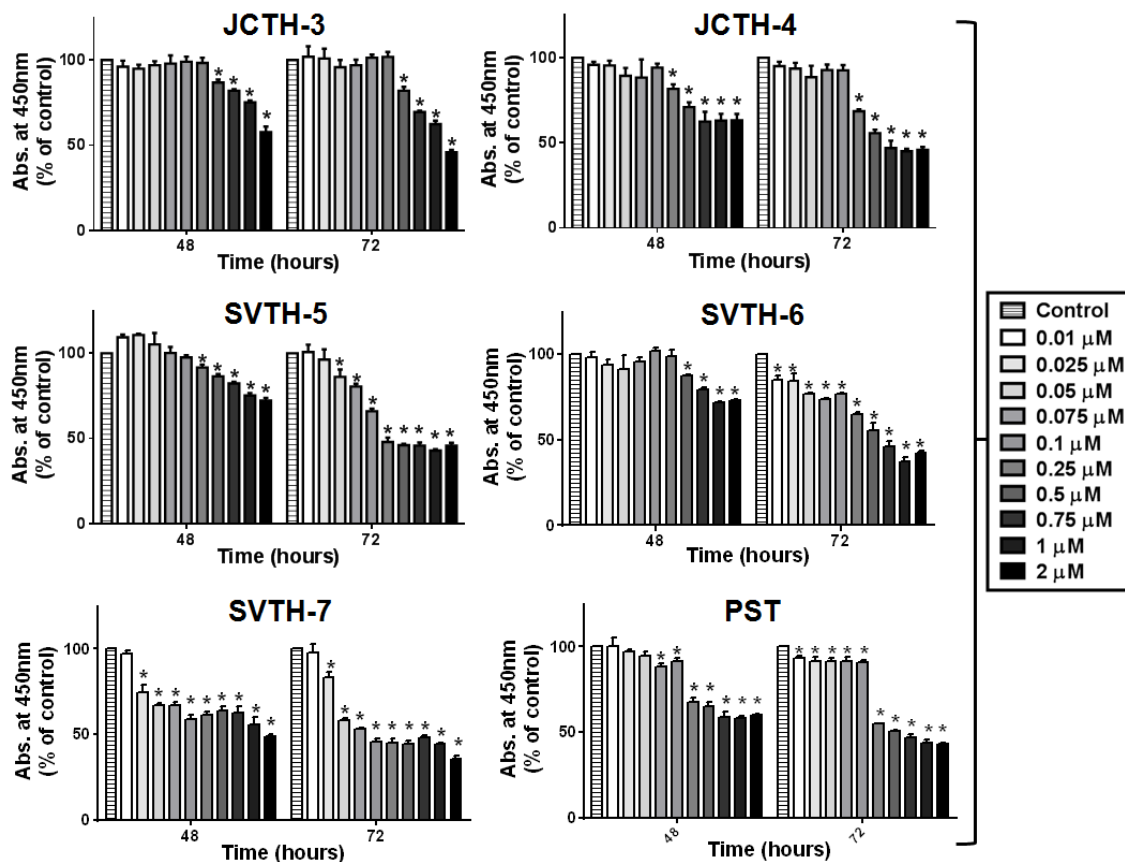
Supplemental Figure S4.1S. PST Analogues & PST Decrease Viability of MCF7 Breast Cancer Cells in a Time and Dose Dependent Manner. The WST-1 colorimetric assay was performed on MCF7 breast cancer cells treated with the indicated concentrations of compounds for the indicated durations. The WST-1 reagent was added and the absorbance of the processed WST-1 reagent formazan, used to quantify cell viability, was read at 450 nm and expressed as a percent of solvent control (DMSO). Values are expressed as mean \pm SD from quadruplicates of 3 independent experiments. * $p < 0.05$ vs. solvent control (DMSO).

DU-145 Prostate Carcinoma Cells (48 h)



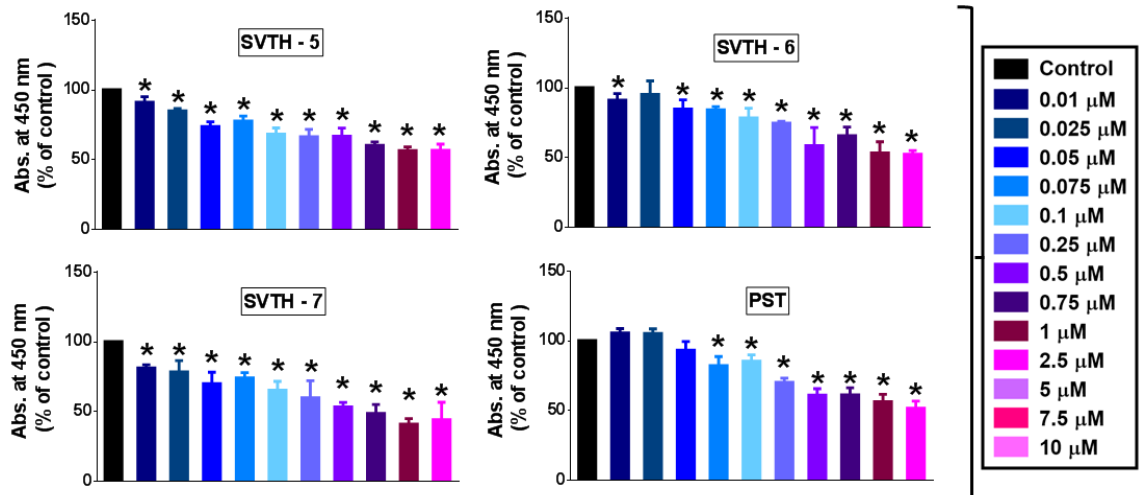
Supplemental Figure S4.1T. PST Analogues Decrease Viability of DU-145 Prostate Carcinoma Cells in a Dose Dependent Manner. The WST-1 colorimetric assay was performed on DU-145 prostate cancer cells treated with the indicated concentrations of compounds for 48 hours. The WST-1 reagent was added and the absorbance of the processed WST-1 reagent formazan, used to quantify cell viability, was read at 450 nm and expressed as a percent of solvent control (DMSO). Values are expressed as mean \pm SD from quadruplicates of 3 independent experiments. * $p < 0.05$ vs. solvent control (DMSO).

Normal Human Fibroblasts (AG09309)



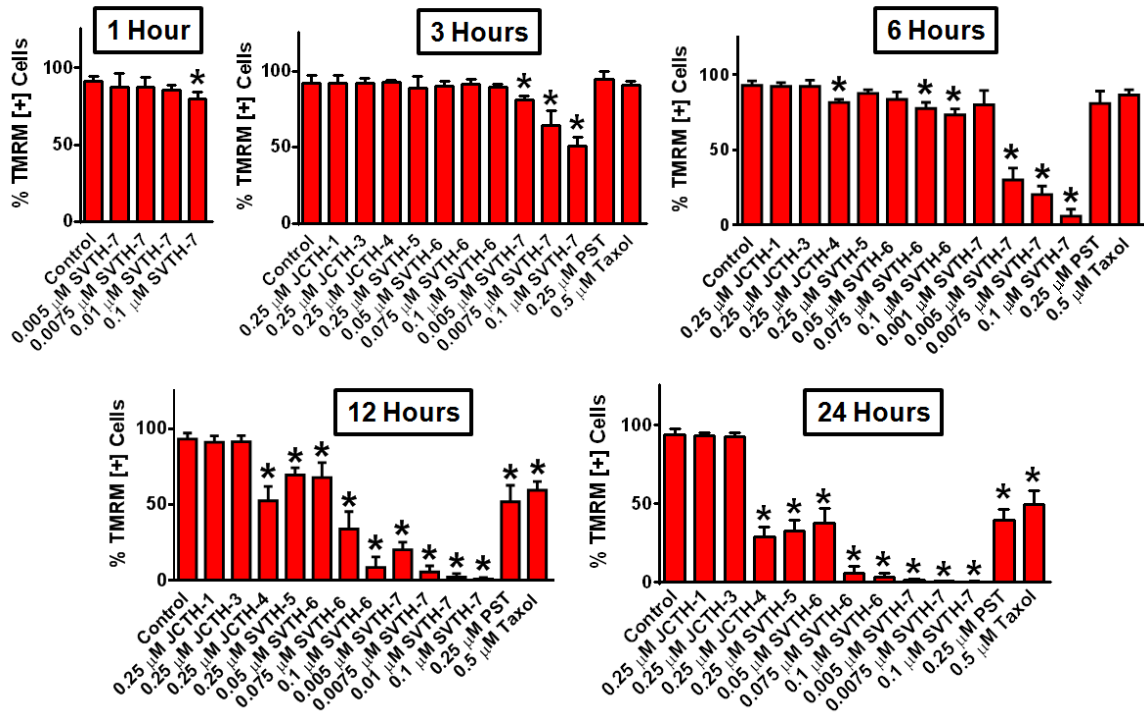
Supplemental Figure S4.1U. PST Analogues & PST have Minimal Toxicity on AG09309 Normal Human Fibroblasts. The WST-1 colorimetric assay was performed on AG09309 normal human fibroblasts treated with the indicated concentrations of compounds for 48 and 72 hours. The WST-1 reagent was added and the absorbance of the processed WST-1 reagent formazan, used to quantify cell viability, was read at 450 nm and expressed as a percent of solvent control (DMSO). Values are expressed as mean \pm SD from quadruplicates of 3 independent experiments. * p <0.05 vs. solvent control (DMSO).

CCD-18Co Normal Colon Fibroblasts (48 h)



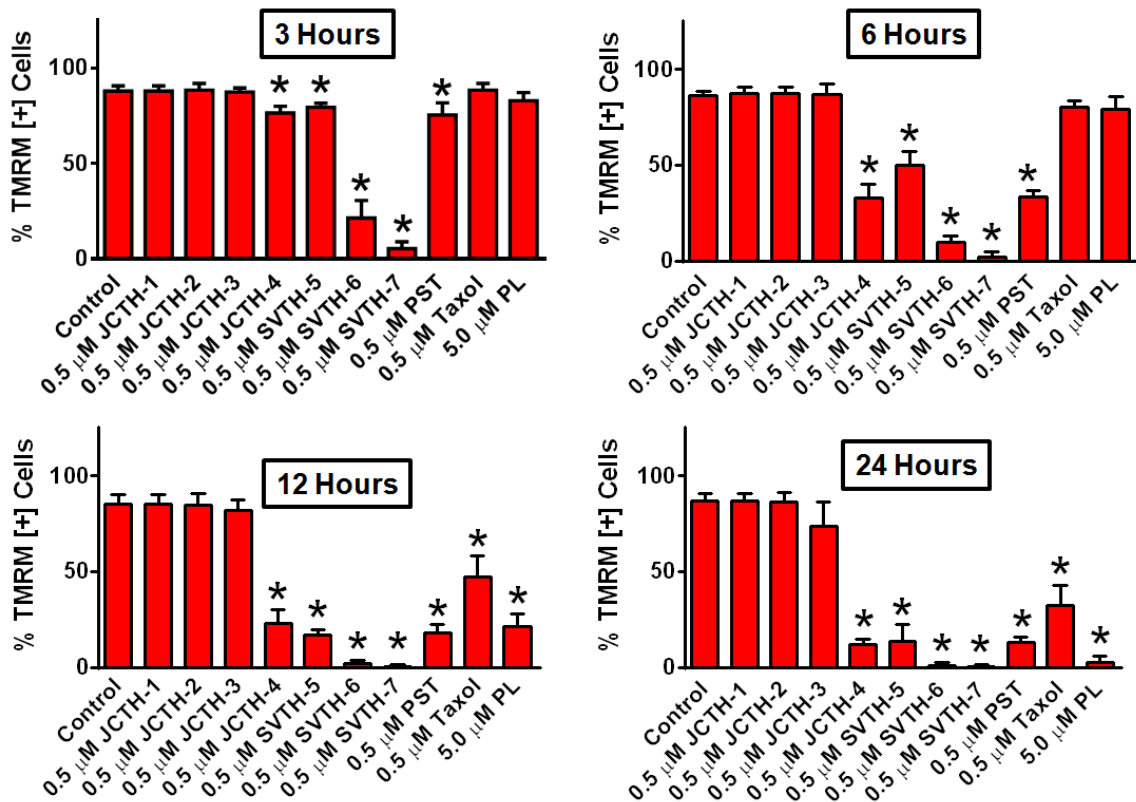
Supplemental Figure S4.1V. PST Analogues & PST have Minimal Toxicity on CCD-18Co Normal Colon Fibroblasts. The WST-1 colorimetric assay was performed on CCD-18Co normal human colon fibroblasts treated with the indicated concentrations of compounds for 48 hours. The WST-1 reagent was added and the absorbance of the processed WST-1 reagent formazan, used to quantify cell viability, was read at 450 nm and expressed as a percent of solvent control (DMSO). Values are expressed as mean \pm SD from quadruplicates of 3 independent experiments. * p <0.05 vs. solvent control (DMSO).

MV-4-11 Biphenotypic B Myelomonocytic Leukemia Cells

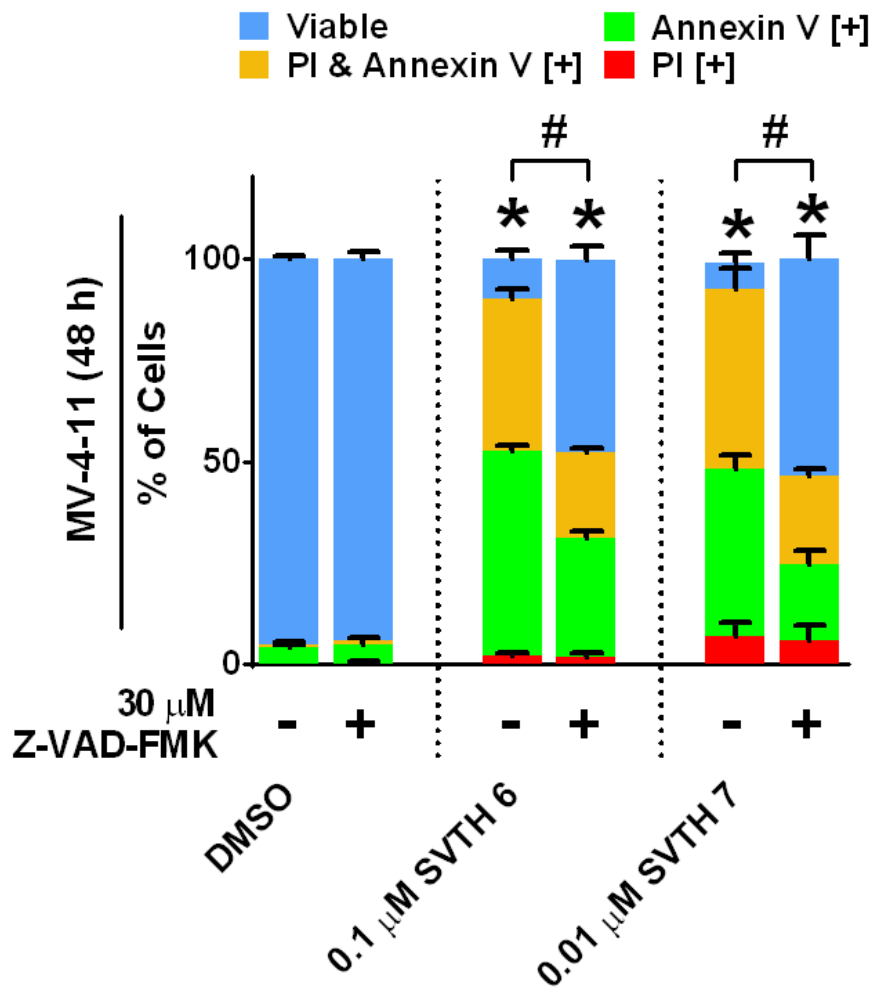


Supplemental Figure S4.3A. PST Analogues & PST Cause Mitochondrial Membrane Potential (MMP) Collapse in a Time Dependent Manner in MV-4-11 Leukemia Cells. TMRM was used to monitor MMP in MV-4-11 leukemia cells with image-based cytometry at the indicated times. * $p < 0.01$ vs. DMSO control. All quantitative values are expressed as mean \pm SD from at least 3 independent experiments. MMP collapse is first observed at 1 and 3 hours with SVTH-7, and at 6 hours with JCTH-4 and SVTH-6. Complete or more pronounced MMP collapse was observed at 12 and 24 hours with JCTH-4 and with SVTH-5, -6, and -7. Taxol was used as a positive control.

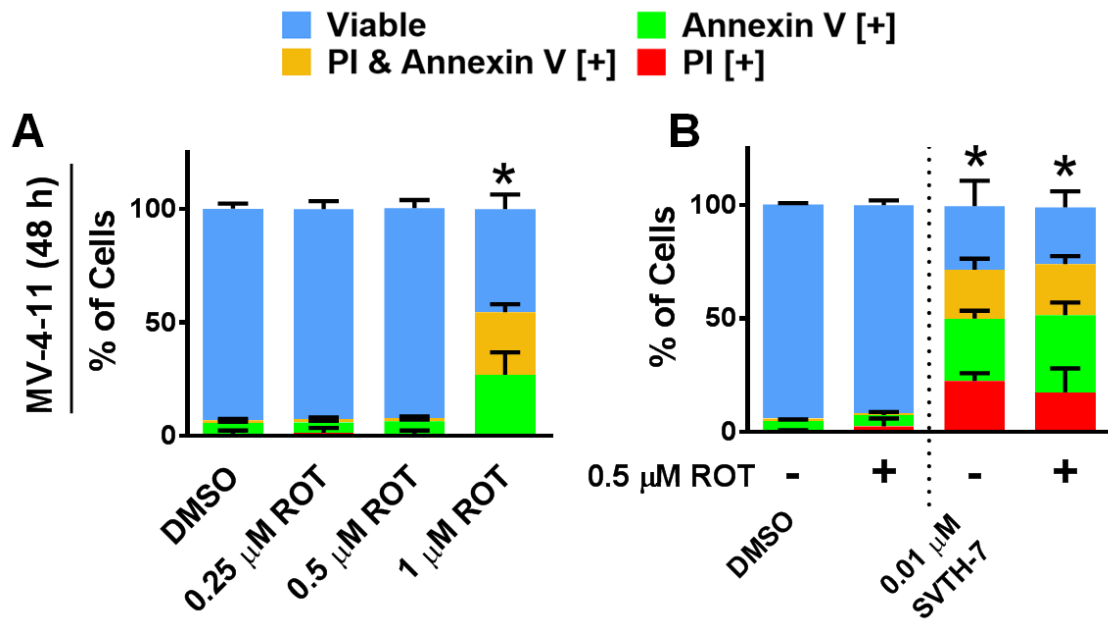
E6-1 Acute T Cell Leukemia Cells



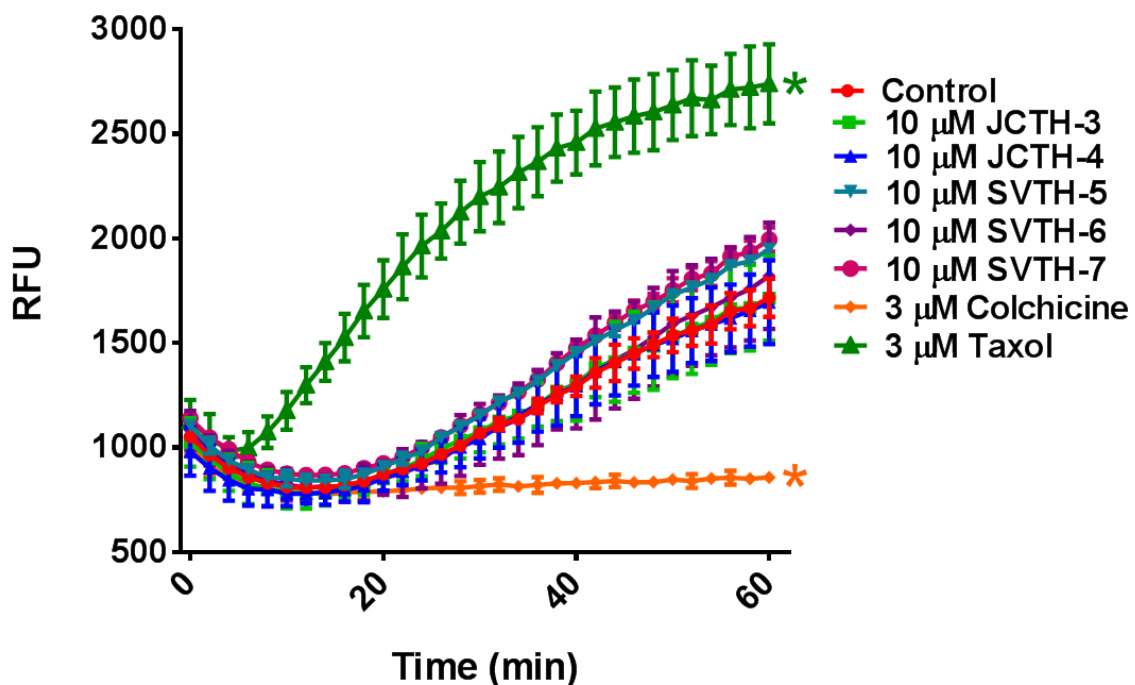
Supplemental Figure S4.3B. PST Analogues & PST Cause Mitochondrial Membrane Potential (MMP) Collapse in a Time Dependent Manner in E6-1 Leukemia Cells. TMRM was used to monitor MMP in E6-1 leukemia cells with image-based cytometry at the indicated times. * $p < 0.01$ vs. DMSO control. All quantitative values are expressed as mean \pm SD from at least 3 independent experiments. MMP collapse is first observed at 3 hours with a more pronounced effect at 6, 12 and 24 hours with JCTH-4 and with SVTH-5, -6, and -7. Taxol and piperlongumine (PL) was used as positive controls.



Supplemental Figure S4.4. PST Analogues Induce Apoptosis in MV-4-11 Leukemia Cells in a Partial Caspase-Dependent Manner. MV-4-11 leukemia cells were pre-treated with 30 μM Z-VAD-FMK broad spectrum caspase inhibitor for 1 hour and then treated with PST analogues to determine the dependence of caspases in PST analogue-induced apoptosis. Values are expressed as mean ± SD from at least 3 independent experiments. * $p < 0.01$ vs. DMSO control (comparison of viable cells only); # $p < 0.001$ vs. respective groups untreated with Z-VAD-FMK (comparison of viable cells only). Z-VAD-FMK was able to partially rescue cells from SVTH-6 and -7, indicating that apoptosis induced by these compounds is partially dependent on caspases.



Supplemental Figure S4.5. PST Analogue-Induced Apoptosis is not Dependent on Functional Complex I of the Mitochondrial Electron Transport Chain. (A) Different doses of the complex I inhibitor rotenone were tested in MV-4-11 leukemia cells to find a concentration that was well tolerated. **(B)** MV-4-11 leukemia cells were pre-treated with the complex I inhibitor rotenone (ROT) at a well tolerated dose for 1 hour and then treated with PST analogue for 48 hours. Annexin V binding (green) and PI staining (PI) (red) was quantified with image based cytometry. * $p < 0.01$ vs. DMSO control (comparison of viable cells only). All values are expressed as mean \pm SD from at least 3 independent experiments. ROT did not appear to affect the apoptosis inducing activity of SVTH-7.



Supplemental Figure S4.6. PST Analogues Do not Evidently Affect Tubulin Polymerization. A tubulin polymerization assay kit (Cytoskeleton Inc., Cat. No. BK011P, Denver, CO, USA) was used to evaluate PST analogues in their ability to alter tubulin polymerization dynamics. A 96-well plate was pre-warmed at 37°C for half an hour prior to the assay. Wells were treated with DMSO solvent control and PST analogues dissolved in PBS. All wells were incubated with 2 mg/mL tubulin in tubulin polymerization buffer (80 mM PIPES pH 6.9, 2 mM MgCl₂, 0.5 mM EGTA, 1 mM GTP and 15% glycerol). Fluorescence was measured (Ex. 360 nm; Em. 450 nm) every 1 minute for 1 hour using a SpectraMax Gemini XS multi-well plate reader (Molecular Devices, Sunnyvale, CA, USA) at 37°C. Fluorescence emission at 450 nm increases as tubulin polymerizes due to the incorporation of a fluorescent reporter. Statistical significance was determined by comparing the relative fluorescence units (RFU) at the 60 minute endpoint between the DMSO solvent control and the compound of interest. All values are expressed as mean ± SD from at least 3 independent experiments. **p*<0.001 vs. DMSO control. Colchicine and Taxol were used as controls for tubulin destabilization and tubulin polymerization respectively.

CHAPTER 5: Exploiting Mitochondrial & Oxidative Vulnerabilities with a Synthetic Analogue of Pancratistatin in Combination with Piperlongumine for Cancer Therapy

Dennis Ma¹, Tyler Gilbert¹, Daniel Tarade¹, Christopher Pignanelli¹, Fadi Mansour¹, Manika Gupta¹, Ian Tuffley¹, Sabrina Ma¹, Sergey Vshyvenko², Tomas Hudlicky², and Siyaram Pandey¹

¹Department of Chemistry and Biochemistry, University of Windsor,
401 Sunset Avenue, Windsor, Ontario N9B 3P4, Canada
Phone: +519-253-3000, ext. 3701
spandey@uwindsor.ca

²Chemistry Department and Centre for Biotechnology, Brock University, 500
Glenridge Avenue, St. Catharines, Ontario L2S 3A1, Canada
thudlicky@brocku.ca

List of Abbreviations

AIF	apoptosis inducing factor
AMA	Antimycin A
CBR1	carbonyl reductase1
Cyto c	cytochrome c
DCF	2', 7'-dichlorofluorescein
ETC	electron transport chain
GSTP1	glutathione S-transferase pi 1
H ₂ DCFDA	2', 7'-dichlorofluorescein diacetate
MMP	mitochondrial membrane potential
NAC	<i>N</i> -Acetyl-L-cysteine
PBMCs	peripheral blood mononuclear cells
PI	propidium iodide
PL	piperlongumine
PST	pancratistatin
ROS	reactive oxygen species
SDHA	succinate dehydrogenase subunit A
TMRM	tetramethylrhodamine methyl ester

Summary

Chemoresistance and harsh side effects as result of non-specific targeting of cancer chemotherapeutics currently pose as large obstacles in cancer therapy; thus, it would be invaluable to devise novel approaches to specifically target cancer cells. The natural compound pancratistatin (PST) has been shown to preferentially induce apoptosis in a variety of cancer cell types. Various analogues of PST were synthesized by *de novo* synthesis and an efficacious analogue, SVTH-6, was found to inflict its cytotoxic effects selectively in a variety of aggressive cancers by way of apoptotic induction via cancer cell mitochondrial targeting; it caused dissipation of mitochondrial membrane potential, decreased oxygen consumption, and with isolated mitochondria, induced the release of apoptogenic factors. The natural compound piperlongumine (PL) has been shown to target the stress response to reactive oxygen species (ROS). Interestingly, when combined with SVTH-6, an increase in mitochondrial dysfunction was observed, leading to an enhanced cytotoxic effect against cancer cells. This enhanced effect was found to dependent on ROS generation as an anti-oxidant was able to rescue cancer cells from this combination treatment. Most importantly, noncancerous cells were markedly less sensitive to this combination of compounds. Hence, we present a combinatorial approach targeting mitochondrial and oxidative vulnerabilities in cancer cells with a novel PST analogue and PL as a potentially safe and effective alternative to current chemotherapeutics.

Introduction

Striking dissimilarities exist between cancer and noncancerous cells which have long been ignored. Cancer cells possess a distinct metabolic phenotype, in which cancer cells depend less on the mitochondria and more on glycolysis for energy (Warburg, 1956); consequently, this glycolytic shift and mitochondrial remodelling confers a proliferative advantage and an acquired resistance to apoptosis, by discouraging mitochondrial membrane permeabilization required for apoptosis execution, in cancer cells (DeBerardinis et al. 2008; Gogvadze, Orrenius, and Zhivotovsky 2008; Gogvadze, Zhivotovsky, and Orrenius 2010; Plas and Thompson 2002; Vander Heiden, Cantley, and Thompson 2009; Pastorino, Shulga, and Hoek 2002; Chen et al. 2010; Green and Kroemer 2004; Casellas, Galiegue, and Basile 2002). Additionally, cancer cells have been observed to possess high basal levels of reactive oxygen species (ROS) (Diehn et al. 2009) while noncancerous cells do not (Schumacker 2006; Fruehauf and Meyskens 2007; Trachootham, Alexandre, and Huang 2009); thus, cancer cells are predicted to be highly dependent on cellular stress response mechanisms to ROS (Gogvadze, Orrenius, and Zhivotovsky 2008; Trachootham, Alexandre, and Huang 2009; Szatrowski and Nathan 1991). Consequently, exploitation of these distinct characteristics may offer selective strategies in targeting cancer cells.

We have found that the natural compound pancratistatin (PST) (**Figure 5.1A**), isolated from the *Hymenocallis littoralis* plant, specifically induces apoptosis in numerous cancer cell types with minimal effect on noncancerous cells by mitochondrial targeting (Kekre et al. 2005; McLachlan et al. 2005;

Siedlakowski et al. 2008; Griffin et al. 2011; Griffin, McNulty, and Pandey 2011). We have previously synthesized and found that JCTH-4 (**Figure 5.1B**), a C-1 acetoxymethyl analogue of 7-deoxypancratistatin, to possess comparable anti-cancer activity to that of PST, inducing apoptosis in numerous cancer cell types by way of mitochondrial targeting (Collins et al. 2010; Ma, Tremblay, et al. 2012; Ma, Collins, et al. 2012). Recently, we have created a C-7 hydroxylated version of JCTH-4, SVTH-6 (**Figure 5.1C**), a C-1 acetoxymethyl analogue of PST, by *de novo* synthesis; this is the first time chemical synthesis of a PST analogue with the full pharmacophore for anti-cancer activity has been achieved. In this study, we report this novel PST analogue to be extremely potent against an array of aggressive cancers, surpassing JCTH-4 in efficacy, while noncancerous cells showed a markedly decrease in sensitivity to this compound. SVTH-6 effectively induced apoptosis in these cancer cells with evidence pointing to a mitochondrial target. Other work has shown preferential targeting of cellular defence mechanisms against ROS by the natural compound piperlongumine (PL) to selectively harm cancer cells (Raj et al. 2011). As we have shown PST and its synthetic analogues to preferentially induce mitochondrial ROS production and dysfunction in cancer cells, we subjected cancer cells to both SVTH-6 and PL in combination and found this treatment to produce an enhanced cytotoxic effect selectively in cancer cells. N-acetyl cysteine (NAC) was able to rescue cancer cells from SVTH-6 alone and in combination with PL. Thus, we demonstrate targeting of both mitochondria and cellular defense mechanisms against oxidative stress as a promising approach for cancer treatment.

Materials and Methods

Cell Culture

The BxPC-3 (ATCC, Cat. No. CRL-1687, Manassas, VA, USA) pancreatic adenocarcinoma cell line was grown in RPMI-1640 media (Sigma-Aldrich Canada, Mississauga, ON, Canada) supplemented with 10% (v/v) FBS standard (Thermo Scientific, Waltham, MA, USA) and 10 mg/mL gentamicin (Gibco BRL, VWR, Mississauga, ON, Canada). The PANC-1 (ATCC, Cat. No. CRL-1469, Manassas, VA, USA), epithelioid carcinoma cell line of the pancreas was grown in Dulbecco's Modified Eagle's Medium (Sigma-Aldrich Canada, Mississauga, ON, Canada) supplemented with 10% (v/v) FBS standard (Thermo Scientific, Waltham, MA, USA) and 10 mg/mL gentamicin (Gibco BRL, VWR, Mississauga, ON, Canada).

The human colorectal cancer cell lines HT-29 and HCT 116 (ATCC, CCL-218 & CCL-247, Manassas, VA, USA) were cultured with McCoy's Medium 5a (Gibco BRL, VWR, Mississauga, ON, Canada) supplemented with 2 mM L-glutamine, 10% (v/v) FBS (Thermo Scientific, Waltham, MA, USA) and 10 mg/ml gentamicin (Gibco, BRL, VWR, Mississauga, ON, Canada).

The OVCAR-3 (American Type Culture Collection, Cat. No. HTB-161, Manassas, VA, USA) ovarian adenocarcinoma cell line was grown and cultured in RPMI-1640 media (Sigma-Aldrich Canada, Mississauga, ON, Canada) supplemented with 0.01 mg/mL bovine insulin, 20% (v/v) fetal bovine serum (FBS) standard (Thermo Scientific, Waltham, MA, USA) and 10 mg/mL gentamicin (Gibco BRL, VWR, Mississauga, ON, Canada).

The MV-4-11 Chronic myelomonocytic leukemia cell line (ATCC, Cat. No. CRL-9591, Manassas, VA, USA). was cultured with Iscove's Modified Dulbecco's Medium (ATCC, Cat. No. 30-2005, Manassas, VA, USA) supplemented with 10% (v/v) FBS standard (Thermo Scientific, Waltham, MA, USA) and 10 mg/mL gentamicin (Gibco BRL, VWR, Mississauga, ON, Canada).

The U-937 histiocytic lymphoma cell line (ATCC, Cat. No. CRL-1593.2, Manassas, VA, USA). was cultured with Iscove's Modified Dulbecco's Medium (ATCC, Cat. No. 30-2005, Manassas, VA, USA) supplemented with 10% (v/v) FBS standard (Thermo Scientific, Waltham, MA, USA) and 10 mg/mL gentamicin (Gibco BRL, VWR, Mississauga, ON, Canada).

The NCI-H23 non-small cell lung cancer cell line (ATCC, Cat. No. CRL-5800, Manassas, VA, USA) was grown and cultured in RPMI-1640 medium (Sigma-Aldrich Canada, Mississauga, ON, Canada) supplemented with 10% (v/v) FBS standard (Thermo Scientific, Waltham, MA, USA) and 10 mg/mL gentamicin (Gibco BRL, VWR, Mississauga, ON, Canada).

The normal-derived colon mucosa NCM460 cell line (INCELL Corporation, LLC., San Antonio, TX, USA) was grown in INCELL's M3Base™ medium (INCELL Corporation, LLC., Cat. No. M300A500) supplemented with 10 % (v/v) FBS and 10 mg/mL gentamicin (Gibco BRL, VWR, Mississauga, ON, Canada).

The normal colon fibroblast CCD-18Co cell line (ATCC, Cat. No. CRL-1459, Manassas, VA, USA) was cultured with Eagle's Minimal Essential Medium supplemented with 10 % (v/v) FBS and 10 mg/mL gentamycin (Gibco BRL, VWR, Mississauga, ON, Canada).

All cells were grown in optimal growth conditions of 37°C and 5 % CO₂. Furthermore, all cells were passaged for less than 6 months and no authentication of cell lines was performed by the authors.

Isolation and Culture of Peripheral Blood Mononuclear cells (PBMCs)

Peripheral blood mononuclear cells (PBMCs) were collected and isolated from healthy volunteers. In brief, whole blood was collected in BD Vacutainer®CPT™ Tubes with Sodium Heparin^N (Becton, Dickinson and Company, Cat. No. 362753, Franklin Lakes, NJ, USA) at room temperature. Tubes were immediately inverted 5 times and centrifuged for 30 minutes at room temperature at 1500-1800 x g. The layer of PBMCs under the plasma layer in each tube was collected, pooled together, resuspended in 50 mL of PBS, and centrifuged at room temperature at 300 x g for 15 minutes. The supernatant was methodically aspirated without disturbing the pellet and PBMCs were resuspended and cultured in RPMI-1640 medium (Sigma-Aldrich Canada, Mississauga, ON, Canada), supplemented with 10% (v/v) FBS standard (Thermo Scientific, Waltham, MA, USA) and 10 mg/mL gentamicin (Gibco BRL, VWR, Mississauga, ON, Canada) at 37 °C and at 5% CO₂. PBMCs from healthy volunteers 1 and 2 (PBMCs V1, PBMCs V2) were taken from a healthy 28 year old female, a healthy 18 year old male respectively.

Cell Treatment

Cells were grown to 60-70% confluence, before being treated with SVTH-6, piperlongumine (PL) (INDOFINE Chemical Company, Inc., Cat. No. P-004, Hillsborough, NJ, USA), and *N*-Acetyl-L-cysteine (NAC) (Sigma-Aldrich Canada, Cat. No. A7250) at the indicated concentrations and time points. SVTH-6, a C-1 acetoxymethyl analogue of PST, was produced by synthesis from bromobenzene (Vshyvenko et al. 2011). NAC was dissolved in sterile water. All other compounds were dissolved in dimethylsulfoxide (DMSO).

WST-1 Assay for Cell Viability

The WST-1 based colorimetric assay was performed as per the manufacturer's protocol (Roche Applied Science, Indianapolis, IN, USA) to quantify cell viability via correlation with active cellular metabolism. 96-well clear bottom tissue culture plates were seeded with cells. Subsequently, the cells were treated with compounds at the indicated concentrations and time points. The treated cells were incubated with WST-1 reagent for 4 hours at 37° C with 5 % CO₂. In actively metabolizing cells, the WST-1 reagent is cleaved to formazan by cellular enzymes. The presence of formazan was quantified via absorbance readings at 450 nm on a Wallac Victor³™ 1420 Multilabel Counter (PerkinElmer, Woodbridge, ON, Canada). Cellular viability through measured absorbance readings expressed as percentages of the solvent control group.

Cell Death Analysis: Annexin V Binding Assay & Propidium Iodide (PI) Staining

The Annexin V binding assay and propidium iodide staining was done in parallel to respectively monitor early apoptosis and cell permeabilization, a marker of necrotic or late apoptotic cell death. Cells were washed with phosphate buffer saline (PBS) and suspended in Annexin V binding buffer (10 mM HEPES, 140 mM NaCl, 2.5 mM CaCl₂, pH 7.4) with green fluorescent Annexin V AlexaFluor-488 (1:20) (Life Technologies Inc, Cat. No. A13201, Burlington, ON, Canada) and 0.01mg/mL of red fluorescent PI (Life Technologies Inc, Cat. No. P3566, Burlington, ON, Canada) for 15 minutes at 37 °C protected from light. The percentage of early (green), late apoptotic cells (green and red), and necrotic cells (red) were quantified using image-based cytometry with a Tali® Image-Based Cytometer (Life Technologies Inc, Cat. No. T10796, Burlington, ON, Canada). Cells from at least 18 random fields were analyzed using both the green (ex. 458 nm; em. 525/20 nm) and red (ex. 530 nm; em. 585 nm) channels. Fluorescent micrographs were taken at 400x magnification using LAS AF6000 software with a Leica DMI6000 fluorescent microscope (Wetzlar, Germany). Cells monitored with microscopy were counterstained with Hoechst 33342 (Molecular Probes, Eugene, OR, USA) to visualize nuclei using a final concentration of 10 µM during the 15 minute incubation.

Tetramethylrhodamine Methyl Ester (TMRM) Staining

Tetramethylrhodamine methyl ester (TMRM) (Gibco BRL, VWR, Mississauga, ON, Canada) was used for the purpose of detecting mitochondrial membrane potential (MMP). Cells were grown on coverslips and treated with various concentrations of drugs for the indicated time points and incubated with 100 nM TMRM for 45 minutes at 37° C. Fluorescent micrographs were taken at 400x magnification on a Leica DM IRB inverted fluorescence microscope (Wetzlar, Germany). The percentage of TMRM cells was quantified using image-based cytometry with a Tali® Image-Based Cytometer (Life Technologies Inc, Cat. No. T10796, Burlington, ON, Canada). Cells from at least 18 random fields were analyzed using the red channel (ex. 530 nm; em. 585 nm). Fluorescent micrographs were taken at 400x magnification using LAS AF6000 software with a Leica DMI6000 fluorescent microscope (Wetzlar, Germany). Cells monitored with microscopy were counterstained with Hoechst 33342 (Molecular Probes, Eugene, OR, USA) to visualize nuclei using a final concentration of 10 µM during the 45 minute incubation.

Oxygen Consumption Quantitation

The MitoXpress® Xtra - Oxygen Consumption Assay [HS Method] (Luxcel Biosciences Ltd., Cat. No. MX-200, Cork, Ireland). 1 000 000 cells/well were seeded in a 96-well black clear bottom tissue culture plate and incubated for an hour at 37° C and 5% CO₂. On a heat pack, 10 µL of MitoXpress® reagent was added to each well excluding the blanks, cells were treated with test compounds,

the plate was shaken with a plate shaker, and 2 drops of pre-warmed high sensitivity mineral oil was added to each well to seal off the air supply. Bottom read fluorescence measurements were taken at Ex. 380 nm and Em. 650, every 2 minutes for 2 hours at 37 °C using a SpectraMax Gemini XS multi-well plate reader (Molecular Devices, Sunnyvale, CA, USA). Increases in fluorescence are indicative of oxygen consumption. Oxygen consumption rates were determined by calculating the slope of the linear regions of the oxygen consumption curves using GraphPad Prism 6 software.

Mitochondrial Isolation

To isolate mitochondria from untreated cancer cells, the cells were washed once in cold PBS. Subsequently, they were resuspended in hypotonic buffer (1 mM EDTA, 5 mM Tris-HCl, 210 mM mannitol, 70 mM sucrose, 10 µM Leu-pep and Pep-A, 100 µM PMSF) and subjected to manual homogenization. The homogenized cells were centrifuged at 600 x g for 5 minutes at 4° C. The supernatant was retrieved and centrifuged at 15000 x g for 15 minutes at 4° C and the mitochondrial pellet was resuspended in cold reaction buffer (2.5 mM malate, 10 mM succinate, 10 µM Leu-pep and Pep-A, 100 µM PMSF in PBS).

Treatment of Isolated Mitochondria & Evaluation of Apoptogenic Factor Release

The isolated mitochondria were treated with SVTH-6, PL or a combination of the two drugs at the indicated concentrations and incubated for 2 hours in cold reaction buffer (2.5 mM malate, 10 mM succinate, 10 μ M Leu-pep, 10 μ M Pep-A, and 100 μ M PMSF in PBS). The control group was treated with solvent (DMSO). Following treatment, the mitochondrial samples were vortexed and centrifuged at 15,000 x g for 15 minutes at 4°C. Western Blot analysis was done on the resulting supernatant and mitochondrial pellet (resuspended in cold reaction buffer) to screen for mitochondrial release or retention of apoptogenic factors.

Western Blot Analyses

Protein samples including mitochondrial pellets and post mitochondrial supernatants were subjected to SDS-PAGE. The samples were transferred onto a nitrocellulose membrane and blocked with 5% w/v milk TBST (Tris-Buffered Saline Tween-20) solution for 1 hour. Membranes were then incubated with an anti-cytochrome c (Cyto c) antibody (1:1000) raised in mice (Abcam, ab13575, Cambridge, MA, USA), an anti-succinate dehydrogenase subunit A antibody (1:1000) raised in mice (Santa Cruz Biotechnology, Inc., sc-59687, Paso Robles, CA, USA), or an anti-apoptosis inducing factor (AIF) antibody raised in rabbits (1:1000) (Abcam, Cat. No. ab1998, Cambridge, MA, USA) overnight at 4° C. Following incubation with primary antibody, the membrane was washed once for 15 minutes and then twice for 5 minutes in TBST. The membranes were then incubated with an anti-mouse (1:2000) or an anti-rabbit (1:2000) horseradish

peroxidase-conjugated secondary antibody (1:2000) (Abcam, ab6728, ab6802, Cambridge, MA, USA) for 1 hour at 25° C. Probing with secondary antibody was followed by three 5 minute washes in TBST. Lastly, chemiluminescence reagent (Sigma-Aldrich, CPS160, Mississauga, ON, Canada) was used to allow for band visualization (Sigma-Aldrich, CPS160, Mississauga, ON, Canada). Densitometry analyses were performed using ImageJ software.

Quantitation of Reactive Oxygen Species (ROS)

The small molecule 2', 7'-dichlorofluorescein diacetate (H₂DCFDA) was used to monitor whole cell ROS generation. H₂DCFDA enters the cell and is deacetylated by esterases and oxidized by ROS to the highly fluorescent 2', 7'-dichlorofluorescein (DCF) (excitation 495 nm; emission 529 nm). Cells were pretreated with 20 µM H₂DCFDA (Sigma-Aldrich Canada, Cat. No. D6883, Mississauga, ON, Canada) for 30 minutes at 37°C protected from light at 5% CO₂. Cells were treated for the indicated durations, centrifuged at 600 x g for 5 minutes and suspended in PBS. Percentage of DCF positive cells was quantified using the Tali® Image-Based Cytometer (Life Technologies Inc, Cat. No. T10796, Burlington, ON, Canada) using 12 random fields per group with the green channel (excitation 458 nm; emission 525/20 nm).

Statistical Analysis

All statistics were performed by GraphPad Prism 6 statistical software. A p-value below 0.05 was considered significant. For the experiments with single variable measurements, which include quantification of MMP, and whole cell ROS, a One-Way ANOVA (nonparametric) was conducted and each sample's mean was compared to the mean of the negative control (DMSO vehicle) unless otherwise specified. For experiments that contained multi-variables (e.g. multiple group comparisons), such as the quantification of live and dead cells, Two-Way ANOVA (nonparametric) was used and each sample's mean was compared to the mean of the negative control (DMSO vehicle) unless otherwise specified.

Results

SVTH-6 Selectively Induces Cytotoxicity in Cancer Cells with Greater Efficacy than JCTH-4

The anti-cancer activity of SVTH-6 was evaluated in various cancer cell types using the WST-1 based colorimetric assay measuring cell viability as a function of cell metabolism. SVTH-6 was shown to be more effective than JCTH-4 as seen in OVCAR-3 ovarian cancer cells and induce apoptotic morphology including cell shrinkage and nuclear condensation (**Figure 5.1D & E**). Importantly after 72 hours, noncancerous NCM460 colon mucosa cells were markedly less sensitive to SVTH-6 compared to the HCT 116 and HT-29 colorectal cancer and the notoriously chemoresistant BxPC-3 pancreatic cancer cells, all of which were very sensitive to SVTH-6 insult; the dose of 0.25 μ M SVTH-6 presented the best therapeutic window (**Figure 5.1F**). Thus, SVTH-6 acts in a selective manner, specifically inducing cytotoxicity in cancer cells with greater anti-cancer activity than JCTH-4.

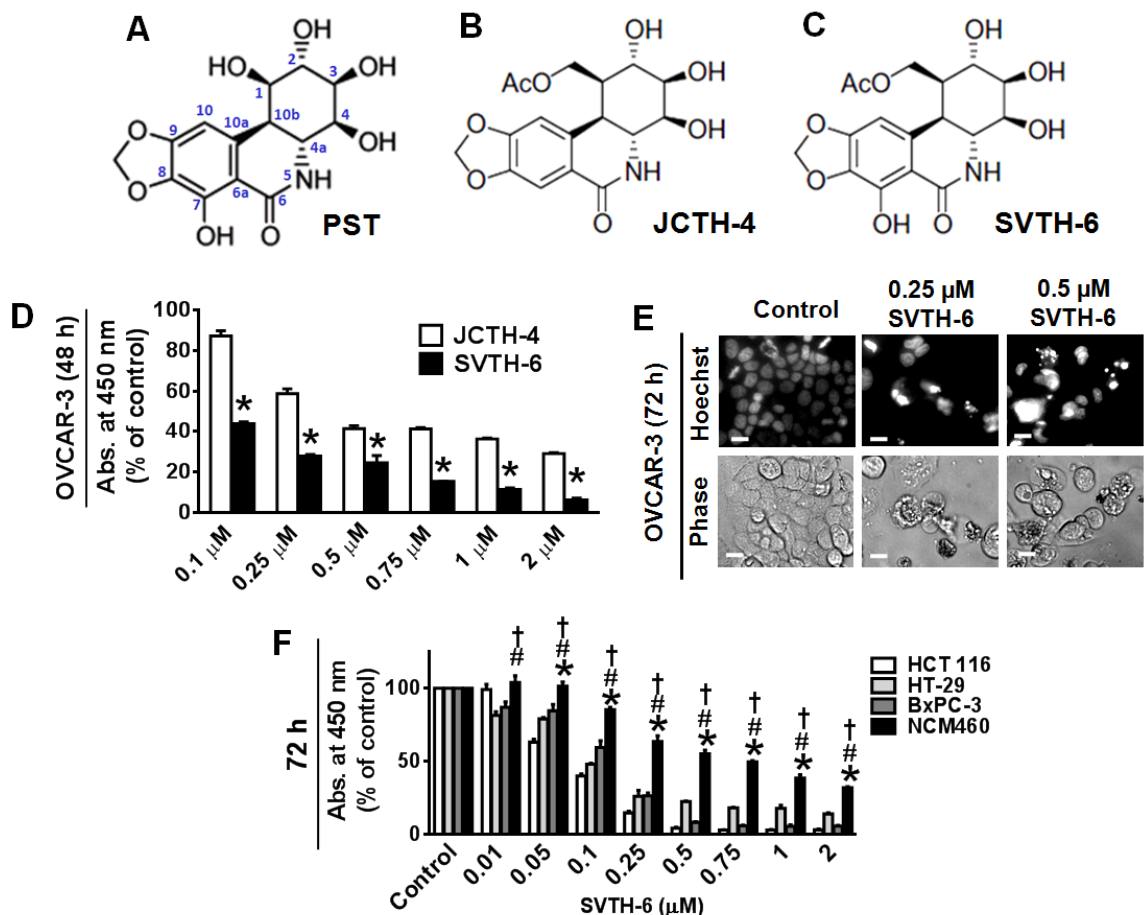


Figure 5.1. SVTH-6 Selectively Induces Cytotoxicity in Cancer Cells with Greater Efficacy than JCTH-4. Structures of (A) PST, (B) JCTH-4, and (C) SVTH-6. (D) WST-1 viability was performed on OVCAR-3 ovarian cancer cells treated for 48 hours. * $p < 0.001$ vs. respective JCTH-4 treated groups. (E) OVCAR-3 ovarian cancer cells treated with SVTH-6 for 72 hours and stained with Hoechst dye. Scale bar = 15 μm . (F) Effect of SVTH-6 on cellular viability of cells was determined by the WST-1 colorimetric assay. HCT-116, HT-29, BxPC-3 and NCM460 cells were treated with SVTH-6 for 72 hours at the indicated concentrations. The WST-1 reagent was used to quantify cell viability. Absorbance was read at 450 nm and expressed as a percent of the solvent control (DMSO). Values are expressed as mean \pm SD from quadruplicates of 3 independent experiments. * $p < 0.01$ vs. HCT 116, # $p < 0.01$ vs. HT-29, † $p < 0.05$ vs. BxPC-3.

PL Enhances Cytotoxicity in Selectively in Cancer Cells

The natural compound PL has previously been demonstrated to preferentially cause cytotoxicity in cancer cells by selectively targeting their stress response mechanisms against ROS (Raj et al. 2011). We have formerly shown PST and JCTH-4 to induce ROS production in cancer cells (McLachlan et al. 2005; Siedlakowski et al. 2008; Collins et al. 2010; Griffin et al. 2011; Griffin, McNulty, and Pandey 2011; Ma et al. 2011; Ma, Tremblay, et al. 2012; Ma, Collins, et al. 2012). Thus, we evaluated the combinatorial effect of both SVTH-6 and PL on cancer cells. Interestingly, an enhanced cytotoxic effect with produced with this combination treatment selectively in cancer cells including BxPC-3 pancreatic cancer, OVCAR-3 ovarian cancer, NCI H23 non-small cell lung cancer, and MV-4-11 leukemia cells (**Figure 5.2A-D**); this combination treatment had minimal effect on noncancerous NCM460 cells (**Figure 5.2E**). Thus, PL is able to enhance the anti-cancer activity of SVTH-6 selectively in cancer cells.

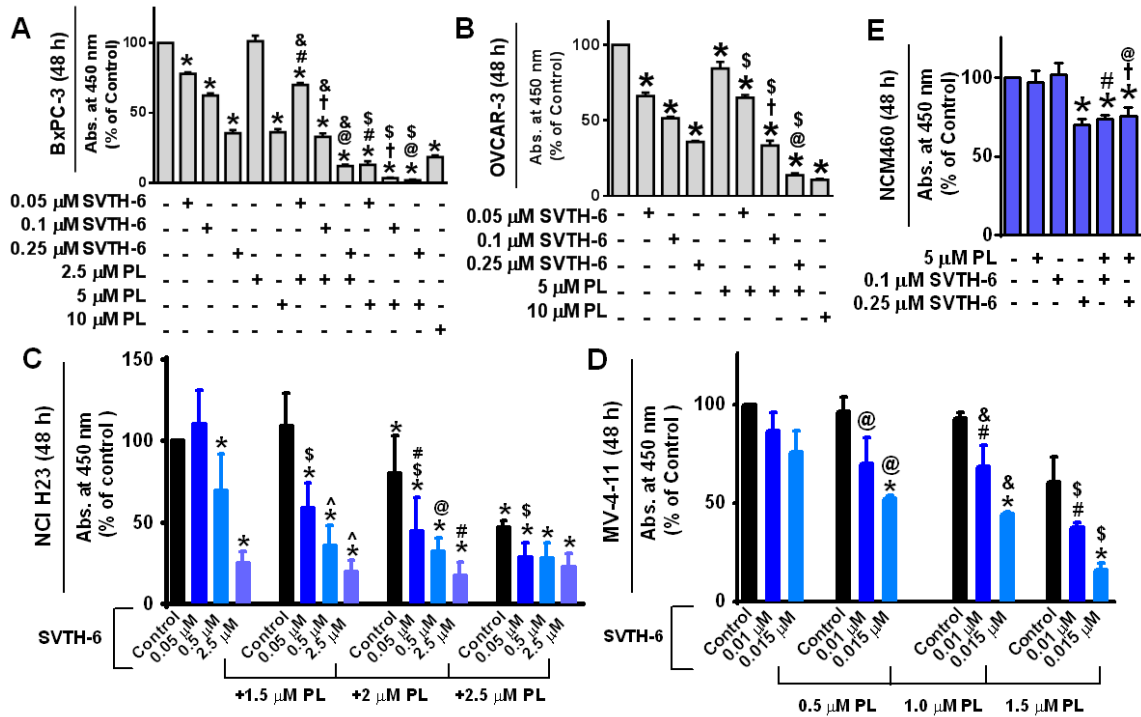
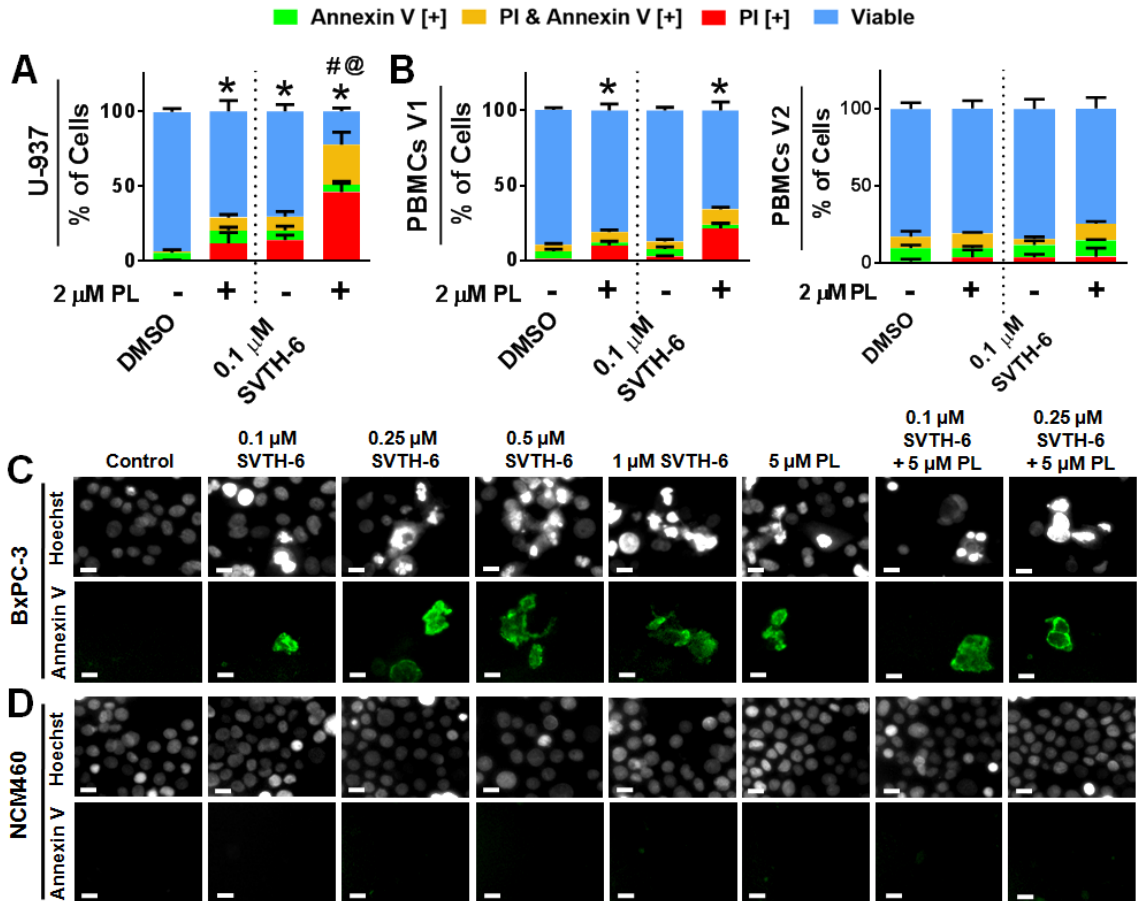


Figure 5.2. PL Enhances Cytotoxicity in Selectively in Cancer Cells. Effect of SVTH-6 and PL on cellular viability was determined by the WST-1 colorimetric assay. **(A)** BxPC-3 pancreatic cancer cells, **(B)** OVCAR-3 ovarian cancer cells, **(C)** NCI H23 non-small cell lung cancer cells and **(D)** MV-4-11 leukemia cells were treated with SVTH-6 and PL for 48 hours at the indicated concentrations. Values are expressed as mean \pm SD from quadruplicates of 3 independent experiments. BxPC-3 & OVCAR-3: * p <0.001 vs. control; # p <0.05 vs. 0.05 μ M SVTH-6; † p <0.005 vs. 0.1 μ M SVTH-6; & p <0.05 vs. 2.5 μ M PL; @ p <0.01 vs. 0.25 μ M SVTH-6; \$ p <0.005 vs. 5 μ M PL. NCI H23: * p < 0.005 vs. Control; \$ p <0.005 vs. 0.05 SVTH-6; @ p <0.005 vs. 0.005 SVTH-6; # p <0.005 vs. 2 PL; ^ p <0.005 vs. 1.5 PL. MV-4-11: * p <0.001 vs. solvent control (DMSO); @ p <0.01 vs. 0.5 μ M PL; & p <0.01 vs. 1.0 PL μ M; \$ p <0.005 vs. 1.5 μ M PL; # p <0.01 vs. 0.01 μ M SVTH-6; % p <0.001 vs. 0.015 μ M SVTH-6. **(E)** Noncancerous NCM460 epithelial cells were also treated for 48 hours with the indicated concentrations of SVTH-6 and PL. Values are expressed as mean \pm SD from quadruplicates of 3 independent experiments; * p <0.01 vs. 0.1 μ M SVTH-6 + 5 μ M PL with BxPC-3 cells (Fig. 2A); # p <0.01 vs. 0.1 μ M SVTH-6 + 5 μ M PL with OVCAR-3 cells (Fig. 2B); † p <0.05 vs. 0.25 μ M SVTH-6 + 5 μ M PL with BxPC-3 cells (Fig. 2A); @ p <0.05 vs. 0.25 μ M SVTH-6 + 5 μ M PL with OVCAR-3 cells (Fig. 2B).

Selective Induction of Cell Death in Cancer Cells by SVTH-6 is Enhanced with PL

To evaluate the ability of SVTH-6 and PL combination to induce apoptosis, cancer cells were treated for 48 hours with SVTH-6 and PL alone and in combination. Subsequently, these cells were monitored for Annexin V binding to externalized phosphatidylserine, a biochemical marker of apoptosis and propidium iodide staining, an indicator of cell membrane permeabilization, and by extension, necrosis and late apoptosis. As determined by image-based cytometry, PL was able to enhance cell death induction in U-937 lymphoma cells after 48 hours of treatment (**Figure 5.3A**). Notably, this combination treatment was well tolerated by peripheral blood mononuclear cells collected from healthy volunteers 1 (PBMCs V1) and 2 (PBMCs V2) at 48 hours (**Figure 5.3B**).

Fluorescence micrographs revealed nuclei of BxPC-3 pancreatic cancer cells treated with SVTH-6 and PL alone and in combination for 48 hours to be brightly stained and condensed, indicative of apoptosis (**Figure 5.3C**). Furthermore, these cells were positive for Annexin V binding, as depicted by the green fluorescence. Such features of apoptosis were not evident in noncancerous NCM460 epithelial cells treated for 48 hours (**Figure 5.3D**). These findings collectively demonstrate this combination treatment to be selective in cancer cells.



PL Selectively Enhances Mitochondrial Membrane Potential (MMP) Dissipation by SVTH-6 in Cancer Cells

We have previously established PST and JCTH-4 to target cancer cell mitochondria (Siedlakowski et al. 2008; McLachlan et al. 2005; Griffin et al. 2011; Griffin, McNulty, and Pandey 2011; Collins et al. 2010; Ma et al. 2011; Ma, Tremblay, et al. 2012). To validate such targeting by SVTH-6, various mitochondrial assays were executed. Cancer cells were treated and stained with TMRM, an indicator of intact MMP and an intact mitochondrial membrane. As depicted with image-based cytometry, SVTH-6 caused dissipation of MMP alone and in combination with PL, as depicted by the loss of red TMRM fluorescence. PL was able to enhance SVTH-6-induced MMP collapse in BxPC-3 pancreatic cancer cells in a time dependent manner (**Figure 5.4A**). This enhancement was also observed in U-937 lymphoma cells at 24 hours (**Figure 5.4B**).

OVCAR-3 ovarian cancer cells treated for 48 hours with SVTH-6 caused dissipation of MMP alone and in combination with PL, indicated by the loss of red TMRM fluorescence, and nuclear condensation as seen with fluorescence microscopy (**Figure 5.4C**). PL insult alone also caused MMP dissipation. MMP dissipation and nuclear apoptotic morphology were not observed in CCD-18Co normal colon fibroblasts after 72 hours (**Figure 5.4D**).

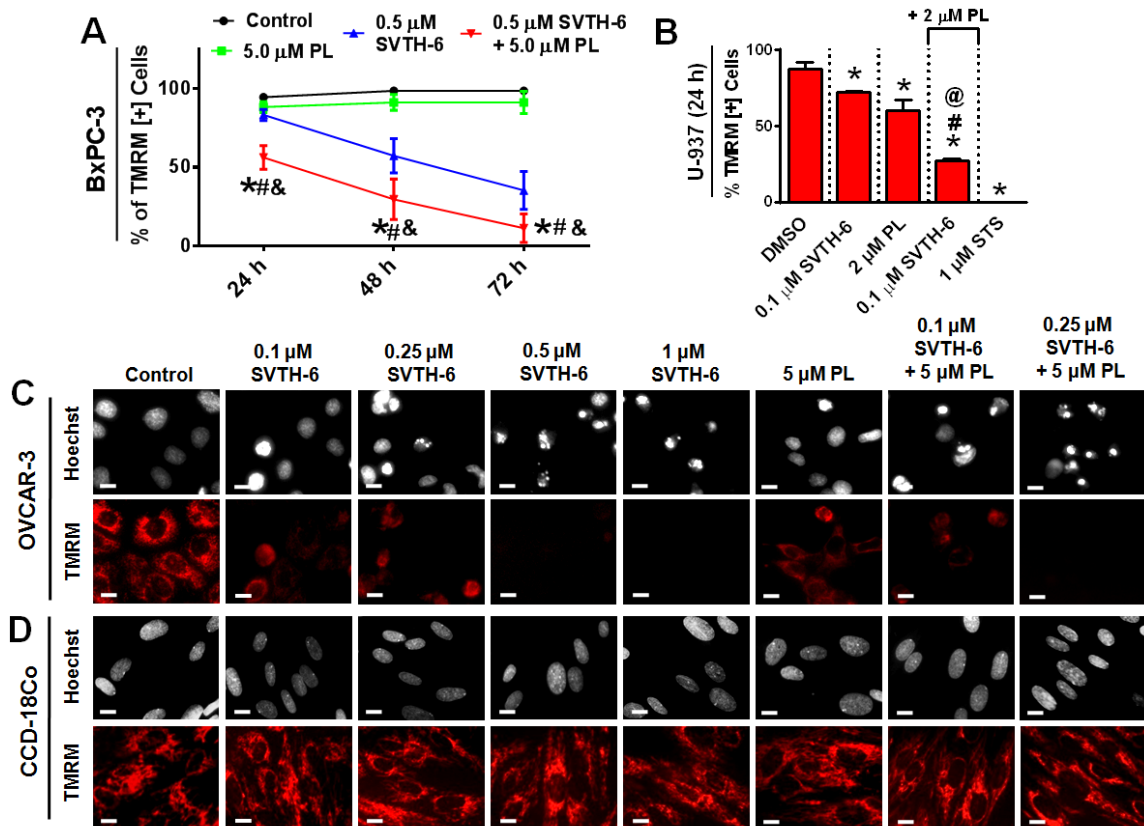


Figure 5.4. PL Selectively Enhances Mitochondrial Membrane Potential (MMP) Dissipation by SVTH-6 in Cancer Cells. TMRM was used to monitor MMP in (A) BxPC-3 and (B) U-937 cancer cells with image-based cytometry. * $p < 0.001$ vs. DMSO control; # $p < 0.01$ SVTH-6 treatment alone; & $p < 0.001$ vs. PL treatment alone. (C) Micrographs of depicting the effect of SVTH-6 and PL on MMP in (C) OVCAR-3 ovarian cancer cells and (D) CCD-18Co normal human fibroblasts after 48 hours with TMRM staining. Red fluorescent punctuate marks are indicative of mitochondria with intact MMP. Scale bar = 15 μm . Micrographs are representative of 3 independent experiments.

PL Enhances Mitochondrial Dysfunction by SVTH-6

A direct indicator on mitochondrial function is oxygen consumption (Brand and Nicholls 2011). To assess the effect of SVTH-6 alone and in combination with PL on oxygen consumption, the MitoXpress® Xtra - Oxygen Consumption Assay was used. SVTH-6 was able to effectively decrease the rate of oxygen consumption in U-937 lymphoma cells (**Figure 5.5A**). PL alone did not have a drastic effect on oxygen consumption, however, it was able to enhance the ability of SVTH-6 to decrease oxygen consumption in U-937 cells. Antimycin A (AMA), a complex III inhibitor of the electron transport chain (ETC), was used as a positive control for hindering oxygen consumption. These results indicate that PL is effective at enhancing the ability of SVTH-6 in reducing oxygen consumption in lymphoma cells, and thus, mitochondrial function.

Subsequent to the collapse of MMP and permeabilization of the mitochondrial membrane, various apoptogenic factors, such as AIF and Cyto c, are released from the mitochondria into the cytosol where they can directly or indirectly execute apoptosis (Earnshaw 1999; Degterev, Boyce, and Yuan 2003). To evaluate the ability of SVTH-6 and PL alone and in combination to act directly on cancer cell mitochondria to cause release of apoptogenic factors, mitochondria from OVCAR-3 cells were isolated and were directly subjected SVTH-6 and PL insult. After 2 hours, samples were vortexed, centrifuged and post mitochondrial supernatants were analyzed by western blot analysis for the release of apoptogenic factors from the mitochondria; mitochondrial pellet samples were probed with succinate dehydrogenase subunit A (SDHA) to serve

as loading controls. Interestingly, SVTH-6 and PL alone and in combination were able to cause release of both Cyto c and AIF from these isolated cancer cell mitochondria, indicative of direct mitochondrial targets by these compounds **(Figure 5.5B)**.

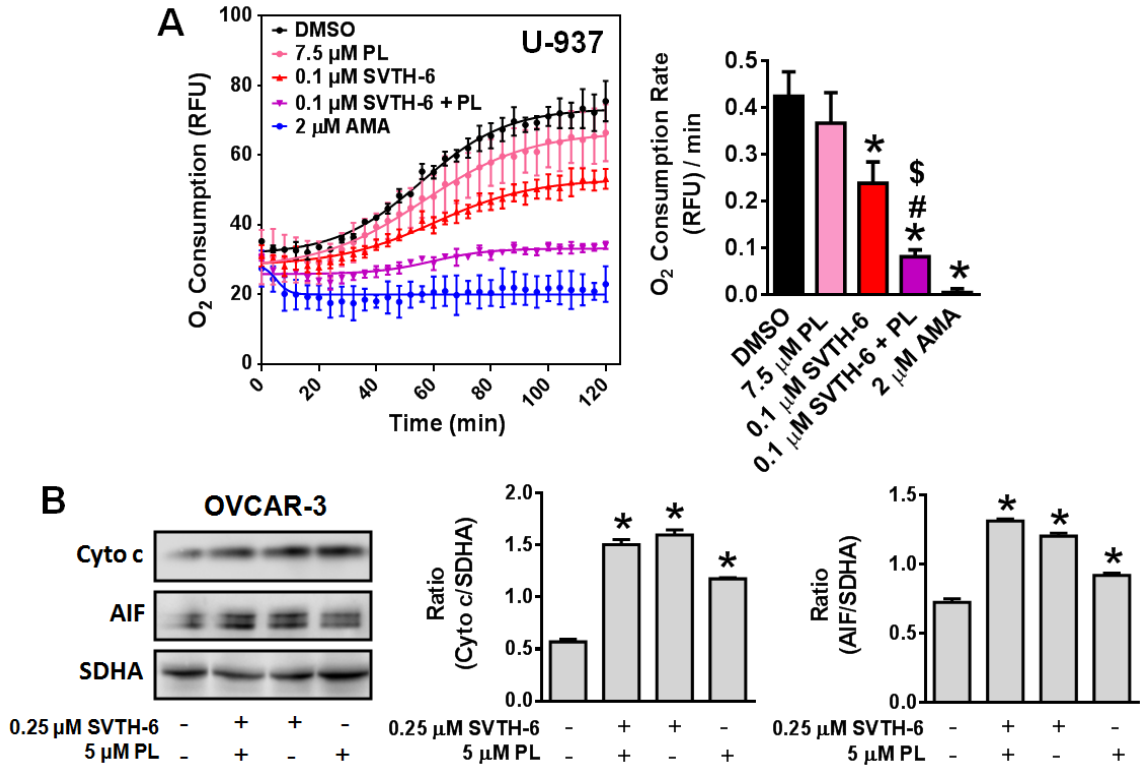


Figure 5.5. PL Enhances Mitochondrial Dysfunction by SVTH-6. (A) The MitoXpress® Xtra - Oxygen Consumption Assay was used to monitor oxygen consumption via fluorescence generation. U-937 Cells were treated, and the fluorescent MitoXpress® reagent monitored at Ex. 380 nm and Em. 650, every 2 minutes for 2 hours at 37 °C. Oxygen consumption rates were calculated by measuring the slopes of the linear regions of the oxygen consumption curves. Values are expressed as mean ± SD from at least 3 independent experiments. * $p < 0.01$ vs. DMSO control; \$ $p < 0.01$ vs. SVTH-6 treatment alone; # $p < 0.01$ vs. PL treatment alone. (B) Isolated mitochondria of OVCAR-3 cells were treated directly with SVTH-6, PL, and solvent control (Me₂SO) for 2 hours. Following treatment, samples were centrifuged, producing post mitochondrial supernatants, which were examined for the release of apoptogenic factors AIF and Cyto c respectively via western blot analyses, and mitochondrial pellets which were probed for SDHA to serve as loading controls. Image is representative of 3 independent experiments demonstrating similar trends. Values are expressed as mean ± SD of quadruplicates of 1 independent experiment; * $p < 0.01$ versus solvent control (DMSO).

Enhancement of SVTH-6 Anti-Cancer Activity by PL is Dependent on Oxidative Stress

To determine the involvement of ROS in SVTH-6 induced cytotoxicity alone and in combination with PL, the antioxidant NAC was utilized. Combination treatment of SVTH-6 and PL yielded an enhancement in ROS production as seen with the H₂DCFDA ROS indicator (**Figure 5.6A**), which was completely diminished with NAC treatment. Interestingly, NAC was able rescue cancer cells from this combination treatment in BxPC-3 and U-937 cancer cells (**Figure 5.6B & C**), and rescued U-937 cells from MMP collapse in U-937 cells (**Figure 5.6D**). Therefore, the enhanced cytotoxic effect produced by this combination treatment selectively in cancer cells is dependent on oxidative stress.

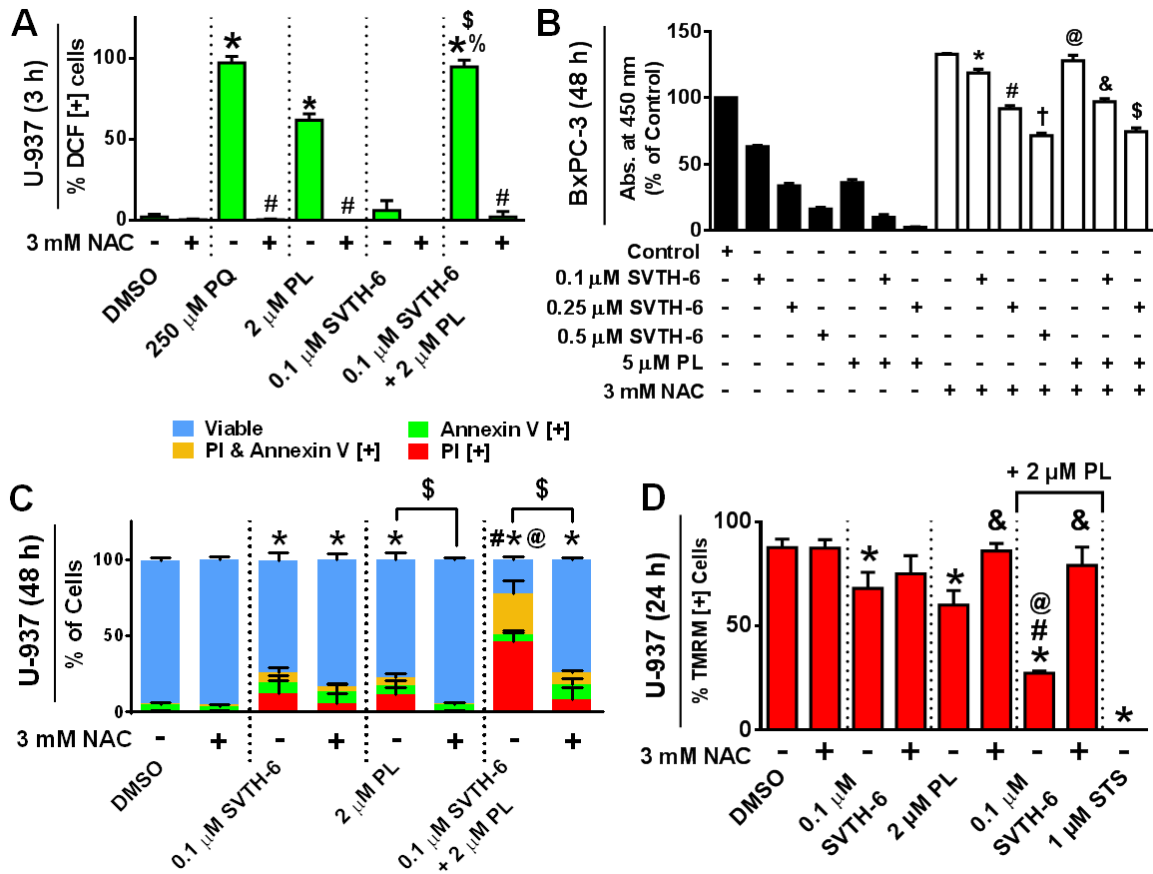


Figure 5.6. Enhancement of SVTH-6 Anti-Cancer Activity by PL is Dependent on Oxidative Stress. (A) ROS production monitored with H₂DCFDA with imaged-based cytometry. **p*<0.001 vs. DMSO control; #*p*<0.001 vs. respective group without NAC; \$*p*<0.001 vs. PL treatment alone; %*p*<0.001 vs. SVTH-6 treatment alone. (B) BxPC-3 cells were treated with SVTH-6 and PL at the indicated concentrations for 48 hours with or without NAC to determine the dependency of ROS. The WST-1 reagent was used to quantify cell viability. Absorbance was read at 450 nm and expressed as a percent of the solvent control (Me₂SO). Values are expressed as mean \pm SD from quadruplicates of 3 independent experiments; **p*<0.001 vs. 0.1 μ M SVTH-6; #*p*<0.01 vs. 0.25 μ M SVTH-6; †*p*<0.005 vs. 0.5 μ M SVTH-6; @*p*<0.01 vs. 5 μ M PL; &*p*<0.01 vs. 0.1 μ M SVTH-6 + 5 μ M PL; \$*p*<0.005 vs. 0.25 μ M SVTH-6 + 5 μ M PL. (C) U-937 cells monitored for Annexin V binding and PI staining with image-based cytometry. **p*<0.01 vs. DMSO control; \$*p*<0.001 vs. respective group without NAC; #*p*<0.001 vs. SVTH-6 treatment alone; @*p*<0.001 vs. PL treatment alone; all comparisons for *p* values are with viable cells only. (D) MMP dissipation of U-937 cells was monitored with TMRM. **p*<0.01 vs. DMSO control; &*p*<0.001 vs. respective group without NAC; #*p*<0.001 vs. SVTH-6 treatment alone; @*p*<0.001 vs. PL treatment alone.

Discussion

We present a synthetic analogue of PST, SVTH-6, which has potent anti-cancer activity by targeting cancer cell mitochondria that was enhanced by exploiting oxidative vulnerabilities in cancer cells with PL. This PST analogue, SVTH-6, effectively caused cytotoxicity in an array of aggressive cancer cell types by way of apoptotic induction as shown by nuclear condensation and Annexin V binding to phosphatidylserine (**Figure 5.3**). This anti-cancer effect was enhanced when combined with the natural compound PL. However, a crucial finding of this study was the selective nature of SVTH-6 alone and in combination with PL; noncancerous PBMCs V1, PBMCs V2, NCM460 and CCD-18Co cells were significantly less sensitive to these treatments (**Figure 5.1F, 5.2E, 5.3B, 5.3D**). This is in contrast to most chemotherapeutics currently available, such as Taxol, which we have previously shown to be very toxic to noncancerous cells (McLachlan et al. 2005).

A new class of compounds collectively known as mitocans, includes anti-cancer agents that directly or indirectly target cancer cell mitochondria to induce apoptosis selectively (Chen et al. 2010); through the findings of this report, SVTH-6 can put into this classification of compounds. We have formerly shown PST and JCTH-4 to selectively target cancer cell mitochondria to selectively induce apoptosis in cancer cells (McLachlan et al. 2005; Siedlakowski et al. 2008; Griffin et al. 2011; Collins et al. 2010; Ma et al. 2011; Ma, Tremblay, et al. 2012). Likewise, this study has shown SVTH-6 to dissipate MMP in cancer cells selectively, decrease oxygen consumption and cause release of apoptogenic

factors Cyto c and AIF from isolated cancer cell mitochondria alone and in combination with PL (**Figure 5.4 & 5.5**). These findings suggest direct mitochondrial targets by SVTH-6.

The development of aggressive malignancies has been associated with elevated levels of oxidative stress (Kumar et al. 2008). Moreover, cancer cells have been found to exhibit higher levels of endogenous ROS compared to noncancerous cells (Diehn et al. 2009; Schumacker 2006). In turn, it is projected that cancer cells are more dependent on cellular defence mechanisms against ROS (Gogvadze, Orrenius, and Zhivotovsky 2008; Trachootham, Alexandre, and Huang 2009). Thus, targeting these oxidative vulnerabilities in cancer cells presents as a promising therapeutic tactic (Fruehauf and Meyskens 2007). Indeed, this strategy proved to be advantageous as demonstrated by SVTH-6 and PL in this study. It has been previously suggested that the anti-cancer effects of PL are a result of selective targeting of the stress response to ROS (Raj et al. 2011). Furthermore, our previous reports have revealed PST and JCTH-4 to induce ROS generation in cancer cells (McLachlan et al. 2005; Siedlakowski et al. 2008; Griffin et al. 2011; Ma, Tremblay, et al. 2012; Ma et al. 2011). When SVTH-6 and PL were used in combination, an enhanced cytotoxic response, MMP dissipation, and generation of ROS was produced in cancer cells (**Figure 5.2A-D, 5.3A & C, 5.4, 5.5, 5.6A**). The cytotoxic effects produced by SVTH-6 alone and in combination with PL were confirmed to be dependent on oxidative stress as the antioxidant NAC was able to rescue cancer cells from these treatments (**Figure 5.6**). Past studies have suggested proteins such as

glutathione S-transferase pi 1 (GSTP1) and carbonyl reductase1 (CBR1) to be direct or indirect targets of PL (Raj et al. 2011). However, increased levels of ROS induced by PL were not affected with the knockdown of GSTP1 or CBR1; thus, it is likely for PL to have multiple targets. Interestingly, we demonstrated PL to cause release of both Cyto c and AIF from isolated cancer cell mitochondria (**Figure 5.5B**) which may point towards mitochondrial target(s) by PL.

There are many distinct differences in cancer cell metabolism and mitochondria which may allow for cancer specific targeting by SVTH-6 and possibly by PL (Gogvadze, Orrenius, and Zhivotovsky 2008; Chen et al. 2010). Cancer cells rely less on the mitochondria and more heavily on glycolytic metabolism for energy, a phenomenon known as the Warburg effect (Vander Heiden, Cantley, and Thompson 2009). Consequently, this metabolic phenotype gives rise to an acidic cytosolic environment, partially contributing to the hyperpolarization of cancer cell mitochondria. Hyperpolarized mitochondria in cancer cells have been associated with increased invasiveness and a heightened ability to evade apoptosis (Heerdt, Houston, and Augenlicht 2006). Nevertheless, it is this very feature that may allow selective targeting of cancer cells; once taken into the cell, SVTH-6 could be processed into a positively charged molecule that can be selectively taken up into hyperpolarized cancer cell mitochondria. Furthermore, there is a differential expression of various antiapoptotic proteins between cancer and noncancerous cells. The glycolytic enzyme hexokinase II and antiapoptotic proteins of the Bcl-2 family, all of which discourage mitochondrial membrane permeabilization, have been shown to be

highly expressed in cancer cells (Green and Kroemer 2004; Casellas, Galiegue, and Basile 2002; Mathupala, Rempel, and Pedersen 1997).

Adverse side effects produced by unspecific targeting and chemoresistance remain as large obstacles with present chemotherapeutics. We have in hand, a novel synthetic analogue of PST, SVTH-6, with highly selective and potent anti-cancer activity against many aggressive malignancies acting through mitochondrial targeting. Combining SVTH-6, shown to cause mitochondrial dysfunction with PL, which cripples cellular defence mechanisms against ROS preferentially in cancer cells, presents a promising strategy in eradicating cancer. We have demonstrated this approach to produce an enhanced response against cancer cells; thus, lower doses of each drug are required for the same desired effect, minimizing any minor side effects these compounds may have at higher doses. This approach targets two or more different vulnerabilities of cancer cells, which may decrease the likelihood of chemoresistance. Elucidating the target protein(s) and pathway(s) of SVTH-6, may give rise to a novel outlook to cancer etiology and provide a scaffold for the design of additional therapeutic approaches. Given the unprecedented selective anti-cancer activity uncovered thus far, we present a promising strategy that may serve as a safer and more effective alternative to the cancer therapies currently available.

Author Contributions

Dennis Ma contributed to the conception and design of experiments, execution of experiments, analysis of data, and preparation of the manuscript. Tyler Gilbert, Daniel Tarade, Christopher Pignanelli, Fadi Mansour, Manika Gupta, Ian Tuffley, and Sabrina Ma contributed to the execution of experiments and preparation of the manuscript. Sergey Vshyvenko and Tomas Hudlicky synthesized and provided SVTH-6 for this study. Siyaram Pandey contributed to design of experiments, analysis of data, preparation of the manuscript and obtained funding for the project.

Acknowledgements

Thank you to Phillip Tremblay, Scott Adams, Colin Curran, Alexander Dowhayko, Megan Noel, Pardis Akbari-Asl, Jashanjit Cheema, Julia Church and Seema Joshi for their initial assistance on this project and continued support and encouragement.

Grant Support

Funding of this work has been provided as generous donations by the Knights of Columbus Chapter 9671 (Windsor, Ontario) and from Dave and Donna Couvillon in memory of Kevin Couvillon. This work has also been supported by a CIHR Frederick Banting and Charles Best Canada Graduate Scholarship, an Ontario Graduate Scholarship, and a Vanier Canada Graduate Scholarship awarded to Dennis Ma.

References

- Brand, Martin D, and David G Nicholls. 2011. "Assessing Mitochondrial Dysfunction in Cells." *The Biochemical Journal* 435 (2): 297–312. doi:10.1042/BJ20110162.
- Casellas, Pierre, Sylvaine Galiegue, and Anthony S Basile. 2002. "Peripheral Benzodiazepine Receptors and Mitochondrial Function." *Neurochemistry International* 40 (6): 475–86.
- Chen, Gang, Feng Wang, Dunyaporn Trachootham, and Peng Huang. 2010. "Preferential Killing of Cancer Cells with Mitochondrial Dysfunction by Natural Compounds." *Mitochondrion* 10 (6): 614–25. doi:10.1016/j.mito.2010.08.001.
- Collins, Jonathan, Uwe Rinner, Michael Moser, Tomas Hudlicky, Ion Ghiviriga, Anntherese E Romero, Alexander Kornienko, Dennis Ma, Carly Griffin, and Siyaram Pandey. 2010. "Chemoenzymatic Synthesis of Amaryllidaceae Constituents and Biological Evaluation of Their C-1 Analogues. The next Generation Synthesis of 7-Deoxypancratistatin and Trans-Dihydrolycoricidine." *The Journal of Organic Chemistry* 75 (9): 3069–84. doi:10.1021/jo1003136.
- DeBerardinis, Ralph J, Julian J Lum, Georgia Hatzivassiliou, and Craig B Thompson. 2008. "The Biology of Cancer: Metabolic Reprogramming Fuels Cell Growth and Proliferation." *Cell Metabolism* 7 (1): 11–20. doi:10.1016/j.cmet.2007.10.002.
- Degterev, Alexei, Michael Boyce, and Junying Yuan. 2003. "A Decade of

- Caspases.” *Oncogene* 22 (53): 8543–67. doi:10.1038/sj.onc.1207107.
- Diehn, Maximilian, Robert W Cho, Neethan A Lobo, Tomer Kalisky, Mary Jo Dorie, Angela N Kulp, Dalong Qian, et al. 2009. “Association of Reactive Oxygen Species Levels and Radioresistance in Cancer Stem Cells.” *Nature* 458 (7239): 780–83. doi:10.1038/nature07733.
- Earnshaw, W C. 1999. “Apoptosis. A Cellular Poison Cupboard.” *Nature* 397 (6718): 387, 389. doi:10.1038/17015.
- Fruehauf, John P, and Frank L Meyskens. 2007. “Reactive Oxygen Species: A Breath of Life or Death?” *Clinical Cancer Research: An Official Journal of the American Association for Cancer Research* 13 (3): 789–94. doi:10.1158/1078-0432.CCR-06-2082.
- Gogvadze, Vladimir, Sten Orrenius, and Boris Zhivotovsky. 2008. “Mitochondria in Cancer Cells: What Is so Special about Them?” *Trends in Cell Biology* 18 (4): 165–73. doi:10.1016/j.tcb.2008.01.006.
- Gogvadze, Vladimir, Boris Zhivotovsky, and Sten Orrenius. 2010. “The Warburg Effect and Mitochondrial Stability in Cancer Cells.” *Molecular Aspects of Medicine* 31 (1): 60–74. doi:10.1016/j.mam.2009.12.004.
- Green, Douglas R, and Guido Kroemer. 2004. “The Pathophysiology of Mitochondrial Cell Death.” *Science (New York, N.Y.)* 305 (5684): 626–29. doi:10.1126/science.1099320.
- Griffin, Carly, Aditya Karnik, James McNulty, and Siyaram Pandey. 2011. “Pancratistatin Selectively Targets Cancer Cell Mitochondria and Reduces Growth of Human Colon Tumor Xenografts.” *Molecular Cancer Therapeutics*

10 (1): 57–68. doi:10.1158/1535-7163.MCT-10-0735.

Griffin, Carly, James McNulty, and Siyaram Pandey. 2011. “Pancratistatin Induces Apoptosis and Autophagy in Metastatic Prostate Cancer Cells.” *International Journal of Oncology* 38 (6): 1549–56. doi:10.3892/ijo.2011.977.

Heerdt, Barbara G, Michele A Houston, and Leonard H Augenlicht. 2006. “Growth Properties of Colonic Tumor Cells Are a Function of the Intrinsic Mitochondrial Membrane Potential.” *Cancer Research* 66 (3): 1591–96. doi:10.1158/0008-5472.CAN-05-2717.

Kekre, Natasha, Carly Griffin, James McNulty, and Siyaram Pandey. 2005. “Pancratistatin Causes Early Activation of Caspase-3 and the Flipping of Phosphatidyl Serine Followed by Rapid Apoptosis Specifically in Human Lymphoma Cells.” *Cancer Chemotherapy and Pharmacology* 56 (1): 29–38. doi:10.1007/s00280-004-0941-8.

Kumar, Binod, Sweaty Koul, Lakshmipathi Khandrika, Randall B Meacham, and Hari K Koul. 2008. “Oxidative Stress Is Inherent in Prostate Cancer Cells and Is Required for Aggressive Phenotype.” *Cancer Research* 68 (6): 1777–85. doi:10.1158/0008-5472.CAN-07-5259.

Ma, Dennis, Jonathan Collins, Tomas Hudlicky, and Siyaram Pandey. 2012. “Enhancement of Apoptotic and Autophagic Induction by a Novel Synthetic C-1 Analogue of 7-Deoxypancratistatin in Human Breast Adenocarcinoma and Neuroblastoma Cells with Tamoxifen.” *Journal of Visualized Experiments : JoVE*, no. 63 (January). doi:10.3791/3586.

Ma, Dennis, Phillip Tremblay, Kevinjeet Mahngar, Pardis Akbari-Asl, Jonathan

- Collins, Tomas Hudlicky, James McNulty, and Siyaram Pandey. 2012. "A Novel Synthetic C-1 Analogue of 7-Deoxypancratistatin Induces Apoptosis in p53 Positive and Negative Human Colorectal Cancer Cells by Targeting the Mitochondria: Enhancement of Activity by Tamoxifen." *Investigational New Drugs* 30 (3): 1012–27. doi:10.1007/s10637-011-9668-7.
- Ma, Dennis, Phillip Tremblay, Kevinjeet Mahngar, Jonathan Collins, Tomas Hudlicky, and Siyaram Pandey. 2011. "Selective Cytotoxicity against Human Osteosarcoma Cells by a Novel Synthetic C-1 Analogue of 7-Deoxypancratistatin Is Potentiated by Curcumin." *PloS One* 6 (12): e28780. doi:10.1371/journal.pone.0028780.
- Mathupala, S P, A Rempel, and P L Pedersen. 1997. "Aberrant Glycolytic Metabolism of Cancer Cells: A Remarkable Coordination of Genetic, Transcriptional, Post-Translational, and Mutational Events That Lead to a Critical Role for Type II Hexokinase." *Journal of Bioenergetics and Biomembranes* 29 (4): 339–43.
- McLachlan, A, N Kekre, J McNulty, and S Pandey. 2005. "Pancratistatin: A Natural Anti-Cancer Compound That Targets Mitochondria Specifically in Cancer Cells to Induce Apoptosis." *Apoptosis: An International Journal on Programmed Cell Death* 10 (3): 619–30. doi:10.1007/s10495-005-1896-x.
- Pastorino, John G, Nataly Shulga, and Jan B Hoek. 2002. "Mitochondrial Binding of Hexokinase II Inhibits Bax-Induced Cytochrome c Release and Apoptosis." *The Journal of Biological Chemistry* 277 (9): 7610–18. doi:10.1074/jbc.M109950200.

- Plas, David R, and Craig B Thompson. 2002. "Cell Metabolism in the Regulation of Programmed Cell Death." *Trends in Endocrinology and Metabolism: TEM* 13 (2): 75–78.
- Raj, Lakshmi, Takao Ide, Aditi U Gurkar, Michael Foley, Monica Schenone, Xiaoyu Li, Nicola J Tolliday, et al. 2011. "Selective Killing of Cancer Cells by a Small Molecule Targeting the Stress Response to ROS." *Nature* 475 (7355): 231–34. doi:10.1038/nature10167.
- Schumacker, Paul T. 2006. "Reactive Oxygen Species in Cancer Cells: Live by the Sword, Die by the Sword." *Cancer Cell* 10 (3): 175–76. doi:10.1016/j.ccr.2006.08.015.
- Siedlakowski, Peter, Amanda McLachlan-Burgess, Carly Griffin, Sridhar S Tirumalai, James McNulty, and Siyaram Pandey. 2008. "Synergy of Pancreatistatin and Tamoxifen on Breast Cancer Cells in Inducing Apoptosis by Targeting Mitochondria." *Cancer Biology & Therapy* 7 (3): 376–84.
- Szatrowski, T P, and C F Nathan. 1991. "Production of Large Amounts of Hydrogen Peroxide by Human Tumor Cells." *Cancer Research* 51 (3): 794–98.
- Trachootham, Dunyaporn, Jerome Alexandre, and Peng Huang. 2009. "Targeting Cancer Cells by ROS-Mediated Mechanisms: A Radical Therapeutic Approach?" *Nature Reviews. Drug Discovery* 8 (7): 579–91. doi:10.1038/nrd2803.
- Vander Heiden, Matthew G, Lewis C Cantley, and Craig B Thompson. 2009. "Understanding the Warburg Effect: The Metabolic Requirements of Cell

Proliferation.” *Science (New York, N.Y.)* 324 (5930): 1029–33.
doi:10.1126/science.1160809.

Vshyvenko, Sergey, Jon Scattolon, Tomas Hudlicky, Anntherese E Romero, and Alexander Kornienko. 2011. “Synthesis of C-1 Homologues of Pancratistatin and Their Preliminary Biological Evaluation.” *Bioorganic & Medicinal Chemistry Letters* 21 (16): 4750–52. doi:10.1016/j.bmcl.2011.06.068.

Warburg, O. 1956. “On the Origin of Cancer Cells.” *Science (New York, N.Y.)* 123 (3191): 309–14.

CHAPTER 6: General Discussion

List of Abbreviations

7-deoxyPST 7-deoxypancratistatin

MMP mitochondrial membrane potential

PST pancratistatin

ROS reactive oxygen species (ROS)

ETC electron transport chain

PL piperlongumine

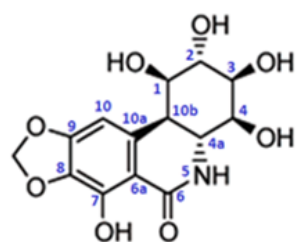
DOX Doxorubicin

GEM Gemcitabine

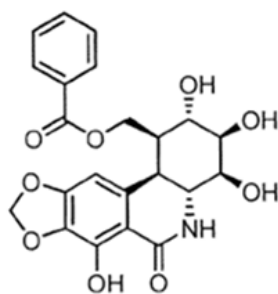
General Discussion

In this dissertation, various synthetic analogues of the natural compound pancratistatin (PST) (**Figure 6.1**), a compound we have found to selectively induce apoptosis in cancer cells, were systematically evaluated for anti-cancer activity in a battery of cancer cell lines. The synthesis and screening of these novel analogues was completed in an effort to overcome the low availability of native PST in nature and to produce more efficacious analogues.

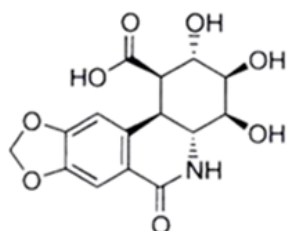
The initial work on this project involved the screening of four 7-deoxypancratistatin (7-deoxyPST) analogues: JCTH-1, JCTH-2, JCTH-3, and JCTH-4 (Collins et al. 2010). JCTH-4 was found to have comparable anti-cancer activity compared to natural PST. JCTH-3 had limited anti-cancer activity while the effects of JCTH-1 and JCTH-2 were very minimal in cancer cells. This was the first time a synthetic analogue of 7-deoxyPST was shown to have comparable anti-cancer activity to PST. JCTH-4, a C-1 acetoxymethyl analogue of 7-deoxyPST, was further evaluated and characterized in various cancer cell types alone in combination with other anti-cancer agents (**Chapter 2 & 3, Appendix A & B**).



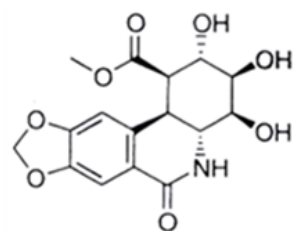
Pancratistatin (PST)



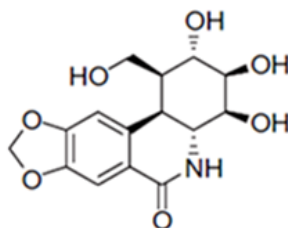
SVTH-7



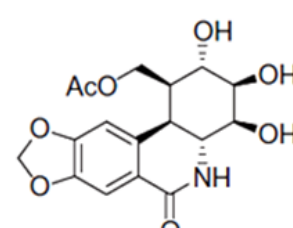
JCTH-1



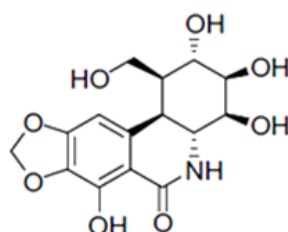
JCTH-2



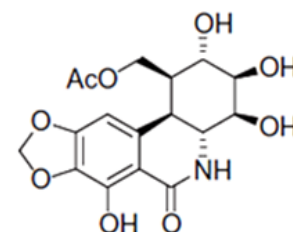
JCTH-3



JCTH-4



SVTH-5



SVTH-6

7-deoxyPST Analogues

Figure 6.1. Structure of PST and Synthetic PST Analogues

JCTH-4 was found to be effective against colorectal cancer cells (**Chapter 2**), osteosarcoma cells (**Chapter 3**), pancreatic cancer cells (**Appendix A**), neuroblastoma cells (**Appendix B**), and breast cancer cells (**Appendix B**). As with natural PST, JCTH-4 was able to induce apoptosis in these cancer cells selectively by targeting mitochondria. Furthermore, the preferential pro-apoptotic effect in cancer cells was potentiated by Tamoxifen (**Chapter 2, Appendix B**) and curcumin (**Chapter 3**), by enhancing mitochondrial dysfunction in cancer cells. This enhancement is proposed to be a result of the ability of Tamoxifen and curcumin to target cancer cell mitochondria, sensitizing this organelle to JCTH-4 insult (Moreira et al. 2006; Ravindran et al. 2009; Aggarwal et al. 2007).

Upon finding potent anti-cancer activity comparable to PST in JCTH-4, a 7-deoxyPST analogue, and drawing from previous structure activity relationship analyses (McNulty et al. 2005; Collins et al. 2008; Collins et al. 2010), additional PST analogues were designed and synthesized in an effort to find chemical modifications to maximize anti-cancer activity. PST analogues containing the full proposed anti-cancer pharmacophore of PST and related alkaloids were synthesized, which incorporated the C-7 hydroxyl group (Vshyvenko et al. 2011). These included SVTH-5 and -6, the C-7 hydroxylated equivalents of JCTH-3 and -4, respectively, and the novel analogue SVTH-7 (**Figure 6.1**).

To evaluate the anti-cancer activity of these compounds, a medium throughput screen was completed on 18 cancer cell lines and non-cancerous cells (**Chapter 4**). PST analogues SVTH-7, -6, and -5 demonstrated potent anti-cancer activity with greater efficacy than natural PST, 7-deoxyPST analogues,

and several standard chemotherapeutics, with SVTH-7 having greatest activity, followed by SVTH-6 and -5. Likewise, they were efficient in disrupting mitochondrial function, activating the intrinsic pathway of apoptosis in both monolayer and spheroid culture, and reducing growth of tumor xenografts *in vivo*. These results demonstrate the ability of PST analogues to target a broad range of different cell types, which demonstrates a possible targeting of a common cancer vulnerability .

Collectively, these findings suggest the anti-cancer activity of these compounds to be highly dependent on the C-7 hydroxyl group and the functional group substitutions on C-1. Notably, the functional group at C-1 dramatically alters analogue potency against cancer cells as seen with JCTH-1 and JCTH-2, compounds nearly devoid of anti-cancer activity, compared to JCTH-4, which only differs in the functional group at the C-1 position (Collins et al. 2010). Moreover, SVTH-7 varies only in the C-1 functional group compared to SVTH-6 and -5, and has much greater efficacy (**Chapter 4**). The findings of these structural activity analyses point to the possible role and importance of the C-7 hydroxyl group and the C-1 functional groups in the interaction between the cellular target(s) of PST and its analogues at very specific binding sites(s). In particular, SVTH-7, the most efficacious PST analogue, has a bulky benzene group at C-1, suggesting an interaction between the C-1 functional group and a specific hydrophobic pocket on the cellular target(s).

Although the exact cellular target of PST and its analogues has not yet been identified and characterized, evidence from this body of work and previous

findings suggest cancer cell mitochondria to play a pivotal role in the anti-cancer activity of these compounds (**Chapter 2-4, Appendix A & B**) (McLachlan et al. 2005; Siedlakowski et al. 2008; Griffin et al. 2011; Ma et al. 2012; Ma et al. 2011). PST and its synthetic analogues have been shown to dissipate mitochondrial membrane potential (MMP) early after treatment, cause an increase in reactive oxygen species (ROS), disrupt oxygen consumption, and promote release of apoptogenic factors from cancer cell mitochondria. Furthermore, isolated cancer cell mitochondria treated with PST and PST analogues were shown to have increases in ROS, and release apoptogenic factors, indicating that these compounds are able to act directly on this organelle.

Like other mitocans, chemical agents that target cancer cell mitochondria to induce apoptosis, these compounds could be interacting with anti-apoptotic Bcl-2 proteins overexpressed in cancer cells, interacting with proteins of the permeability transition pore to induce mitochondrial permeabilization, functionally mimicking the activity of various pro-apoptotic Bcl-2 family proteins, or targeting complexes of the electron transport chain (ETC) (Neuzil et al. 2013; Ralph et al. 2006). Interestingly, inhibiting ETC complex II was able to abolish the anticancer activity of SVTH-7 (**Chapter 4**). A similar but less pronounced effect was observed with complex III inhibition.

This surprising observation could be the result targeting of these complexes directly or through interacting partners. Alternatively, studies have shown complex II to be a mediator of apoptosis (Guzzo et al. 2014; Lemarie et al. 2011), however, the exact role of complex II and III in PST analogue-induced

apoptosis remains unclear. Further experiments involving functional ETC complex activity assays, siRNAs or shRNAs for ETC complexes, and overexpression of ETC complexes are needed to characterize the role of complex II and III. However, to identify direct binding partners of PST analogues, affinity chromatography with a PST analogue-linked resin can be employed. These additional studies may reveal specific cancer vulnerabilities that can be used for the design of novel therapeutic strategies.

Targeting ETC complexes has been shown to increase ROS, which can selectively induce apoptosis in cancer cells as they have been demonstrated to be more vulnerable to oxygen radical insult (Trachootham et al. 2006; Trachootham et al. 2009). Therefore, mitocans that target mitochondria in combination with agents that can increase oxidative stress could be an effective way to eliminate cancer cells. Indeed, the ability of SVTH-6 to induce mitochondrial dysfunction and apoptosis selectively in cancer cells was enhanced with piperlongumine (PL), a compound found to target cellular defense mechanisms against oxidative stress (**Chapter 5**). Such findings demonstrate the potential of exploiting cancer cell mitochondria and oxidative vulnerabilities to selectively induce apoptosis in cancer cells.

Although, the broad spectrum caspase inhibitor Z-VAD-FMK was unable to prevent JCTH-4-induced cytotoxicity (**Chapter 2**), this result was obtained using the WST-1 assay which measures active cell metabolism. The dependence of caspases in PST analogue-induced apoptosis was more appropriately evaluated by monitoring early and late apoptosis induction with Annexin V

binding and propidium iodide staining (**Chapter 4**). These studies revealed Z-VAD-FMK to only partially rescue cancer cells from PST analogues, indicating that caspases are only partially but not completely necessary in the induction of apoptosis. This supports the case for PST analogues targeting cancer cell mitochondria which are upstream of executioner caspases and can cause release of various apoptogenic factors involved in both caspase dependent and independent pathways of apoptosis.

Marked differences in cancer cell mitochondria provide opportunities for selectively promoting cell death. (Gogvadze et al. 2008; Gogvadze et al. 2010). In contrast, many chemotherapeutics currently in use targeting DNA or tubulin dynamics do not discriminate between normal and cancerous cells, and exert their effects on fast dividing cells in the body which can lead to a variety of side effects (Jordan & Wilson 2004). At low concentrations, PST analogues demonstrated potent anti-cancer activity with minimal effect in normal cells, which may be a result of its ability to exploit cancer cell mitochondria. In addition to selectively targeting cancer cells, SVTH-7, -6, and -5 were shown to be more effective than common chemotherapeutics, Taxol, Doxorubicin (DOX), Gemcitabine (GEM), and Cisplatin in a multitude of cancer cell types including leukemia, triple negative breast cancer, glioblastoma, and non-small cell lung cancer in vitro. Notably, GEM, a nucleoside analogue and the standard chemotherapeutic for notoriously chemoresistant pancreatic cancer (Berlin & Benson 2010), was surpassed in efficacy by these PST analogues.

As we have shown these compounds to be both selective and more effective than multiple standard chemotherapeutics, it presents a strong case for their clinical development. More importantly, these analogues were able to reduce growth of tumor spheroids and human tumor xenografts *in vivo* in mice. No apparent toxicity to mice was observed as there was no reduction in body mass and decrease in normal activity. However, further toxicology and pathological analyses are required to fully characterize their tolerance in animals. Additional *in vivo* studies using various modes of drug administration including oral feeding, intraperitoneal injection and intravenous injection will further validate our findings. In summary, these *in vivo* studies demonstrate the ability of these analogues to penetrate tumor architecture and remain stable and effective in physiological systems, warranting their investigation for human use. Future work involving rigorous pharmacokinetic and pharmacodynamic studies are required to characterize how these analogues are absorbed, distributed, metabolized, and excreted, as well as identifying potentially dangerous interactions these compounds may have in the body. These will be crucial prerequisites for the approval of these analogues for human clinical trials by Health Canada.

Conclusion

This dissertation has addressed the initial hurdles in advancing the development of PST as a chemotherapeutic including its low availability in nature. SVTH-7 had the most anti-cancer activity, followed by -6, and -5. These compounds can be made in abundance and their chemical modification of the C-1 functional group has provided greater anti-cancer activity compared to natural PST and multiple chemotherapeutics in various aggressive cancer cell types in two- and three-dimensional cell culture. Further validation of the efficacy and selectivity of these analogues was found in animal models. Evidence from this work suggests a mitochondrial target in cancer cells. The requirement of functional complex II and III for the anti-cancer activity of SVTH-7 points to a potential vulnerability in cancer cells that can be further characterized and exploited for the development of novel therapeutic regimes. In addition, this work has demonstrated the potential benefit of using novel non-genotoxic anti-cancer agents targeting mitochondrial and oxidative susceptibilities in combination. Consequently, using these analogues as sensitizing agents in adjuvant therapy with standard chemotherapeutics could potentially bring down the effective concentrations of these drugs needed for therapeutic benefit while minimizing any known toxic effects observed at higher doses. Therefore, this work provides a basis for characterizing and exploiting distinct mitochondrial and metabolic vulnerabilities in cancer cells with synthetic analogues of PST with high therapeutic potential.

References

- Aggarwal, B.B. et al., 2007. Targeting cell signaling pathways for drug discovery: an old lock needs a new key. *Journal of cellular biochemistry*, 102(3), pp.580–92.
- Berlin, J. & Benson, A.B., 2010. Chemotherapy: Gemcitabine remains the standard of care for pancreatic cancer. *Nature reviews. Clinical oncology*, 7(3), pp.135–7.
- Collins, J. et al., 2010. Chemoenzymatic synthesis of Amaryllidaceae constituents and biological evaluation of their C-1 analogues. The next generation synthesis of 7-deoxypancratistatin and trans-dihydrolycoricidine. *The Journal of organic chemistry*, 75(9), pp.3069–84.
- Collins, J. et al., 2008. Total synthesis of 7-deoxypancratistatin-1-carboxaldehyde and carboxylic acid via solvent-free intramolecular aziridine opening: phenanthrene to phenanthridone cyclization strategy. *Organic letters*, 10(3), pp.361–4.
- Gogvadze, V., Orrenius, S. & Zhivotovsky, B., 2008. Mitochondria in cancer cells: what is so special about them? *Trends in cell biology*, 18(4), pp.165–73.
- Gogvadze, V., Zhivotovsky, B. & Orrenius, S., 2010. The Warburg effect and mitochondrial stability in cancer cells. *Molecular aspects of medicine*, 31(1), pp.60–74.
- Griffin, C. et al., 2011. Pancratistatin selectively targets cancer cell mitochondria and reduces growth of human colon tumor xenografts. *Molecular cancer therapeutics*, 10(1), pp.57–68.

- Guzzo, G. et al., 2014. Inhibition of succinate dehydrogenase by the mitochondrial chaperone TRAP1 has anti-oxidant and anti-apoptotic effects on tumor cells. *Oncotarget*, 5(23), pp.11897–908.
- Jordan, M.A. & Wilson, L., 2004. Microtubules as a target for anticancer drugs. *Nature Reviews Cancer*, 4(4), pp.253–265.
- Lemarie, A. et al., 2011. Specific disintegration of complex II succinate:ubiquinone oxidoreductase links pH changes to oxidative stress for apoptosis induction. *Cell death and differentiation*, 18(2), pp.338–49.
- Ma, D. et al., 2012. A novel synthetic C-1 analogue of 7-deoxypancratistatin induces apoptosis in p53 positive and negative human colorectal cancer cells by targeting the mitochondria: enhancement of activity by tamoxifen. *Investigational new drugs*, 30(3), pp.1012–27.
- Ma, D. et al., 2011. Selective cytotoxicity against human osteosarcoma cells by a novel synthetic C-1 analogue of 7-deoxypancratistatin is potentiated by curcumin. *PloS one*, 6(12), p.e28780.
- McLachlan, A. et al., 2005. Pancratistatin: a natural anti-cancer compound that targets mitochondria specifically in cancer cells to induce apoptosis. *Apoptosis: an international journal on programmed cell death*, 10(3), pp.619–30.
- McNulty, J., Larichev, V. & Pandey, S., 2005. A synthesis of 3-deoxydihydrolycoricidine: refinement of a structurally minimum pancratistatin pharmacophore. *Bioorganic & medicinal chemistry letters*, 15(23), pp.5315–8.

- Moreira, P.I. et al., 2006. Tamoxifen and estradiol interact with the flavin mononucleotide site of complex I leading to mitochondrial failure. *The Journal of biological chemistry*, 281(15), pp.10143–52.
- Neuzil, J. et al., 2013. Classification of mitocans, anti-cancer drugs acting on mitochondria. *Mitochondrion*, 13(3), pp.199–208.
- Ralph, S.J. et al., 2006. Mitocans: mitochondrial targeted anti-cancer drugs as improved therapies and related patent documents. *Recent patents on anti-cancer drug discovery*, 1(3), pp.327–46.
- Ravindran, J., Prasad, S. & Aggarwal, B.B., 2009. Curcumin and cancer cells: how many ways can curry kill tumor cells selectively? *The AAPS journal*, 11(3), pp.495–510.
- Siedlakowski, P. et al., 2008. Synergy of Pancratistatin and Tamoxifen on breast cancer cells in inducing apoptosis by targeting mitochondria. *Cancer biology & therapy*, 7(3), pp.376–84.
- Trachootham, D. et al., 2006. Selective killing of oncogenically transformed cells through a ROS-mediated mechanism by beta-phenylethyl isothiocyanate. *Cancer cell*, 10(3), pp.241–52.
- Trachootham, D., Alexandre, J. & Huang, P., 2009. Targeting cancer cells by ROS-mediated mechanisms: a radical therapeutic approach? *Nature reviews. Drug discovery*, 8(7), pp.579–91.
- Vshyvenko, S. et al., 2011. Synthesis of C-1 homologues of pancratistatin and their preliminary biological evaluation. *Bioorganic & medicinal chemistry letters*, 21(16), pp.4750–2.

Appendices

APPENDIX A: Induction of Apoptosis and Autophagy in Human Pancreatic Cancer Cells by a Novel Synthetic C-1 Analogue of 7-deoxypancratistatin

Dennis Ma¹, Phillip Tremblay¹, Kevinjeet Mahngar¹, Pardis Akbari-Asl¹, Jonathan Collins², Tomas Hudlicky², and Siyaram Pandey^{1*}

^{1*}Department of Chemistry and Biochemistry, University of Windsor,
401 Sunset Avenue, Windsor, Ontario N9B 3P4, Canada
Phone: +519-253-3000, ext. 3701
spandey@uwindsor.ca

²Chemistry Department and Centre for Biotechnology, Brock University, 500
Glenridge Avenue, St. Catharines, Ontario L2S 3A1, Canada
thudlicky@brocku.ca

Summary

Pancreatic cancer is amongst the deadliest cancers in the world. It is associated with poor prognosis, is notorious for developing chemoresistance, and very few approved chemotherapeutics are available to treat this disease. The natural compound pancratistatin (PST) has shown to effectively induce cytotoxicity selectively in numerous cancer cell types. However, it is present in only minute quantities in its natural source and many complications have burdened its chemical synthesis. We have overcome these bottlenecks by synthesizing a C-1 acetoxymethyl analogue of 7-deoxypancratistatin, JC-TH-acetate-4 (JCTH-4), which we have shown to have similar selective anti-cancer activity to that of PST. In this report, we show JCTH-4 to be a potent chemotherapeutic against pancreatic cancer cells (BxPC-3, PANC-1). It induced apoptosis selectively in BxPC-3 and PANC-1 cells by targeting the mitochondria; it dissipated mitochondrial membrane potential, caused release of apoptogenic factors, and in isolated mitochondria, increased the generation of reactive oxygen species. Furthermore, JCTH-4 selectively induced autophagy in pancreatic cancer cells while normal human fetal fibroblasts were markedly less sensitive to JCTH-4 insult. Altogether, this study outlines JCTH-4 as a potentially safe and effective chemotherapeutic agent in treating notoriously chemoresistant pancreatic cancer.

Introduction

Type I programmed cell death or apoptosis induction can arise extrinsically, as a result of death receptor ligation at the plasma membrane or intrinsically, as a response to internal cellular stress [1]. Such internal stress, including DNA damage, triggers upregulation of proapoptotic proteins which cause permeabilization of the mitochondrial membrane, dissipation of mitochondrial membrane potential (MMP), and release of apoptogenic factors [2,3]. Once released from the mitochondria, these factors can execute apoptosis directly or indirectly via activation of caspases, a family of cysteine proteases [2,3].

Alternatively, type II programmed cell death, or autophagic cell death, results from the extensive activation of autophagy, a process which normally functions as a pro-survival stress response that allows cells to persist under unfavourable conditions [4]. Autophagy can be triggered by various forms of cellular stress such as oxidative stress, dysfunctional organelles, deficiencies in growth factors and nutrients, hypoxia, and pathogens [5]. Upon autophagic induction a membrane sac, a phagophore, engulfs portions of cytoplasm containing proteins and organelles to be degraded [6]. This gives rise to double-membrane vesicles termed autophagosomes which subsequently fuse with lysosomes to yield autolysosomes; previously engulfed contents are then degraded via lysosomal hydrolases [6]. Avoidance of programmed cell death has been implicated in cancer etiology and restoration or selective induction of these pathways may prove to be advantageous strategies in cancer therapy [7,8].

Pancreatic cancer is notoriously one of the most deadly cancers worldwide [9,10]. Most patients are diagnosed at advanced stages of this disease and consequently few live longer than 6 months post diagnosis [11,12]. The standard therapy for pancreatic cancer has been gemcitabine, increasing quality of life and survival time [13]. However, the largest obstacles in combating this malignancy are inherent and developed resistance against chemotherapy [14,15]. Currently, there are only a few other approved chemotherapeutic agents available for treating pancreatic cancer, and thus, it would be invaluable to find and develop novel compounds with greater efficacy and specificity towards these malignancies.

In preceding studies, we have reported the Amaryllidaceae alkaloid pancratistatin (PST) to induce apoptosis selectively in a variety of cancer cell types at low doses and decrease the volume of human tumors *in vivo*; PST is well tolerated in mice and non-cancerous cells are drastically less sensitive to this compound [16-22]. Nevertheless, the availability of this compound has impeded its preclinical and clinical work; PST is present in only minuscule quantities in the *Hymenocallis littoralis* plant and many difficulties have been encountered with its chemical synthesis. To overcome these issues, we have produced 7-deoxypancratistatin derivatives via chemoenzymatic synthesis from bromobenzene and have screened them for similar anti-cancer activity; one C-1 acetoxymethyl analogue, JC-TH-acetate-4 (JCTH-4), was identified to have comparable efficacy and specificity to PST in several cancer cell types [23]. Herein, we report JCTH-4 to be an effective inducer of apoptosis and autophagy

selectively in pancreatic cancer cells. Such activity in pancreatic cancer may be attributed to mitochondrial targeting by JCTH-4; this compound caused the release of apoptogenic factors from the mitochondria, dissipated mitochondrial membrane potential, and in isolated mitochondria, increased the production of reactive oxygen species (ROS). Such cytotoxicity was not observed in normal human fetal fibroblasts (NFF). Thus, these results present JCTH-4 as a potential selective and potent chemotherapeutic against pancreatic cancer.

Materials and Methods

Cell Culture

A pancreatic adenocarcinoma cell line, BxPC-3 (American Type Culture Collection, Cat. No. CRL-1687, Manassas, VA, USA), was cultured in RPMI-1640 medium (Sigma-Aldrich Canada, Mississauga, ON, Canada) supplemented with 10% (v/v) fetal bovine serum (FBS) standard (Thermo Scientific, Waltham, MA, USA) and 10 mg/mL gentamicin (Gibco BRL, VWR, Mississauga, ON, Canada). A pancreatic epithelioid carcinoma cell line, PANC-1 (American Type Culture Collection, Cat. No. CRL-1469, Manassas, VA, USA), was cultured in Dulbecco's Modified Eagle's Medium (Sigma-Aldrich Canada, Mississauga, ON, Canada) supplemented with 10% (v/v) FBS standard (Thermo Scientific, Waltham, MA, USA) and 10 mg/mL gentamicin (Gibco BRL, VWR, Mississauga, ON, Canada). Apparently normal human fetal fibroblast (NFF) cells (Coriell Institute for Medical Research, Cat. No. AG04431B, Camden, NJ, USA) were grown in Dulbecco's Modified Eagle's Medium, High Glucose (Thermo Scientific, Waltham, MA, USA) supplemented with 15% (v/v) FBS standard (Thermo Scientific, Waltham, MA, USA) and 10 mg/mL gentamicin (Gibco BRL, VWR, Mississauga, ON, Canada). All cells were maintained at 37° C and 5 % CO₂.

Cell Treatment

In this study, cells were cultured to 60–70 % confluence and subsequently treated with tamoxifen (TAM) citrate salt (Sigma-Aldrich Canada, Cat. No. T9262, Mississauga, ON, Canada), the broad spectrum caspase inhibitor Z-VAD-FMK (EMD Chemicals, Gibbstown, NJ, USA), and JC-TH-acetate-4 (JCTH-4) at the indicated concentrations and durations. As previously described, JCTH-4 was created by chemoenzymatic synthesis from bromobenzene [23]. Compounds were dissolved in dimethylsulfoxide (Me₂SO).

Nuclear Staining

Following treatment and incubation with the aforementioned drugs, cells were incubated with 10 µM Hoechst 33342 dye (Molecular Probes, Eugene, OR, USA) for 5 minutes to visualize the nuclei. Images were acquired at 400x magnification on a Leica DM IRB inverted fluorescence microscope (Wetzlar, Germany).

Annexin V Binding Assay

The Annexin V binding assay was carried out to validate apoptosis. After drug treatment, cells were washed with phosphate buffer saline (PBS) twice, resuspended in Annexin V binding buffer (10 mM HEPES, 10 mM NaOH, 140 mM NaCl, 1 mM CaCl₂, pH 7.6), and incubated with Annexin V AlexaFluor-488 (1:50) (Sigma-Aldrich Canada, Mississauga, ON, Canada) for 15 minutes.

Fluorescent micrographs were acquired at 400x magnification on a Leica DM IRB inverted fluorescence microscope (Wetzlar, Germany).

WST-1 Assay for Cell Viability

The WST-1 based colorimetric assay was carried out as per the manufacturer's protocol (Roche Applied Science, Indianapolis, IN, USA) to quantify cell viability as a function of active cell metabolism. Clear bottom 96-well tissue culture plates were seeded with approximately 4.0×10^3 BxPC-3 cells/well, 6.0×10^3 PANC-1 cells/well, or 5.0×10^3 NFF cells/well and subsequently, cells were treated with JCTH-4 and Z-VAD-FMK at the indicated doses and durations. After treatment, the WST-1 reagent, which is converted to formazan by cellular enzymes, was administered into each well and incubated for 4 hours at 37° C. Absorbance readings were taken at 450 nm on a Wallac Victor³™ 1420 Multilabel Counter (PerkinElmer, Woodbridge, ON, Canada) to quantify the formazan product. Absorbance readings were expressed as percentages of the solvent control groups.

Tetramethylrhodamine Methyl Ester (TMRM) Staining

To detect MMP, tetramethylrhodamine methyl ester (TMRM) (Gibco BRL, VWR, Mississauga, ON, Canada) was used. Cells were grown on coverslips and treated with JCTH-4 at the indicated concentrations and for the indicated durations. After treatment, cells were incubated with 200 nM TMRM for 45 minutes at 37° C. Fluorescent micrographs were taken at 400x magnification on a Leica DM IRB inverted fluorescence microscope (Wetzlar, Germany).

Mitochondrial Isolation

Mitochondria were isolated from untreated BxPC-3 cells. BxPC-3 cells were washed two times in cold PBS, resuspended in hypotonic buffer (1 mM EDTA, 5 mM Tris-HCl, 210 mM mannitol, 70 mM sucrose, 10 μ M Leu-pep, 10 μ M Pep-A, and 100 μ M PMSF), homogenized, and centrifuged at 600 x g for 5 minutes at 4° C. The supernatant was centrifuged at 15,000 x g for 15 minutes at 4° C. The resulting cytosolic supernatant was discarded and the mitochondrial pellet was resuspended in cold reaction buffer (2.5 mM malate, 10 mM succinate, 10 μ M Leu-pep, 10 μ M Pep-A, and 100 μ M PMSF in PBS).

Amplex Red Assay

ROS production was measured with Amplex Red (Molecular Probes, Eugene, OR, USA). Isolated mitochondria suspended in cold reaction buffer were loaded into wells of an opaque 96-well plate (20 μ g of protein/well) with the indicated concentrations of drugs. Paraquat (PQ) (Sigma-Aldrich Canada, Mississauga, ON, Canada) was used as a positive control at 250 μ M. Amplex Red reagent was added to each well at a final concentration of 50 μ M and horseradish peroxidase (HRP) (Sigma-Aldrich Canada, Mississauga, ON, Canada) was added in the ratio of 6 U/200 μ L. Fluorescence readings were taken after 2 hours of incubation at Ex. 560 nm and Em. 590 nm on a spectrofluorometer (SpectraMax Gemini XS, Molecular Devices, Sunnyvale, CA, USA). Fluorescence readings were expressed as relative fluorescence units (RFU).

Cellular Lysate Preparation

After 72 hours of treatment with the indicated concentrations of JCTH-4 and TAM, cells were manually homogenized in cold hypotonic buffer (10 mM Tris HCl at pH 7.2, 5 mM KCl, 1 mM MgCl₂, 1 mM EGTA, 1% Triton-X-100; 10 μM Leu-pep, 10 μM Pep-A, and 100 μM PMSF). Cell lysates were stored at -20° C until use.

Western Blot Analyses

Protein samples were subjected to SDS-PAGE and transferred to a nitrocellulose membrane. Membranes were blocked with a 5% w/v milk TBST (Tris-Buffered Saline with Tween-20) solution for 1 hour and probed overnight at 4° C with either: an anti-LC3 antibody raised in rabbits (1:500) (Novus Biologicals, Cat. No. NB100-2220, Littleton, CO, USA), an anti-β-Actin antibody raised in mice (1:1000) (Santa Cruz Biotechnology, Inc., Cat. No. sc-81178, Paso Robles, CA, USA), an anti-cytochrome C (Cyto C) antibody raised in mice (1:1000) (Abcam, Cat. No. ab13575, Cambridge, MA, USA), an anti-apoptosis inducing factor (AIF) antibody raised in rabbits (1:1000) (Abcam, Cat. No. ab1998, Cambridge, MA, USA), an anti-endonuclease G (EndoG) antibody raised in rabbits (1:1000) (Abcam, Cat. No. ab9647, Cambridge, MA, USA), or an anti-succinate dehydrogenase subunit A (SDHA) antibody raised in mice (1:1000) (Santa Cruz Biotechnology, Cat. No. sc-59687, Paso Robles, CA, USA). Membranes were subjected to one 15 minute and two 5 minute washes in TBST

and were incubated with an anti-mouse (1:2000) (Abcam, Cat. No. ab6278, Cambridge, MA, USA) or an anti-rabbit (1:2000) (Abcam, Cat. No. ab6802, Cambridge, MA, USA) horseradish peroxidase-conjugated secondary antibody for 1 hour at 25° C. Membranes were washed three times for 5 minutes in TBST. Enhanced chemiluminescence reagent (Sigma-Aldrich Canada, CPS160, Mississauga, ON, Canada) was used to visualize the bands. ImageJ software was used to perform densitometry analyses.

Monodansylcadaverine (MDC) Staining

Monodansylcadaverine (MDC) (Sigma-Aldrich Canada, Mississauga, ON, Canada) was used to visualize autophagic vacuoles. Cells were grown on coverslips and treated with the indicated concentrations of drugs and durations. Subsequent to drug treatment, cells were incubated with 0.1 mM MDC for 15 minutes. Micrographs were acquired at 400x magnification on a Leica DM IRB inverted fluorescence microscope (Wetzlar, Germany).

Propidium Iodide (PI) Staining

Cell lysis was observed using Propidium iodide (PI) dye (Sigma-Aldrich Canada, Mississauga, ON, Canada). For 10 minutes, cells were incubated with PI at a concentration of 1 µg/mL. Subsequently, micrographs were acquired with a Leica DM IRB inverted fluorescence microscope (Wetzlar, Germany) at 400x magnification.

Results

JCTH-4 Selectively Induces Cytotoxicity in Pancreatic Carcinoma Cells in a Time & Dose-Dependent Manner

To circumvent the issues surrounding the low availability of PST (**Figure 1A**), a potent and selective inducer of cytotoxicity in numerous cancer cell types, synthetic analogues of PST were synthesized and evaluated for similar activity in BxPC-3 and PANC-1 pancreatic cancer cell lines. Using the WST-1 colorimetric assay for cell viability, it was found that JCTH-4 (**Figure 1B**), a C-1 acetoxymethyl analogue of 7-deoxypancratistatin, was able to effectively induce cytotoxicity in BxPC-3 and PANC-1 cells in a time and dose dependent manner (**Figure 2A & B**). After 96 hours, JCTH-4 had an approximate half-maximal inhibitory concentration (IC_{50}) value of 0.25 μ M in BxPC-3 cells and 0.5 μ M in PANC-1 cells. Notably, NFF cells were markedly less sensitive to JCTH-4 insult (**Figure 2C**).

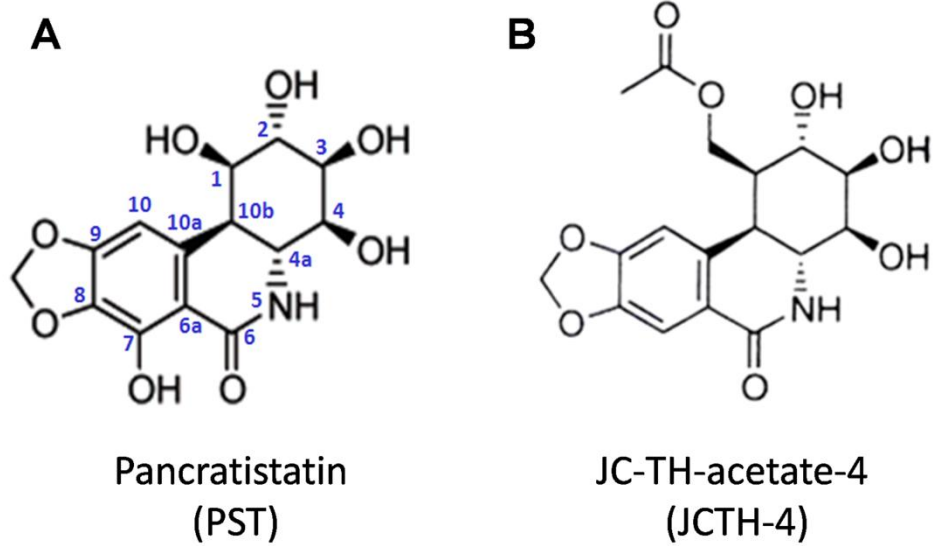


Figure 1: Comparison of Chemical Structures. The structures of **(A)** Pancratistatin (PST) and **(B)** JC-TH-acetate-4 (JCTH-4).

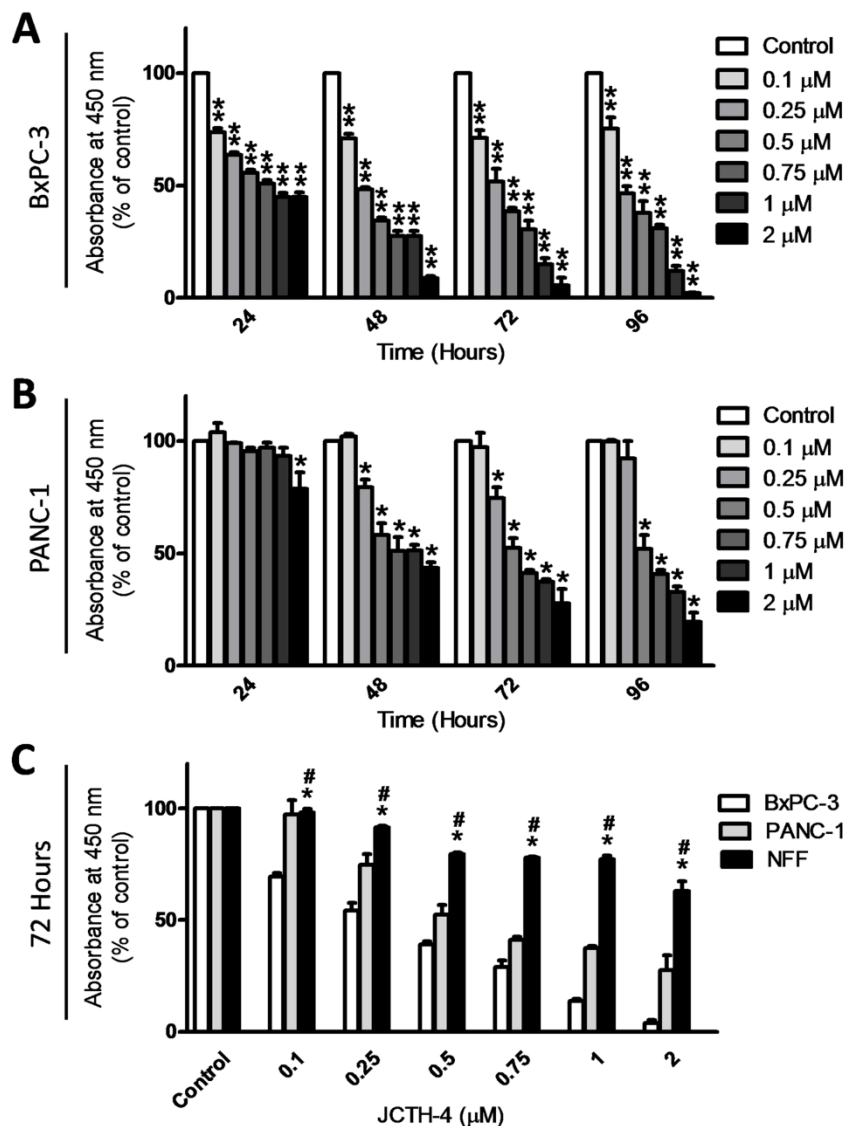


Figure 2: JCTH-4 Selectively Induces Cytotoxicity in Pancreatic Carcinoma Cells in a Time & Dose-Dependent Manner. Effect of JCTH-4 on cellular viability of cells was determined by the WST-1 colorimetric assay. **(A)** BxPC-3 and **(B)** PANC-1 cells were treated with JCTH-4 at the indicated concentrations and times. The WST-1 reagent was used to quantify cell viability. Absorbance was read at 450 nm and expressed as a percent of the solvent control (Me_2SO). Values are expressed as mean \pm SD from quadruplicates of 3 independent experiments. * p <0.05, ** p <0.01 versus solvent control (Me_2SO). **(C)** Viability of NFF cells treated with JCTH-4 at the indicated concentrations compared to BxPC-3 and PANC-1 cells after 72 hours was determined by the WST-1 colorimetric assay. The WST-1 reagent was used to quantify viability. Absorbance was read at 450 nm and expressed as a percent of the solvent control (Me_2SO). Values are expressed as mean \pm SD from quadruplicates of 3 independent experiments. * p <0.01 versus BxPC-3 cells, # p <0.05 versus PANC-1 cells.

JCTH-4 Selectively Induces Apoptosis in Pancreatic Carcinoma Cells

Apoptotic morphology was observed in pancreatic cancer cells treated with JCTH-4 as seen with Hoechst nuclear staining and phase microscopy; cell shrinkage, blebbing, brightly stained and condensed nuclei, and apoptotic bodies were produced by JCTH-4 in BxPC-3 cells at 0.5 μ M and 1 μ M and in PANC-1 cells at 1 μ M and 2 μ M (**Figure 3A and B**). Such morphology was absent in NFF cells treated with JCTH-4 (**Figure 3C**). Selective induction of apoptosis in pancreatic cancer cells was confirmed with the binding of Annexin V to exposed phosphatidylserine, a biochemical marker of apoptosis, as indicated by the green fluorescence (**Figure 3D-F**). These results illustrate JCTH-4 to be a potent and selective agent against BxPC-3 and PANC-1 cells via induction of apoptotic cell death.

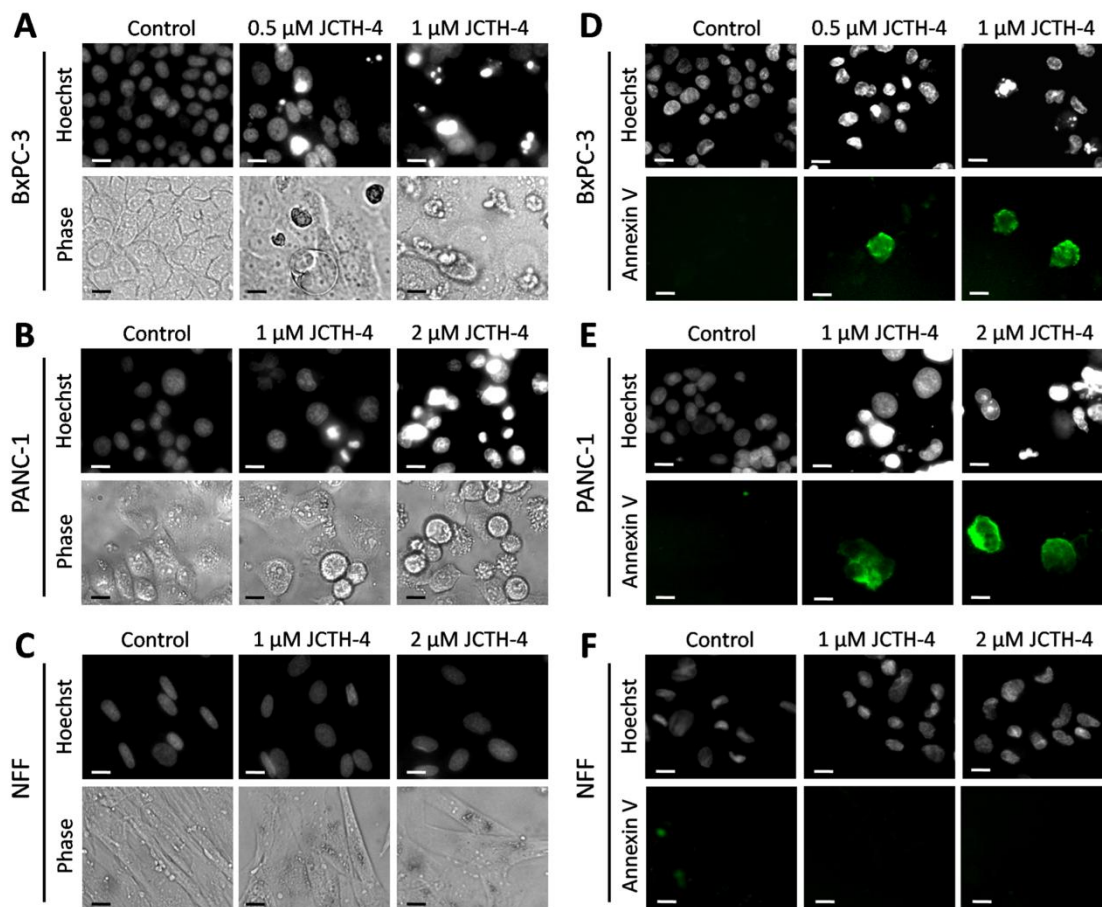


Figure 3: JCTH-4 Selectively Induces Apoptosis in Pancreatic Carcinoma Cells. Nuclear morphology of (A) BxPC-3, (B) PANC-1 and (C) NFF cells after 72 hours of treatment. Cells were treated with JCTH-4 at the indicated concentrations and solvent control (Me₂SO). Afterwards, the cells were stained with Hoechst 33342 dye. Images were taken at 400x magnification on a fluorescent microscope. The accompanying phase images are shown below the Hoechst images. Apoptosis is evident in cells with bright and condensed nuclei accompanied by apoptotic bodies. Annexin V binding to externalized phosphatidylserine, a marker for apoptosis, was monitored in (D) BxPC-3, (E) PANC-1, and (F) NFF cells. Cells were treated with the indicated concentrations of JCTH-4 and solvent control (Me₂SO) for 72 hours. Green fluorescence is indicative of Annexin V binding to phosphatidylserine. Cells were also stained with Hoechst 33342 dye. Images were taken at 400x magnification on a fluorescent microscope. Scale bar = 15 μm.

JCTH-4 Selectively Induces Apoptosis by Targeting Mitochondria in Pancreatic Carcinoma Cells

In previous reports, we have attributed the apoptosis-inducing capabilities of PST to mitochondrial targeting [17-22]. To substantiate such targeting by JCTH-4, mitochondria in pancreatic cancer cells were monitored following JCTH-4 insult. Following 72 hours of treatment with JCTH-4, cells were evaluated for MMP dissipation, an indicator of mitochondrial membrane permeabilization, with TMRM dye. Loss of MMP, illustrated by the decrease of red TMRM fluorescence, was observed in BxPC-3 and PANC-1 cells but not in NFF cells with the indicated concentrations of JCTH-4 (**Figure 4A-C**).

Subsequent to mitochondrial membrane permeabilization, various apoptogenic factors are released from the mitochondria into the cytosol which can then directly or indirectly execute apoptosis [2]. To verify whether or not JCTH-4 is able to cause release of these factors, pancreatic cancer cells were treated with 1 μ M JCTH-4 for 72 hours. Following treatment, cells were lysed and centrifuged to produce cytosolic and mitochondrial fractions that were analyzed for the release or retention of apoptogenic factors respectively with JCTH-4 insult. Indeed, JCTH-4 caused the release of the apoptogenic factors AIF and Cyto c from mitochondria of BxPC-3 cells and a decreased retention of the apoptogenic factor EndoG in PANC-1 mitochondria (**Figure 4D-F**). Complementary to these findings, isolated mitochondria from BxPC-3 cells were treated directly with 1 μ M JCTH-4 for 2 hours, and exhibited an increase in ROS production, an indicator of mitochondrial dysfunction (**Figure 4G**). PQ was used

as a positive control as it is known to induce ROS generation in mitochondria [24]. Collectively, these findings clearly demonstrate the mitochondria to be the target of JCTH-4.

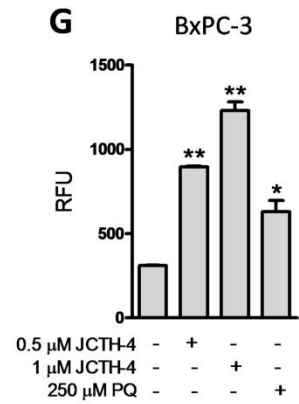
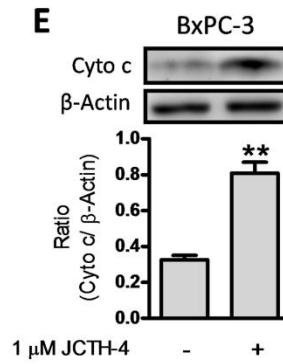
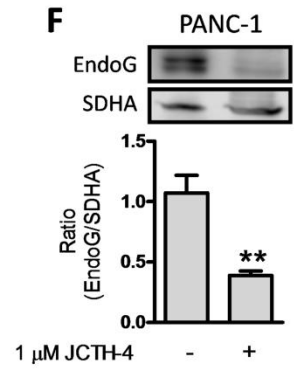
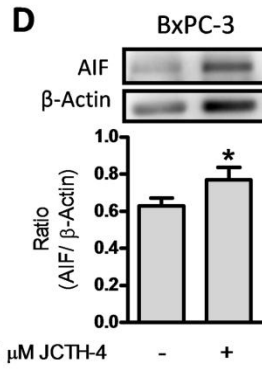
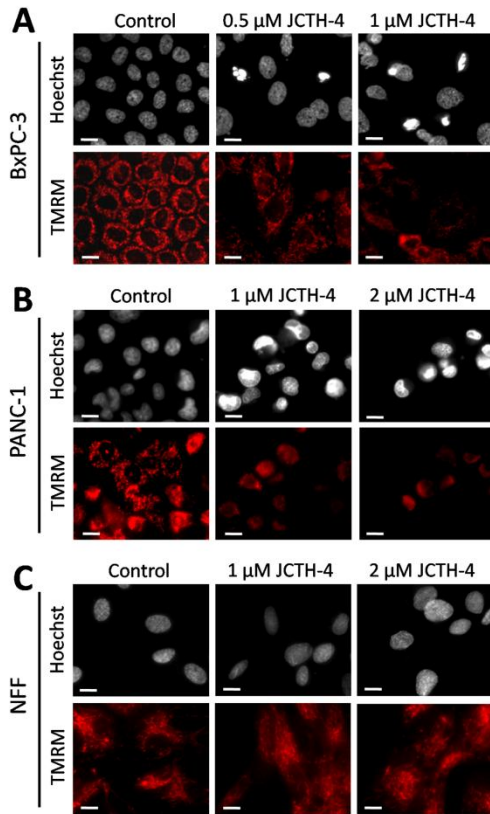


Figure 4: JCTH-4 Selectively Induces Apoptosis by Targeting Mitochondria in Pancreatic Carcinoma Cells. (A) BxPC-3, (B) PANC-1 and (C) NFF cells were treated with the indicated concentrations of JCTH-4 and solvent control (Me₂SO) for 72 hours and stained with TMRM and Hoechst dye. Red fluorescent punctuate marks are indicative of mitochondria with intact MMP. Images were taken at 400x magnification on a fluorescent microscope. Scale bar = 15 μm. Cytosolic fractions, separated from mitochondria by centrifugation, of BxPC-3 cells treated with JCTH-4 or solvent control (Me₂SO) for 72 hours were monitored for (D) AIF and (E) Cyto c release from mitochondria by western blot analysis; β-Actin was probed as a loading control. Mitochondrial fractions, produced by centrifugation, of PANC-1 cells treated with JCTH-4 or solvent control (Me₂SO) for 72 hours were monitored for the retention of (F) EndoG in the mitochondria by western blot analysis; SDHA was probed as a loading control. Densitometric analyses were performed using ImageJ software and statistics were calculated using GraphPad Prism version 5.0. Values are expressed as mean ± SD. **p*<0.05, ***p*<0.01 versus solvent control (Me₂SO). (G) Isolated mitochondria of BxPC-3 cells were treated directly with JCTH-4 and solvent control (Me₂SO). ROS was measured with Amplex Red substrate in the presence of horseradish peroxidase (HRP). Paraquat (PQ) was used as positive control. Fluorescence readings were taken after 2 hours of incubation at Ex. 560 nm and Em. 590 nm and were expressed as relative fluorescence units (RFU). Statistics were performed using GraphPad Prism version 5.0. Image is representative of 3 independent experiments demonstrating similar trends. Values are expressed as mean ± SD of quadruplicates of 1 independent experiment. **p*<0.05, ***p*<0.001 versus solvent control (Me₂SO).

Activity of JCTH-4 is Independent of Caspase Activation

Upon their expulsion from the mitochondria, apoptogenic factors can execute apoptosis directly or indirectly; factors such as AIF and EndoG are able to translocate to the nucleus to execute apoptosis directly while Cyto c activates a caspase signalling cascade to achieve apoptosis [2,25,26,3]. To assess the involvement of caspases in JCTH-4-induced apoptosis, the broad spectrum caspase inhibitor Z-VAD-FMK was used in conjunction with 1 μ M JCTH-4 on BxPC-3 cells for 72 hours. As seen using the WST-1 colorimetric assay for cell viability, the inhibitor was unable to protect the BxPC-3 cells from JCTH-4, demonstrating a caspase-independent mode of action (**Figure 5**).

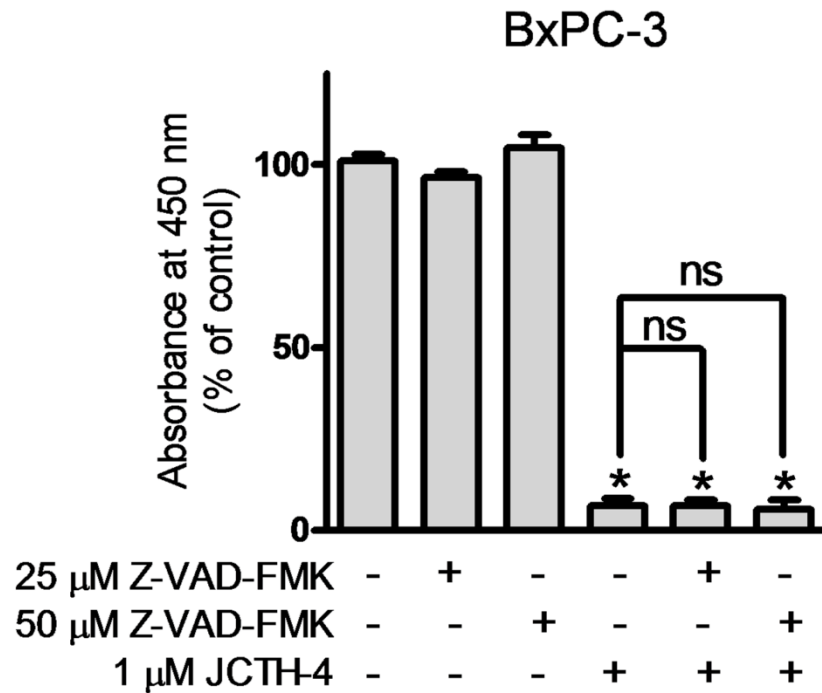


Figure 5: Activity of JCTH-4 is Independent of Caspase Activation. Effect of broad spectrum caspase inhibition on JCTH-4-induced cytotoxicity in pancreatic cancer cells. BxPC-3 cells were treated with Z-VAD-FMK, a broad spectrum caspase inhibitor, at the indicated concentrations with and without the presence of 1 μ M JCTH-4 treatment for 72 hours and the WST-1 reagent was used to quantify cell viability. Absorbance was read at 450 nm and expressed as a percent of solvent control (Me₂SO). Values are expressed as mean \pm SD from quadruplicates of 3 independent experiments. * p <0.001 versus solvent control (Me₂SO); ns = not significant.

Selective Autophagic Induction Occurs in Pancreatic Carcinoma Cells Treated with JCTH-4

Both pro-death and pro-survival autophagic responses have been implicated following chemotherapeutic insult [4]. As JCTH-4 causes oxidative stress in pancreatic cancer cells, a known inducer of autophagy, we monitored pancreatic cancer cells for autophagic induction. PANC-1 cells were treated with TAM, a known inducer of autophagy as a positive control, and JCTH-4 at 1 and 2 μ M for 72 hours and stained with MDC, an indicator of autophagosomes. Bright blue punctate MDC staining was present in cells treated with JCTH-4, comparable to the TAM treated cells (**Figure 6A**). PANC-1 cells were also stained with PI, but none of the aforementioned treatments yielded positive PI staining (**Figure 6A**). Interestingly, JCTH-4 did not induce autophagy in NFF cells as seen with MDC staining (**Figure 6B**).

The conversion of microtubule-associated protein1 light chain 3 (LC3) localized in the cytosol as LC3-I, to LC3-II which is recruited to autophagosomal membranes occurs with the induction of autophagy [27]. To validate autophagic induction by JCTH-4 in PANC-1 cells, western blot analyses were performed on cell lysates of PANC-1 cells treated with 1 μ M JCTH-4 for 72 hours to analyze the conversion of LC3-I to LC3-II; this conversion was observed with JCTH-4 treatment and produced at greater autophagic response than the TAM treated cells used as a positive control (**Figure 6C**). Thus, JCTH-4 is capable of selectively inducing apoptosis in pancreatic cancer cells.

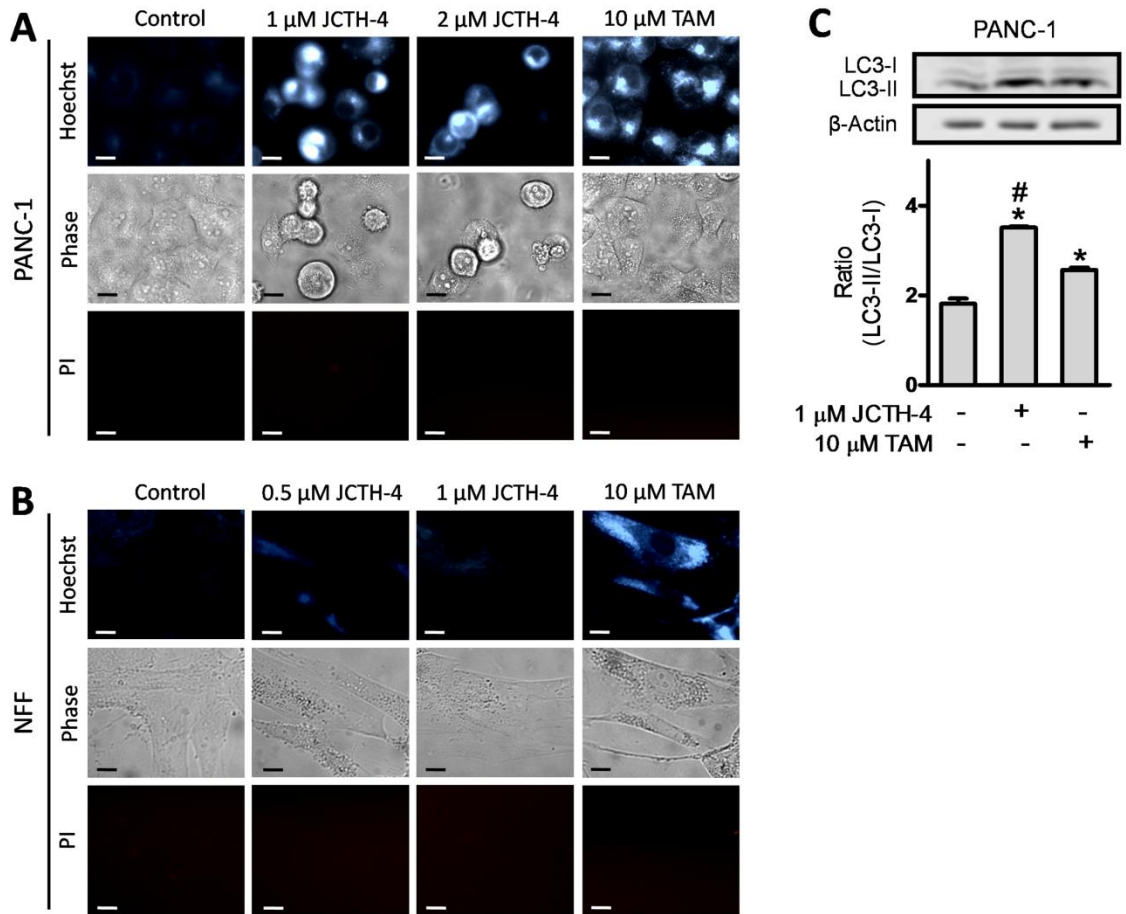


Figure 6: Selective Autophagic Induction Occurs in Pancreatic Carcinoma Cells Treated with JCTH-4. (A) PANC-1 and (B) NFF cells were stained with MDC after treatment with JCTH-4, TAM, or solvent control (Me_2SO) at the indicated concentrations for 72 hours. Bright blue MDC punctate marks are indicative of autophagic vacuoles. Accompanying phase and propidium iodide-stained images are shown below the MDC images. Scale bar = 15 μm . (C) Western Blot analysis were performed on lysates of PANC-1 cells treated with JCTH-4, TAM, and solvent control (Me_2SO) at the indicated concentrations for 72 hours to monitor the conversion of LC3-I to LC3-II, a marker of autophagy. β -actin was probed as a loading control. Densitometric analyses were done using ImageJ software and statistics were calculated using GraphPad Prism version 5.0. Values are expressed as mean \pm SD. * $p < 0.01$ versus solvent control (Me_2SO); # $p < 0.01$ versus 10 μM TAM.

Discussion

Currently, pancreatic cancer stands as one of the most fatal malignancies in the world [9,10]. As this disease lacks distinct and evident symptoms, it is difficult to diagnose in its early stages. Thus, pancreatic cancer is often found in its advanced stages with most patients showing metastases to the liver, lungs, or proximal lymph nodes at the time of diagnosis [11,12]. Very few anti-cancer drugs are available for the treatment of this disease as most standard chemotherapeutics have been shown to be ineffective; doxorubicin, 5-5-fluorouracil, and cisplatin have been shown to be ineffective both *in vitro* and *in vivo* [28]. The nucleoside analogue gemcitabine has been shown to be moderately effective and currently serves as the standard chemotherapeutic treatment for pancreatic cancer [29]. Despite various efforts to enhance the effectiveness of this drug with other chemotherapeutics such as erlotinib, gemcitabine still remains only moderately potent against pancreatic cancer and is often rendered ineffective with the onset of chemoresistance [30,29]. Consequently, the necessity for a more potent treatment presently remains unfulfilled.

In this study, we report the activity of a synthetic analogue of PST, JCTH-4, against human pancreatic cancer cells. JCTH-4 was able to effectively induce cytotoxicity in the BxPC-3 and PANC-1 pancreatic cancer cells by way of apoptotic induction in a selective manner. Necrotic cell death, characterized by lysis of the plasma membrane, by JCTH-4 was ruled out as cells subjected to JCTH-4 were negative for PI staining, a DNA stain impermeable to the plasma

membrane (**Figure 6A**) [31]. Most importantly, we report JCTH-4 to be more effective against BxPC-3 and PANC-1 cells than gemcitabine by comparison to other studies also utilizing colorimetric tetrazolium salt-based assays for cell viability [29]. Although gemcitabine has been previously shown to be effective in BxPC-3 cells at submicromolar concentrations, other studies have shown the effectiveness of this drug to quickly plateau as the dose is increased [29]. Consequently, such reports show only a decrease in cell viability to a range between 30% and 40% of the control after 72 hours of treatment with 1 μ M gemcitabine in BxPC-3 cells [29]. However, we show 1 μ M JCTH-4 to be more potent after 72 hours in BxPC-3 cells, decreasing cell viability to approximately 13% of the control (**Figure 2A**). Furthermore, other work has shown minimal sensitivity to gemcitabine by PANC-1 cells; gemcitabine was reported to have an IC_{50} value of 25 μ M after 72 hours of treatment [29]. In contrast, JCTH-4 was more effective in inducing cytotoxicity in PANC-1 cells and had an IC_{50} value of 0.5 μ M after 72 hours (**Figure 2B**). Similar to PST, JCTH-4 is selective against cancer cells, showing minimal toxicity in normal human fibroblasts, non-cancerous peripheral blood mononuclear cells, and NFF cells; NFF cells proved to be markedly less sensitive to JCTH-4 compared to both BxPC-3 and PANC-1 cells (**Figure 2C**), did not exhibit any observable signs of apoptotic induction (**Figure 3F**), and were not affected in terms of their dividing capacity after removal of JCTH-4 (Data not shown) [23]. On the contrary, other chemotherapeutics currently available such as Taxol and VP-16 have been shown to produce cytotoxicity in normal human fibroblasts at their effective doses

[17]. Thus, these findings illustrate JCTH-4 to be a potentially more effective chemotherapeutic alternative to current cancer therapies.

Previously, we have shown the natural compound PST to be a potent and selective anti-cancer agent; PST was able to induce apoptosis in numerous cancer cell types with minimal cytotoxicity in non-cancerous cells [16-20]. Furthermore, PST was able to decrease the volume of human tumor xenografts *in vivo* and was non-toxic to mice [21,22]. PST however, is only present in parts per million quantities in the buds of the *Hymenocallis littoralis* plant and many difficulties have burdened its chemical synthesis. In an attempt to circumvent these issues, we subsequently synthesized various analogues of PST and found similar anti-cancer activity with JCTH-4 in human neuroblastoma and leukemia cell lines, with no evident toxicity to various non-cancerous cell types [23]. The findings presented in this study demonstrate JCTH-4 to also be a potent agent against BxPC-3 and PANC-1 cells, two different cell lines of a very aggressive and deadly cancer. Thus, previous limitations hindering the preclinical and clinical work with PST have been surpassed.

As with PST, our results indicate the mechanistic target of JCTH-4 is likely to be the mitochondria; JCTH-4 was shown to dissipate MMP (**Figure 4A & B**), cause the release of apoptogenic factors from the mitochondria (**Figure 4D & E**), and in isolated mitochondria, increase ROS production (**Figure 4G**). Such mitochondrial targeting was not evident in NFF cells (**Figure 4C**), complementing previous work with PST; mitochondrial ROS production selectively increased in isolated mitochondria of cancer cells but not in normal human fibroblast

mitochondria with PST treatment [17]. In response to various forms of cellular stress, the tumor suppressor p53 transcriptionally activates various proapoptotic proteins that can give rise to mitochondrial membrane permeabilization [32]. Although moderately differing in sensitivities, both BxPC-3 and PANC-1, two different p53-mutated pancreatic cancer cell lines, were responsive to JCTH-4 [33,34]. Thus, signalling of p53 and its transcriptional targets, all of which are cellular events upstream of mitochondrial permeabilization, play an insignificant role in JCTH-4-induced apoptosis, supporting the notion of a direct mitochondrial target by JCTH-4. The caspase-independent nature of JCTH-4-induced apoptosis (**Figure 5**) further supports mitochondrial targeting by JCTH-4 as caspase signalling can occur upstream of the mitochondria to permeabilize it. Although caspases are required for the execution apoptosis through Cyto c, JCTH-4 may yield apoptosis through the release of other apoptogenic factors such as AIF and EndoG which can directly execute apoptosis in a caspase-independent manner [2,25,26,3].

Various differences exist between normal and cancer cell mitochondria which may serve as the basis by which JCTH-4 targets cancer cells specifically. The Warburg effect, a phenomenon in which cancer cells rely heavily on glycolysis for ATP generation, is postulated to be a result of mitochondrial dysfunction [35]. It is therefore possible for JCTH-4 to target these differences in metabolism. Moreover, an acidic cytosolic environment is created as result these alterations in metabolic activity which in part contributes to elevated MMP in cancer cell mitochondria. Heightened MMP in cancer cell mitochondria has been

linked to an increased capacity to evade apoptosis, invade neighbouring tissue, and promote angiogenesis [36]. It is this elevation in MMP however, that may be exploited by JCTH-4 for cancer selectivity. Upon entering the cell, JCTH-4 may acquire a positive charge through enzymatic processing which may then be preferentially taken up selectively by cancer cell mitochondria as a result of their increased MMP. Additionally, cancer cells have been reported to overexpress various proteins which act to inhibit mitochondrial outer membrane permeabilization such as antiapoptotic proteins of the Bcl-2 family and hexokinase II [37-39]. All of these proteins could serve as potential targets of JCTH-4.

Cellular stress, such as oxidative stress, can trigger the induction of autophagy. As JCTH-4 was found to increase the production of ROS in isolated mitochondria of pancreatic cancer cells (**Figure 4G**), we monitored PANC-1 for autophagic induction following JCTH-4 insult. Indeed, autophagy was induced selectively in pancreatic cancer cells by JCTH-4 (**Figure 6A-C**). Increased ROS production triggered by JCTH-4-induced mitochondrial dysfunction is most likely responsible for selective autophagic induction in these pancreatic cancer cells, which provides additional evidence of a mitochondrial target by JCTH-4. Nevertheless, these cells ultimately die as a result of mitochondrial membrane permeabilization and the subsequent release of apoptogenic factors.

In summary, the novel analogue of PST, JCTH-4, is effective in inducing apoptosis and autophagy selectively in pancreatic cancer cells by means of mitochondrial targeting. Furthermore, this compound was shown to be very

effective against one of the most aggressive and notoriously chemoresistant malignancies, surpassing its current standard chemotherapeutic agent in efficacy. Thus, the unprecedented activity of this compound presents a potentially safe and effective treatment for pancreatic cancer.

Acknowledgements

This work has been supported by the Knights of Columbus Chapter 9671 (Windsor, Ontario), and a CIHR Frederick Banting and Charles Best Canada Graduate Scholarship awarded to Dennis Ma.

References

1. Hengartner MO. The biochemistry of apoptosis. *Nature* 2000; 407(6805):770-6.
2. Earnshaw WC. Apoptosis. A cellular poison cupboard. *Nature* 1999; 397(6718):387- 389.
3. Degterev A, Boyce M, Yuan J. A decade of caspases. *Oncogene* 2003; 22(53):8543-67.
4. Dalby KN, Tekedereli I, Lopez-Berestein G, Ozpolat B. Targeting the prodeath and prosurvival functions of autophagy as novel therapeutic strategies in cancer. *Autophagy* 2010; 6(3): 322-9. [Epub 2010 Apr 26]
5. Kroemer G, Mariño G, Levine B. Autophagy and the integrated stress response. *Mol Cell*. 2010; 40(2):280-93.
6. Xie Z, Klionsky DJ. Autophagosome formation: core machinery and adaptations. *Nat Cell Biol*. 2007; 9(10):1102-9.
7. Borst P, Rottenberg S. Cancer cell death by programmed necrosis? *Drug Resist Updat*. 2004; 7(6):321-4. [Epub 2005 Jan 11]
8. Liu JJ, Lin M, Yu JY, Liu B, Bao JK. Targeting apoptotic and autophagic pathways for cancer therapeutics. *Cancer Lett*. 2011; 300(2):105-14. [Epub 2010 Oct 30]
9. Eckel F, Schneider G, Schmid RM. Pancreatic cancer: a review of recent advances. *Expert Opin Investig Drugs* 2006; 15:1395-1410.
10. Matsuno S, Egawa S, Fukuyama S, Motoi F, Sunamura M, Isaji S, Imaizumi T, Okada S, Kato H, Suda K, Nakao A, Hiraoka T, Hosotani R, Takeda K. Pancreatic cancer registry in Japan: 20 years of experience. *Pancreas* 2004; 28:219-230.
11. Hruban RH. Pancreatic cancer: from genes to patient care. *J. Gastrointest. Surg*. 2001; 5:583–587.
12. Jemal A, Siegel R, Xu J, Ward E. Cancer statistics, 2010. *CA Cancer J. Clin*. 2010; 60:277–300.
13. Burris HA 3rd, Moore MJ, Andersen J, Green MR, Rothenberg ML, Modiano MR, Cripps MC, Portenoy RK, Storniolo AM, Tarassoff P, Nelson R, Dorr FA,

Stephens CD, Von Hoff DD Improvements in survival and clinical benefit with gemcitabine as first-line therapy for patients with advanced pancreas cancer: a randomized trial. *J Clin Oncol* 1997; 15:2403–2413.

14. Sultana A, Ghaneh P, Cunningham D, Starling N, Neoptolemos JP, Smith CT. Gemcitabine based combination chemotherapy in advanced pancreatic cancer-indirect comparison. *BMC Cancer* 2008; 8:192.

15. Cunningham D, Chau I, Stocken DD, Valle JW, Smith D, Steward W, Harper PG, Dunn J, Tudur-Smith C, West J, Falk S, Crellin A, Adab F, Thompson J, Leonard P, Ostrowski J, Eatock M, Scheithauer W, Herrmann R, Neoptolemos JP. Phase iii randomized comparison of gemcitabine versus gemcitabine plus capecitabine in patients with advanced pancreatic cancer. *J Clin Oncol* 2009; 27(33):5513-5518.

16. Kekre N, Griffin C, McNulty J, Pandey S. Pancreatistatin causes early activation of caspase-3 and the flipping of phosphatidyl serine followed by rapid apoptosis specifically in human lymphoma cells. *Cancer Chemother Pharmacol* 2005; 56(1): 29-38.

17. McLachlan A, Kekre N, McNulty J, Pandey S. Pancreatistatin: a natural anti-cancer compound that targets mitochondria specifically in cancer cells to induce apoptosis. *Apoptosis* 2005; 10(3):619-630.

18. Siedlakowski P, McLachlan-Burgess A, Griffin C, Tirumalai SS, McNulty J, Pandey S. Synergy of Pancreatistatin and Tamoxifen on breast cancer cells in inducing apoptosis by targeting mitochondria. *Cancer Biol Ther* 2007; 7(3):376-384.

19. Chatterjee SJ, McNulty J, Pandey S. Sensitization of human melanoma cells by tamoxifen to apoptosis induction by pancreatistatin, a nongenotoxic natural compound. *Melanoma Res.* 2010 [Epub 2010 Mar 17 ahead of print]

20. Griffin C, Hamm C, McNulty J, Pandey S. Pancreatistatin induces apoptosis in clinical leukemia samples with minimal effect on non-cancerous peripheral blood mononuclear cells. *Cancer Cell Int.* 2010; 10:6.

21. Griffin C, Karnik A, McNulty J, Pandey S. Pancreatistatin selectively targets cancer cell mitochondria and reduces growth of human colon tumor xenografts. *Molecular Cancer Therapeutics* 2011a; 10(1):57-68.

22. Griffin C, McNulty J, Pandey S. Pancreatistatin induces apoptosis and autophagy in metastatic prostate cancer cells. *Int J Oncol.* 2011b; 38(6):1549-56.

23. Collins J, Rinner U, Moser M, Hudlicky T, Ghiviriga I, Romero AE, Kornienko A, Ma D, Griffin C, Pandey S. Chemoenzymatic synthesis of Amaryllidaceae constituents and biological evaluation of their C-1 analogues. The next generation synthesis of 7-deoxypancratistatin and trans-dihydrolycoricidine. *J Org Chem* 2010; 75(9):3069-84.
24. Cochemé HM, Murphy MP. Complex I is the major site of mitochondrial superoxide production by paraquat. *J Biol Chem*. 2008; 283(4):1786-98. [Epub 2007 Nov 26]
25. Susin SA, Lorenzo HK, Zamzami N, Marzo I, Snow BE, Brothers GM, Mangion J, Jacotot E, Costantini P, Loeffler M, Larochette N, Goodlett DR, Aebersold R, Siderovski DP, Penninger JM, Kroemer G. Molecular characterization of mitochondrial apoptosis-inducing factor. *Nature* 1999; 397(6718):441-6.
26. Li LY, Luo X, Wang X. Endonuclease G is an apoptotic DNase when released from mitochondria. *Nature* 2001; 412(6842):95-9.
27. Kabeya Y, Mizushima N, Ueno T, Yamamoto A, Kirisako T, Noda T, Kominami E, Ohsumi Y, Yoshimori T. LC3, a mammalian homologue of yeast Apg8p, is localized in autophagosome membranes after processing. *EMBO J*. 2000; 19(21):5720-8.
28. Schultz RM, Merriman RL, Toth JE, Zimmermann JE, Hertel LW, Andis SL, Dudley DE, Rutherford PG, Tanzer LR, Grindey GB. Evaluation of new anticancer agents against the MIA PaCa-2 and PANC-1 human pancreatic carcinoma xenografts. *Oncol Res*. 1993; 5(6-7):223-8.
29. Giroux V, Malicet C, Barthelet M, Gironella M, Archange C, Dagorn JC, Vasseur S, Iovanna JL. p8 is a new target of gemcitabine in pancreatic cancer cells. *Clin Cancer Res*. 2006; 12(1):235-41.
30. Squadroni M, Fazio N. Chemotherapy in pancreatic adenocarcinoma. *Eur Rev Med Pharmacol Sci*. 2010; 14(4):386-94.
31. Pollack M, Leeuwenburgh C. Apoptosis and Aging: Role of the Mitochondrial. *Journal of Gerontology* 2001; 11:475-482.
32. Zilfou JT, Lowe SW. Tumor suppressive functions of p53. *Cold Spring Harb Perspect Biol*. 2009; 1(5):a001883.
33. Berrozpe G, Schaeffer J, Peinado MA, Real FX, Perucho M. Comparative analysis of mutations in the p53 and K-ras genes in pancreatic cancer. *Int J Cancer* 1994; 58(2):185-91.

34. Butz J, Wickstrom E, Edwards J. Characterization of mutations and loss of heterozygosity of p53 and K-ras2 in pancreatic cancer cell lines by immobilized polymerase chain reaction. *BMC Biotechnol.* 2003; 3:11. [Epub 2003 Jul 23].
35. Warburg O. On the origin of cancer cells. *Science* 1956; 123(3191):309-14.
36. Heerdt BG, Houston MA, Augenlicht LH. Growth properties of colonic tumor cells are a function of the intrinsic mitochondrial membrane potential. *Cancer Res.* 2006; 66(3):1591-6.
37. Green DR, Kroemer G. The pathophysiology of mitochondrial cell death. *Science* 2004; 305(5684):626-9.
38. Casellas P, Galiegue S, Basile AS. Peripheral benzodiazepine receptors and mitochondrial function. *Neurochem Int.* 2002; 40(6):475-86.
39. Mathupala SP, Rempel A, Pedersen PL. Aberrant glycolytic metabolism of cancer cells: a remarkable coordination of genetic, transcriptional, post-translational, and mutational events that lead to a critical role for type II hexokinase. *J Bioenerg Biomembr.* 1997; 29(4):339-43.

Appendices

APPENDIX B: Enhancement of Apoptotic and Autophagic Induction by a Novel Synthetic C-1 Analogue of 7-deoxypancratistatin in Human Breast Adenocarcinoma and Neuroblastoma Cells with Tamoxifen

Dennis Ma¹, Jonathan Collins², Tomas Hudlicky², and Siyaram Pandey^{1*}

^{1*}Department of Chemistry and Biochemistry, University of Windsor,
401 Sunset Avenue, Windsor, Ontario N9B 3P4, Canada
Phone: +519-253-3000, ext. 3701
spandey@uwindsor.ca

²Chemistry Department and Centre for Biotechnology, Brock University, 500
Glenridge Avenue, St. Catharines, Ontario L2S 3A1, Canada
thudlicky@brocku.ca

To view videos, please refer to the publication
at the Journal of Visualized Experiments:

<http://www.jove.com/video/3586/enhancement-apoptotic-autophagic-induction-novel-synthetic-c-1>

Ma et al. 2012. J Vis Exp. 30;(63). pii: 3586. doi: 10.3791/3586

List of Abbreviations

ER	estrogen receptor
FMN	flavin mononucleotide
JCTH-4	JC-TH-acetate-4
LC3	microtubule-associated protein 1 light chain 3
MDC	monodansylcadaverine
MMP	mitochondrial membrane potential
MRC	mitochondrial respiratory chain
NFF	normal human fetal fibroblast
PQ	paraquat
PST	pancratistatin
RFU	relative fluorescence units
ROS	reactive oxygen species
TAM	tamoxifen
TMRM	tetramethylrhodamine methyl ester

Summary

Breast cancer is one of the most common cancers amongst women in North America. Many current anti-cancer treatments, including ionizing radiation, induce apoptosis via DNA damage. Unfortunately, such treatments are unselective and produce similar effects in normal cells. We have reported selective induction of apoptosis in cancer cells by the natural compound pancratistatin (PST). Recently, a novel PST analogue, a C-1 acetoxymethyl derivative of 7-deoxypancratistatin (JCTH-4), was produced by de novo synthesis and exhibits comparable selective apoptosis inducing activity in several cancer cell lines. Recently, autophagy has been implicated in malignancies as both pro-survival and pro-death mechanisms in response to chemotherapy. Tamoxifen (TAM) has invariably demonstrated induction of pro-survival autophagy in numerous cancers. In this study, the efficacy of JCTH-4 alone and in combination with TAM to induce cell death in human breast cancer (MCF7) and neuroblastoma (SH-SY5Y) cells was evaluated. TAM alone induced autophagy, but insignificant cell death whereas JCTH-4 alone caused significant induction of apoptosis with some induction of autophagy. Interestingly, the combinatory treatment yielded a drastic increase in apoptotic and autophagic induction. We monitored time-dependent morphological changes in MCF7 cells undergoing TAM-induced autophagy, JCTH-4-induced apoptosis and autophagy, and accelerated cell death with combinatorial treatment using time-lapse microscopy. We have demonstrated these compounds to induce apoptosis/autophagy by mitochondrial targeting in these cancer cells. Importantly, these treatments did

not affect the survival of noncancerous human fibroblasts. Thus, these results indicate that JCTH-4 in combination with TAM could be used as a safe and very potent anti-cancer therapy against breast cancer and neuroblastoma cells.

Short Abstract

We have synthesized a novel synthetic analogue of pancratistatin with comparable anti-cancer activity; interestingly, combinatory treatment with tamoxifen yielded a drastic enhancement in apoptotic and autophagic induction by mitochondrial targeting with minimal effect on noncancerous fibroblasts. Thus, JCTH-4 in combination with tamoxifen could be used as a safe anti-cancer therapy.

Introduction

Apoptosis, or type I programmed cell death, is a physiological process that can operate extrinsically, via binding of a death ligand to a death receptor, or intrinsically. The intrinsic pathway of apoptosis is initiated by intracellular stress such as DNA damage and mitochondrial dysfunction; this ultimately leads to the permeabilization of the mitochondria, dissipation of mitochondrial membrane potential (MMP), release of apoptogenic factors from the mitochondrial intermembrane space, and subsequent execution of apoptosis¹.

Autophagy is a process in which a cell breaks, degrades, and recycles its own intracellular components while maintaining plasma membrane integrity; it is triggered by different types of cellular stresses including oxidative stress, hypoxia, protein aggregates, nutrient deprivation, growth factor deprivation, and damaged organelles². In the initial stages of this process, cytosolic material is engulfed by autophagosomes, double-membraned vesicles, which fuse to lysosomes to form autolysosomes. Post lysosomal fusion, cytosolic materials previously taken up by autophagosomes are degraded by lysosomal enzymes². Extensive activation of this pathway yields extensive degradation of intracellular components which may lead to autophagic cell death or type II programmed cell death³.

Evasion of cell death has been considered one of the hallmarks of cancer⁴. Cancer is a disease characterized by uncontrolled cell growth and proliferation⁵. In particular, neuroblastoma arises from developing nerve cells of the sympathetic nervous system from the neural crest⁶. It is the most common

solid tumor occurring in young children, accounting for approximately 9% of all childhood cancers⁷. Although much progress has been made to date, this disease remains problematic to both basic scientists and clinicians. On the other hand, breast cancer is the most common cancer amongst females⁸. Tamoxifen (TAM) has been frequently used for therapy in hormone-responsive breast cancers as an estrogen receptor (ER) antagonist⁹. Nonetheless, other reports provide evidence of additional independent mechanisms of apoptosis induction by TAM. In particular, TAM interacts with Complex I of the mitochondrial respiratory chain (MRC) at its flavin mononucleotide (FMN) site¹⁰.

PST is a natural compound isolated from the *Hymenocallis littoralis* plant. Contrasting from many chemotherapeutics currently in use, it has been shown to induce apoptosis, in a non-genotoxic manner, selectively in various cancer cell types via mitochondrial targeting¹¹⁻¹⁵. However, preclinical and clinical work has been hindered by its availability; it is present at very low amounts in its natural source and many complications burden its chemical synthesis. We have synthesized and screened synthetic analogues of 7-deoxypancratistatin and observed similar anti-cancer activity in a C-1 acetoxymethyl derivative, JC-TH-acetate-4 (JCTH-4)¹⁶. We now have in hand a synthetic PST analogue with potent anti-cancer activity. Its synthesis has been standardized and can be scaled up to produce sufficient quantities for preclinical and clinical work. Since natural PST and TAM both target the mitochondria, it would be interesting to investigate the combined effect of a synthetic analogue of PST on human breast cancer and neuroblastoma cells in combination with TAM.

Herein, we report selective cytotoxicity of JCTH-4 in human neuroblastoma (SH-SY5Y) and breast adenocarcinoma (MCF7) cells. JCTH-4 was able to induce apoptosis in both cell lines by mitochondrial targeting; JCTH-4 caused dissipation of MMP and an increase in reactive oxygen species (ROS) production in isolated mitochondria from these cancer cells. Furthermore, autophagy was induced by JCTH-4 in MCF7 cells. Interestingly, the addition of TAM to JCTH-4 insult enhanced the aforementioned effects of JCTH-4 in SH-SY5Y and MCF7 cells. Morphological changes induced by JCTH-4 and TAM alone and in combination in MCF7 cells were monitored via time-lapse microscopy of phase contrast or bright field pictures. Normal human fetal fibroblasts (NFF) exhibited a marked decrease in sensitivity to JCTH-4 both alone and in combination with TAM. Therefore, these observations suggest JCTH-4, alone and in with TAM, to be a safe and effect chemotherapeutic agent against breast cancer and neuroblastoma.

Materials and Methods

1) Cell Culture

1.1) Grow and culture SH-SY5Y human neuroblastoma cells (ATCC, Cat. No. CRL-2266, Manassas, VA, USA) with Dulbecco's Modified Eagles Medium F-12 HAM (Sigma-Aldrich, Mississauga, ON, Canada) supplemented with 2 mM L-glutamine, 10 % fetal bovine serum (FBS) and 10 mg/ml gentamicin (Gibco BRL, VWR, Mississauga, ON, Canada). Maintain cells at 37° C and 5 % CO₂.

1.2) Grow and culture MCF7 human breast adenocarcinoma cells (ATCC, Cat. No. HTB-22, Manassas, VA, USA) in RPMI-1640 medium (Sigma-Aldrich Canada, Mississauga, ON, Canada) supplemented with 10% FBS standard (Thermo Scientific, Waltham, MA) and 10 mg/mL gentamicin (Gibco BRL, VWR, Mississauga, ON, Canada). Maintain cells at 37° C and 5 % CO₂.

1.3) Grow and culture the apparently normal human fetal fibroblast (NFF) cell line (Coriell Institute for Medical Research, Cat. No. AG04431B, Camden, NJ, USA) in Dulbecco's Modified Eagle's Medium, High Glucose (Thermo Scientific, Waltham, MA, USA) supplemented with 15 % FBS and 10 mg/mL gentamicin (Gibco BRL, VWR, Mississauga, ON, Canada). Maintain cells at 37° C and 5 % CO₂.

2) Drug Preparation

2.1) Weigh out tamoxifen (TAM) citrate salt (Sigma-Aldrich, Cat. No. T9262, Mississauga, ON, Canada) and dissolve it in DMSO to prepare a 10 mM stock solution. Store stock solution at -20° C until use. All vehicle controls used in this study contained DMSO at less than 0.5%.

2.2) Repeat step 2.1 to prepare a 1 mM stock solution dissolved in DMSO of JC-TH-acetate-4 (JCTH-4), produced by chemoenzymatic synthesis from bromobenzene as previously described¹⁶. Store stock solution at -20° C until use. All vehicle controls used in this study contained DMSO at less than 0.5%.

3) Time-Lapse Microscopy

3.1) Plate approximately 2.0×10^5 MCF7 cells in 35 mm glass bottom culture dishes (MatTek Corporation, Cat. No. P35G-014-C, Ashland, MA, USA) in sterile conditions of a class II biosafety cabinet and allow them to grow at 37° C and 5 % CO₂.

3.2) When cells reach 60 to 70 % confluence, treat them with 1 μM JCTH-4 using a 1 mM stock solution dissolved in DMSO and 10 μM TAM using a 10 mM stock solution dissolved in DMSO, alone and in combination in a class II biosafety cabinet.

3.3) After treatment of cells for 48 hours, place cells in a heated chamber at 37° C with 5 % CO₂ on a stage of a Leica DMI6000 fluorescent microscope (Leica Microsystems, Wetzlar, Germany).

3.4) Using LAS AF6000 software, set the microscope to take phase contrast or bright field micrographs at 400x magnification every 5 minutes for 18 hours.

4) Nuclear Staining

4.1) Plate approximately 2.0×10^5 MCF7 or SH-SY5Y cells in each well of a 6 well clear bottom tissue culture plate in a class II biosafety cabinet and allow them to grow at 37° C and 5 % CO₂.

4.2) When cells reach 60 to 70 % confluence, treat them with 1 μM JCTH-4 using a 1 mM stock solution dissolved in DMSO and 10 μM TAM using a 10 mM stock solution dissolved in DMSO, both alone and in combination in a class II biosafety cabinet.

4.3) Incubate cells with the aforementioned treatments at 37° C and 5 % CO₂ for 48 hours (SH-SY5Y cells) or 72 hours (MCF7 cells). After treatment and incubation of cells with drugs, directly add Hoechst 33342 dye (Molecular Probes, Eugene, OR, USA) to the media of the treated cells to a final concentration of 10 μM to stain the nuclei.

4.4) Incubate the cells with the Hoechst dye for 5 to 10 minutes protected from light.

4.5) Place the plate on the stage of a Leica DM IRB inverted fluorescence microscope (Leica Microsystems, Wetzlar, Germany).

4.6) Take fluorescent and phase micrographs at 400x magnification.

5) Annexin V Binding Assay

5.1) Plate approximately 5.0×10^5 MCF7, SH-SY5Y, or NFF cells in 10 mL tissue culture plates in a class II biosafety cabinet and allow them to grow at 37° C and 5 % CO₂.

5.2) When cells reach 60 to 70 % confluence, treat them with 1 μM JCTH-4 using a 1 mM stock solution dissolved in DMSO and 10 μM TAM using a 10 mM stock solution dissolved in DMSO, both alone and in combination in a class II biosafety cabinet.

5.3) Incubate cells with the aforementioned treatments at 37° C and 5 % CO₂ for 48 hours (SH-SY5Y cells) or 72 hours (MCF7 and NFF cells).

5.4) Prepare Annexin V binding buffer in ddH₂O with 10 mM HEPES, 10 mM NaOH, 140 mM NaCl, and 1 mM CaCl₂ at pH 7.6 and store at 4° C until use.

5.5) After treatment and incubation of cells with drugs, remove the media from the plates containing suspended cells and place it into a separate 15 mL conical tube for each different treatment group labelled with the proper treatment.

5.6) Detach adherent cells from the plates using trypsin.

5.7) After the cells lifted from the plate as a result of the trypsin, aspirate the media placed in the 15 mL conical tube in step 5.4 and place it back in their original plates with the trypsin suspended cells.

5.8) With the electronic pipette filler and serological pipettes, mix the media with the trypsin cell solution and place this mixture back into the corresponding 15 mL conical tubes.

5.9) Centrifuge the cells at 600 x g for 5 minutes at 4° C, remove the supernatant from each tube, and resuspend cells in PBS.

5.10) Centrifuge the cells at 600 x g for 5 minutes, remove the supernatant from each tube, and resuspend cells in labelled microfuge tubes with about 50 to 70 µL of Annexin V binding buffer.

5.11) Add Annexin V AlexaFluor-488 (1:50) (Sigma-Aldrich, Mississauga, ON, Canada) and Hoechst dye to a final concentration of 10 μ M and incubate for 15 minutes protected from light.

5.12) Following incubation, vortex one of the microfuge tubes, add 7 to 10 μ L of the cell mixture to a microscope slide, place a coverslip overtop of the cell mixture on the microscope slide and take fluorescent micrographs, both Annexin V and Hoechst images for each view, at 400x magnification on a Leica DM IRB inverted fluorescence microscope (Leica Microsystems, Wetzlar, Germany). Repeat for each experimental sample in each of the remaining microfuge tubes.

6) Water Soluble Tetrazolium Salt (WST-1) Assay for Cell Viability

6.1) Trypsinize a confluent T75 flask or 10 cm tissue culture dish of MCF7, SH-SY5Y, or NFF cells in a class II biosafety cabinet.

6.2) After the cells have been lifted, add 5 to 10 mL of media to the trypsin and place the media cell suspension in a 15 mL conical tube.

6.3) Centrifuge the cells at 600 x g for 5 minutes, place the tube back into the biosafety cabinet, remove the supernatant from each tube, and resuspend the cells in about 1 to 3 mL of media depending on the cell pellet size.

6.4) Place 10 μL of the cell suspension in a microfuge tube, add 10 μL of Trypan Blue dye (Sigma-Aldrich, Mississauga, ON, Canada), and mix with a micropipette.

6.5) Load 10 μL of Trypan Blue suspended cells on a haemocytometer (Hausser Scientific, USA), count the cells, and calculate the concentration of cells of the cell suspension in the original 15 mL conical tube.

6.6) Use this concentration to determine the volume of original cell suspension needed to create diluted cell suspensions with concentrations of 1.5×10^5 cells/mL for MCF7 and SH-SY5Y and 5.0×10^4 for NFF cells needed for plating.

6.7) Use the diluted cell suspensions to plate 15×10^3 MCF7 or SH-SY5Y cells/well or 5.0×10^3 NFF cells/well by adding 100 μL of the diluted cell suspensions to each well of a 96 well clear bottom tissue culture plate. Incubate the cells at 37°C and 5 % CO_2 overnight.

6.8) Treat the cells with 1 μM JCTH-4 and 10 μM TAM both alone and in combination in a class II biosafety cabinet for 72 hours for MCF7 and NFF cells, and for 48 hours for SH-SY5Y cells.

6.9) After treatment and incubation of drugs, add 10 μL of WST-1 reagent (Roche Applied Science, Indianapolis, IN, USA) to each well and incubate the plate for 4 hours at 37° C and 5 % CO_2 . Take absorbance readings at 450 nm on a Wallac Victor³™ 1420 Multilabel Counter (PerkinElmer, Woodbridge, ON, Canada) and express them as percentages of the solvent control groups.

7) Tetramethylrhodamine Methyl Ester (TMRM) Staining

7.1) Place a coverslip into each well of a 6 well clear bottom tissue culture plate and plate MCF7 cells in each well of a 6 well tissue culture plate in a class II biosafety cabinet. Allow them to grow at 37° C and 5 % CO_2 .

7.2) When cells reach 60 to 70 % confluence, treat them with 1 μM JCTH-4 using a 1 mM stock solution dissolved in DMSO and 10 μM TAM using a 10 mM stock solution dissolved in DMSO, both alone and in combination in a class II biosafety cabinet.

7.3) Incubate cells with the aforementioned treatments at 37° C and 5 % CO_2 for 72 hours.

7.4) After treatment and incubation of cells with drugs, directly add Hoechst 33342 dye (Molecular Probes, Eugene, OR, USA) to the media of the treated cells to a final concentration of 10 μM to stain the nuclei as well as tetramethylrhodamine methyl ester (TMRM) (Gibco BRL, VWR, Mississauga, ON, Canada) at a final concentration of 200 nM.

7.5) Incubate the cells with the dyes at 5 % CO_2 and 37° C for 45 minutes protected from light.

7.6) Pipette 8 μL of media or PBS onto a microscope slide and take a coverslip from the 6 well plate and place it on top of the media or PBS on the microscope slide with the cells facing downwards with tweezers.

7.7) Take fluorescent micrographs, both Hoechst and TMRM micrographs for each view, with a Leica DM IRB inverted fluorescence microscope (Leica Microsystems, Wetzlar, Germany) at 400x magnification.

8) Mitochondrial Isolation

8.1) Prepare about 10 mL of hypotonic buffer (1 mM EDTA, 5 mM Tris-HCl, 210 mM mannitol, 70 mM sucrose, 10 μM Leu-pep, 10 μM Pep-A, and 100 μM PMSF) and reaction buffer and keep both solutions on ice.

8.2) With about 8 to 10 confluent T75 tissue culture flasks of SH-SY5Y cells, trypsinize the cells, add media to neutralize the trypsin, collect the cell suspensions in 50 mL conical tubes, and centrifuge the tubes at 600 x g for 5 minutes at 4° C.

8.3) Remove the supernatant and resuspend cell pellets in about 10 to 20 mL of cold PBS, centrifuge the tubes at 600 x g for 5 minutes at 4° C, and repeat this wash process once.

8.4) Remove the supernatant and resuspend the cells in cold hypotonic buffer. Homogenize cells manually with a glass tissue grinder and centrifuge the cell lysate at 600 x g for 5 minutes at 4° C.

8.5) Centrifuge the resultant supernatant at 15,000 x g for 15 minutes at 4° C. Remove the cytosolic supernatant and resuspend the mitochondrial pellet in cold reaction buffer.

9) Amplex Red Assay

9.1) After isolating mitochondria from cells, estimate the concentration of protein of the sample of isolated mitochondria using a standard curve of known concentrations of 1mg/mL BSA (Bovine Serum Albumin) with the BioRad protein assay (Bio-Rad Laboratories, Hercules, CA USA).

9.2) Using the estimated concentration of protein of the isolated mitochondria solution, calculate the volume of this solution to give 20 µg of protein. Pipette this volume into each well of an opaque 96-well plate to load 20 µg of protein/well.

9.3) Fill each well in the plate to a total volume of 100 µL with reaction buffer, drug treatment (with a final concentration of 1 µM JCTH-4, and/or 10 µM TAM, or 250 µM PQ (Sigma-Aldrich, Mississauga, ON, Canada) used as a positive control), Amplex Red reagent at a final concentration of 50 µM, and horseradish peroxidase (HRP) (Sigma-Aldrich, Mississauga, ON, Canada) in the ratio of 6 U/200 µL.

9.4) After a 2 hour incubation, take fluorescence readings at Ex. 560 nm and Em. 590 nm on a spectrofluorometer (SpectraMax Gemini XPS, Molecular Devices, Sunnyvale, CA, USA).

10) Cellular Lysate Preparation

10.1) Grow MCF7 cells to 60 to 70 % confluence in 10 cm tissue culture plates.

10.2) Treat cells with 1 µM JCTH-4 and 10 µM TAM alone and in combination for 72 hours with about 10 to 15 plates per treatment group.

10.3) Prepare cell lysis buffer (10 mM Tris HCl at pH 7.2, 5 mM KCl, 1 mM MgCl₂, 1 mM EGTA, 1% Triton-X-100; 10 μM Leu-pep, 10 μM Pep-A, and 100 μM PMSF) and store at 4° C until use.

10.4) Mechanically dislodge cells from the plate surfaces with a cell scraper and collect cells in labelled 50 mL conical tubes.

10.5) Centrifuge the tubes at 600 x g for 5 minutes at 4° C, remove the supernatant and resuspend cell pellets in about 10 to 20 mL of cold PBS, centrifuge the tubes at 600 x g for 5 minutes at 4° C, and repeat this wash process once.

10.6) Remove the supernatant and resuspend the cells in cold cell lysis buffer. Homogenize cells manually with a glass tissue grinder and centrifuge the cell lysate at 600 x g for 5 minutes at 4° C.

10.7) Discard the pellets and store the cell lysates at -20° C until use.

11) Western Blot Analyses

11.1) Determine the protein concentration of cell lysates using the BioRad protein assay (Bio-Rad Laboratories, Hercules, CA USA). Subject the protein samples to SDS-PAGE and transfer protein to a nitrocellulose membrane.

11.2) After transfer, block membranes with a 5% w/v milk TBST (Tris-Buffered Saline Tween-20) solution for 1 hour.

11.3) Probe membranes with an anti-LC3 antibody raised in rabbit (1:500) (Novus Biologicals, Cat. No. NB100-2220, Littleton, CO, USA), or an anti- β -Actin antibody raised in mouse (1:1000) (Santa Cruz Biotechnology, Inc., Cat. No. sc-81178, Paso Robles, CA, USA) overnight at 4° C.

11.4) Subject membranes to one 15 minute and two 5 minute washes in TBST and incubate with an anti-mouse (1:2000) or an anti-rabbit (1:2000) horseradish peroxidase-conjugated secondary antibody (Abcam, Cat. No. ab6728 & ab6802, Cambridge, MA, USA) for 1 hour at at 4° C.

11.5) Subject membranes to three consecutive 5 minute washes in TBST and visualize protein bands with enhanced chemiluminescence reagent (Sigma-Aldrich, CPS160, Mississauga, ON, Canada).

11.6) Performed densitometry analyses using ImageJ software.

12) Monodansylcadaverine (MDC) Staining

12.1) Place a coverslip into each well of a 6 well clear bottom tissue culture plate and plate MCF7 cells in each well of a 6 well clear bottom tissue culture plate in a class II biosafety cabinet. Allow them to grow at 37° C and 5 % CO₂.

12.2) When cells reach 60 to 70 % confluence, treat them with 1 μ M JCTH-4 using a 1 mM stock solution dissolved in DMSO and 10 μ M TAM using a 10 mM stock solution dissolved in DMSO, both alone and in combination in a class II biosafety cabinet.

12.3) Incubate cells with the aforementioned treatments at 37° C and 5 % CO₂ for 72 hours.

12.4) After treatment and incubation of cells with drugs, directly add Monodansylcadaverine (MDC) (Sigma-Aldrich, Mississauga, ON, Canada) to a final concentration of 0.1 mM to each well for 15 min.

12.5) Incubate the cells with the dye at 5 % CO₂ and 37° C for 15 minutes protected from light.

12.6) Pipette 30 μ L of media or PBS onto a microscope slide and take a coverslip from the 6 well plate and place it on top of the media or PBS on the microscope slide with the cells facing downwards with tweezers.

12.7) Take fluorescent MDC and phase micrographs, for each view, with a Leica DM IRB inverted fluorescence microscope (Leica Microsystems, Wetzlar, Germany) at 400x magnification.

Results

Please refer to the *Journal of Visualized Experiments* for videos:

Ma et al. 2012. *J Vis Exp.* 30;(63). pii: 3586. doi: 10.3791/3586

Selective Induction of Apoptosis in Human Breast Adenocarcinoma and Neuroblastoma Cells by JCTH-4: Enhancement of Activity by TAM

Selective induction of apoptosis was shown in various cancer cells by natural PST (**Fig. 1a**)¹¹⁻¹³. Because of the low availability of PST, we have synthesized analogues of 7-deoxypancratistatin (JCTH-4) (**Fig. 1b**) and screened them for similar anti-cancer activity in human breast adenocarcinoma (MCF7) and neuroblastoma cells (SH-SY5Y). In the first phase of experiments, we wanted to monitor morphological changes over time following treatment with JCTH-4 and TAM alone and in combination in MCF7 cells. MCF7 cells were monitored for 18 hours, as seen in **Video 1** produced by time-lapse microscopy with phase contrast pictures, with solvent treatment (control) for 48 hours; these cells exhibited no major changes in morphology. In contrast, after 48 hours of 1 μ M JCTH-4 treatment, these cells exhibited morphological changes associated with apoptosis such as shrinkage, blebbing, apoptotic body formation as seen in **Video 2**. On the other hand, TAM treatment alone in MCF7 cells produced a very distinct morphology including punctate inclusions indicative of autophagosomes associated with autophagy (**Video 3**). Very minimal apoptotic morphology was observed and cells generally exhibited healthy morphology comparable to the solvent control treated MCF7 cells. Interestingly, in the presence of TAM, the apoptotic induction by JCTH-4 was drastically enhanced as indicated by

increased apoptotic morphology in MCF7 cells after 48 hours as illustrated in **Video 4**.

In the second phase of experiments we utilized fluorescent dyes to evaluate the induction of apoptosis. After 72 hours and 48 hours of 1 μ M JCTH-4 treatment in MCF7 and SH-SY5Y cells respectively, Hoechst dye was used and to monitor nuclear morphology. Results indicated condensed, brightly stained nuclei accompanied by apoptotic bodies in MCF7 and SH-SY5Y cells, indicative of apoptotic induction (**Fig. 2a,b**). TAM treatment alone yielded minimal apoptotic nuclear morphology in MCF7 and SH-SY5Y cells; nuclei were large, round, and dimly stained with Hoechst comparable to solvent control group (**Fig. 2a,b**). In agreement with **Video 4**, nuclei of MCF7 and SH-SY5Y cells displayed a marked increase in apoptotic morphology with the combination treatment after 72 hours (**Fig. 2a,b**).

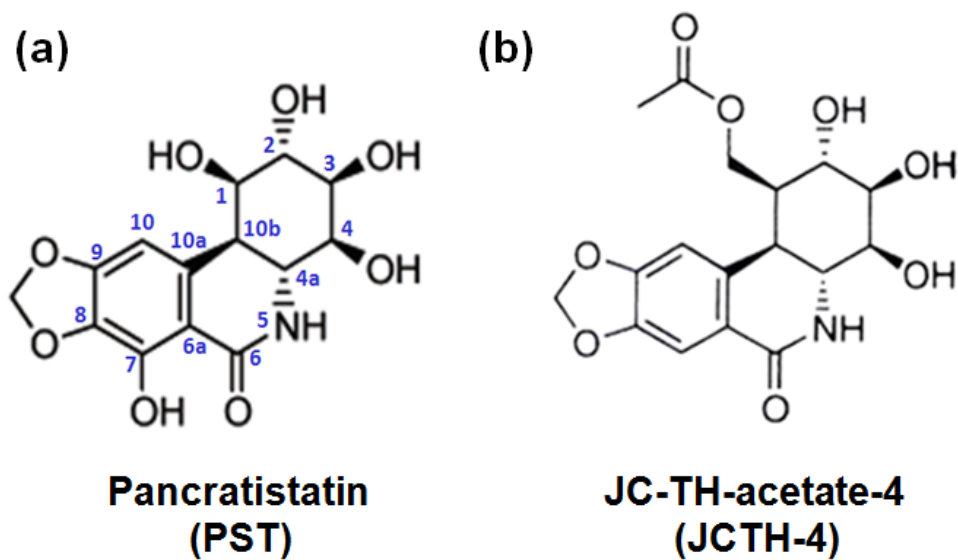


Figure 1. Structural comparison of PST to a synthetic 7-deoxy analogue. (a) Chemical structure of pancreatistatin (PST). **(b)** Chemical structure of JC-TH-acetate-4 (JCTH-4).

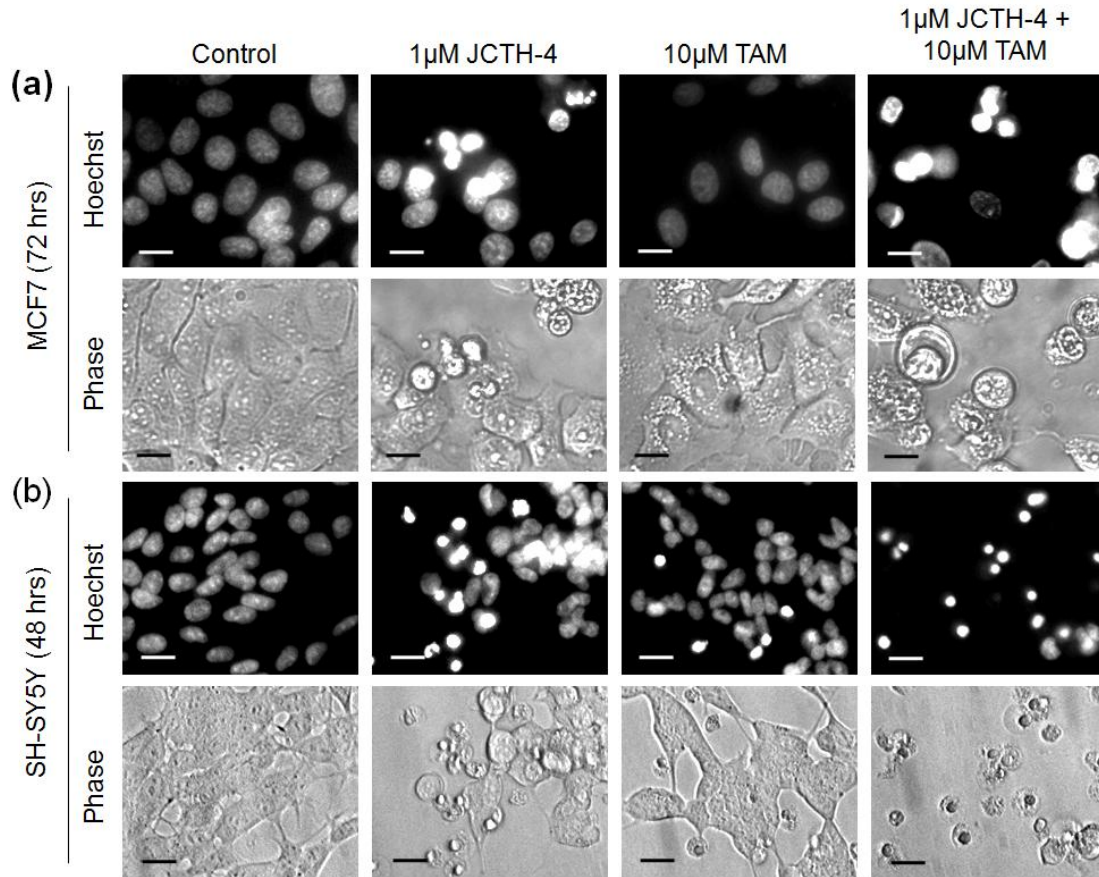


Figure 2. JCTH-4 induces nuclear apoptotic morphology with enhanced activity with TAM. Nuclear morphology of **(a)** MCF7 and **(b)** SH-SY5Y cells treated for 72 and 48 hours respectively with the indicated concentrations of TAM and JCTH-4 stained with Hoechst dye. Control groups were treated with solvent (DMSO). Images were taken at 400x magnification on a fluorescent microscope. Scale bar= 15 μ m.

To verify apoptotic induction, cells were evaluated for phosphatidylserine externalization, a marker for apoptosis, via an Annexin V binding assay¹⁷. MCF7 and SH-SY5Y cells treated for 72 and 48 hours respectively with 1 μ M JCTH-4 alone and in combination with 10 μ M TAM were positive for Annexin V binding, indicated by the green fluorescence, confirming the induction of apoptosis (**Fig 3a,b**). No evident externalization of phosphatidylserine was observed in MCF7 and SH-SY5Y cells treated with TAM alone, as well as in NFF cells treated with all the aforementioned treatments groups after 72 hours (**Fig. 3c**). Therefore, JCTH-4 alone and in combination with TAM selectively induces apoptosis in MCF7 and SH-SY5Y cells.

To quantify the effect of JCTH-4 alone and in combination with TAM, a WST-1 based colorimetric assay for cell viability, an indicator of active cell metabolism, was performed on MCF7 and NFF cells treated for 72 hours and SH-SY5Y cells treated for 48 hours. Compared to the solvent control groups, 1 μ M JCTH-4 decreased active cell metabolism by over 50%, while 10 μ M TAM alone exhibited no significant difference in both MCF7 and SH-SY5Y cells (**Fig 4a,b**). Interestingly in MCF7 and SH-SY5Y cells, the addition of TAM to JCTH-4 insult resulted in a synergistic decrease in cell metabolism. NFF cells were drastically less sensitive to both JCTH-4 alone and JCTH-4 with TAM (**Fig. 4c**). Hence, JCTH-4 demonstrates selective synergistic activity with TAM in MCF7 and SH-SY5Y cells.

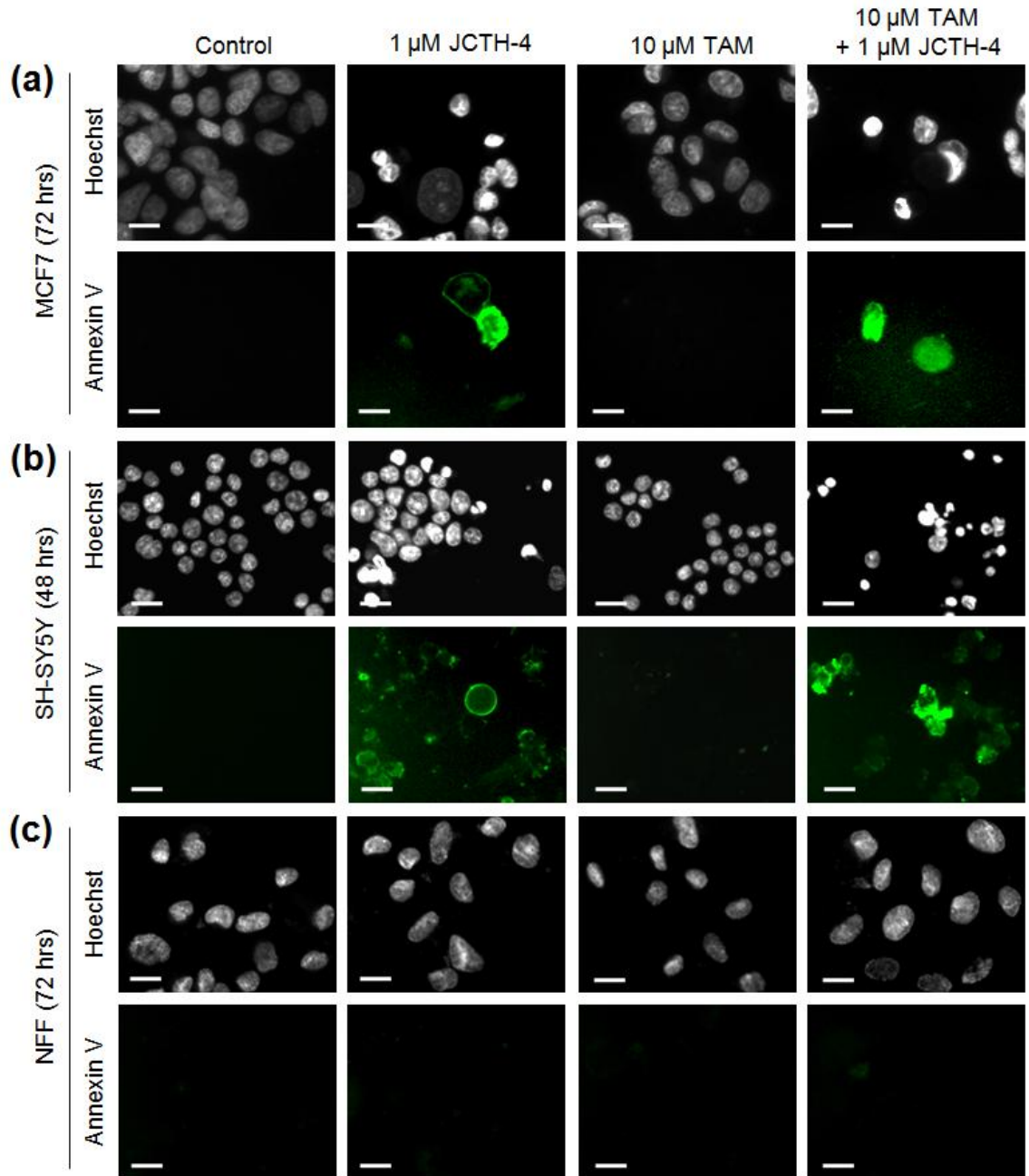


Figure 3. JCTH-4 causes phosphatidylserine externalization alone and in combination with TAM selectively in cancer cells. Annexin V binding to externalized phosphatidylserine was evaluated to verify induction of apoptosis in **(a)** MCF7 (72 hours), **(b)** SH-SY5Y (48 hours), and **(c)** NFF (72 hours) cells treated with JCTH-4 and TAM at the indicated concentrations. Control groups were treated with solvent (DMSO). Images were taken at 400x magnification on a fluorescent microscope. Scale bar= 15 μ m.

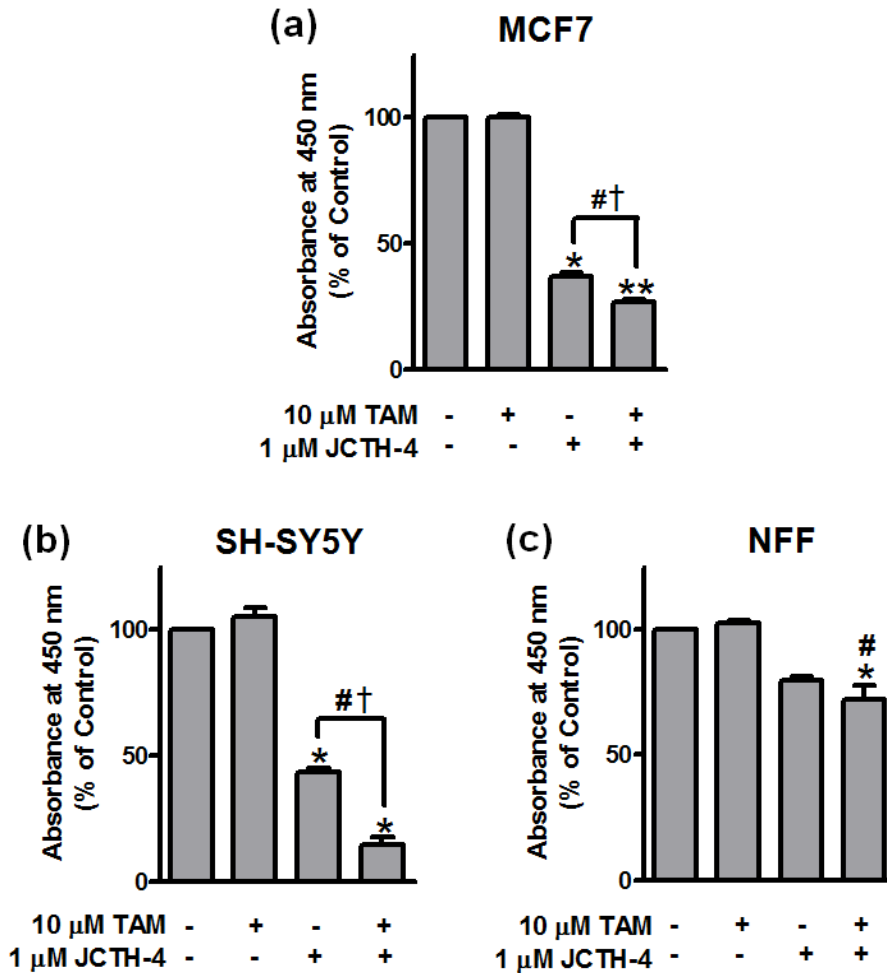


Figure 4. TAM enhances viability decrease by JCTH-4 selectively in cancer cells. 96-well plates were seeded with (a) MCF7, (b) SH-SY5Y, and (c) NFF cells and treated with JCTH-4 and TAM at the indicated concentrations. MCF7 and NFF cells were treated for 72 hours and SH-SY5Y were treated for 48 hours. Post drug treatment and incubation, WST-1 reagent was added to each well, and absorbance readings were taken at 450 nm and expressed as a percentage of the control (DMSO). Statistics were performed using GraphPad Prism version 5.0. Values are expressed as mean \pm SD from quadruplicates of 3 independent experiments. MCF7: * p <0.001, ** p <0.0001 versus control; # p <0.05 versus 1 μ M JCTH-4; † p <0.0001 versus 10 μ M TAM. SH-SY5Y: * p <0.0005 versus control; # p <0.005 versus 1 μ M JCTH-4; † p <0.005 versus 10 μ M TAM. NFF: * p <0.005 versus 10 μ M TAM + 1 μ M JCTH-4 in MCF7 cells; # p <0.01 versus 10 μ M TAM + 1 μ M JCTH-4 in SH-SY5Y cells.

Mitochondrial Targeting of JCTH-4

To see if JCTH-4 is targeting the mitochondria to induce apoptosis mitochondrial membrane potential in whole cells and ROS generation in isolated mitochondria was monitored. MCF7 cells were treated for 72 hours and stained with TMRM. 1 μ M JCTH-4 decreased MMP, indicated by the loss of red fluorescence (**Fig 5a**). However, with the addition of 10 μ M TAM, a greater dissipation of MMP was observed, while 10 μ M TAM alone had no evident effect on MMP.

As increases ROS generation have been associated to mitochondrial membrane permeabilization and apoptosis induction, the production of ROS was assessed with Amplex Red dye in isolated mitochondria from SH-SY5Y cells treated with 1 μ M JCTH-4 and 10 μ M TAM, alone and in combination¹⁸⁻²⁰. Fluorescence readings were expressed as relative fluorescence units (RFU). Increases in ROS generation were observed with JCTH-4 and TAM alone (**Fig 5b**). Interestingly, combination treatment yielded a greater increase in ROS production. A well-known inducer of ROS production in mitochondria, PQ, was utilized as a positive control.

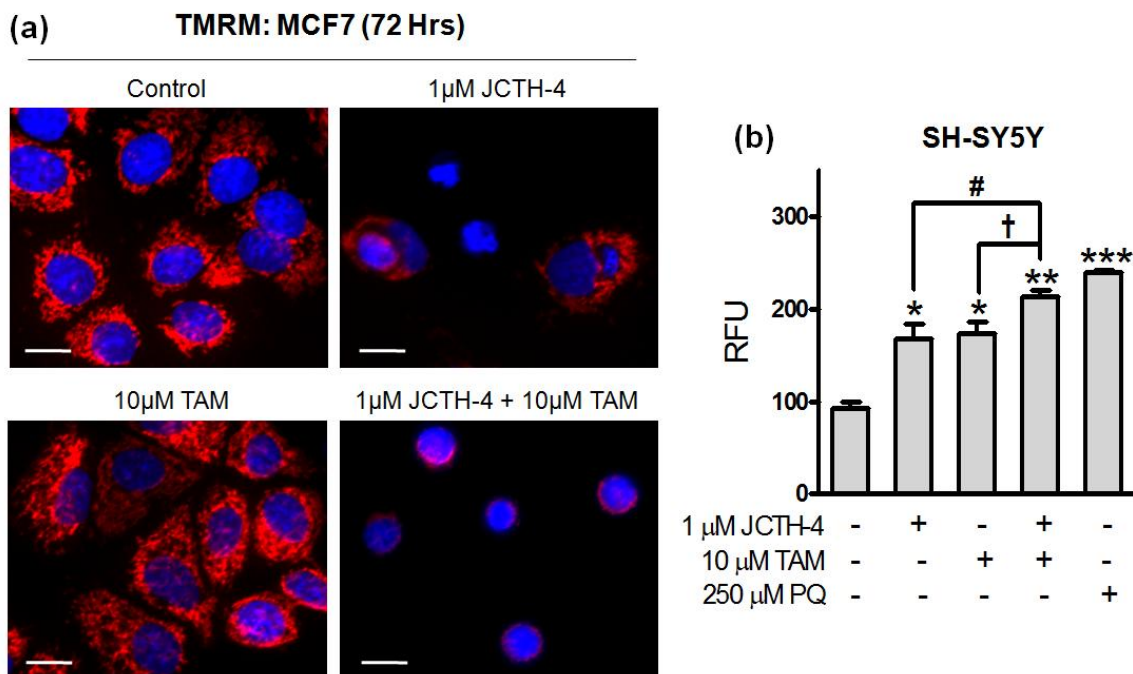


Figure 5. JCTH-4 and TAM act on the mitochondria. (a) MCF7 cells were grown on coverslips and treated with the indicated concentrations of drugs for 72 hours and stained with TMRM to evaluate MMP. Cells of the control group were treated with solvent (DMSO). Images were captured at 400x magnification on a fluorescence microscope. Scale bar= 15 µm. **(b)** Isolated mitochondria from SH-SY5Y cells were treated with JCTH-4 and TAM at the indicated concentrations and ROS production was assessed with Amplex Red substrate in presence of horseradish peroxidase (HRP). The control group cells were treated with solvent (DMSO). Paraquat (PQ) was used at a concentration of 250 µM as a positive control. Fluorescence readings were obtained after 2 hours of treatment at Ex. 560 nm and Em. 590 nm and expressed as relative fluorescence units (RFU). Statistics were obtained using GraphPad Prism version 5.0. Data is representative of 3 independent experiments with similar trends. Values are expressed as mean ± SD of quadruplicates of 1 independent experiment. * $p < 0.05$, ** $p < 0.005$, *** $p < 0.001$ versus control; # $p < 0.05$ versus 1 µM JCTH-4; † $p < 0.05$ versus 10 µM TAM; @ $p < 0.05$ versus 250 µM PQ.

Induction of Autophagy by JCTH-4 and TAM

Autophagic induction has been associated to chemotherapeutic insult by many different compounds³. To evaluate the induction of autophagy, MDC staining was performed on MCF7 cells treated with 1 μ M JCTH-4 and 10 μ M TAM alone and in combination for 72 hours. Blue punctate fluorescence, indicative of autophagosomes, was present in MCF7 cells treated with JCTH-4 and TAM alone and in combination (**Fig 6a**). Notably, the intensity of MDC staining was greatest with the combination treatment, followed by TAM alone, and JCTH-4 alone.

During autophagy, microtubule-associated protein 1 light chain 3 (LC3) normally situated in the cytosol (LC3-I), is lipidated with phosphatidylethanolamine and subsequently localized to the autophagosomal membranes (LC3-II)². To verify the induction of autophagy, levels of LC3-II were assessed in MCF7 cells treated for 72 hours via western blot analyses. 1 μ M JCTH-4 slightly induced the conversion of LC3-I to LC3-II while 10 μ M TAM produced a greater autophagic response (**Fig. 6b**). Interestingly, combination treatment resulted in the greatest induction of autophagy, yielding a LC3-II to LC3-I ratio greater than 3. Therefore, these results demonstrate autophagic induction in MCF7 cells by JCTH-4 and TAM alone and in combination, with the greatest response in cells with the combination treatment.

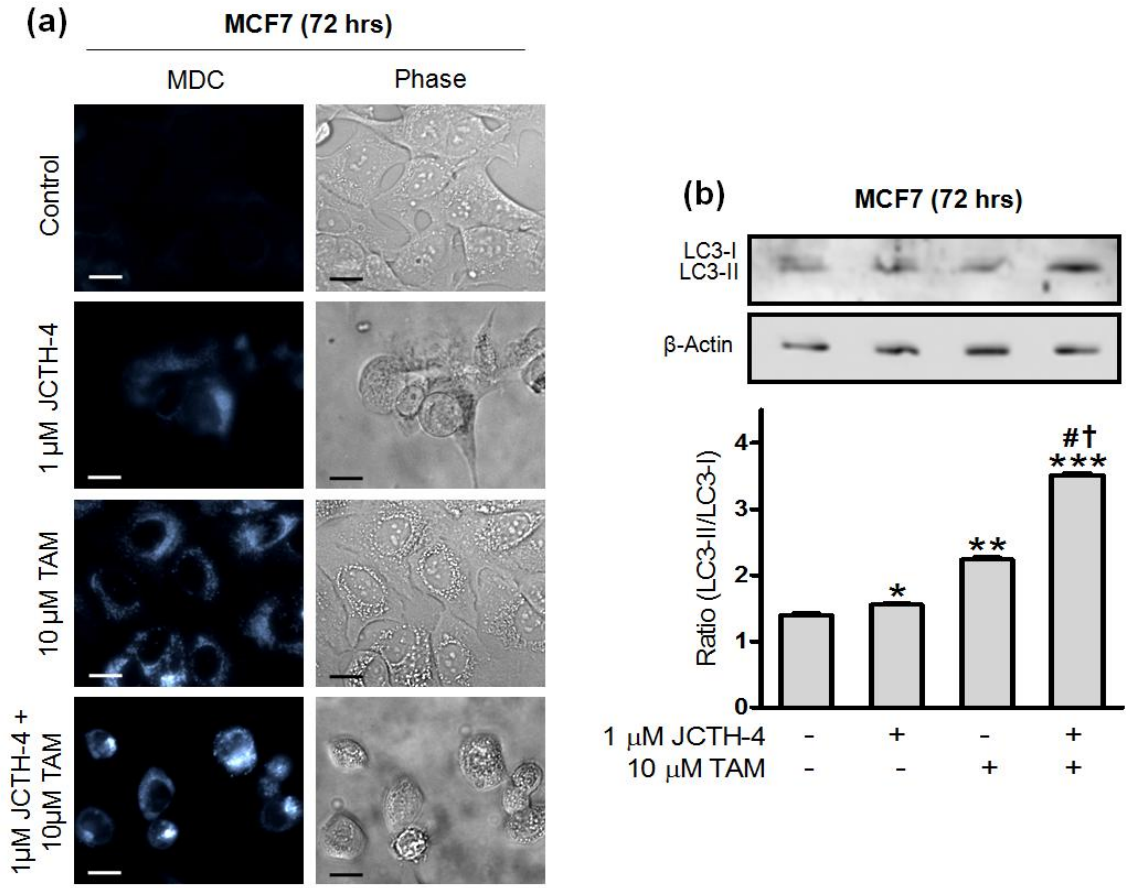


Figure 6. TAM enhances autophagic induction of JCTH-4. (a) MCF7 cells were grown on coverslips and subjected to JCTH-4 and TAM insult at the indicated concentrations for 72 hours. Control group cells were treated with solvent (DMSO). Post treatment, MCF7 cells were stained with MDC to detect autophagic vacuoles. Images were captured at 400x magnification on a fluorescence microscope. Scale bar= 15 μ m. (b) Western blot analyses were carried out for LC3 and β -Actin on cell lysates of MCF7 cells treated with the indicated concentrations of drugs for 72 hours. Densitometric analyses were executed using ImageJ software. Statistics were performed using GraphPad Prism version 5.0. Values are expressed as mean \pm SD. * p <0.05, ** p <0.005, *** p <0.0005 versus control; # p <0.001 versus 1 μ M JCTH-4; † p <0.001 versus 10 μ M TAM.

Discussion

PST and similar compounds have been shown to have anti-cancer properties^{11-15,21}. We have previously reported natural PST to destabilize the mitochondria selectively in cancer cells, which thereby induces apoptosis by the release of apoptogenic factors^{12,14}. It is most likely that JCTH-4 acts through the same mechanism; JCTH-4 caused MMP collapse in MCF7 cells as seen with TMRM staining (**Fig. 5a**), and increased generation of ROS in isolated mitochondria from SH-SY5Y cells (**Fig. 5b**), indicative of mitochondrial dysfunction. Thus, induction of apoptosis by JCTH-4 is most probably through mitochondrial targeting in cancer cells.

Numerous differences exist between noncancerous and cancer cells which could serve as the basis for cancer selectivity by JCTH-4. Cancer cells are highly dependent on glycolysis and less on mitochondria for energy production; this phenomenon is referred to as the Warburg effect²². Such metabolic activity in the cancer cells leads to high acidity in the cytosol. Consequently, the acidic cytosolic environment contributes cancer cell mitochondria hyperpolarization which has been linked to an enhanced ability to invade and evade apoptosis²³. Hyperpolarization of cancer cell mitochondria however, may render cancer cells vulnerable to JCTH-4; once taken into the cell, JCTH-4 may acquire a positive charge through enzymatic processing and may selectively be taken up into cancer cell mitochondria due to their hyperpolarized nature. Moreover, an array of mitochondria associated antiapoptotic proteins have been shown to be highly expressed in cancer cells that prohibit mitochondrial membrane permeabilization

and subsequent execution of apoptosis such as antiapoptotic proteins of the Bcl-2 family of proteins²⁴⁻²⁶.

In the presence of various forms of cellular stress, autophagy is triggered as a pro-survival response, allowing cells to survive under unfavourable conditions². Over stimulation of this pathway however, can lead to extensive breakdown of vital intracellular components giving rise to autophagic cell death³. Both the pro-survival and pro-death autophagic responses have been associated to chemotherapeutic insult³. Mitochondrial dysfunction by JCTH-4 leading to oxidative stress could trigger an automatic default autophagic response. Indeed we did observe some autophagic induction along with apoptosis with JCTH-4 treatment (**Fig. 2a,b 3a,b 6a,b**). Although TAM has been well established as an ER antagonist in ER positive breast cancer cells, it has been recently shown to interact with the mitochondria, binding to the FMN site of Complex I¹⁰. Furthermore, TAM is a well-known inducer of autophagy across many cancer cell types³. Indeed, TAM did cause an increase in ROS generation in isolated mitochondria (**Fig. 5b**). However, such interaction proved to be insufficient to cause MMP collapse (**Fig. 5a**), but sufficient to induce a typical pro-survival autophagic response. Extensive autophagic induction was observed when JCTH-4 and TAM were used in combination (**Fig. 6a,b**), which was accompanied by an enhanced cytotoxic response (**Fig. 4a,b**), suggestive of a pro-death autophagic response; nonetheless, the cancer cells eventually die from apoptosis as a result of mitochondrial permeabilization and apoptogenic factor release. Such sensitization by TAM to JCTH-4 insult may be attributed to the increase in

ROS generation by TAM. Because both TAM and JCTH-4 are able to generate oxidative stress, the combinatorial production of such stress with both compounds may lead to extensive autophagic induction giving rise to a detrimental autophagic response and/or extensive mitochondrial permeabilization and subsequent apoptosis. This combined treatment does not affect viability of noncancerous fibroblasts (**Fig. 4c**). These findings indicate that JCTH-4 alone and in combination with TAM can be used efficiently to treat breast cancer and neuroblastoma without causing adverse effects on noncancerous cells.

Acknowledgements

This work has been supported by the Knights of Columbus Chapter 9671 (Windsor, Ontario), and a CIHR Frederick Banting and Charles Best Canada Graduate Scholarship awarded to Dennis Ma. Thank you to Robert Hodge and Elizabeth Fidalgo da Silva for their assistance with the time-lapse microscopy. Thank you to Katie Facecchia for editing the time-lapse microscopy videos. We would also like to thank Sudipa June Chatterjee and Phillip Tremblay for the critical review of this manuscript.

References

1. Earnshaw, W.C. Apoptosis. A cellular poison cupboard. *Nature* **397** (6718), 387- 389 (1999).
2. Kroemer, G., Mariño, G., Levine, B. Autophagy and the integrated stress response. *Mol Cell.* **40** (2), 280-93 (2010).
3. Dalby, K.N., Tekedereli, I., Lopez-Berestein, G., Ozpolat, B. Targeting the prodeath and prosurvival functions of autophagy as novel therapeutic strategies in cancer. *Autophagy* **6** (3), 322-9 (2010). [Epub 2010 Apr 26]
4. Hanahan, D., Weinberg, R.A. Hallmarks of cancer: the next generation. *Cell* 2011 **144** (5), 646-74 (2011).
5. Fearon, E.R. Human Cancer Syndromes: Clues to the Origin and Nature of Cancer. *Science* **278**, 1043-1050 (1997).
6. Tsokos, M., Scarpa, S., Ross, R.A., Triche, T.J. Differentiation of human neuroblastoma recapitulates neural crest development. Study of morphology, neurotransmitter enzymes, and extracellular matrix proteins. *The American Journal of Pathology* **128** (3), 484-496 (1987).
7. Schwab, M., Westermann, F., Hero, B., Berthold, F. Neuroblastoma: biology and molecular and chromosomal pathology. *Lancet Oncol.* **4**, 472–480 (2003).
8. Jemal, A., Siegel, R., Ward, E., Hao, Y., Xu, J., Thun, M.J. Cancer statistics, 2009. *CA Cancer J Clin.* **59**, 225–249 (2009).
9. Howell, A. The endocrine prevention of breast cancer. *Best Pract Res Clin Endocrinol Metab* **22**, 615-623 (2008).
10. Moreira, P., Custodio, J., Morena, A., Oliveira, C., Santos, M. Tamoxifen and estradiol interact with the flavin mononucleotide site of complex I leading to mitochondrial failure. *J Biol Chem* **281**, 10143–10152 (2006).
11. Kekre, N., Griffin, C., McNulty, J., Pandey, S. Pancreatistatin causes early activation of caspase-3 and the flipping of phosphatidyl serine followed by rapid apoptosis specifically in human lymphoma cells. *Cancer Chemother Pharmacol* **56** (1), 29-38 (2005).
12. McLachlan, A., Kekre, N., McNulty, J., Pandey, S. Pancreatistatin: a natural anti-cancer compound that targets mitochondria specifically in cancer cells to induce apoptosis. *Apoptosis* **10** (3), 619-630 (2005).

13. Griffin, C., Hamm, C., McNulty, J., Pandey, S. Pancreatistatin induces apoptosis in clinical leukemia samples with minimal effect on noncancerous peripheral blood mononuclear cells. *Cancer Cell Int.* **10**, 6 (2010).
14. Griffin, C., Karnik, A., McNulty, J., Pandey, S. Pancreatistatin selectively targets cancer cell mitochondria and reduces growth of human colon tumor xenografts. *Molecular Cancer Therapeutics* **10** (1), 57-68 (2011a).
15. Griffin, C., McNulty, J., Pandey, S. Pancreatistatin induces apoptosis and autophagy in metastatic prostate cancer cells. *Int J Oncol.* **38** (6),1549-56 (2011b).
16. Collins, J., Rinner, U., Moser, M., Hudlicky, T., Ghiviriga, I., Romero, A.E., Kornienko, A., Ma, D., Griffin, C., Pandey, S. Chemoenzymatic synthesis of Amaryllidaceae constituents and biological evaluation of their C-1 analogues. The next generation synthesis of 7-deoxypancreatistatin and trans-dihydrolycoricidine. *J Org Chem* **75** (9), 3069-84 (2010).
17. Zhang, G., Gurtu, V., Kain, S.R., Yan, G. Early detection of apoptosis using a fluorescent conjugate of annexin V. *Biotechniques* **23** (3), 525-31 (1997).
18. Madesh, M., Hajnóczy, G. VDAC-dependent permeabilization of the outer mitochondrial membrane by superoxide induces rapid and massive cytochrome c release. *J Cell Biol.* **155** (6),1003-15 (2001). [Epub 2001 Dec 10]
19. Simon, H.U., Haj-Yehia, A., Levi-Schaffer, F. Role of reactive oxygen species (ROS) in apoptosis induction. *Apoptosis* **5** (5), 415-8 (2000).
20. Batandier, C., Leverve, X., Fontaine, E. Opening of the mitochondrial permeability transition pore induces reactive oxygen species production at the level of the respiratory chain complex I. *J Biol Chem.* **279** (17), 17197-204 (2004). [Epub 2004 Feb 11]
21. Lefranc, F., Sauvage, S., Van Goietsenoven, G., Mégalizzi, V., Lamoral-Theys, D., Debeir, O., Spiegl-Kreinecker, S., Berger, W., Mathieu, V., Decaestecker, C., Kiss, R. Narciclasine, a plant growth modulator, activates Rho and stress fibers in glioblastoma cells. *Mol Cancer Ther.* **8** (7),1739-50 (2009). [Epub 2009 Jun 16]
22. Warburg, O. On the origin of cancer cells. *Science* **123** (3191), 309-14 (1956).
23. Heerdt, B.G., Houston, M.A., Augenlicht, L.H. Growth properties of colonic tumor cells are a function of the intrinsic mitochondrial membrane potential. *Cancer Res.* **66** (3), 1591-6 (2006).

24. Green, D.R., Kroemer, G. The pathophysiology of mitochondrial cell death. *Science* **305** (5684), 626-9 (2004).
25. Casellas, P., Galiegue, S., Basile, A.S. Peripheral benzodiazepine receptors and mitochondrial function. *Neurochem Int.* **40** (6), 475-86 (2002).
26. Mathupala, S.P., Rempel, A., Pedersen, P.L. Aberrant glycolytic metabolism of cancer cells: a remarkable coordination of genetic, transcriptional, post-translational, and mutational events that lead to a critical role for type II hexokinase. *J Bioenerg Biomembr.* **29** (4), 339-43 (1997).

Video Legends

Please refer to the Journal of Visualized Experiments for videos:

Ma et al. 2012. J Vis Exp. 30;(63). pii: 3586. doi: 10.3791/3586

Video 1. Cellular morphology of MCF7 cells treated with solvent control. MCF7 cells were monitored between 48 and 66 hours post solvent control treatment (DMSO) using time-lapse microscopy with phase contrast pictures. Cells were maintained at 37° C and 5% CO₂. Images were captured at 400x magnification.

Video 2. Induction of apoptotic cellular morphology in MCF7 cells treated with JCTH-4. MCF7 cells were monitored between 48 and 66 hours post treatment with 1 μM JCTH-4 using time-lapse microscopy with phase contrast pictures. Cells were maintained at 37° C and 5% CO₂. Images were captured at 400x magnification.

Video 3. Induction of autophagic cellular morphology in MCF7 cells treated with TAM. MCF7 cells were monitored between 48 and 66 hours post treatment with 10 μM TAM using time-lapse microscopy with phase contrast pictures. Cells were maintained at 37° C and 5% CO₂. Images were captured at 400x magnification.

Video 4. Enhanced apoptotic morphology by JCTH-4 with TAM in MCF7 cells. MCF7 cells were monitored between 48 and 66 hours post treatment with both 1 μM JCTH-4 and 10 μM TAM using time-lapse microscopy with phase contrast pictures. Cells were maintained at 37° C and 5% CO₂. Images were captured at 400x magnification.

Appendices

APPENDIX C: Copyright Transfer Agreement Forms

SPRINGER LICENSE

TERMS AND CONDITIONS

May 18, 2016

This Agreement between Dennis Ma ("You") and Springer ("Springer") consists of your license details and the terms and conditions provided by Springer and Copyright Clearance Center.

License Number	3872240118867
License date	May 18, 2016
Licensed Content Publisher	Springer
Licensed Content Publication	Investigational New Drugs
Licensed Content Title	A novel synthetic C-1 analogue of 7deoxypancratistatin induces apoptosis in p53 positive and negative human colorectal cancer cells by targeting the mitochondria: enhancement of activity by tamoxifen
Licensed Content Author	Dennis Ma
Licensed Content Date	Jan 1, 2011
Licensed Content Volume Number	30
Licensed Content Issue Number	3
Type of Use	Thesis/Dissertation
Portion	Full text
Number of copies	1
Author of this Springer article	Yes and you are a contributor of the new work
Order reference number	None
Title of your thesis / dissertation	Exploiting Cancer Cell Mitochondria as a Therapeutic Strategy: Structure Activity Relationship Analyses of Synthetic Analogues of Pancreatistatin
Expected completion date	May 2016

Estimated size(pages)	None
Requestor Location	Dennis Ma 1154 Langlois Avenue Windsor, ON N9A2H5 Canada Attn: Dennis Ma
Billing Type	Invoice
Billing Address	Dennis Ma 1154 Langlois Avenue Windsor, ON N9A2H5 Canada Attn: Dennis Ma
Total	0.00 USD

Terms and Conditions

Introduction

The publisher for this copyrighted material is Springer. By clicking "accept" in connection with completing this licensing transaction, you agree that the following terms and conditions apply to this transaction (along with the Billing and Payment terms and conditions established by Copyright Clearance Center, Inc. ("CCC"), at the time that you opened your Rightslink account and that are available at any time at <http://myaccount.copyright.com>).

Limited License

With reference to your request to reuse material on which Springer controls the copyright, permission is granted for the use indicated in your enquiry under the following conditions:

- Licenses are for onetime use only with a maximum distribution equal to the number stated in your request.
- Springer material represents original material which does not carry references to other sources. If the material in question appears with a credit to another source, this permission is not valid and authorization has to be obtained from the original copyright holder.
- This permission
 - is nonexclusive
 - is only valid if no personal rights, trademarks, or competitive products are infringed.
 - explicitly excludes the right for derivatives.
- Springer does not supply original artwork or content.

According to the format which you have selected, the following conditions apply accordingly:

- Print and Electronic: This License include use in electronic form provided it is password protected, on intranet, or CDRom/DVD or Ebook/Ejournal.

It may not be republished in electronic open access.

- Print: This License excludes use in electronic form.

- Electronic: This License only pertains to use in electronic form provided it is password protected, on intranet, or CDRom/DVD or Ebook/Ejournal.

It may not be republished in electronic open access.

For any electronic use not mentioned, please contact Springer at permissions.springer@spiglobal.com.

Although Springer controls the copyright to the material and is entitled to negotiate on rights, this license is only valid subject to courtesy information to the author (address is given in the article/chapter).

If you are an STM Signatory or your work will be published by an STM Signatory and you are requesting to reuse figures/tables/illustrations or single text extracts, permission is granted according to STM Permissions Guidelines:

<http://www.stmassoc.org/permissionsguidelines/>

For any electronic use not mentioned in the Guidelines, please contact Springer at permissions.springer@spiglobal.com. If you request to reuse more content than stipulated in the STM Permissions Guidelines, you will be charged a permission fee for the excess content.

Permission is valid upon payment of the fee as indicated in the licensing process.

If permission is granted free of charge on this occasion, that does not prejudice any rights we might have to charge for reproduction of our copyrighted material in the future.

If your request is for reuse in a Thesis, permission is granted free of charge under the following conditions:

This license is valid for onetime use only for the purpose of defending your thesis and with a maximum of 100 extra copies in paper. If the thesis is going to be published, permission needs to be reobtained.

-includes use in an electronic form, provided it is an authorcreated version of the thesis on his/her own website and his/her university's repository, including UMI (according to the definition on the Sherpa website:

<http://www.sherpa.ac.uk/romeo/>); is subject to courtesy information to the coauthor or corresponding author.

Geographic Rights: Scope

Licenses may be exercised anywhere in the world.

Altering/Modifying Material: Not Permitted

Figures, tables, and illustrations may be altered minimally to serve your work.

You may not alter or modify text in any manner. Abbreviations, additions, deletions and/or any other alterations shall be made only with prior written authorization of the author(s).

Reservation of Rights

Springer reserves all rights not specifically granted in the combination of (i) the license details provided by you and accepted in the course of this licensing transaction and (ii) these terms and conditions and (iii) CCC's Billing and Payment terms and conditions.

License Contingent on Payment

While you may exercise the rights licensed immediately upon issuance of the license at the end of the licensing process for the transaction, provided that you have disclosed complete and accurate details of your proposed use, no license is finally effective unless and until full payment is received from you (either by Springer or by CCC) as provided in CCC's Billing and Payment terms and conditions. If full payment is not received by the date due, then any license preliminarily granted shall be deemed automatically revoked and shall be void as if never granted. Further, in the event that you breach any of these terms and conditions or any of CCC's Billing and Payment terms and conditions, the license is automatically revoked and shall be void as if never granted. Use of materials as described in a revoked license, as well as any use of the materials beyond the scope of an unrevoked license, may constitute copyright infringement and Springer reserves the right to take any and all action to protect its copyright in the materials.

Copyright Notice: Disclaimer

You must include the following copyright and permission notice in connection with any reproduction of the licensed material:

"Springer book/journal title, chapter/article title, volume, year of publication, page, name(s) of author(s), (original copyright notice as given in the publication in which the material was originally published) "With permission of Springer"

In case of use of a graph or illustration, the caption of the graph or illustration must be included, as it is indicated in the original publication.

Warranties: None

Springer makes no representations or warranties with respect to the licensed material and adopts on its own behalf the limitations and disclaimers established by CCC on its behalf in its Billing and Payment terms and conditions for this licensing transaction.

Indemnity

You hereby indemnify and agree to hold harmless Springer and CCC, and their respective officers, directors, employees and agents, from and against any and all claims arising out of your use of the licensed material other than as specifically authorized pursuant to this license.

No Transfer of License

This license is personal to you and may not be sublicensed, assigned, or transferred by you without Springer's written permission.

No Amendment Except in Writing

This license may not be amended except in a writing signed by both parties (or, in the case of Springer, by CCC on Springer's behalf).

Objection to Contrary Terms Springer hereby objects to any terms contained in any purchase order, acknowledgment, check endorsement or other writing prepared by you, which terms are inconsistent with these terms and conditions or CCC's Billing and Payment terms and conditions. These terms and conditions, together with CCC's Billing and Payment terms and conditions (which are incorporated herein), comprise the entire agreement between you and Springer (and CCC) concerning this licensing transaction. In the event of any conflict between your obligations established by these terms and conditions and those established by CCC's Billing and Payment terms and conditions, these terms and conditions shall control.

Jurisdiction

All disputes that may arise in connection with this present License, or the breach thereof, shall be settled exclusively by arbitration, to be held in the Federal Republic of Germany, in accordance with German law.

Other conditions:

V 12AUG2015

Questions? customercare@copyright.com or +18552393415
(toll free in the US) or
+19786462777.

Wed, May 18, 2016 at 2:26 AM

plosone <plosone@plos.org>

Dear Dr. Ma,

Thank you for your message. PLOS ONE publishes all of the content in the articles under an open access license called "CC-BY." This license allows you to download, reuse, reprint, modify, distribute, and/or copy articles or images in PLOS journals, so long as the original creators are credited (e.g., including the article's citation and/or the image credit). Additional permissions are not required. You can read about our open access license here: <http://www.plos.org/about/open-access/>.

There are many ways to access our content, including HTML, XML, and PDF versions of each article. Higher resolution versions of figures can be downloaded directly from the article.

Thank you for your interest in PLOS ONE and for your continued support of the Open Access model. Please do not hesitate to be in touch with any additional questions.

Kind Regards,

Emma Darkin
Staff EO
PLOS ONE

Case Number: 04575878

Thu, May 19, 2016 at 6:21 AM

From: **Kevin AJBMS** <editor2_ajbms@nwpii.com>

Dear Dennis Ma,

Thanks for your request.

Your following publication is permitted to be included in your doctoral dissertation:

Am. J. Biomed. Sci. 2011, 3(4), 278-291; doi: 10.5099/aj110400278.

Please let me know if you have any questions.

Best wishes,

Kevin
Production Editor
AJBMS
editor2_ajbms@nwpii.com
<http://www.nwpii.com/ajbms>

Wed, May 18, 2016 at 12:07 PM

From: Kathleen Doyle <kathleen.doyle@jove.com>

signed-by: jove-com.20150623.gappssmtp.com

Dear Mr. Ma,

You have our permission to use your JoVE article "Ma, D., Collins, J., Hudlicky, T., Pandey, S. Enhancement of Apoptotic and Autophagic Induction by a Novel Synthetic C-1 Analogue of 7-deoxypancratistatin in Human Breast Adenocarcinoma and Neuroblastoma Cells with Tamoxifen. *J. Vis. Exp.* (63), e3586, doi:10.3791/3586 (2012)." in your dissertation as requested.

Please be sure to cite the article accordingly and consider this email as approval. Do not hesitate to email me with any other questions and have a great day.

Best Regards,
Katie

Vita Auctoris

NAME: Dennis Ma

PLACE OF BIRTH: Windsor ON, Canada

YEAR OF BIRTH: 1987

EDUCATION

Jan 2010-
May 2016 **PhD Biochemistry**
Department of Chemistry & Biochemistry, University of Windsor,
Windsor, ON, Canada

- Supervised by Dr. Siyaram Pandey, Professor

2005-2010 **BSc (Honours) Biology with Great Distinction**
Department of Biological Sciences, University of Windsor,
Windsor, ON, Canada

- Undergraduate thesis supervised by Dr. Siyaram Pandey, Professor

LABORATORY EXPERIENCE

Jan 2006-
Current **Research Assistant, Lab Manager, Lab Safety Manager**
Department of Chemistry & Biochemistry, University of Windsor

- 2D & 3D cell culture, drug screening, enzymatic assays, western blots, flow cytometry, molecular techniques, fluorescence & confocal microscopy, animal models
- Mentored, trained, managed and led 27 undergraduate and 2 graduate students on projects in cancer and neurodegenerative research
- conducted and kept records of lab safety trainings, enforced safety, catalogued hazardous materials, drafted emergency and standard operating protocols for hazardous materials, and ensured safety requirements were maintained

Jan 2010-
Current **Teaching Assistant**
Department of Chemistry & Biochemistry, University of Windsor

- Taught basic lab techniques and instructed 1st to 4th year undergraduate students in course-based chemistry and biochemistry laboratories
- Mentored students with homework problems and equipped them with exam writing strategies and writing skills

AWARDS

- 2015 - 2016 **Ontario Graduate Scholarship (OGS):** award for doctoral studies
- 2012 - 2015 **Vanier Canada Graduate Scholarship:** most prestigious doctoral award in Canada
- 2012 - 2015 **Canadian Institutes of Health Research (CIHR) – Frederick Banting and Charles Best Canada Graduate Scholarships:** Doctoral Award (ranked in top 1% in Canada) - declined for the Vanier Canada Graduate Scholarship
- Aug. 2015 **Best Poster Award:** Natural Health Product Research Society Conference, London, ON
- May 2013 **Best Oral Presentation:** Natural Health Product Research Society Conference, Windsor, ON
- May 2013 **CIHR Training Program in Neurodegenerative Lipidomics Research Scholarship:** Travel award for Natural Health Product Research Society Conference, Windsor, ON
- 2011 - 2012 **Ontario Graduate Scholarship (OGS):** award for doctoral studies
- Nov. 2011 **Cancer Society-Ontario Trainee Travel Award:** Canadian Cancer Research Alliance (CCRA): 2011 Canadian Cancer Research Conference, Toronto, ON
- 2011 **Golden Key Research Grant Award:** Travel award for the Natural Health Product Research Society Conference, Montreal, QC
- May 2011 **Best Oral Presentation:** Natural Health Product Research Society Conference, Montreal, QC
- 2011 **Casino Windsor Cares Gail Rosenblum Memorial Breast Cancer Research Scholarship**
- Nov. 2010 **Travel Award for Top 10 International abstracts:** Society for Free Radical Biology and Medicine (SFRBM) 17th Annual Meeting, Orlando, FL
- 2010 - 2011 **CIHR–Frederick Banting & Charles Best Canada Graduate Scholarships - Master's Award**
- 2010 **Ontario Graduate Scholarships in Science & Tech.:** declined for CIHR Master's Award

- 2010 - 2014 **University of Windsor – Graduate Tuition Scholarship**
- 2005 - 2009 **University of Windsor – Dean’s Renewable Entrance Scholarship**
- 2005 - 2009 **Queen Elizabeth II Aiming for the Top Scholarship**
- 2009 **Natural Sciences & Engineering Research Council of Canada (NSERC) – Undergraduate Student Research Award:** Award to conduct summer undergraduate research
- 2008 **NSERC – Undergraduate Student Research Award**
- 2008 **Canadian Society for Chemistry Silver Medal:** for highest academic standing in Biochemistry at the University of Windsor
- 2007 **Canada Millennium Excellence Scholarship**

REFEREED PUBLICATIONS

McNulty J, van den Berg S, **Ma D**, Tarade D, Joshi S, Church J, Pandey S. Antimitotic activity of structurally simplified biaryl analogs of the anticancer agents colchicine and combretastatin-A4. *Bioorg Med Chem Lett*. 2014;25(1):117-121. doi: 10.1016/j.bmcl.2014.10.090. Published January 1, 2015.

Ovadge P, **Ma D**, Tremblay P, Roma A, Steckle M, Guerrero J, Arnason JT, Pandey S. Evaluation of the Efficacy & Biochemical Mechanism of Cell Death Induction by Long Pepper Extract Selectively in In-Vitro and In-Vivo models of Human Cancer Cells. *PLoS One* 2014;9(11):e113250. doi: 10.1371/journal.pone.0113250. eCollection 2014. Published November 17, 2014.

Ma D, Stokes K, Mahngar K, Domazet-Damjanov D, Sikorska M, Pandey S. Inhibition of stress induced premature senescence in presenilin-1 mutated cells with water soluble Coenzyme Q₁₀. *Mitochondrion* 2014; 17:106-15. doi: 10.1016/j.mito.2014.07.004. Epub Jul 15, 2014

Vshyvenko S, Scattolon J, Hudlicky T, Romero AE, Kornienko A, **Ma D**, Tuffley I, Pandey S. Unnatural C-1 homologues of pancratistatin - Synthesis and promising biological activities. *Canadian Journal of Chemistry* 2012;90(11): 932-943. doi: 10.1139/v2012-073. Published September 19, 2012.

Ma D, Collins J, Hudlicky T, Pandey S. Enhancement of apoptotic and autophagic induction by a novel synthetic C-1 analogue of 7-deoxypancratistatin in human breast adenocarcinoma and neuroblastoma cells with tamoxifen. *J Vis Exp*. 2012;(63). pii: 3586. doi: 10.3791/3586. Published May 30, 2012.

Pandey S, **Ma D**, Griffin C, Hamm C, McNulty J. Selective induction of apoptosis in cancer cells by Pancratistatin that targets mitochondria. *Int. J. of Mol. Medicine* 2011; Vol. 28 supplement 1. S23. *Published Abstract. Abstract #: 173.*

Ma D, Tremblay P, Mahngar K, Collins J, Hudlicky T, Pandey S. Selective Cytotoxicity Against Human Osteosarcoma Cells by a Novel Synthetic C-1 Analogue of 7-deoxypancratistatin is Potentiated by Curcumin. *PLoS One* 2011;6(12):e28780. doi: 10.1371/journal.pone.0028780. Epub December 21, 2011.

Ma D, Tremblay P, Mahngar K, Akbari-Asl P, Collins J, Hudlicky T, Pandey S. Induction of Apoptosis and Autophagy in Human Pancreatic Cancer Cells by a Novel Synthetic C-1 Analogue of 7-deoxypancratistatin. *Am. J. Biomed. Sci.* 2011;3(4):278-291; doi: 10.5099/aj110400278. Published September 5, 2011.

Ma D, Tremblay P, Mahngar K, Akbari-Asl P, Collins J, Hudlicky T, McNulty J, Pandey S. A Novel Synthetic C1 Analog of 7-deoxypancratistatin Induces Apoptosis in p53 Positive and Negative Human Colon Cancer Cells by Targeting the Mitochondria: Enhancement of Activity by Tamoxifen. *Investigational New Drugs* 2012;30(3):1012-27. doi: 10.1007/s10637-011-9668-7. Epub April 15, 2011.

Collins J, Rinner U, Moser M, Hudlicky T, Ghiviriga I, Romero AE, Kornienko A, **Ma D**, Griffin C, Pandey S. Chemoenzymatic synthesis of Amaryllidaceae constituents and biological evaluation of their C-1 analogues. The next generation synthesis of 7-deoxypancratistatin and trans-dihydrolycoricidine. *J Org Chem* 2010;75(9):3069-84. doi: 10.1021/jo1003136. Published May 7, 2010.

ORAL PRESENTATIONS

Pignanelli C, **Ma D**, Wang Y, Liang G, Pandey S. Improved Anti-Cancer Activity of Novel Curcumin Analogs in Combination with Trigonelline, an Inhibitor of the Nrf2 Pro-Survival Pathway in Non-Small Cell Lung Carcinoma. (2015) *12th Annual Natural Health Product Research Society Conference: Convergence: Multi-sector Integration for Advancing Transdisciplinary NHP R&D*, Western University, London, ON, Canada, Aug. 14-17, 2015. *International Conference*. I contributed to design and execution of experiments, analysis of data, and preparation of the presentation.

Noel M, **Ma D**, Pignanelli C, Wang Y, Liang G, Pandey S. Anti-Cancer Properties of Novel Curcumin Analogues are Enhanced with Piperlongumine in Triple Negative Breast Cancer Cells. (2015) *12th Annual Natural Health Product Research Society Conference: Convergence: Multi-sector Integration for Advancing Transdisciplinary NHP R&D*, Western University, London, ON, Canada, Aug. 14-17, 2015. *International Conference*. I contributed to design and execution of experiments, analysis of data, and preparation of the presentation.

Tarade D, Mansour F, Pignanelli C, **Ma D**, Van den Berg S, McNulty J, Pandey S. Natural Compound Combretastatin A4 and Structurally-Simplified Analogues Possess Potent Anti-Cancer Activity Dependent on Prolonged Mitotic Arrest and Mitochondrial Depolarisation. (2015) *12th Annual Natural Health Product Research Society Conference: Convergence: Multi-sector Integration for Advancing Transdisciplinary NHP R&D*, Western University, London, ON, Canada, Aug. 14-17, 2015. *International Conference*. I contributed to design and execution of experiments, analysis of data, and preparation of the presentation.

Mansour F, Tarade D, Pignanelli C, **Ma D**, Van den Berg S, McNulty J, Pandey S. The Current and Future Developments of Structurally-Simplified Analogues of the Natural Compound Combretastatin A4. (2015) *12th Annual Natural Health Product Research Society Conference: Convergence: Multi-sector Integration for Advancing Transdisciplinary NHP R&D*, Western University, London, ON, Canada, Aug. 14-17, 2015. *International Conference*. I contributed to design and execution of experiments, analysis of data, and preparation of the presentation.

Cowell M, **Ma D**, Vshyvenko S, Hudlicky T, Pandey S. Anti-Cancer Activity of Synthetic Analogues of Pancratistatin Alone & in Combination with Piperlongumine in Glioblastoma. (2015) *12th Annual Natural Health Product Research Society Conference: Convergence: Multi-sector Integration for Advancing Transdisciplinary NHP R&D*, Western University, London, ON, Canada, Aug. 14-17, 2015. *International Conference*. (PhD work) I contributed to design and execution of experiments, analysis of data, and preparation of the presentation.

Tarade D, **Ma D**, Vshyvenko S, Hudlicky T, Pandey S. Piperlongumine Enhances the Anti-cancer Effect of Natural Pancreatistatin and Synthetic Analogs. (2014) *11th Annual Natural Health Product Research Society Conference: From East and West - A Shifting Cultural Landscape of Natural Health Products*, Delta Grand Okanagan Resort, Kelowna, BC, May 13-16. International Conference. (PhD work) I contributed to design and execution of experiments, analysis of data, and preparation of the presentation.

Ma D, Joshi S, Church J, Stokes K, Tarade D, Kadri A, Vshyvenko S, Hudlicky T, McNulty J, Pandey S. Using Natural Pancreatistatin and Synthetic Analogues to Target Cancer Cell Mitochondria for Cancer Therapy: Potentiation of Anti-cancer Activity with Tamoxifen. (2013) *10th Annual Natural Health Product Research Society Conference: The Best of Both Worlds -Traditional & Modern Approaches*, Caesars, Windsor, ON, May 12-15, 2013. International Conference. (PhD work) I contributed to design and execution of experiments, analysis of data, and preparation of the presentation.

Church J, **Ma D**, Stokes K, Vshyvenko S, Hudlicky T, Pandey S. (2013) Evaluating the Anti-Cancer Activity of Synthetic Analogues of Pancreatistatin in Colorectal Cancer and Leukemia Cells and in Colon Tumor Xenografts. *41th Southern Ontario Undergraduate Student Chemistry Conference (SOU SCC 2013)*, McMaster University, Hamilton, ON, Mar. 30, 2013. Provincial Conference. (PhD work) I contributed to design and execution of experiments, analysis of data, and preparation of the presentation.

Joshi S, **Ma D**, Tarade D, Vshyvenko S, Hudlicky T, Pandey S. Targeting Mitochondrial and Oxidative Vulnerabilities Using Synthetic Analogues of Pancreatistatin in Breast Cancer. (2013) *41th Southern Ontario Undergraduate Student Chemistry Conference (SOU SCC 2013)*, McMaster University, Hamilton, ON, Mar. 30, 2013. Provincial Conference. (PhD work) I contributed to design and execution of experiments, analysis of data, and preparation of the presentation.

Ma D, Gupta M, Tuffley I, Joshi S, Church J, Vshyvenko S, Hudlicky, Pandey S. Targeting Mitochondrial & Oxidative Vulnerabilities in Cancer Cells with Synthetic Analogues of Pancreatistatin in Combination with Piperlongumine, Curcumin, & Tamoxifen. (2012) *Windsor Cancer Reserach Group (WCRG) First Annual Conference*, Caesars Windsor Casino. November 16-17, 2012. Provincial Conference. (PhD work) I contributed to design and execution of experiments, analysis of data, and preparation of the presentation.

Ma D, Tremblay P, Mahngar K, Akbari-Asl P, Collins J, Hudlicky T, Pandey S (2011) A Novel Synthetic C1 Analogue of 7-deoxypancreatistatin Selectively Induces Cytotoxicity in Cancer Cells, Exhibits Enhanced Activity with Curcumin and Tamoxifen and Reduces Human Tumour Growth in Xenograft Models. *8th Annual Natural Health Product Research Society Conference "Multidisciplinary*

Approaches to Modern Therapeutics”, Hilton Montreal Bonaventure, Montreal, QC, May 24-27, 2011. *International Conference*. (PhD work) I contributed to design and execution of experiments, analysis of data, and preparation of the presentation.

Pandey S, Griffin C, Chatterjee S, **Ma D** (2011) Targeting Mitochondria in Cancer Cells to Induce Apoptosis by Pancreatistatin, a Natural Products from Spider Lily. *8th Annual Natural Health Product Research Society Conference “Multidisciplinary Approaches to Modern Therapeutics”*, Hilton Montreal Bonaventure, Montreal, QC, May 24-27, 2011. *International Conference*. Abstract #: NHPRS-01-06 (M.Sc. work) I contributed to design and execution of experiments, analysis of data, and preparation of the presentation.

Pandey S, Griffin C, Chatterjee P, Ovadje P, **Ma D**, Tran C, Akbari-Asl P (2010) Targeting Mitochondria in Cancer Cells to Induce Apoptosis by Natural Products From Spider Lily, Dandelion and Turmeric. *Third Annual Cancer Drug Discovery Symposium*, Regional Cancer Centre, Sudbury, ON, May 28-29, 2010. *Provincial Conference*. (M.Sc. work) I contributed to design and execution of experiments, analysis of data, and preparation of the presentation.

Ma D, Collins J, Hudlicky T, Tran C, Garg S, Griffin C, Pandey S (2010) Evaluating the Efficacy of a Novel Synthetic Derivative of Pancreatistatin and its Synergism with Curcumin and Dandelion Root Extract in Inducing Apoptosis in Cancer Cells. *7th Annual Natural Health Product Research Conference “The Next Wave”*, Westin, Halifax, NS, May 23-26, 2010. *International Conference*. (M.Sc. work) I contributed to design and execution of experiments, analysis of data, and preparation of the presentation.

Mahngar K, Domazet-Damjanov D, **Ma D**, Pandey S (2010) Effect of Coenzyme Q10 on fibroblast cells of Alzheimer’s disease patients. *38th Southern Ontario Undergraduate Student Chemistry Conference (SOU SCC 2010)*, University of Western Ontario, ON, Mar. 20, 2010. *Provincial Conference*.

POSTER PRESENTATIONS

Ma D, Gilbert T, Pignanelli C, Tarade D, Cowell M, Noel M, Dowhayko A, Curran C, Vshyvenko S, Hudlicky T, Pandey S. Exploiting Cancer Mitochondrial & Oxidative Vulnerabilities with Pancreatistatin & Analogues with Other Anti-Cancer Agents. (2015) *12th Annual Natural Health Product Research Society Conference: Convergence: Multi-sector Integration for Advancing Transdisciplinary NHP R&D*, Western University, London, ON, Canada, Aug. 14-17, 2015. *International Conference*. (PhD work) I contributed to design and execution of experiments, analysis of data, and preparation of the presentation.

Tarade D, **Ma D**, Church J, Joshi S, Kadri A, Van den Berg S, McNulty J, Pandey, S (2014) Medium Throughput Screen: Novel Anti-cancer Compounds Identified & Characterized. *11th Annual Natural Health Product Research Society Conference: From East and West - A Shifting Cultural Landscape of Natural Health Products*, Delta Grand Okanagan Resort, Kelowna, BC, May 13-16. *International Conference*. I contributed to design and execution of experiments, analysis of data, and preparation of the presentation.

Ma D, Adams S, Larocque K, Pignanelli C, Cowell M, Noel M, Yi W, Guang L, Pandey S (2014) Evaluation of Anti-Cancer Activity of Synthetic Analogues of Curcumin Alone & in Combination with Piperlongumine. *Windsor Cancer Research Group Cancer Research Conference*, Caesars Windsor, Windsor, ON, Canada, Nov 22. *Provincial Conference*. I contributed to design and execution of experiments, analysis of data, and preparation of the presentation.

Ma D, Tarade D, Church J, Joshi S, Stokes K, Kadri A, Vshyvenko S, Hudlicky T, Pandey S (2013) Exploiting Mitochondrial Vulnerabilities with Pancreatistatin & Pancreatistatin Analogues in Combination with Curcumin, Tamoxifen, & Piperlongumine for Cancer Therapy. *Canadian Cancer Research Conference*. Sheraton Centre Toronto Hotel, Toronto, ON, Nov. 3-6, 2013. *National Conference*. (PhD work) I contributed to design and execution of experiments, analysis of data, and preparation of the presentation.

Stokes K, **Ma D**, Sikorska M, Pandey S (2013) Prevention of Stress Induced Premature Senescence in Fibroblasts from Alzheimer's Disease Patients with a Water Soluble Formulation of Coenzyme Q₁₀. *10th Annual Natural Health Product Research Society Conference: The Best of Both Worlds -Traditional & Modern Approaches*, Caesars Windsor, Windsor, ON, May 12-15, 2013. *International Conference*. (PhD work) I contributed to design and execution of experiments, analysis of data, and preparation of the presentation.

Ma D, Tarade D, Church J, Joshi S, Stokes K, Kadri A, Vshyvenko S, Hudlicky T, Pandey S (2013) Exploiting Mitochondrial Vulnerabilities with Pancreatistatin & Pancreatistatin Analogues in Combination with Curcumin, Tamoxifen, & Piperlongumine for Cancer Treatment. *10th Annual Natural Health Product*

Research Society Conference: The Best of Both Worlds -Traditional & Modern Approaches, Caesars Windsor, Windsor, ON, May 12-15, 2013. *International Conference*. (PhD work) I contributed to design and execution of experiments, analysis of data, and preparation of the presentation.

Roma A, Ovadge P, **Ma D**, Pandey S (2013) Ethanolic Extract of Long Pepper Targets Cancer Cell Mitochondria for the Induction of Apoptosis. *10th Annual Natural Health Product Research Society Conference: The Best of Both Worlds - Traditional & Modern Approaches*, Caesars Windsor, Windsor, ON, May 12-15, 2013. *International Conference*. (PhD work) I contributed to design and execution of experiments, analysis of data, and preparation of the presentation.

Ma D, Tremblay P, Vshyvenko S, Hudlicky T, Pandey S (2011) Targeting Mitochondrial Vulnerabilities Using Synthetic Analogues of Pancreatistatin in Combination with Curcumin, Tamoxifen & Piperlongumine for Cancer Treatment. *Canadian Cancer Research Conference*, Sheraton Centre Toronto Hotel, Toronto, ON, Nov. 27-30, 2011. *National Conference*. (PhD work) I contributed to design and execution of experiments, analysis of data, and preparation of the presentation.

Ma D, Tremblay P, Mahngar K, Akbari-Asl P, Collins J, Hudlicky T, Pandey S (2011) A Novel Synthetic C1 Analogue of 7-deoxypancratistatin Induces Cytotoxicity Specifically in Human Leukemia, Neuroblastoma, Glioblastoma, and Colorectal Cancers and Reduces Growth of p53 Positive and Negative Colon Tumour Xenografts. *Bringing Together Communities- Student Research Conference*, University of Windsor CAW Student Center, Windsor, ON, Feb. 4, 2011. *Local Conference*. (M.Sc. work) I contributed to design and execution of experiments, analysis of data, and preparation of the presentation.

Tremblay P, **Ma D**, Mahngar K, Akbari-Asl P, Collins J, Hudlicky T, Pandey S (2011) Chemo-resistant osteosarcoma and pancreatic cancer cells are sensitive to an analogue of Pancreatistatin and displays synergism with curcumin. *Bringing Together Communities- Student Research Conference*, University of Windsor CAW Student Center, Windsor, ON, Feb. 4, 2011. *Local Conference*. (M.Sc. work) I contributed to design and execution of experiments, analysis of data, and preparation of the presentation.

K, Tremblay P, **Ma D**, Sikorska M, Weinstock S, Pandey S (2010) Inhibition of Premature Senescence of Fibroblast Cells From Alzheimer's Disease Patients by Water Soluble Coenzyme Q₁₀. *The Gerontological Society of America's 63rd Annual Scientific Meeting*, New Orleans, LA, Nov. 19-23, 2010. *National Conference*. I contributed to design and execution of experiments, analysis of data, and preparation of the presentation.

Ma D, Tremblay P, Mahngar K, Akbari-Asl P, Griffin C, Garg S, Collins J, Hudlicky T, Pandey S (2010) A Novel Synthetic Derivative of Pancratistatin Induces Apoptosis Selectively in Cancer Cells, Reduces Colon Tumor Growth in Xenograft Models and Exhibits Synergistic Effects with Tamoxifen. *SFRBM 17th Annual Meeting*, Caribe Royale Hotel & Conference Center, Orlando, FL, Nov. 17-21, 2010. *International Conference*. (M.Sc. work) I contributed to design and execution of experiments, analysis of data, and preparation of the presentation.

STUDENT MENTORSHIP & SUPERVISION

Master's Thesis Students, University of Windsor, Windsor ON, Canada

- Sept. 2014- **Cory Philion**
Aug. 2016 Project: Evaluation and Characterization of Anti-Cancer Activity of White Tea & Lemongrass (Expected) Extract in Lymphoma Cells
Present Position: Master's student at the University of Windsor, Windsor, ON, Canada
- Sept. 2012- **Kristen Larocque**
Aug. 2014 Project: Sensitizing Triple Negative Breast Cancer Cells to Novel Synthetic Analogues of Curcumin with Piperlongumine
Present Position: Clinical Trial Researcher at the Ontario Institute of Cancer Research, Kingston, ON, Canada

Bachelor's Honours Thesis Students, University of Windsor, Windsor ON, Canada

- Jun. 2015- **Colin Curran**
Jun. 2019 Project: To be determined
Present Position: Undergraduate Researcher, University of Windsor, Windsor, ON, Canada
- Sept. 2014- **Alexander Dowhayko**
Jun. 2018 Project: Evaluation of Toxicity of Various Anti-Cancer Agents on Peripheral Blood Mononuclear Cells from Healthy Volunteers
Present Position: Undergraduate Researcher, University of Windsor, Windsor, ON, Canada
- Sept. 2014- **Fadi Mansour**
Jun. 2018 Project: Evaluation of Anti-Cancer Activity of Phosphate Derivatives of Combretastatin A4 in Mouse Models of Osteosarcoma
Present Position: Undergraduate Researcher, University of Windsor, Windsor, ON, Canada
- Sept. 2014- **Megan Noel**
Jun. 2017 Project: Exploiting Oncogenic Pathways & Oxidative Vulnerabilities with Piperlongumine & Novel Synthetic Analogues of Curcumin in Triple Negative Breast Cancer Cells
Present Position: Undergraduate Researcher, University of Windsor, Windsor, ON, Canada

- Jan. 2014 - **Christopher Pignanelli**
 Jun. 2016 Project: Pleiotropic Effects of Novel Curcumin Analogues in Leukemia Cells
 Present Position: Undergraduate Thesis Student, University of Windsor, Windsor, ON, Canada
- Sept. 2013- **Tyler Gilbert**
 Jun. 2016 Project : Targeting Actin Dynamics to Sensitive Lymphoma Cells to Mitochondrial Mediated Apoptosis with Novel Analogues of Pancratistatin
 Present Position: Undergraduate Thesis Student, University of Windsor, Windsor, ON, Canada
- Sept. 2013- **Melissa Cowell**
 Jun. 2016 Project : Modulation of NF-kappaB Activity with Novel Analogues of Curcumin in Lymphoma
 Present Position: Undergraduate Thesis Student, University of Windsor, Windsor, ON, Canada
- Sept. 2012- **Fatmeh Hourani**
 Jun. 2015 Project Title: Modulating Heat Shock Protein 70 Activity with Synthetic Analogues of Curcumin in Colorectal Cancer Cells
 Present Position: Dental Student at Western University, London, ON, Canada
- Sept. 2012- **Daniel Tarade**
 Jun. 2015 Project Title: Structure Activity Relationship Study of Novel Analogues of Combretastatin A-4
 Present Position: PhD Student, Dept. of Laboratory Medicine and Pathobiology, University of Toronto, Toronto, ON, Canada
- Sept. 2012- **Kyle Stokes**
 Jun. 2015 Project: Induction of Autophagy by a Water Soluble Formulation of Coenzyme Q10 in Presenilin 1 Mutated Fibroblasts from Alzheimer's Disease Patients
 Present Position: PhD Student in the Department of Biological Sciences, University of Windsor, Windsor, ON, Canada
- Sept. 2012- **Adam Kadri**
 Jun. 2015 Project: Evaluation of Pancratistatin Analogues Against Prostate Cancer Cells
 Present Position: Pharmacy Student at the University of Toronto, Toronto, ON, Canada

- Aug. 2012- **Julia Church**
 Jun. 2013 Project: Evaluation of Novel Pancreatistatin Analogues in Models of Leukemia
 Present Position: Medical Student at Michigan State University, Lansing, Michigan, USA
- Sept. 2011- **Seema Joshi**
 Jun. 2013 Project: Targeting Mitochondria with Pancreatistatin Analogues in Triple-Negative Breast Cancer
 Present Position: Medical Student in Cyprus
- Sept. 2011- **Sabrina Ma**
 Aug. 2012 Project : Dandelion Root Extract & Resveratrol in Combination against Colon Cancer Cells
 Present Position: Dental Student at Detroit Mercy Dental School, Detroit, MI, USA
- Jun. 2011- **Ian Tuffley**
 Jun. 2012 Project: Exploitation of Oxidative Vulnerabilities of Colon Cancer Cells with Piperlongumine and Pancreatistatin Analogues
 Present Position: Master of Biotechnology Graduate, University of Toronto, Mississauga, ON, Canada
- May 2011- **Manika Gupta**
 Aug. 2012 Project: Piperlongumine & Pancreatistatin Analogues Combination Therapy for Ovarian Cancer
 Present Position: Resident Physician, London, ON, Canada
- May 2010 **Phillip Tremblay**
 Aug. 2011 Project: Selective Cytotoxicity Against Human Osteosarcoma Cells by A Novel Anaglogue of Pancreatistatin is Potentiated by Curcumin
 Present Position: Resident Physician, Windsor, ON, Canada
- Sept. 2009 **Kevinjeet Mahngar**
 Jun. 2010 Project: Inhibition of Stress-Induced Premature Senescence of Presenilin 1 Mutated Fibroblasts from Alzheimer's Disease Patients
 Present Position: Resident Physician, London, ON, Canada
- Sept. 2009- **Pardis Akbari-Asl**
 Jun. 2010 Project: Evaluation of Anti-Cancer Activity of Dandelion Root Extract in Pancreatic Cancer Cells
 Present Position: Pharmacist at Windsor Regional Hospital, Windsor, ON, Canada

Sept. 2009- **Cynthia Tran**
Jun 2010 Project: Anti-Cancer Activity of Dandelion Root Extract in
Osteosarcoma Cells
Present Position: Master's Graduate in Political Science, University
of Calgary, Calgary, AB, Canada

Sept. 2009- **Surbhi Garg**
Jun. 2010 Project: Characterization of Combination Therapy of 7-Deoxy
Pacratsistatin analogues & Tamoxifen for Colorectal Cancer
Current Position: Rotman School of Management Master's
Graduate, University of Toronto, Toronto, ON, Canada

INTERNATIONAL PROJECTS & STUDIES

- May 2011 **Golden Future South Africa Project: Khayelitsha, South Africa**
- Educated students in HIV and AIDS awareness, overall health and wellness, life skills, and educational paths/opportunities via classroom workshops in schools in the impoverished community of Khayelitsha, South Africa
- July 2008 **“Contemporary Molecular Approaches to the Study of Human Breast Cancer” Research Workshop: The St. John’s Research Institute, Bangalore, India**
- Shadowed and worked with medical doctors, molecular biologists, and pathologists, learning state of the art techniques in primary culture and molecular biology as approaches used to studying human breast cancer using actual patient specimens
 - Aided in establishing a research collaboration between The St. John’s Research Institute, Bangalore, India and the University of Windsor, Windsor ON, Canada

COMMUNITY/UNIVERSITY OF WINDSOR INVOLVEMENT

- 2011 **University of Windsor Faculty of Science Council**
- Graduate Student representative for the Dept. of Chemistry and Biochemistry for the Faculty of Science Council responsible for program review and academic policies regarding programs in the sciences
- 2008 – 2010 **University of Windsor Science Society Vice President of Academic Affairs**
- Mentored undergraduate science students in course selection
 - Provided guidance regarding professional and grad school applications
 - Coordinator of 4 professor meet and greet sessions attended by professors from the entire Faculty of Science and science undergraduate students
- 2007 – 2009 **Canadian Cystic Fibrosis Foundation – Shinerama (Windsor)**
- Raised funds supporting cystic fibrosis research
- 2007 **University of Windsor Students' Alliance (UWSA) Board of Directors**
- Represented over 12,000 students at the University of Windsor managing an organization and a 6.2 million budget, a staff of 150, and several business operations
- 2006 – 2008 **University of Windsor Walksafe Volunteer Program**
- responsible for walking people safely around campus at night
- 2006 – 2008 **Chemistry and Biochemistry Association**
- assisted in organizing student social events
 - helped organize and put on fundraisers to support the Children's World Education Foundation, a non-profit organization financially supporting the education of children of widowed mothers
- 1999 – 2006 **Windsor Figure Skating Club**
- Can Skate Program volunteer assistant teaching children from ages 3 to 14 how to ice skate and perform basic to intermediate skating skills

ATHLETIC ACCOMPLISHMENTS

Figure Skating

2006 BMO Skate Canada Junior Nationals - 8th in Novice Pairs, Moncton, NB
2005 BMO Skate Canada Junior Nationals- 4th in Pre-Novice Pairs, Ste. Foy, QC
2004 BMO Financial Group Skate Canada Sectionals- 3rd in Novice Men
2003 BMO Skate Canada Junior Nationals- 3rd in Juvenile Pairs, Brampton, ON

Swimming and Running

2002 WECSSAA Junior Boys Swimming- team finished 1st overall
2001 SWOSSAA Midget Boys Cross Country- team finished 2nd in midget boys
2001 OFSAA Midget Boys Cross Country- team finished 22nd